

Small Molecule Dynamics and Partner Fidelity in an Ancient Host-microbe
Symbiosis

By
Heidi A. Horn

A dissertation submitted in partial fulfillment of the
requirements for the degree of

Doctor of Philosophy
(Zoology)

At the
UNIVERSITY OF WISCONSIN-MADISON
2018

Date of final oral examination: December 18, 2018

The dissertation is approved by the following members of the Final Oral Committee:

Cameron R. Currie, Professor, Bacteriology

Richard Lindroth, Professor, Entomology

David A. Baum, Professor, Botany

David R. Andes, Professor, Medical Microbiology and Immunology

Lingjun Li, Professor, Pharmacy

Dissertation Abstract

Small molecule dynamics and partner fidelity in an ancient host-microbe symbiosis

By

Heidi A. Horn

Under the supervision of Professor Cameron R. Currie

at the University of Wisconsin-Madison

Microbes engage in complex behaviors including cooperation, competition, and predation to engage in a range of mutualistic and pathogenic interactions with other organisms. These interactions are mediated through the production of small molecules that are diverse in structure and function. Of these small molecules, the ecology of those with antimicrobial properties are particularly poorly understood, as the behaviors they facilitate and the contexts in which they are produced are often complicated and difficult to observe. In this dissertation, I use interdisciplinary approaches to shed light on host-microbe interactions and their influence on small molecule production within the fungus-growing ant symbiosis. In chapter 1, I outline the fungus-growing ant symbiosis as a model to explore antibiotic-mediated interactions and argue that defensive mutualisms are especially well-suited for study of the ecological dynamics of antimicrobial small molecules. Chapter 2 of this thesis uses quantitative polymerase chain reaction to examine the role of *Pseudonocardia*, a defensive symbiont, in the context of social immunity of an ant colony. In chapter 3, I develop a mass spectrometry imaging method to allow detection of small molecules that are produced by *Pseudonocardia* on the ant exoskeleton. In chapter 4, I use this mass spectrometry imaging technique to examine species interactions that influence small molecule production in the leaf-cutter ant system. I find that interactions between

Pseudonocardia and pathogens induce small molecules as well as the induction of small molecules *in vivo* that are not observed *in vitro*. Chapter 5 assesses the role of partner fidelity between ant host and bacterium on small molecule production. I perform host-symbiont switches and assess the effect of conspecific and allospecific switches on small molecule production. Preliminary results indicate that a combination of *Pseudonocardia* phylotype and ant host in conspecific switches may significantly alter small molecule production. Together, these works suggest that complex interactions between ant host and its defensive mutualist are influencing small molecule production and dynamics in a host-microbe symbiosis.

Acknowledgments

I take a lesson from the ants that I study and recognize that collaboration is an efficient way to be productive and successful. The work in this thesis would not be possible without the collaboration and support of many people. First and foremost, I thank my advisor and mentor, Dr. Cameron Currie. Thank you for your patience and humor over the last ten years. I appreciate the freedom you have given me to pursue my own questions that have stimulated my scientific curiosity. You have encouraged me when I lack confidence, corrected me when I am wrong, and challenged my reasoning when it was flawed. Few people have impacted my life as much as you have—thank you. I am also grateful for the members of my thesis committee, Dr. Richard Lindroth, Dr. David Baum, Dr. Lingjun Li, Dr. David Andes, for challenging my thought process and greatly improving my work.

I am equally grateful to all members of the Currie lab, past and present. I am particularly appreciative of Gina Lewin, Bradon McDonald, Gaspar Bruner, Marc Chevrette, Jenny Bratburd, Camila Carlos, Reed Stubbendieck, Evelyn Wendt-Pienkowski, Kirk Grubbs, and Lily Khadempour. Debates and discussion (especially over a beer) have undoubtedly improved my work and made graduate school more enjoyable.

Interdisciplinary work is crucial in any scientific endeavor and I have wonderful collaborators across the globe. I thank Adrian Tomas-Pinto and his students as well as Monica Tallarico-Pupo and her students for their help facilitating field work and for expanding my world view. I also thank Erin Gemperline and Kellen DeLaney, wonderful collaborators who much of the work in this thesis is dependent upon.

I am blessed to be part of wonderful faith communities in Madison that have supported me on this journey. In particular, I thank Bob and Anne Woodson, Melissa and Maurice Cheeks

(and Hannah and Cyrus), Holly Heinrichs, Deb Flanders, Daniel and Leanne Seemuth, Brittany Ederer, Michelle Prost for supporting me and praying for me and feeding me. I especially thank Tyler Steier—you have comforted me, encouraged me, and made me laugh when I needed it. I am so grateful for your support, and I would not have been able to finish these final stages without you.

And lastly I thank my family: my parents, sister, aunt and uncle, grandma, and oma and opa. You have all been a constant source of strength and encouragement. Any success or achievement in my life is only possible because of the support I have from you. I love you and thank you.

Table of Contents

Small molecule dynamics and partner fidelity in an ancient host-microbe symbiosis.....	i
Dissertation Abstract.....	ii
Acknowledgments.....	iii
Table of contents.....	v
Chapter 1: The ecological diversity and dynamics of small molecule production in defensive symbioses.....	1
1.1 Microbial interactions.....	1
1.2 Fungus-growing ant multi-partite symbiosis as a model.....	3
1.2.1 Multipartite symbiosis.....	3
1.2.2 Coevolutionary dynamics within the fungus-growing ant symbiosis.....	6
1.3 Small molecules: the language of microbes.....	9
1.3.1 Developing models to characterize antibiotic-mediated interactions.....	10
1.4 Symbiosis as a framework.....	11
1.4.1 Insect-microbe defensive symbioses.....	11
1.4.2 Chemistry in the fungus-growing ant symbiosis.....	11
1.4.3 Other model insect-microbe defensive symbioses.....	13
1.5 Small molecule diversity and dynamics in the leaf-cutter ant defensive symbiosis.....	15
1.6 Figures.....	18
1.7 References.....	20
Chapter 2: Integration of <i>Pseudonocardia</i> defensive symbiont in the social structure of <i>Acromyrmex</i> leaf-cutter ants.....	29
2.1 Abstract.....	29
2.2 Introduction.....	30
2.3 Methods.....	32
2.3.1 qPCR primer design.....	33
2.3.2 Ant collection and maintenance.....	34
2.3.3 Experimentally manipulated ants.....	34
2.3.4 Symbiont-free ants.....	35
2.3.5 qPCR from ant exoskeletons.....	35
2.4 Results.....	37
2.4.1 qPCR primer specificity and efficiency.....	37

2.4.2 Variation in abundance of <i>Pseudonocardia</i> between age-based ant castes.....	38
2.4.3 No detection of <i>Streptomyces coelicolor</i> in experimentally manipulated symbiont acquisition	38
2.5 Discussion.....	39
2.6 Acknowledgments.....	42
2.7 Table and Figures.....	43
2.8 References.....	49
Chapter 3: Imaging with mass spectrometry of bacteria on exoskeleton of fungus-growing ants.....	51
3.1 Abstract.....	51
3.2 Introduction.....	52
3.3 Results and discussion.....	54
3.3.1 MSI Method.....	54
3.3.2 MSI of Ant/ <i>Pseudonocardia</i> / <i>Escovopsis</i> Interactions.....	56
3.4 Methods.....	58
3.4.1 Sample Preparation for MALDI-MSI.....	58
3.4.2 MALDI-Orbitrap MSI.....	59
3.4.3 Metabolite Identifications.....	60
3.5 Acknowledgements.....	60
3.6 Figures.....	61
3.7 References.....	65
Chapter 4: Specialized chemical responses to pathogens in the defensive symbionts of fungus-growing ants..	68
4.1 Abstract.....	68
4.2 Introduction.....	69
4.3 Methods.....	72
4.3.1 Ant colony collection and maintenance.....	72
4.3.2 <i>In vitro</i> bioassays.....	73
4.3.3 Genome sequencing.....	73
4.3.4 Subcolony preparation and pathogen treatment.....	74
4.3.5 Sample preparation for MALDI.....	75
4.3.6 MALDI-Orbitrap MSI.....	76
4.3.7 MALDI-MSI data processing and analysis.....	76
4.3.8 Statistical analysis.....	77

4.4 Results.....	78
4.4.1 Genomics.....	78
4.4.2 <i>In vitro</i> small molecule induction.....	79
4.4.3 <i>in vitro-in vivo</i> comparison.....	82
4.4.4 Specificity of pathogen interaction.....	84
4.5 Discussion.....	86
4.6 Acknowledgments.....	92
4.7 Figures and tables.....	92
4.8 References.....	97
Chapter 5: Partner fidelity of host-microbe symbiosis influences small molecule production <i>in vivo</i> in the leaf-cutter ant symbiosis.....	105
5.1 Abstract.....	105
5.2 Introduction.....	106
5.3 Methods.....	109
5.3.1 Colony collection and maintenance.....	109
5.3.2 Conspecific switches.....	109
5.3.3 Allospecific switches.....	110
5.3.4 MALDI-Mass spectrometry imaging.....	111
5.3.5 Data analysis.....	112
5.4 Results.....	113
5.4.1 Conspecific switches.....	113
5.4.2 Allospecific switches.....	113
5.5 Discussion.....	114
5.6 Acknowledgments.....	116
5.7 Figures and tables.....	117
5.8 References.....	124
Chapter 6: Conclusion and future directions.....	127
Appendix 1: Supplementary materials for Chapter 3.....	131
Appendix 2: Supplementary materials for Chapter 4.....	141
Appendix 3: Convergent evolution of complex structures for ant-bacterial defensive symbiosis in fungus-farming ants.....	149
A3.1 Abstract.....	149

A3.2 Introduction.....	150
A3.3 Results and discussion.....	152
A3.3.1 Ancient Ant- <i>Pseudonocardia</i> symbiosis.....	152
A3.3.2 Evolutionary trajectory of <i>Pseudonocardia</i> maintenance in fungus-farming ants.....	156
A3.3.3 Caste differences in maintenance of <i>Pseudonocardia</i> symbionts.....	158
A3.3.4 Repeated loss of symbiosis.....	158
A3.4 Conclusion.....	159
A3.5 Experimental procedures.....	160
A3.5.1 Taxon sampling and UCE data preparation.....	160
A3.5.2 Phylogenetic inference.....	161
A3.5.3 Divergence-dating analysis.....	162
A3.5.4 Fossil ants.....	163
A3.5.5 Electron microscopy.....	163
A3.5.6 qPCR.....	163
A3.5.7 Ancestral-state reconstruction.....	164
A3.6 Acknowledgments.....	164
A3.7 Figures.....	164
A3.8 References.....	167
A3.9 Supplementary material.....	170
Appendix 4: Microbes are trophic analogs of animals.....	173
A4.1 Abstract.....	173
A4.2 Introduction.....	174
A4.3 Results.....	177
A4.3.1 Controlled-feeding studies (TDFglu-phe and TPglu-phe estimates).....	177
A4.3.2 Fungus-garden study.....	180
A4.4 Discussion.....	180
A4.5 Materials and methods.....	184
A4.5.1 Culturing of consumer species.....	184
A4.5.2 Compound-specific isotope analysis.....	184
A4.5.3 Trophic computations and statistics.....	185
A4.6 Acknowledgments.....	185
A4.7 Figures.....	186

A4.8 References.....	191
A4.9 Supplementary material.....	193

Chapter 1

The ecological diversity and dynamics of small molecule production in defensive symbioses

1.1 Microbial interactions

The diversity of life is shaped by interactions between species. The complex range of these intra- and interspecific interactions range from competition and cooperation to predation and parasitism (Bailey, Kelsic, & Kishony, 2016; Hardin, 1960; Levin, 1970; May, 1988; Volterra, 1928; Williams & Martinez, 2000). Ecologists have observed and studied the complex interactions between organisms, populations, communities and ecosystems since the origin of the field of Ecology. Likewise evolutionary biologists have explored how these associations drive diversity. Darwin famously concludes ‘On the origin of species’ with

"It is interesting to contemplate a tangled bank, clothed with many plants of many kinds, with birds singing on the bushes, with various insects flitting about, and with worms crawling through the damp earth, and to reflect that these elaborately constructed forms, so different from each other, and dependent upon each other in so complex a manner, have all been produced by laws acting around us."

Darwin's quote highlights the interconnections between species and how the ‘laws acting around us’ mediate these interactions and shape populations and generate biological diversity.

The complex interactions occurring between plants and animals are now recognized as being shaped, in part, by microbial symbionts. Almost all organisms are influenced by or rely on some symbiosis with microbes that enables their host to occupy a niche or utilize an otherwise inaccessible resource. Mutualistic symbioses between microbes and eukaryotic hosts influence

host processes including nutrient acquisition, immune system functioning, and defense against pathogens. Lichens, the first described microbial symbiosis, are composed of fungus and either alga or cyanobacterium which provide a supply of carbon through photosynthesis (Honegger, 1991). Other well-studied examples of microbes enabling nutrient acquisition include plants that obtain nitrogen through symbioses with nitrogen-fixing microorganisms Rhizobia (Andrews & Andrews, 2017; Young & Johnston, 1989; Zahran, 1999) and cyanobacteria (Lindblad, 2008). While the previously listed symbioses occur through an external association with a microbe, pea aphids maintain a nutritional symbiosis with an intracellular mutualist, *Buchnera*. The bacterium resides in specialized bacteriocytes and produces essential amino acids that the host does not receive in its diet (Baumann et al., 1995; Douglas & Prosser, 1992; Hansen & Moran, 2011).

The previous examples are interactions between one host and one microbial symbiont, although multispecies communities of microbes are also important to the ecology of most organisms. The complex interplay between microbial communities and humans is now being explored to greater depth (Eckburg et al., 2005). Gut microbial communities have been implicated in human immune functioning, aging, brain function, and nutrient uptake (Hsiao et al., 2013; Kau, Ahern, Griffin, Goodman, & Gordon, 2011; Kundu, Blacher, Elinav, & Pettersson, 2017; Sharon, Sampson, Geschwind, & Mazmanian, 2016). The interactions between organisms in these communities and between microbes and their hosts are difficult to elucidate, yet these interactions and their influences are important to define as they are necessary to understand the diversity of extant life.

As microbial symbioses allow macroorganisms to occupy new niches, they can, by consequence, influence the evolution and diversity of their associated hosts. Host-pathogen dynamics are a key selective pressure and drive diversity in both host and pathogen populations

and have been well-studied particularly in human-pathogen interactions (Barreiro & Quintana-Murci, 2010; Betts, Gray, Zelek, MacLean, & King, 2018; Haerter, Mitarai, & Sneppen, 2014; Shapiro et al., 2018; Spurgin & Richardson, 2010). Mutualistic interactions further contribute to the evolution of extant life. Even the origin of eukaryotes is attributed to a microbial-derived endosymbiosis (Sagan, 1967). The evolutionary dynamics of symbioses vary depending on the nature of the interaction. These symbioses can be tight intracellular associations, like the pea aphid/*Buchnera* association, or diverse communities of bacteria interacting within or on a single host, each with their own evolutionary implications and dynamics (Moran & Telang, 1998).

Despite the recognized importance of microbial symbionts in mediating the ecology and evolution of plants and animals, and the complexity of ecological interactions among the microbes embedded within and around them, our understanding of microbe-host and microbe-microbe interactions remains extremely limited. Model symbioses are necessary to better understand the processes driving microbial species interactions and the diversity they generate. Here, we discuss a model multipartite symbiosis and pose questions to further shed light upon the nature of microbial interactions within a symbiosis.

1.2 Fungus-growing ant multi-partite symbiosis as a model

1.2.1 Multipartite symbiosis

Fungus-growing ants (subtribe Attina) participate in an ancient, multi-partite symbiosis whose microbial associations span from mutualistic to parasitic (**Figure 1.1**). Fungus-growers, also referred to as attine ants, are a New World group that engage in the cultivation of basidiomycetous fungi that they consume as their primary food source (Chapela, Rehner, Schultz, & Mueller, 1994; Hölldobler & Wilson, 1990; Shik et al., 2016; Weber, 1966; Wilson, 1971). The ants forage for substrate that they feed to the fungus, *Leucoagaricus*; in return, the queen and brood are fed the

fungus as their sole food source (Quinlan & Cherrett, 1979). The fungal cultivar is vertically transmitted – founding queens carry a piece of fungus from their parent colony to their founding colony in a specialized infrabuccal pocket in their oral cavity (Quinlan & Cherrett, 1978) allowing a tight and specific association between ant and fungal food source. This obligate mutualism is ancient in origin and arose approximately 55 million years ago (Nygaard et al., 2016; Schultz & Brady, 2008).

Attine ants have diversified along with their fungal cultivar and are subdivided into two groups, conventionally called ‘higher’ attines and ‘lower’ attines, based on the fungus they cultivate. Lower attines cultivate a range of fungi, most belonging to the Leucocoprinae (Chapela et al. 1994; Shultz & Brady, 2008). Some ants cultivate fungi from lineages derived from the origin of attine fungiculture and other ants have domesticated fungal cultivars from free-living fungi (Schultz & Brady, 2008). Higher attines cultivate a single, derived fungal cultivar, *Leucoagaricus gongylophorus*, and include the leaf-cutter ants (*Atta* and *Acromyrmex*) along with the genera *Sericomyrmex* and *Trachymyrmex* (Schultz & Brady, 2008). *Leucoagaricus gongylophorus* evolved specialized structures called gongylidia that the ants feed upon. Gongylidia resemble hyphal swellings and contain high concentrations of lipid and carbohydrate nutrients (De Fine Licht, Boomsma, & Tunlid, 2014; Quinlan & Cherrett, 1979). The relationship between attine ants and their fungal cultivar is highly specialized and enables the ants to obtain energy, indirectly through their fungus gardens, from many different resources.

The fungal cultivar is grown in a monoculture within colonies and as such is highly susceptible to pathogens, including the specialized fungal pathogen *Escovopsis* (Ascomycete; Hypocreales) which is capable of overgrowing the ants’ food source (C. R. Currie, Mueller, & Malloch, 1999). *Escovopsis* is found in approximately 50% of higher attine fungus gardens and

in 30-40% percent of lower attine colonies sampled in Panama (Currie et al., 1999). It is not found in foundress queen infrabuccal pockets or in incipient colonies supporting that the pathogen is horizontally transmitted. Although there are several hypotheses of how *Escovopsis* may be horizontally transmitted, the mode of transmission is unknown. Interestingly, the pathogen maintains a degree of host specificity and associates tightly with particular lineages of fungal cultivar (Currie et al., 2003a; Gerardo, Mueller, & Currie, 2006). There is some evidence of host switching, although congruent phylogenies at deep levels indicate *Escovopsis* diversified along with the fungal host (Currie et al., 2003b; Gerardo et al., 2006).

The ants, to protect their food source, have evolved several defense mechanisms, including a defensive mutualism with a bacterium in the genus *Pseudonocardia* (Currie et al. 1999; C R Currie, Bot, & Boomsma, 2003). *Pseudonocardia* provides protection in the form of antimicrobial molecules that are active against *Escovopsis*, helping defend the fungus garden from infection (Currie et al. 1999; Currie et al., 2003; Michael Poulsen et al., 2010). It resides as a white biofilm on the ant exoskeleton (**Figure 1.1d**) and removal from the ants results in faster overgrowth of *Escovopsis* (Currie et al., 2003). Culture assays, when *Pseudonocardia* and *Escovopsis* are grown together in a Petri plate, reveal patterns of inhibition and resistance between the two organisms suggesting interesting population and interaction dynamics (Cafaro et al., 2011; Michael Poulsen et al., 2010). Several of the antibiotics produced by *Pseudonocardia* have been characterized (Carr, Derbyshire, Caldera, Currie, & Clardy, 2012; Oh, Poulsen, Currie, & Clardy, 2009; Van Arnam et al., 2016) although the full diversity of antibiotics used is unknown.

Pseudonocardia transmission occurs vertically as foundress queens carry the symbiont on their exoskeleton and transfer the bacterium to new workers (Currie et al.1999). Once the colony

is established, workers that carry the symbiont transfer *Pseudonocardia* to developing workers within 1-2 hours of eclosion (Marsh, Poulsen, Pinto-Tomás, & Currie, 2014; M. Poulsen, Bot, Currie, Nielsen, & Boomsma, 2003). Once acquired on the ant exoskeleton, abundance of *Pseudonocardia* varies over the lifespan of an individual ant (Poulsen et al., 2003), however the bacterial strain maintained within an individual colony is stable over time. DNA sequencing of *Acromyrmex* colonies maintained in the laboratory for 10 years revealed that colonies maintain primarily one strain of *Pseudonocardia* and that it is the dominant bacterial member on the exoskeleton (Andersen, Hansen, Sapountzis, Sørensen, & Boomsma, 2013). Together, the mode of transmission and stability of the association supports a specific association between ant host and *Pseudonocardia*.

The basic ecology of the ants, their fungal cultivar, the pathogen *Escovopsis*, and the mutualistic *Pseudonocardia* has been well-characterized. The interactions between these players have generated genetic diversity within this system and provide a model framework in which to pose evolutionary questions. Specifically, the ants, cultivar, and *Pseudonocardia* are all under selective pressure to defend against *Escovopsis*, possibly resulting in coevolution at different levels between these organisms.

1.2.2 Coevolutionary dynamics within the fungus-growing ant symbiosis

Comparisons of phylogenetic topologies suggest that reciprocal selection may be shaping parts of this multipartite symbiosis. Congruent phylogenies at deeper phylogenetic levels support a pattern of codiversification between the ants, their fungal cultivar, and the pathogen *Escovopsis* supporting long term coevolutionary dynamics in the system (C. Currie et al., 2003a). There is evidence of specialization between symbiont phylogenies at finer phylogenetic levels, as

Escovopsis phylogenies are congruent with fungal cultivar but not ant host phylogenies (Gerardo et al., 2006; Gerardo, Mueller, Price, & Currie, 2004). Pairwise assays between players reveal complex dynamics and host-pathogen specificity between cultivar and *Escovopsis* lineages at finer phylogenetic scales. Fungal cultivar in two lower attines, *Cyphomyrmex* and *Apterostigma*, is more likely to be infected by *Escovopsis* from its own colony than an *Escovopsis* with which it does not typically associate (Gerardo et al., 2006, 2004). These patterns demonstrate the complexity of interactions across geographic and phylogenetic scales and is consistent with a geographic mosaic framework where diverse species interactions may be observed at local or population levels (J. Thompson, 1999, 2005; J. N. Thompson & Cunningham, 2002).

Several lines of evidence suggest that *Pseudonocardia* is also undergoing coevolutionary dynamics with its ant host. Significant morphological and physiological changes in the ant host supports coevolution between the ants and *Pseudonocardia*. Depending on the ant lineages, *Pseudonocardia* resides in specialized crypts embedded within the exoskeleton of the ant (Cameron R Currie, Poulsen, Mendenhall, Boomsma, & Billen, 2006; Li et al., 2018). Recent work revealed that these crypts evolved at least three independent times in attine evolution and diversified over 50 million years leading to a variety of structures in extant lineages (Li et al., 2018). Additionally, the ants have glands associated with the corresponding crypts that provide nutrients to *Pseudonocardia* for growth and survival (Cameron R Currie et al., 2006; Steffan et al., 2015). Lineages of ants that do not have visible associations with *Pseudonocardia*, apparently having secondarily lost the symbiont, do not exhibit these morphological adaptations (Cameron R Currie et al., 2006; Li et al., 2018). These morphological adaptations indicate the ants have evolved to maintain the symbiont and *Pseudonocardia* may have similarly adapted to utilize the resources available on the ant host. Analysis of *Pseudonocardia* across several ant

genera suggests that *Pseudonocardia* displays a significant degree of phylogenetic specificity with its ant host, as there appear to be clades of *Pseudonocardia* that associate with only a few genera of fungus-growing ants (Cafaro et al., 2011; Cafaro & Currie, 2005). There is evidence of some host switching and horizontal acquisition of the bacterium suggesting that it is possible for the ants to acquire new symbionts or symbionts colonize new ant hosts.

It is hypothesized that *Pseudonocardia* and *Escovopsis* may be engaging in an evolutionary arms race and shaped by Red Queen dynamics. This has largely been studied from the perspective of *Pseudonocardia* and its ability to inhibit *Escovopsis* through antibiotic production. *Pseudonocardia* exhibits variation in its inhibition of *Escovopsis* at the population level, supporting the hypothesis that selective pressure from a pathogen drives diversity of small molecules (Cafaro et al., 2011; Cafaro & Currie, 2005; Michael Poulsen et al., 2010). Several of the antibiotics produced by ant-associated *Pseudonocardia* that inhibit *Escovopsis* have been characterized, including dentigerumycin and pseudonocardone (Carr et al., 2012; Oh, Poulsen, et al., 2009; Sit et al., 2015; Van Arnam et al., 2016). However, recent genomic and metabolomics analysis suggests that ant-associated *Pseudonocardia* possess diverse secondary metabolite potential that varies even within populations (Horn et al., in review; McDonald, in prep). In addition to this population level variation in *Pseudonocardia*, the population structures of *Pseudonocardia* and *Escovopsis* are correlated and are suggestive of coevolutionary dynamics (Caldera & Currie, 2012). These findings indicates that *Escovopsis* may play a role in shaping the diversity of antimicrobial small molecules produced by *Pseudonocardia*.

These microbially-produced small molecules are putatively traits under reciprocal selection in these *Pseudonocardia*-*Escovopsis* interactions. Exploring the dynamics of these small molecules is necessary to understand how these organisms interact and how chemical diversity is

generated. Further, characterizing small molecule dynamics in a well-described symbiosis is important to better understand general microbial species interactions that are mediated by chemistry.

1.3 Small molecules: the language of microbes

Microbial species interactions are difficult to explore due, in part, to the microscopic nature of microbes. In contrast, ecologists that study plants and animals have an advantage in their ability to physically observe organisms of interest, and also be informed by the hundreds of years of natural history conducted on macroorganisms. This historical legacy is lacking in microbial ecology. However, new technologies are now enabling us to rapidly fill this knowledge gap. It is now appreciated that microbes engage in many of the same behaviors as macroorganisms and form the same classes of interactions, ranging from competition and predation to cooperation and mutualism. Many of these interactions occur through the production of small molecules. Small molecules (also referred to as secondary metabolites or natural products), such as those discussed above produced by ant-associated *Pseudonocardia*, are low molecular weight organic compounds (ranging from 100-1700 Da). The molecules produced by microbes are diverse spanning quorum sensing molecules, siderophores, and antibiotics. These molecules mediate a wide array of microbial behaviors and interactions at several ecological levels within species, across phyla, and across kingdoms.

Antimicrobial or antibiotic molecules, compounds that inhibit the growth or kill bacteria or fungi, mediate microbial interactions. These compounds span a diversity of molecule classes including terpenes, peptides, polyketides, among others that inhibit the growth of other organisms. Antibiotics have been explored in detail due to their application in treating human

infectious disease, though their ecological function and relevance is largely unknown (Bérdy, 2005; Clardy, Fischbach, & Currie, 2009; Romero, Traxler, López, & Kolter, 2011). While it is thought that microbes use antibiotics to engage in warfare and competition, the actual ecology of antibiotic production is likely more complicated (Chevrette & Currie, 2018; Davies, 2006; Yim, Wang, & Davies, 2007).

At sub-inhibitory concentrations these same compounds can act as signaling molecules between microbes and influence transcription rather than arrest bacterial growth (Davies, Spiegelman, & Yim, 2006; Goh et al., 2002). Further complicating our understanding of these secondary metabolites is that most bacteria possess the genomic potential to produce many molecules that are never observed under laboratory conditions (Bentley et al., 2002; Nett, Ikeda, & Moore, 2009; Rutledge & Challis, 2015). It is hypothesized that these cryptic molecules are only produced under certain conditions or in response to ecologically-relevant species interactions. Recent effort to induce these compounds include co-culture techniques, where microbes are grown together in the same Petri Plate, to induce the production of so-called cryptic gene clusters by species interactions (Adnani et al., 2017; Bertrand et al., 2014; Lim, Sanchez, Wang, & Keller, 2012; Scherlach & Hertweck, 2009; Seyedsayamdost, 2014). While informative, this method is still lacks the complexity of interactions found in a microbes' native niche. It appears that bacteria use antimicrobial molecules to mediate complex behavior, although the diversity of these molecules and the context in which they are employed remains unknown.

1.3.1 Developing models to characterize antibiotic-mediated interactions

Most work examining antimicrobial small molecules is done *in vitro*, and little is known about the antimicrobial chemistry of *in vivo* interactions or interactions within a microbe's native

niche. There is a recent call to develop model systems to elucidate what the chemical interactions are between multispecies microbial interactions (O'Brien & Wright, 2011; Zhalnina, Zengler, Newman, & Northen, 2018). This is historically difficult due to technological constraints in observing small molecules, as most microbes produce antibiotic compounds in low abundance *in vivo* compared to culture conditions. Furthermore, microbes are likely interacting with multiple organisms as in Darwin's tangled bank. New models and techniques are necessary to shed insight into antibiotic small molecule dynamics.

1.4 Defensive symbiosis as a framework

1.4.1 Insect-microbe defensive symbioses

Here, we argue that microbial defensive mutualisms, such as the fungus-growing ant-*Pseudonocardia* symbiosis, provide a framework to begin unraveling antibiotic-mediated interactions more generally. Defensive mutualisms are symbioses between a host organism and a microbe where the microbial player provides defense for the host. Insect hosts are particularly interesting to explore as they are some of the most diverse organisms on the planet and occupy a wide array of niches. The pathogens and parasites they encounter are equally diverse and, the selective pressure to protect larvae and protect food sources is strong. Defensive mutualisms with microbes are one adaptation to protect vulnerable life stages. The interaction between defensive symbionts and pathogen likely drives chemical diversity. The following section reviews several well-characterized defensive symbioses, primarily between insect hosts and bacterial mutualists, and highlights evolutionary questions that are key in unraveling the complicated small molecule interactions in a multi-player symbiosis.

1.4.2 Chemistry in the fungus-growing ant symbiosis

The small molecule interactions within the fungus-growing ant system have been characterized to varying degrees. The antibiotic molecules produced by *Pseudonocardia* are perhaps the best characterized in the system, although they have been studied largely in laboratory culture. Inhibition bioassays between different lineages of *Pseudonocardia* and *Escovopsis* reveal variation in *Pseudonocardia*'s ability to inhibit the pathogen (Cafaro et al., 2011; Poulsen et al., 2010). This suggests that population level dynamics between the players may be shaping the antibiotic compounds *Pseudonocardia* produces. Indeed, several novel antibiotics have been discovered including dentigerumycin (Oh, Poulsen, et al., 2009), pseudonocardone (Carr et al., 2012), and selvamycin (Van Arnam et al., 2016) (**Figure 1.2**). Many other derivatives of known molecules with antimicrobial activity have also been characterized in ant-associated *Pseudonocardia* (Barke et al., 2010; Van Arnam, Ruzzini, Sit, Currie, & Clardy, 2015). Comparative genomic analysis between two closely related strains of *Pseudonocardia*, isolated from sympatric ant populations, reveal biosynthetic gene cluster (BGC) differences between the two strains (Holmes et al., 2016). One phylotype had 14-15 BGC and the other phylotype had 11-15 BGC with only 6 BGC shared among all strains (Holmes et al., 2016). This indicates that there is variation in the biosynthetic gene potential of ant-associated *Pseudonocardia* even at local population level although the ecological effects of this variation is unknown.

Two studies have attempted to examine small molecules produced *in vivo*, when *Pseudonocardia* resides on the ant exoskeleton (Gemperline, Horn, DeLaney, Currie, & Li, 2017; Schoenian et al., 2011). Valinomycins and actinomycins were found distributed across the body of an *Acromyrmex* worker however this study could not determine if antibiotic production occurs where the symbiont resides on the ant exoskeleton (Schoenian et al., 2011). More recent

work used improved methods to visualize small molecules localized to *Pseudonocardia* on the ant exoskeleton (Gemperline et al., 2017). Although this method is not capable of identifying individual metabolites it does allow for detection of whole small molecule profiles (Gemperline et al., 2017). It is a powerful tool to compare small molecule profiles of *Pseudonocardia* on different ant hosts and determine the *in vivo* variation and response to pathogen infection. It is yet to be observed if the variation seen in inhibition bioassays is reflected in *in vivo* interactions.

This model system is well-suited to address questions regarding small molecule diversity and dynamics for several reasons, including: i) The ecology has been studied for many years and the basic interactions between players are well-described; ii) Colonies act as a unit and can be easily manipulated; and iii) Individual players can be isolated from the system and studied in reduced interactions. A combination of mass spectrometry, inhibition bioassays, population ecology, and experimental manipulations can be used to address questions regarding when and how antibiotic molecules are produced in this system. Study of the interactions mediating antibiotic production may inform on the evolutionary processes driving this chemical diversity.

1.4.3 Other model insect-microbe defensive symbioses

Beewolves (solitary digger wasps) are another well-described example of an insect using a bacterium for antibiotic production (Kaltenpoth, Göttler, Herzner, & Strohm, 2005; Kroiss et al., 2010). Mother beewolves inoculate their brood chambers with a *Streptomyces* that coats the entire chamber. The *Streptomyces* produces a combination of 9 different antibiotics (Kroiss et al., 2010) that prevent pathogen growth in the chamber, and the beewolf larvae then develop in this *Streptomyces*-protected chamber. The mode of transmission is particularly interesting in this symbiosis –the *Streptomyces* resides within the antennae of the mother beewolf and she

inoculates the brood chamber by an elaborate shaking of her head across the chamber (Kaltenpoth et al., 2005; Koehler, Doubský, & Kaltenpoth, 2013). The dynamics of symbiont transmission have been well-characterized in this system. Only a few bacterial cells are taken up by the emerging female and grows logistically in her antennae just days after she emerges (Kaltenpoth, Goettler, Koehler, & Strohm, 2010). It is suggested that partner fidelity is maintained by this strict vertical transmission however biogeographic analysis of beewolf-associated *Streptomyces* indicates frequent horizontal acquisition or switching (Kaltenpoth, Roeser-Mueller, Stubblefield, Seger, & Strohm, 2014). *In situ* analysis of 25 beewolf-*Streptomyces* pairs reveals combinations of up to 49 antibiotic derivatives with particular differences associated with species and geography. While these antibiotic interactions are complex, it appears that local pressures may be shaping the chemical diversity in this system.

Lagria beetles maintain a dynamic association with *Burkholderia gladioli* that protects *Lagria* larvae (Flórez & Kaltenpoth, 2017). *Burkholderia gladioli* is transmitted vertically by female beetles through application of the bacterium to the developing larvae which maintain special structures for bacterial localization (Flórez et al., 2017). This association protects the larvae from pathogen infection. The beetles can also horizontally acquire the bacterium from plants that the beetles reside on—the bacterium acts as pathogen of the host plant and transitions to a mutualistic lifestyle in association with the *Lagria* beetle. While the basic ecology of the *Lagria-Burkholderia* association has been well-described, the chemical diversity and potential is still unknown.

Other insect-microbe systems are less well-characterized but represent promising systems for further exploration. *Wolbachia* appear to prevent the dengue virus from replicating in *Aedes aegypti* (Bian, Xu, Lu, Xie, & Xi, 2010) as well as prevent RNA viral infection in *Drosophila*

melanogaster (Teixeira, Ferreira, & Ashburner, 2008) although the mechanism of these interactions is unknown. Host-associated bacteria and active antibiotic molecules have been characterized in ambrosia beetles, dung beetles (S.-H. Kim et al., 2013), and southern pine beetles (Oh, Scott, Currie, & Clardy, 2009; Scott et al., 2008). Active compounds have been isolated from these systems but the interaction between host and bacteria is not characterized. Hundreds of strains of *Streptomyces* were isolated from two species of mud-dauber wasps and many of them exhibited bioactivity against bacteria and fungi (Oh, Poulsen, Currie, & Clardy, 2011; Michael Poulsen, Oh, Clardy, & Currie, 2011). However, the specificity of the interactions between wasp and bacterium has yet to be assessed and the ecological relevance of these compounds is unknown. Several novel compounds have been isolated from bacteria from fungus-growing termites (Beemelmans et al., 2017; K. H. Kim et al., 2014), however a large-scale bacterial survey, accounting for geography and host phylogeny, found no specificity of an association between fungus-growing termites and a particular Actinobacteria species or any target-specific bioactivity (Visser, Nobre, Currie, Aanen, & Poulsen, 2012). The compounds isolated from these interactions have been reviewed in several recent publications (Flórez, Biedermann, Engl, & Kaltenpoth, 2015; Van Arnam, Currie, & Clardy, 2018). While these compounds are of interest, the association between host and microbe are not well described in these cases. Questions regarding the specificity and biogeography of the association have yet to be answered.

1.5 Small molecule diversity and dynamics in the leaf-cutter ant defensive symbiosis

While these works represent key experiments that establish the ecology of microbial defense symbioses, questions regarding partner fidelity and small molecule diversity are still to be explored. Indeed, it is necessary to address these questions to understand the evolution of

microbial associations. Patterns of diversity and specificity often give clues to the evolution of populations and these clues in microbial associations are found in the small molecules they produce. Here, we suggest that defensive microbial symbioses between microbes and a host are a natural starting point to ask these questions and develop new methods. The natural history and ecological characterization of these associations provide a starting place that allows for better identification of microbial-produced small molecules and their roles in their native niches. Here, I use the fungus-growing ant multi-partite symbiosis as a model to understand microbial interactions, particularly elucidating small molecule interactions between players *in vivo*.

In the chapters of this dissertation, I examine how interactions between ant host and *Pseudonocardia* influence the nature of the symbioses, particularly how small molecule production is influenced. In Chapter 2, I develop molecular methods to measure the abundance of *Pseudonocardia* on the ant exoskeleton. I then demonstrate how this method can be used to test questions regarding the dynamics between host and symbiont. Specifically, I find evidence of caste-based differences in *Pseudonocardia* abundance supporting a connection between symbiont and social organization of the ant colony. Chapter 3 outlines development of a matrix-assisted laser desorption ionization (MALDI) mass spectrometry imaging (MSI) approach to examine small molecules produced by *Pseudonocardia* while it resides on the ant exoskeleton, effectively assessing the chemistry produced *in vivo*. This method is used in chapter 4 to ask ecologically relevant questions about *in vivo* small molecule dynamics. Specifically, I address the following questions: i) Does the interaction with a pathogen induce the production of different small molecules by *Pseudonocardia*? ii) Are the same small molecules produced when the bacterium resides on its ant host (*in vivo*) compared to when it is grown in culture (*in vitro*) iii) Do different pathogens induce the production of different small molecules by

Pseudonocardia? Finally, chapter 5 uses MALDI MSI to assess the effects of specificity between ant host and *Pseudonocardia* on small molecule production. The work in this dissertation provides insight into ecological interactions that influence microbially-produced small molecules.

1.6 Figures

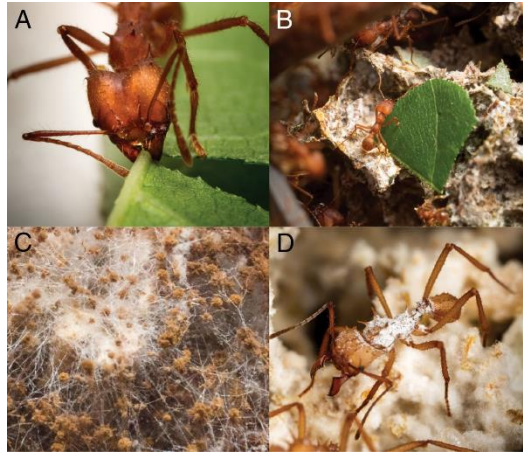
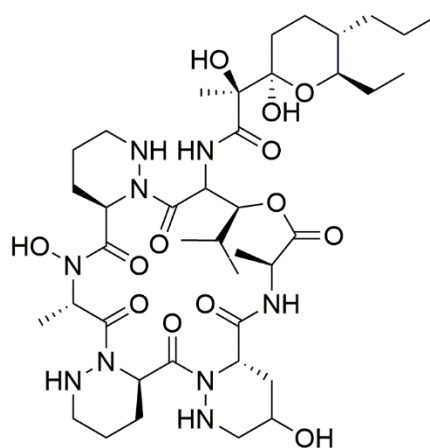
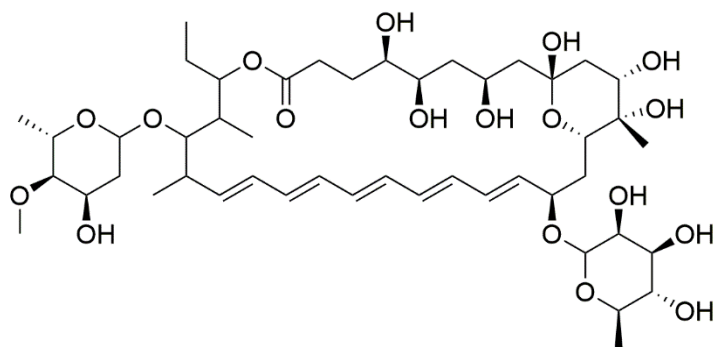


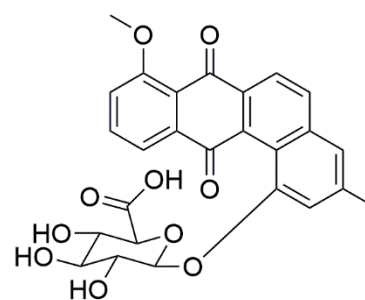
Figure 1.1 Components of a leaf-cutter ant fungus garden. A) Forager ant cutting a leaf fragment. B) Incorporation of leaf material into the fungus garden. C) Brown spores of *Escovopsis* consuming the fungal cultivar. D) *Pseudonocardia*, white substance, growing on the ant cuticle. (Adapted from Steffan et al. 2015)



Dentigerumycin



Selvamycin



Pseudonocardone B

Figure 1.2 Diversity of antibiotic small molecules isolated from *Pseudonocardia* of fungus-growing ants. Adapted from Oh et al. 2009, Carr et al. 2012, and Van Arnam et al. 2015.

1.7 References

- Adnani, N., Chevrette, M. G., Adibhatla, S. N., Zhang, F., Yu, Q., Braun, D. R., ... Bugni, T. S. (2017). Coculture of Marine Invertebrate-Associated Bacteria and Interdisciplinary Technologies Enable Biosynthesis and Discovery of a New Antibiotic, Keyicin. *ACS Chemical Biology*, *12*(12), 3093–3102. <http://doi.org/10.1021/acscchembio.7b00688>
- Andersen, S. B., Hansen, L. H., Sapountzis, P., Sørensen, S. J., & Boomsma, J. J. (2013). Specificity and stability of the Acromyrmex-Pseudonocardia symbiosis. *Molecular Ecology*, *22*(16), 4307–21. <http://doi.org/10.1111/mec.12380>
- Andrews, M., & Andrews, M. E. (2017). Specificity in Legume-Rhizobia Symbioses. *International Journal of Molecular Sciences*, *18*(4), 705. <http://doi.org/10.3390/ijms18040705>
- Bairey, E., Kelsic, E. D., & Kishony, R. (2016). High-order species interactions shape ecosystem diversity. *Nature Communications*, *7*(1), 12285. <http://doi.org/10.1038/ncomms12285>
- Barke, J., Seipke, R. F., Grünschow, S., Heavens, D., Drou, N., Bibb, M. J., ... Hutchings, M. I. (2010). A mixed community of actinomycetes produce multiple antibiotics for the fungus farming ant Acromyrmex octospinosus. *BMC Biology*, *8*, 109. <http://doi.org/10.1186/1741-7007-8-109>
- Barreiro, L. B., & Quintana-Murci, L. (2010). From evolutionary genetics to human immunology: how selection shapes host defence genes. *Nature Reviews Genetics*, *11*(1), 17–30. <http://doi.org/10.1038/nrg2698>
- Baumann, P., Baumann, L., Lai, C.-Y., Rouhbakhsh, D., Moran, N. A., & Clark, M. A. (1995). *GENETICS, PHYSIOLOGY, AND EVOLUTIONARY RELATIONSHIPS OF THE GENUS BUCHNERA: Intracellular Symbionts of Aphids*. *Annu. Rev. Microbiol* (Vol. 49). Retrieved from www.annualreviews.org
- Beemelmans, C., Ramadhar, T. R., Kim, K. H., Klassen, J. L., Cao, S., Wyche, T. P., ... Clardy, J. (2017). Macrotermycins A–D, Glycosylated Macrolactams from a Termite-Associated *Amycolatopsis* sp. M39. *Organic Letters*, *19*(5), 1000–1003. <http://doi.org/10.1021/acs.orglett.6b03831>
- Bentley, S. D., Chater, K. F., Cerdeño-Tárraga, A.-M., Challis, G. L., Thomson, N. R., James, K. D., ... Hopwood, D. A. (2002). Complete genome sequence of the model actinomycete *Streptomyces coelicolor* A3(2). *Nature*, *417*(6885), 141–7. <http://doi.org/10.1038/417141a>
- Bérdy, J. (2005). Bioactive microbial metabolites. *The Journal of Antibiotics*, *58*(1), 1–26. <http://doi.org/10.1038/ja.2005.1>
- Bertrand, S., Bohni, N., Schnee, S., Schumpp, O., Gindro, K., & Wolfender, J.-L. (2014). Metabolite induction via microorganism co-culture: A potential way to enhance chemical

- diversity for drug discovery. *Biotechnology Advances*, 32(6), 1180–1204.
<http://doi.org/10.1016/J.BIOTECHADV.2014.03.001>
- Betts, A., Gray, C., Zelek, M., MacLean, R. C., & King, K. C. (2018). High parasite diversity accelerates host adaptation and diversification. *Science*, 360(6391), 907–911.
<http://doi.org/10.1126/SCIENCE.AAM9974>
- Bian, G., Xu, Y., Lu, P., Xie, Y., & Xi, Z. (2010). The Endosymbiotic Bacterium Wolbachia Induces Resistance to Dengue Virus in *Aedes aegypti*. *PLoS Pathogens*, 6(4), e1000833.
<http://doi.org/10.1371/journal.ppat.1000833>
- Cafaro, M. J., & Currie, C. R. (2005). Phylogenetic analysis of mutualistic filamentous bacteria associated with fungus-growing ants, 446, 441–446. <http://doi.org/10.1139/W05-023>
- Cafaro, M. J., Poulsen, M., Little, A. E. F., Price, S. L., Gerardo, N. M., Wong, B., ... Currie, C. R. (2011). Specificity in the symbiotic association between fungus-growing ants and protective *Pseudonocardia* bacteria. *Proceedings. Biological Sciences / The Royal Society*, 278(1713), 1814–22. <http://doi.org/10.1098/rspb.2010.2118>
- Caldera, E. J., & Currie, C. R. (2012). The population structure of antibiotic-producing bacterial symbionts of *Apterostigma dentigerum* ants: impacts of coevolution and multipartite symbiosis. *The American Naturalist*, 180(5), 604–17. <http://doi.org/10.1086/667886>
- Carr, G., Derbyshire, E. R., Caldera, E., Currie, C. R., & Clardy, J. (2012). Antibiotic and antimalarial quinones from fungus-growing ant-associated *Pseudonocardia* sp. *Journal of Natural Products*, 75(10), 1806–9. <http://doi.org/10.1021/np300380t>
- Chapela, I. H., Rehner, S. A., Schultz, T. R., & Mueller, U. G. (1994). Evolutionary history of the symbiosis between fungus-growing ants and their fungi. *Science (New York, N.Y.)*, 266(5191), 1691–4. <http://doi.org/10.1126/science.266.5191.1691>
- Chevrette, M. G., & Currie, C. R. (2018). Emerging evolutionary paradigms in antibiotic discovery. *Journal of Industrial Microbiology & Biotechnology*, 1–15.
<http://doi.org/10.1007/s10295-018-2085-6>
- Clardy, J., Fischbach, M. A., & Currie, C. R. (2009). The natural history of antibiotics. *Current Biology : CB*, 19(11), R437-41. <http://doi.org/10.1016/j.cub.2009.04.001>
- Currie, C. R., Bot, A. N. M., & Boomsma, J. J. (2003). Experimental evidence of a tripartite mutualism : bacteria protect ant fungus gardens from specialized parasites. *Oikos*, 1(July 2002), 91–102.
- Currie, C. R., Mueller, U. G., & Malloch, D. (1999). The agricultural pathology of ant fungus gardens. *Proceedings of the National Academy of Sciences*, 96(14), 7998–8002.
<http://doi.org/10.1073/pnas.96.14.7998>
- Currie, C. R., Poulsen, M., Mendenhall, J., Boomsma, J. J., & Billen, J. (2006). Coevolved crypts and exocrine glands support mutualistic bacteria in fungus-growing ants. *Science (New York, N.Y.)*, 311(5757), 81–3. <http://doi.org/10.1126/science.1119744>
- Currie, C., & Scott, James A, Summerbell, Richard, and Malloch, D. (1999). Fungus-growing ants use antibiotic-producing bacteria to control garden parasites, 398(April), 701–705.

- Currie, C., Wong, B., Stuart, A. E., Schultz, T. R., Rehner, S. A., Mueller, U. G., ... Straus, N. A. (2003a). Ancient tripartite coevolution in the attine ant-microbe symbiosis. *Science (New York, N.Y.)*, 299(5605), 386–8. <http://doi.org/10.1126/science.1078155>
- Currie, C., Wong, B., Stuart, A. E., Schultz, T. R., Rehner, S. a, Mueller, U. G., ... Straus, N. a. (2003b). Ancient tripartite coevolution in the attine ant-microbe symbiosis. *Science (New York, N.Y.)*, 299(5605), 386–8. <http://doi.org/10.1126/science.1078155>
- Davies, J. (2006). Are antibiotics naturally antibiotics? *Journal of Industrial Microbiology & Biotechnology*, 33(7), 496–9. <http://doi.org/10.1007/s10295-006-0112-5>
- Davies, J., Spiegelman, G. B., & Yim, G. (2006). The world of subinhibitory antibiotic concentrations. *Current Opinion in Microbiology*, 9(5), 445–453. <http://doi.org/10.1016/J.MIB.2006.08.006>
- De Fine Licht, H. H., Boomsma, J. J., & Tunlid, A. (2014). Symbiotic adaptations in the fungal cultivar of leaf-cutting ants. *Nature Communications*, 5(1), 5675. <http://doi.org/10.1038/ncomms6675>
- Douglas, A. E., & Prosser, W. A. (1992). Synthesis of the essential amino acid tryptophan in the pea aphid (*Acyrtosiphon pisum*) symbiosis. *Journal of Insect Physiology*, 38(8), 565–568. [http://doi.org/10.1016/0022-1910\(92\)90107-O](http://doi.org/10.1016/0022-1910(92)90107-O)
- Eckburg, P. B., Bik, E. M., Bernstein, C. N., Purdom, E., Dethlefsen, L., Sargent, M., ... Relman, D. A. (2005). Diversity of the Human Intestinal Microbial Flora. *Science*, 308(5728), 1635–1638. <http://doi.org/10.1126/science.1110591>
- Flórez, L. V., Biedermann, P. H. W., Engl, T., & Kaltenpoth, M. (2015). Defensive symbioses of animals with prokaryotic and eukaryotic microorganisms. *Natural Product Reports*, 32(7), 904–936. <http://doi.org/10.1039/C5NP00010F>
- Flórez, L. V., & Kaltenpoth, M. (2017). Symbiont dynamics and strain diversity in the defensive mutualism between *Lagria* beetles and *Burkholderia*. *Environmental Microbiology*, 19(9), 3674–3688. <http://doi.org/10.1111/1462-2920.13868>
- Flórez, L. V., Scherlach, K., Gaube, P., Ross, C., Sitte, E., Hermes, C., ... Kaltenpoth, M. (2017). Antibiotic-producing symbionts dynamically transition between plant pathogenicity and insect-defensive mutualism. *Nature Communications*, 8, 15172. <http://doi.org/10.1038/ncomms15172>
- Gemperline, E., Horn, H. A., DeLaney, K., Currie, C. R., & Li, L. (2017). Imaging with Mass Spectrometry of Bacteria on the Exoskeleton of Fungus-Growing Ants. *ACS Chemical Biology*, 12(8), 1980–1985. <http://doi.org/10.1021/acscchembio.7b00038>
- Gerardo, N. M., Mueller, U. G., & Currie, C. R. (2006). Complex host-pathogen coevolution in the *Apterostigma* fungus-growing ant-microbe symbiosis. *BMC Evolutionary Biology*, 6(1), 88. <http://doi.org/10.1186/1471-2148-6-88>
- Gerardo, N. M., Mueller, U. G., Price, S. L., & Currie, C. R. (2004). Exploiting a mutualism: parasite specialization on cultivars within the fungus-growing ant symbiosis. *Proceedings. Biological Sciences*, 271(1550), 1791–8. <http://doi.org/10.1098/rspb.2004.2792>

- Goh, E.-B., Yim, G., Tsui, W., McClure, J., Surette, M. G., & Davies, J. (2002). Transcriptional modulation of bacterial gene expression by subinhibitory concentrations of antibiotics. *Proceedings of the National Academy of Sciences of the United States of America*, 99(26), 17025–30. <http://doi.org/10.1073/pnas.252607699>
- Haerter, J. O., Mitarai, N., & Sneppen, K. (2014). Phage and bacteria support mutual diversity in a narrowing staircase of coexistence. *The ISME Journal*, 8(11), 2317–2326. <http://doi.org/10.1038/ismej.2014.80>
- Hansen, A. K., & Moran, N. A. (2011). Aphid genome expression reveals host-symbiont cooperation in the production of amino acids. *Proceedings of the National Academy of Sciences of the United States of America*, 108(7), 2849–54. <http://doi.org/10.1073/pnas.1013465108>
- Hardin, G. (1960). The competitive exclusion principle. *Science (New York, N.Y.)*, 131(3409), 1292–7. <http://doi.org/10.1126/SCIENCE.131.3409.1292>
- Hölldobler, B., & Wilson, E. O. (1990). *The Ants*. Harvard University Press. Retrieved from <https://books.google.com/books?hl=en&lr=&id=R-7TaridBX0C&pgis=1>
- Holmes, N. A., Innocent, T. M., Heine, D., Bassam, M. Al, Worsley, S. F., Trottmann, F., ... Hutchings, M. I. (2016). Genome Analysis of Two Pseudonocardia Phylotypes Associated with Acromyrmex Leafcutter Ants Reveals Their Biosynthetic Potential. *Frontiers in Microbiology*, 7, 2073. <http://doi.org/10.3389/fmicb.2016.02073>
- Honegger, R. (1991). *FUNCTIONAL ASPECTS OF THE LICHEN SYMBIOSIS**. *Annu. Rev. Plant Physiol. Plant Mol. Biol.* (Vol. 42). Retrieved from www.annualreviews.org
- Hsiao, E. Y., McBride, S. W., Hsien, S., Sharon, G., Hyde, E. R., McCue, T., ... Mazmanian, S. K. (2013). Microbiota modulate behavioral and physiological abnormalities associated with neurodevelopmental disorders. *Cell*, 155(7), 1451–63. <http://doi.org/10.1016/j.cell.2013.11.024>
- Kaltenpoth, M., Goettler, W., Koehler, S., & Strohm, E. (2010). Life cycle and population dynamics of a protective insect symbiont reveal severe bottlenecks during vertical transmission. *Evolutionary Ecology*, 24(2), 463–477. <http://doi.org/10.1007/s10682-009-9319-z>
- Kaltenpoth, M., Göttler, W., Herzner, G., & Strohm, E. (2005). Symbiotic bacteria protect wasp larvae from fungal infestation. *Current Biology : CB*, 15(5), 475–9. <http://doi.org/10.1016/j.cub.2004.12.084>
- Kaltenpoth, M., Roeser-Mueller, K., Stubblefield, J. W., Seger, J., & Strohm, E. (2014). Biogeography of a defensive symbiosis. *Communicative & Integrative Biology*, 7(6), e993265. <http://doi.org/10.4161/19420889.2014.993265>
- Kau, A. L., Ahern, P. P., Griffin, N. W., Goodman, A. L., & Gordon, J. I. (2011). Human nutrition, the gut microbiome and the immune system. *Nature*, 474(7351), 327–336. <http://doi.org/10.1038/nature10213>
- Kim, K. H., Ramadhar, T. R., Beemelmans, C., Cao, S., Poulsen, M., Currie, C. R., & Clardy, J.

- (2014). Natalamycin A, an ansamycin from a termite-associated *Streptomyces* sp. *Chem. Sci.*, 5(11), 4333–4338. <http://doi.org/10.1039/C4SC01136H>
- Kim, S.-H., Kwon, S. H., Park, S.-H., Lee, J. K., Bang, H.-S., Nam, S.-J., ... Oh, D.-C. (2013). Tripartin, a Histone Demethylase Inhibitor from a Bacterium Associated with a Dung Beetle Larva. *Organic Letters*, 15(8), 1834–1837. <http://doi.org/10.1021/ol4004417>
- Koehler, S., Doubský, J., & Kaltenpoth, M. (2013). Dynamics of symbiont-mediated antibiotic production reveal efficient long-term protection for beewolf offspring. *Frontiers in Zoology*, 10(1), 3. <http://doi.org/10.1186/1742-9994-10-3>
- Kroiss, J., Kaltenpoth, M., Schneider, B., Schwinger, M.-G., Hertweck, C., Maddula, R. K., ... Svatos, A. (2010). Symbiotic Streptomyces provide antibiotic combination prophylaxis for wasp offspring. *Nature Chemical Biology*, 6(4), 261–3. <http://doi.org/10.1038/nchembio.331>
- Kundu, P., Blacher, E., Elinav, E., & Pettersson, S. (2017). Our Gut Microbiome: The Evolving Inner Self. *Cell*, 171(7), 1481–1493. <http://doi.org/10.1016/J.CELL.2017.11.024>
- Levin, S. A. (1970). Community Equilibria and Stability, and an Extension of the Competitive Exclusion Principle. *The American Naturalist*. The University of Chicago Press/The American Society of Naturalists. <http://doi.org/10.2307/2459310>
- Li, H., Sosa-Calvo, J., Horn, H. A., Pupo, M. T., Clardy, J., Rabeling, C., ... Currie, C. R. (2018). Convergent evolution of complex structures for ant–bacterial defensive symbiosis in fungus-farming ants. *Proceedings of the National Academy of Sciences*, 201809332. <http://doi.org/10.1073/pnas.1809332115>
- Lim, F. Y., Sanchez, J. F., Wang, C. C. C., & Keller, N. P. (2012). Toward awakening cryptic secondary metabolite gene clusters in filamentous fungi. *Methods in Enzymology*, 517, 303–24. <http://doi.org/10.1016/B978-0-12-404634-4.00015-2>
- Lindblad, P. (2008). Cyanobacteria in Symbiosis with Cycads (pp. 225–233). Springer, Berlin, Heidelberg. http://doi.org/10.1007/7171_2008_118
- Marsh, S. E., Poulsen, M., Pinto-Tomás, A., & Currie, C. R. (2014). Interaction between workers during a short time window is required for bacterial symbiont transmission in *Acromyrmex* leaf-cutting ants. *PloS One*, 9(7), e103269. <http://doi.org/10.1371/journal.pone.0103269>
- May, R. M. (1988). How many species are there on Earth? *Science (New York, N.Y.)*, 241(4872), 1441–9. <http://doi.org/10.1126/science.241.4872.1441>
- Moran, N. A., & Telang, A. (1998). Bacteriocyte-Associated Symbionts of Insects. *BioScience*, 48(4), 295–304. <http://doi.org/10.2307/1313356>
- Nett, M., Ikeda, H., & Moore, B. S. (2009). Genomic basis for natural product biosynthetic diversity in the actinomycetes. *Natural Product Reports*, 26(11), 1362–84. <http://doi.org/10.1039/b817069j>
- Nygaard, S., Hu, H., Li, C., Schiøtt, M., Chen, Z., Yang, Z., ... Tunlid, A. (2016). Reciprocal genomic evolution in the ant–fungus agricultural symbiosis. *Nature Communications*, 7, 12233. <http://doi.org/10.1038/ncomms12233>

- O'Brien, J., & Wright, G. D. (2011). An ecological perspective of microbial secondary metabolism. *Current Opinion in Biotechnology*, 22(4), 552–8. <http://doi.org/10.1016/j.copbio.2011.03.010>
- Oh, D.-C., Poulsen, M., Currie, C. R., & Clardy, J. (2009). Dentigerumycin: a bacterial mediator of an ant-fungus symbiosis. *Nature Chemical Biology*, 5(6), 391–3. <http://doi.org/10.1038/nchembio.159>
- Oh, D.-C., Poulsen, M., Currie, C. R., & Clardy, J. (2011). Sceliphrolactam, a Polyene Macrocyclic Lactam from a Wasp-Associated *Streptomyces* sp. *Organic Letters*, 13(4), 752–755. <http://doi.org/10.1021/ol102991d>
- Oh, D.-C., Scott, J. J., Currie, C. R., & Clardy, J. (2009). Mycangimycin, a Polyene Peroxide from a Mutualist *Streptomyces* sp. *Organic Letters*, 11(3), 633–636. <http://doi.org/10.1021/ol802709x>
- Poulsen, M., Bot, A. N. M., Currie, C. R., Nielsen, M. G., & Boomsma, J. J. (2003). Within-colony transmission and the cost of a mutualistic bacterium in the leaf-cutting ant *Acromyrmex octospinosus*. *Functional Ecology*, 17(2), 260–269. <http://doi.org/10.1046/j.1365-2435.2003.00726.x>
- Poulsen, M., Cafaro, M. J., Erhardt, D. P., Little, A. E. F., Gerardo, N. M., Tebbets, B., ... Currie, C. R. (2010). Variation in *Pseudonocardia* antibiotic defence helps govern parasite-induced morbidity in *Acromyrmex* leaf-cutting ants. *Environmental Microbiology Reports*, 2(4), 534–540. <http://doi.org/10.1111/j.1758-2229.2009.00098.x>
- Poulsen, M., Oh, D.-C., Clardy, J., & Currie, C. R. (2011). Chemical Analyses of Wasp-Associated *Streptomyces* Bacteria Reveal a Prolific Potential for Natural Products Discovery. *PLoS ONE*, 6(2), e16763. <http://doi.org/10.1371/journal.pone.0016763>
- Quinlan, R. J., & Cherrett, J. M. (1978). Studies on the role of the infrabuccal pocket of the leaf-cutting ant *Acromyrmex octospinosus* (Reich) (Hym., Formicidae). *Insectes Sociaux*, 25(3), 237–245. <http://doi.org/10.1007/BF02224744>
- Quinlan, R. J., & Cherrett, J. M. (1979). The role of fungus in the diet of the leaf-cutting ant *Atta cephalotes* (L.). *Ecological Entomology*, 4(2), 151–160. <http://doi.org/10.1111/j.1365-2311.1979.tb00570.x>
- Romero, D., Traxler, M. F., López, D., & Kolter, R. (2011). Antibiotics as signal molecules. *Chemical Reviews*, 111(9), 5492–505. <http://doi.org/10.1021/cr2000509>
- Rutledge, P. J., & Challis, G. L. (2015). Discovery of microbial natural products by activation of silent biosynthetic gene clusters. *Nature Reviews Microbiology*, 13(8), 509–523. <http://doi.org/10.1038/nrmicro3496>
- Sagan, L. (1967). On the origin of mitosing cells. *Journal of Theoretical Biology*, 14(3), 225–IN6. [http://doi.org/10.1016/0022-5193\(67\)90079-3](http://doi.org/10.1016/0022-5193(67)90079-3)
- Scherlach, K., & Hertweck, C. (2009). Triggering cryptic natural product biosynthesis in microorganisms. *Organic & Biomolecular Chemistry*, 7(9), 1753–60. <http://doi.org/10.1039/b821578b>

- Schoenian, I., Spiteller, M., Ghaste, M., Wirth, R., Herz, H., & Spiteller, D. (2011). Chemical basis of the synergism and antagonism in microbial communities in the nests of leaf-cutting ants. *Proceedings of the National Academy of Sciences of the United States of America*, *108*(5), 1955–60. <http://doi.org/10.1073/pnas.1008441108>
- Schultz, T. R., & Brady, S. G. (2008). Major evolutionary transitions in ant agriculture. *Proceedings of the National Academy of Sciences of the United States of America*, *105*(14), 5435–40. <http://doi.org/10.1073/pnas.0711024105>
- Scott, J. J., Oh, D.-C., Yuceer, M. C., Klepzig, K. D., Clardy, J., & Currie, C. R. (2008). Bacterial protection of beetle-fungus mutualism. *Science (New York, N.Y.)*, *322*(5898), 63. <http://doi.org/10.1126/science.1160423>
- Seyedsayamdost, M. R. (2014). High-throughput platform for the discovery of elicitors of silent bacterial gene clusters. *Proceedings of the National Academy of Sciences of the United States of America*, *111*(20), 7266–71. <http://doi.org/10.1073/pnas.1400019111>
- Shapiro, L. R., Paulson, J. N., Arnold, B. J., Scully, E. D., Zhaxybayeva, O., Pierce, N. E., ... Kolter, R. (2018). An Introduced Crop Plant Is Driving Diversification of the Virulent Bacterial Pathogen *Erwinia tracheiphila*. *MBio*, *9*(5), e01307-18. <http://doi.org/10.1128/mBio.01307-18>
- Sharon, G., Sampson, T. R., Geschwind, D. H., & Mazmanian, S. K. (2016). The Central Nervous System and the Gut Microbiome. *Cell*, *167*(4), 915–932. <http://doi.org/10.1016/J.CELL.2016.10.027>
- Shik, J. Z., Gomez, E. B., Kooij, P. W., Santos, J. C., Wcislo, W. T., & Boomsma, J. J. (2016). Nutrition mediates the expression of cultivar-farmer conflict in a fungus-growing ant. *Proceedings of the National Academy of Sciences of the United States of America*, *113*(36), 10121–6. <http://doi.org/10.1073/pnas.1606128113>
- Sit, C. S., Ruzzini, A. C., Van Arnem, E. B., Ramadhar, T. R., Currie, C. R., & Clardy, J. (2015). Variable genetic architectures produce virtually identical molecules in bacterial symbionts of fungus-growing ants. *Proceedings of the National Academy of Sciences*, *112*(43), 13150–13154. <http://doi.org/10.1073/pnas.1515348112>
- Spurgin, L. G., & Richardson, D. S. (2010). How pathogens drive genetic diversity: MHC, mechanisms and misunderstandings. *Proceedings. Biological Sciences*, *277*(1684), 979–88. <http://doi.org/10.1098/rspb.2009.2084>
- Steffan, S. A., Chikaraishi, Y., Currie, C. R., Horn, H., Gaines-Day, H. R., Pauli, J. N., ... Ohkouchi, N. (2015). Microbes are trophic analogs of animals. *Proceedings of the National Academy of Sciences*, *112*(49), 201508782. <http://doi.org/10.1073/pnas.1508782112>
- Teixeira, L., Ferreira, Á., & Ashburner, M. (2008). The Bacterial Symbiont *Wolbachia* Induces Resistance to RNA Viral Infections in *Drosophila melanogaster*. *PLoS Biology*, *6*(12), e1000002. <http://doi.org/10.1371/journal.pbio.1000002>
- Thompson, J. (1999). Specific hypotheses on the geographic mosaic of coevolution. *The American Naturalist*. Retrieved from <http://www.jstor.org/stable/10.1086/303208>

- Thompson, J. (2005). *The geographic mosaic of coevolution*. Retrieved from https://books.google.com/books?hl=en&lr=&id=SFsfGrcwwWsC&oi=fnd&pg=PR5&ots=s9_S5Mmr_U&sig=OSJoZGvSnPaBGZGoc3vWQetd87o
- Thompson, J. N., & Cunningham, B. M. (2002). Geographic structure and dynamics of coevolutionary selection. *Nature*, *417*(6890), 735–8. <http://doi.org/10.1038/nature00810>
- Van Arnam, E. B., Currie, C. R., & Clardy, J. (2018). Defense contracts: molecular protection in insect-microbe symbioses. *Chemical Society Reviews*, *47*(5), 1638–1651. <http://doi.org/10.1039/C7CS00340D>
- Van Arnam, E. B., Ruzzini, A. C., Sit, C. S., Currie, C. R., & Clardy, J. (2015). A Rebeccamycin Analog Provides Plasmid-Encoded Niche Defense. *Journal of the American Chemical Society*, *137*(45), 14272–14274. <http://doi.org/10.1021/jacs.5b09794>
- Van Arnam, E. B., Ruzzini, A. C., Sit, C. S., Horn, H., Pinto-Tomás, A. A., Currie, C. R., & Clardy, J. (2016). Selvamycin, an atypical antifungal polyene from two alternative genomic contexts. *Proceedings of the National Academy of Sciences of the United States of America*, *113*(46), 12940–12945. <http://doi.org/10.1073/pnas.1613285113>
- Visser, A. A., Nobre, T., Currie, C. R., Aanen, D. K., & Poulsen, M. (2012). Exploring the Potential for Actinobacteria as Defensive Symbionts in Fungus-Growing Termites. *Microbial Ecology*, *63*(4), 975–985. <http://doi.org/10.1007/s00248-011-9987-4>
- Volterra, V. (1928). Variations and Fluctuations of the Number of Individuals in Animal Species living together. *ICES Journal of Marine Science*, *3*(1), 3–51. <http://doi.org/10.1093/icesjms/3.1.3>
- Weber, N. A. (1966). Fungus-growing ants. *Science (New York, N.Y.)*, *153*(3736), 587–604. <http://doi.org/10.1126/science.153.3736.587>
- Williams, R. J., & Martinez, N. D. (2000). Simple rules yield complex food webs. *Nature*, *404*(6774), 180–183. <http://doi.org/10.1038/35004572>
- Wilson, E. O. (1971). The insect societies. Retrieved from <http://www.cabdirect.org/abstracts/19720503745.html?freeview=true>
- Yim, G., Wang, H. H., & Davies, J. (2007). Antibiotics as signalling molecules. *Philosophical Transactions of the Royal Society of London. Series B, Biological Sciences*, *362*(1483), 1195–200. <http://doi.org/10.1098/rstb.2007.2044>
- Young, J. P., & Johnston, A. W. (1989). The evolution of specificity in the legume-rhizobium symbiosis. *Trends in Ecology & Evolution*, *4*(11), 341–9. [http://doi.org/10.1016/0169-5347\(89\)90089-X](http://doi.org/10.1016/0169-5347(89)90089-X)
- Zahran, H. H. (1999). Rhizobium-legume symbiosis and nitrogen fixation under severe conditions and in an arid climate. *Microbiology and Molecular Biology Reviews : MMBR*, *63*(4), 968–89, table of contents. Retrieved from <http://www.ncbi.nlm.nih.gov/pubmed/10585971>
- Zhalnina, K., Zengler, K., Newman, D., & Northen, T. R. (2018). Need for Laboratory Ecosystems To Unravel the Structures and Functions of Soil Microbial Communities

Mediated by Chemistry. *MBio*, 9(4), e01175-18. <http://doi.org/10.1128/mBio.01175-18>

Chapter 2

Integration of *Pseudonocardia* defensive symbionts in the social structure of *Acromyrmex* leaf-cutter ants

Authors: Heidi A. Horn, Gasper Bruner, Rolando Soto Moiera, Adrian Tomas-Pinto and Cameron R. Currie

Author Contributions: Conceived of project (HAH, GB, CRC), designed experiment (HAH, GB), performed field collections (HAH, GB, RSM, ATP), performed manipulation experiments (HAH), performed qPCR (HAH), performed statistical analysis (HAH), and wrote manuscript (HAH, CRC).

*This manuscript is written to be submitted for publication in 2019 after revisions and insertion of additional data.

2.1 Abstract

Defensive symbioses between insects and bacteria appear to be common, helping insects defend against pathogens and predators. Leaf-cutter ants in the genus *Acromyrmex* engage in a defensive mutualism with *Pseudonocardia* bacteria, which reside on the ant exoskeleton and produce antibiotics important in protecting the colony from pathogen infection. The interaction between the ant host and *Pseudonocardia* symbiont is dynamic as bacterial abundances visibly vary over the lifetime of a single ant worker. Here we examine the dynamics of this ant-bacterium association by combining a quantitative polymerase chain (qPCR) reaction approach and experimental manipulations of the host-microbe interaction. Using qPCR, we observe a significantly higher abundance of *Pseudonocardia* on garden workers compared to foragers of *A. octospinosus* ants. Garden workers of *A. echinaior* also had a higher abundance of *Pseudonocardia* than foragers, although lower in abundance than *A. octospinosus* garden workers. These results are consistent with visual assessment of *Pseudonocardia* abundance.

Acromyrmex gynes displayed a significant amount of *Pseudonocardia* supporting symbiont vertical transmission of the symbiont from parent to offspring nestmates. In addition, we experimentally manipulated symbiont acquisition to determine if *Streptomyces*, a related genus of Actinobacteria, can be acquired in detectable amounts. Although workers successfully acquired their native *Pseudonocardia* symbiont in these experiments, ant workers were unable to acquire the non-native *Streptomyces*, as detected by qPCR. Here we show higher abundance of *Pseudonocardia* in *A. octospinosus* garden tending worker castes, indicating integration of the defensive symbiont in the social structure of these ants, as well as evidence indicating an inability of a non-native symbiont to colonize workers.

2.2 Introduction

Microbial symbionts are ubiquitous and important for the functioning of many eukaryotes (Moran, 2007). Defensive symbioses, where one player provides protection to another, enable organisms to defend against predators, parasites, and pathogens (Bentley et al., 2002; Clay, 2014; Kaltenpoth & Engl, 2014; Oliver, Russell, Moran, & Hunter, 2003). In insects, which occupy a diverse array of niches and encounter diverse groups of pathogens, defensive symbioses appear particularly common. For example, several insect hosts associate with bacteria that play a defensive role, often through the production of antibiotics. The associations between insects and mutualistic bacteria likely varies over time and space, as the need for the mutualist is not static and maintenance of these symbionts is known to be energetically expensive (Poulsen, Bot, Currie, Nielsen, & Boomsma, 2003). Exploring the temporal dynamics of these associations in

model defensive symbioses is important for understanding the complex interactions within these associations.

Many fungus-growing ants (subtribe Attina), including many leaf-cutters, engage in a defensive symbiosis with Actinobacteria in the genus *Pseudonocardia*. These ants engage in an obligate mutualisms with a fungi that they cultivate for food (Hölldobler & Wilson, 1990). To protect this important food source from pathogens, the ants maintain a mutualistic association with a bacterium in the genus *Pseudonocardia* (C R Currie, Bot, & Boomsma, 2003; Cameron R Currie & Scott, 1999). *Pseudonocardia* protects the fungus garden from pathogens through the production of antibiotics (Carr, Derbyshire, Caldera, Currie, & Clardy, 2012; Oh, Poulsen, Currie, & Clardy, 2009; Van Arnam et al., 2016). In *Acromyrmex* spp. that engage in a defensive symbiosis with *Pseudonocardia*, the bacteria reside on the ant exoskeleton and are visible as a white coating (Cameron R Currie & Scott, 1999; Li et al., 2018). The abundance of the symbiont is temporally dynamic as different ant castes visibly maintain varying abundances of *Pseudonocardia* (Marsh, Poulsen, Pinto-Tomás, & Currie, 2014). Furthermore, *Pseudonocardia* abundance appears to change over the lifespan of a single ant (Poulsen et al., 2003).

Defensive symbiotic *Pseudonocardia* appear to be transmitted vertically, initially from the queen to her daughters and subsequently from daughter worker to daughter worker (Cameron R Currie & Scott, 1999; Marsh et al., 2014). Callow or newly eclosed *Acromyrmex* spp. worker ants must be exposed to their symbiont within a tight 1-2 hour window of eclosion or they will not acquire the bacterium (Marsh et al., 2014). Bacterial coverage is not consistent between workers, and ant caste appears to influence the abundance of the bacterium present. Leaf-cutter ant workers are divided into castes determined by size of worker (Hölldobler & Wilson, 1990; Wilson, 1980). The smallest workers, minima, typically maintain less visible *Pseudonocardia*

while major workers, ants with a larger head size, maintain greater abundances of the symbiont (C R Currie et al., 2003; Marsh et al., 2014). The ants also utilize an age-based division of labor—the youngest workers perform tasks within the fungus garden, while older workers perform tasks outside the colony such as foraging for leaf material or tending the dump system (Camargo, Forti, Lopes, Andrade, & Ottati, 2007). Major workers appear to have a higher abundance of *Pseudonocardia* when they are younger and working inside the fungus garden compared to when they transition to work outside the colony (Poulsen et al., 2003). Age-based division of labor is part of a highly organized social structure that influences the social defenses of the colony, and variation in *Pseudonocardia* abundance among ant caste may also contribute to this structure.

Previous work has relied largely on visual confirmation of bacterial abundance (c.f. Poulsen et al., 2003). Here we developed a quantitative polymerase chain reaction (qPCR) protocol to quantify the abundance of the *Pseudonocardia* symbiont on the ant exoskeleton. We ask the following questions: i) Do garden workers maintain a higher abundance of *Pseudonocardia*, as compared to foragers, as predicted by the functional role of defensive symbiont in protecting the fungal cultivar from pathogens? ii) Do gynes carry a significant abundance of *Pseudonocardia*, supporting vertical transmission of the defensive symbionts? iii) Do *Acromyrmex* ants exposed to *Streptomyces coelicolor* in their window of acquisition acquire detectable abundances of this non-native bacterium? To address these questions, we use qPCR to quantify and compare abundances of *Pseudonocardia* in the leaf-cutter ants *Acromyrmex echinator* and *A. octospinosus*. We also perform experimental manipulations of the ant-symbiont association to confirm acquisition of detectable amounts of either *Pseudonocardia* or *Streptomyces* in manipulated ants.

2.3 Methods

2.3.1 qPCR primer design

DNA was extracted from all bacterial strains using an Epicentre MasterPure Complete DNA & RNA Purification Kit (catalogue MC89010, Epicentre technologies, Madison) following manufacturer's protocol. DNA was stored at -20°C until processing.

CLC Workbench (CLC Bio, a QIAGEN Company, Aarhus, Denmark) was used to design primers that target elongation factor tu (EFTu) of *Pseudonocardia* and 16S rRNA of *Streptomyces coelicolor*. Primers were first tested using polymerase chain reaction (PCR) on *Pseudonocardia* sp. CC0420-04 and *Streptomyces Dv14*, *S. di88*, *S. flavogriseus*, *Streptomyces* sp. *igat1*, *S. lividans*, *S. hygroscopicus*, *Streptomyces* sp. *actF*, *Streptosporangium roseum* and *Kitasatospora* sp. *ss2h* (**Table 2.3**). EFTu was amplified for each organisms using the designed primers: EFTuf 5'-GGCTTCGGCGTTCGACAT-3' and EFTu 227r 5'-GTTCTTCACGTAGTCGGCG-3'. As a control, the 16S rRNA gene was amplified for all organisms using universal bacterial primers 27f and 1492r. Reactions included 1 µl forward primer, 1 µl reverse primer, 1µ template DNA (50-150 ng DNA), 12 µl EconoTaq® PLUS Green Master Mix (Lucigen Corporation, Madison,WI) , and 5 µl nuclease free water. PCR was performed with the following parameters for EFTu primers: 5 minutes at 94°C; 35 cycles of: 45 seconds at 94°C, 50 seconds at 56°C, 2 minutes at 72°C; 10 minutes at 72°C; and 4°C forever. PCR of 16s rRNA was amplified with the following parameters: 5 minutes at 95°C; 35 cycles of: 1 minute at 95°C, 1 minute at 55°C, 2 minutes at 72°C; 7 minutes at 72°C; and 4°C forever.

qPCR was performed at the University of Wisconsin-Madison Gene Expression Center using a Roche LightCycler® 480 Real-Time PCR System. Genes were amplified using the following reaction conditions: 10 µl Roche Lightcycler® 480 SYBR Green I Master

(04707516001), 150 μ M forward primer, 150 μ M reverse primer, 2 μ l template DNA (concentrations between 5.0 ng/ μ l to 100 ng/ μ l), and 5 μ l nuclease free water. Each reaction was run in triplicate. Cycling parameters for each gene amplified varied. A range of annealing temperatures between 56°C and 64°C were tested to determine the annealing temperature with highest amplification efficiency. Primer efficiency was calculated using the ThermoFisher Scientific qPCR Efficiency Calculator. The annealing temperature with the highest primer efficiency was determined and used in subsequent qPCR reactions (**Table 2.1**).

2.3.2 *Ant collection and maintenance*

Colonies of *Acromyrmex* leaf-cutter ants were collected in Gamboa, Panama between 2003 and 2009 (Table 1) and were subsequently maintained in Madison, WI, USA in a temperature-controlled room and fed leaves from *Quercus palustris* or *Acer saccharum* three times a week. Two colonies were used in this experiment: an *Acromyrmex octospinosus* colony (colony code CC031210-22) and an *Acromyrmex echinator* colony (colony code Ae288). *Pseudonocardia* from these colonies was isolated upon arrival in the lab following the methods from Pouslen et al. 2005.

Acromyrmex queens were collected in Costa Rica on the University of Costa Rica campus in May and June of 2014. Ant caste was defined based on location and observed behavior of each worker: foragers were collected outside the fungus garden chamber and were actively cutting or carrying leaf material; garden workers were found inside the fungus garden tending and grooming the fungus. Both foragers and garden workers were all major workers with a head width of approximately 1 mm (Wilson, 1980).

2.3.3 *Experimentally manipulated ants*

Artificial bacterial inoculation was performed by manipulating the critical acquisition window (Marsh et al., 2014). *Acromyrmex* pupae were placed in Petri dish subcolonies containing a wet piece of cotton, a weigh boat with approximately 1 g fungus garden, and 6 worker ants. The pupae was monitored and raised to eclosion and then inoculated with 2 μ l of a solution of bacterial cells within 2 hours of eclosion. Eclosion was monitored under a dissection microscope and was considered complete when the pupal casing was completely removed. The bacterial solution was prepared by taking an agar plug (1 cm diameter) of freshly grown bacterial cells and vortexed in 1 mL of sterilized water for 30 seconds. The ant was then allowed to develop for 2 weeks or until bacterial bloom visibly covered the ant, after which the ant was preserved in 95 percent ethanol for further processing.

2.3.4 *Symbiont-free ants*

Acromyrmex workers were raised to be free of *Pseudonocardia*. One *Acromyrmex* pupa was placed in a Petri dish subcolony containing the following: ~1-5g fungus garden from an *Atta cephalotes* colony (colony *A.c* 3 collected in Gamboa, Panama), 8 *Atta cephalotes* workers, and wet cotton. The *Atta* workers raised the *Acromyrmex* pupa until eclosion. The *Acromyrmex* worker was then removed and placed in its own subcolony containing fungus garden and no other ant worker. The ant was raised until it was 2 weeks old (when bacterial bloom is the highest abundance (Poulsen et al., 2003)) and then preserved in 95 percent ethanol for further processing.

2.3.5 *qPCR from ant exoskeletons*

The ants from different castes and from the artificially inoculated experiment were collected and preserved in 95% ethanol and frozen at -20°C until processing. Workers were

dissected prior to DNA extraction to minimize amplification of bacteria in the thoracic tissue and digestive tract. The head, appendages, and abdomen were systematically removed using a dissecting scope and sterile dissecting scissors and forceps. The propleural plates were removed following Anderson and colleagues 2015. Additionally, the digestive tract was removed by cutting down the right ventral side of the thorax and scraping out digestive and thoracic tissue. DNA was then extracted from the remaining exoskeleton and propleural plates.

The dissected thorax and propleural plates were placed in an impact resistant microcentrifuge tube (USA Scientific 1420-9600) containing one 3 mm steel bead to prevent tube breakage during beadbeating. DNA was subsequently extracted using an Epicentre MasterPure Complete DNA & RNA Purification Kit (catalogue MC89010, Epicentre technologies, Madison) following manufacturer's protocol. DNA was stored at -4° Celsius until processing.

qPCR was performed as described above using both the EFTu specific primers as well as the 16S rRNA primers and EF1 α primers (**Table 2.1**). Serial dilutions of each target organism were also included to calculate a standard curve: *Pseudonocardia* for EFTu, *Streptomyces coelicolor* for 16S rRNA, and extracted ant DNA for EF1 α . Using the slope of the standard curve, final gene concentration was calculated and then normalized by determining the ratio of bacterial gene concentration to EF1 α gene concentration. A repeated measures ANOVA was performed in JMP®, Version 11, SAS Institute Inc., Cary, NC, 1989-2007. Mean EFTu:EF1 α of garden workers and foragers were compared using a Welch's T-test due to unequal variance in the groups.

2.4 Results

2.4.1 qPCR primer specificity and efficiency

Primer set EFTuf and EFTu 227r was developed to amplify the EFTu gene specific to *Pseudonocardia* (**Table 2.1**). Polymerase chain reaction (PCR) using this primer pair successfully yielded EFTu amplicons for *Pseudonocardia* sp. CC0420-04 and did not generate EFTu amplicons for closely related bacteria *Streptomyces* sp. *Dv14*, *Streptomyces* sp. *di88*, *S. flavogriseus*, *Streptomyces* sp. *igat1*, *S. lividans*, *S. hygroscopicus*, or *Streptomyces* sp. *actF* (**Figure 2.1a**). Amplification of the target amplicon was determined by observation of the appropriate size (227 bp for *Pseudonocardia* EFTu gene). For *S. griseus*, the primer set yielded multiple amplicons, all of which corresponded to a size far larger than targeted by the primer pair. This indicates nonspecific binding that would result in multiple t_m peaks in qPCR and be distinguishable from *Pseudonocardia* amplification. Additionally, there is a faint product detected when the primers amplify genes in *Streptosporangium roseum* and *Kitasatospora* sp. *ss2*. However, the amplicon is much larger than the EFTu gene amplified in *Pseudonocardia* and again would be a distinguishable t_m peak in qPCR. As a control, the 16S rRNA gene of these strains did all amplify using universal bacterial primers 27f and 1492r (Lane 1991) (**Figure 2.1b**).

EFTu primer efficiency during qPCR was approximately equivalent for all *Pseudonocardia* strains tested (**Table 2.2**). *Pseudonocardia* from ant colony CC030328-02, isolated from *Mycetarotes parallelus* in Argentina, amplified the EFTu gene with the lowest efficiency at 76.6%, and *Pseudonocardia* from colonies CC011120-05 (*Apterostigma dentigerum* in Panama) and SES030406-01 (*Acromyrmex* sp. in Argentina) both displayed the

highest amplification efficiency of 80.2% (**Table 2.2**). The *Pseudonocardia* tested are from a wide range of ant host lineages and geographic locations (clade refers to *Pseudonocardia* phylogenetic clade in Cafaro et al. 2011). The EFTu gene of all strains amplified with similar primer efficiency using this primer set.

2.4.2 Variation in abundance of *Pseudonocardia* between age-based ant castes

To examine the dynamics of *Pseudonocardia* abundance between different ant castes, we amplified the EFTu gene from workers of different castes based on age (**Figure 2.2a**) in *Acromyrmex echinator* and *Acromyrmex octospinosus*. *Pseudonocardia* EFTu was normalized to the amount of the ant gene, EF1 α (**Table 2.1**). Garden workers of *A. echinator* maintain slightly greater abundance of *Pseudonocardia* than *A. echinator* foragers, an average of 0.0065 ng EFTu/ng EF1 α and .001421 ng EFTu/ng EF1 α respectively (p=0.0682). Garden workers of *A. octospinosus* (average of 0.0135 ng EFTu/ng EF1 α) had a significantly greater abundance of *Pseudonocardia* compare to *A. octospinosus* foragers (average of 0.0041 ng EFTu/ng EF1 α) (p=0.0093) (**Figure 2.2b**). *Acromyrmex octospinosus* garden workers also had significantly more *Pseudonocardia* compared to *A. echinator* foragers (p=0.0034). Foragers of both species had similar abundance of the defensive symbiont (p=0.8588). A significant abundance of *Pseudonocardia* was detected in *Acromyrmex* gynes (0.006208 ng EFTu/ng EF1 α) (**Figure 2.2b**).

2.4.3 No detection of *Streptomyces coelicolor* in experimentally manipulated symbiont acquisition

To test acquisition of potential defensive symbionts, *A. octospinosus* newly eclosed ant workers were experimentally exposed to either *Pseudonocardia* - their native symbiont,

Streptomyces coelicolor – a nonnative bacterium, or no bacteria. qPCR was used to determine which bacterium was acquired in detectable amounts on the exoskeleton. Callow worker ants that were not exposed to either *Pseudonocardia* or *Streptomyces* did not acquire any detectable amounts of either bacteria (**Figure 2.3**). *Pseudonocardia* was detected by qPCR on ants that were exposed to their native *Pseudonocardia*, ranging in abundance from 0.02056 ng EFTu/ng EF1 α to 0.02706 ng EFTu/ng EF1 α . Further, no *Streptomyces* was detected on these ants (n=3) (**Figure 2.3**). The group of ants, n=3, exposed to *Streptomyces coelicolor* did not acquire *Streptomyces* as detectable by *Streptomyces*-specific primers. One worker in this group acquired visible bacteria (0.0119 ng EFTu/ng EF1 α). However this bacterium was amplified by *Pseudonocardia*-specific primers and not *Streptomyces* primers indicating that this ant acquired its native *Pseudonocardia* and not the *Streptomyces* it was exposed to (**Figure 2.3**).

2.5 Discussion

Quantifying bacterial symbionts can be challenging and qPCR is a useful approach to quantify bacterial abundances from environmental samples. qPCR, compared to other sequence based techniques, allows for amplification of small amounts of starting DNA. Furthermore, primers can be optimized for high specificity that target specific organisms within mixed communities. Here, we use qPCR to characterize temporal dynamics between a leaf-cutter ant and its bacterial mutualist. We explore differences in *Pseudonocardia* abundance between three ant castes (determined by ant age) and ask if leaf-cutter ants can acquire detectable abundances of a non-*Pseudonocardia* mutualist.

We observe differences in the relative abundances of *Pseudonocardia* between castes of garden tending workers versus foragers. *Acromyrmex octospinosus* and *A. echinator* garden

workers had a significantly higher average abundance of *Pseudonocardia* compared to foragers. This is consistent with the visual observations of Poulsen et al. 2003. Foragers work outside the colony and primarily cut leaf material while garden workers are ants found within the fungus garden and are engaged in care of the cultivar. All ant workers in this experiment were major workers so the shift in role is due to the age of the worker, not the size of the ant (Wilson, 1980). Young garden workers maintaining greater abundance of *Pseudonocardia* is congruent with the primary role of *Pseudonocardia* being to help defend the fungus garden from pathogens. As workers age and move to tasks outside the fungus garden and colony, they may stop providing nutrients to *Pseudonocardia* as it is no longer as necessary for colony health (Poulsen et al., 2003; Steffan et al., 2015). Thus the association between the ants and their defensive symbionts appears integrated into the social structure of the colony.

We found that *Acromyrmex* gynes maintain an abundance of *Pseudonocardia*. Although gynes reside within the fungus garden, they do not engage in garden tending, so may have a lower abundance of the defensive symbiont as they only need to transmit the bacterium to the initial workers she lays. (Cameron R Currie & Scott, 1999; Marsh et al., 2014). Subsequent transmission occurs worker to worker when the colony is established. All gynes used in this experiment were collected on the nuptial flight and were in the process of founding their colonies. These results support the important role gynes play in the vertically transmission of *Pseudonocardia*, just as they carry inoculum of their fungal mutualists, gynes transmit *Pseudonocardia* from their parent colony to founding nest.

The *Streptomyces* strain tested here was unable to colonize on the ant exoskeleton. *Streptomyces coelicolor* is a common soil bacterium known for antibiotic production and is likely a good defensive mutualist due to its antibiotic potential (Bentley et al., 2002). However, it

appears that the bacterium is unable to utilize the resources available on the ant exoskeleton or are inhibited by the glandular secretions produced by ants associated with the defensive symbiont (Cameron R Currie, Poulsen, Mendenhall, Boomsma, & Billen, 2006; Li et al., 2018). One ant in the *S. coelicolor* treatment group did acquire visible bacteria on its exoskeleton, however this was not amplified using *S. coelicolor*-specific primers. The *Pseudonocardia* EFTu gene was amplified indicating that this ant acquired its native symbiont. The *Pseudonocardia* likely came from the ant workers raising the pupae—each subcolony consisted of several minor *Acromyrmex* workers to assist the developing pupae (Marsh et al., 2014). A symbiont recruitment hypothesis has been proposed suggesting fungus-growing ants acquire Actinobacteria from the surrounding soil as their symbiont, rather than transmission through strict vertical inheritance (Mueller, 2012). Our results suggest this appears unlikely, although experiments testing if other antibiotic-producing bacteria can colonize the ant exoskeleton may help test this hypothesis.

The technique described here can be used to further characterize the relationship between leaf-cutter ants and their defensive mutualists. Questions of partner choice and mutualist maintenance are of particular importance and interest in the field of symbiosis. qPCR can be used in future experiments to quantify the abundance differences in host-symbiont manipulations. The association between *Pseudonocardia* and the ants is temporally dynamic and perhaps strain specific.

2.6 Acknowledgments

We would like to thank the UW Sequencing Center for assistance and use of the Roche Lightcycler®. We acknowledge the University of Costa Rica and Ministerio del Ambiente y Energia for collection and export permits. We are also grateful to the Smithsonian Tropical Research Institute for logistical support and facilitation of export permits in Panama. We thank for L. Khadempour for assistance in qPCR primer design and J. Bratburd for comments on the final manuscript.

2.7 Tables and Figures

Table 2.1 Primers used in this study and their specifications. One primer set targets the EFTu gene of *Pseudonocardia* sp., two primers target the 16S rRNA gene of *Streptomyces*, and one primer set targets the ant gene, EF1 α

Target organism	Primer name	Primer sequence	Annealing temperature (°C)	Amplicon length (bp)
<i>Pseudonocardia</i> (modified from Poulsen et al. 2005)	EFTuf EFTu 227r	5'-GGCTTCGGCGTTCGACAT-3' 5'-GTTCTTCACGTAGTCGGCG-3'	60	227
<i>Streptomyces coelicolor</i>	Coelf3 Strep 261r	5'-CGCAGGCATCTGCGAGGTTTCG-3' 5'-GTCTGGGCCGTGTCTCAGTC-3'	55	120
Ant (Anderson et al. 2012)	EF1 α f EF1 α r	5'-ACGGAAGCTCTGCCCCGGTGA-3' 5'-TGGCAGTCAAGCACTGGCGT-3'	62	

Table 2.2 *Pseudonocardia* strains used to calculate qPCR primer efficiency of primers EFTuf and EFTu227r. Colony code, ant host species, collection location of each strain as reported by Cafaro et al. 2011. Ant host species number and clade corresponds to data and phylogenetic clades of *Pseudonocardia* in Cafaro et al. 2011.

Colony Code	Ant host species	Collection location	Clade	Primer efficiency
CC030404-04	<i>Trachymyrmex zeteki</i> 117	Argentina	III	79.55%
CC030328-02	<i>Mycetarotes parallelus</i> 081	Argentina	III	76.60%
CC030328-06	<i>Mycetarotes parallelus</i> 082	Argentina	III	80.00%
CC011213-24	<i>Apterostigma dentigerum</i> 048	Panama	IV	77.95%
CC011120-05	<i>Apterostigma dentigerum</i> 052	Panama	IV	80.20%
CC010320-02	<i>Acromyrmex</i> sp. 035	Panama	VI	79.51%
CC030402-02	<i>Acromyrmex</i> sp. 040	Argentina	VI	78.05%
ST040116-01	<i>Acromyrmex octospinosus</i> 019	Panama	VI	77.90%
CC030406-01	<i>Acromyrmex echinator</i> 002	Panama	VI	78.70%
SES030406-01	<i>Acromyrmex</i> sp. 042	Argentina	VI	80.20%
UGM030402-04	<i>Acromyrmex hispidus fallax</i> 013	Argentina	VI	79.50%

Table 2.3 Bacterial strain abbreviation used in Figure 2.1 and associated full isolate name and origin. NCBI accession number included if applicable.

Abbreviation (this study)	Full Isolate Name	Source	Accession number
S. Dv14	<i>Streptomyces</i> sp Dv14	Currie lab	PRJNA319210
S. di88	<i>Streptomyces</i> sp di88	Currie lab	
S. flavogriseus	<i>Streptomyces flavogriseus</i> ATCC33331	NCBI	PRJNA40839
S. griseus	<i>Streptomyces griseus</i> NBRC13350	NCBI	PRJNA58983
S. l gat1	<i>Streptomyces</i> sp igat1	Currie lab	
S. lividans	<i>Streptomyces lividans</i> TK24	NCBI	PRJNA55825
S. actF	<i>Streptomyces</i> sp SA3-ActF	Currie lab	PRJNA61901
S. hygrosopicus	<i>Streptomyces hygrosopicus</i> ATCC53653	NCBI	PRJNA33605
Streptosporangium roseum	<i>Streptosporangium roseum</i>	Currie lab	
Kitasatospora ss2h	<i>Kitasatospora</i> sp. ss2h	Currie lab	
P. CC0420-04	<i>Pseudonocardia</i> sp. CC0420-04	Currie lab	

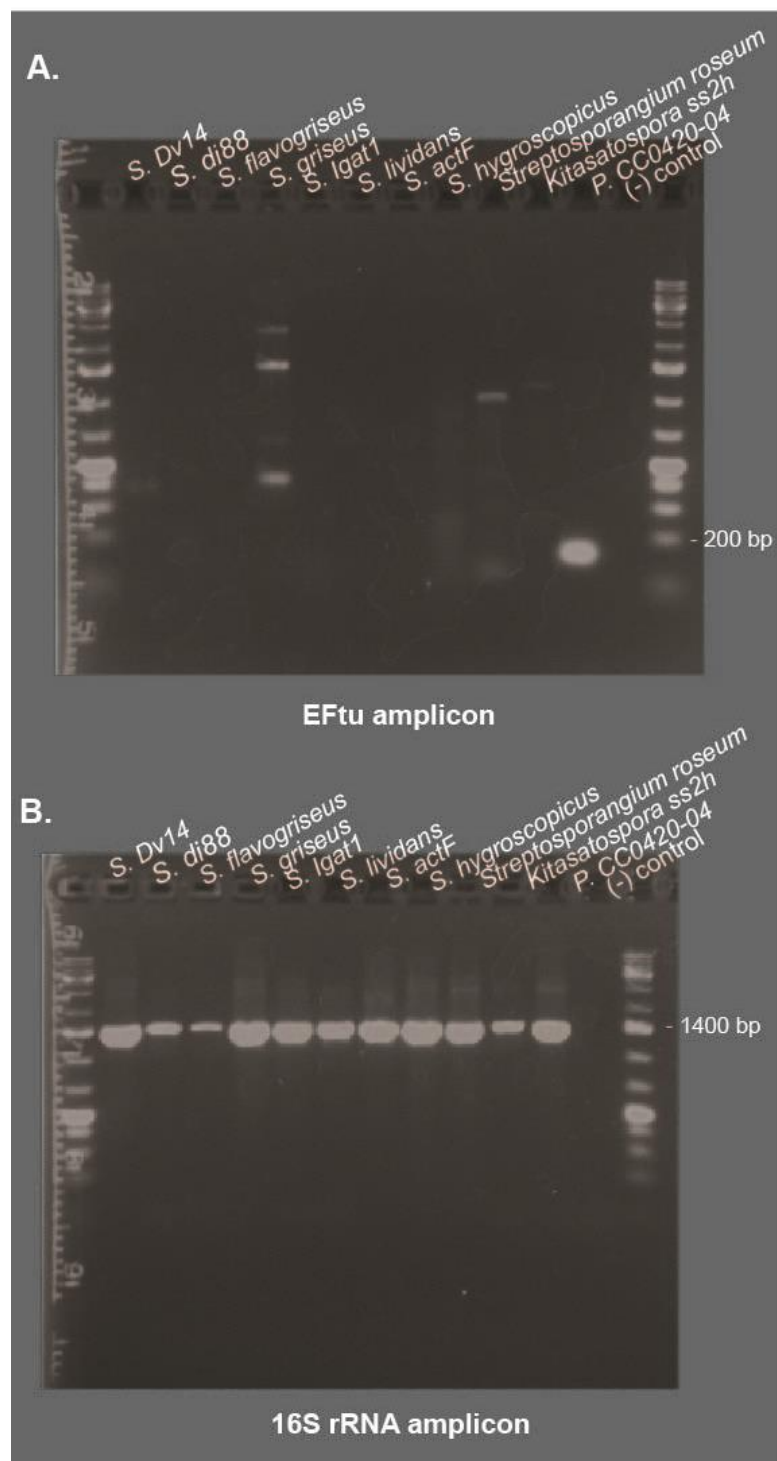


Figure 2.1 A) Agarose gel picture of PCR product of amplification of the EFTu gene using primers EFTuf and EFTu 227r. B) Agarose gel picture of PCR product of amplification of the 16S rRNA gene using universal bacterial primers 27f and 1492r. Strain abbreviations and information found in Table 2.3.

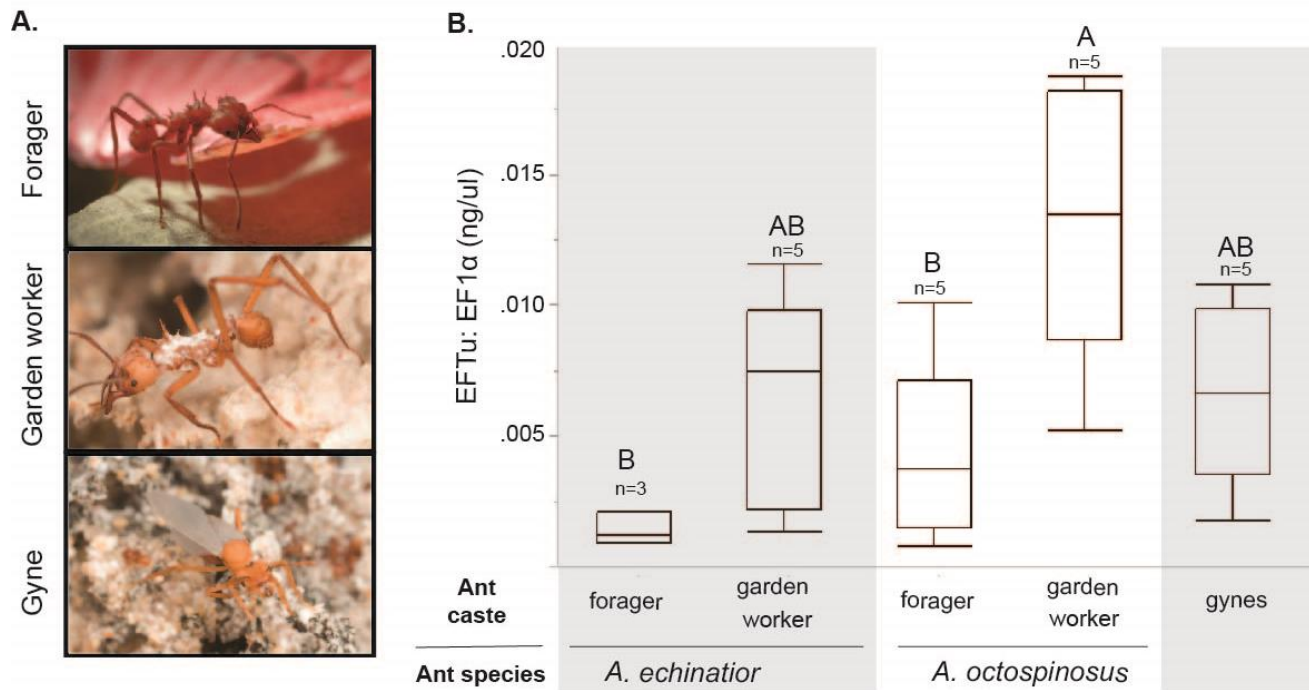


Figure 2.2 A) Photos depicting the three ant castes used in this study. Foragers are located outside the colony and primarily cut leaves; garden workers are found within the fungus garden. Photos courtesy of Don Parsons. B) Box plot of the average concentration of *Pseudonocardia* (ng EFTu:ng EF1 α) for different ant castes (foragers, workers, and gynes) of both *A. echinator* and *A. octospinosus* ants. Connecting letters denote treatments that are significantly the same. The number of ant replicates is indicated above the box plot.

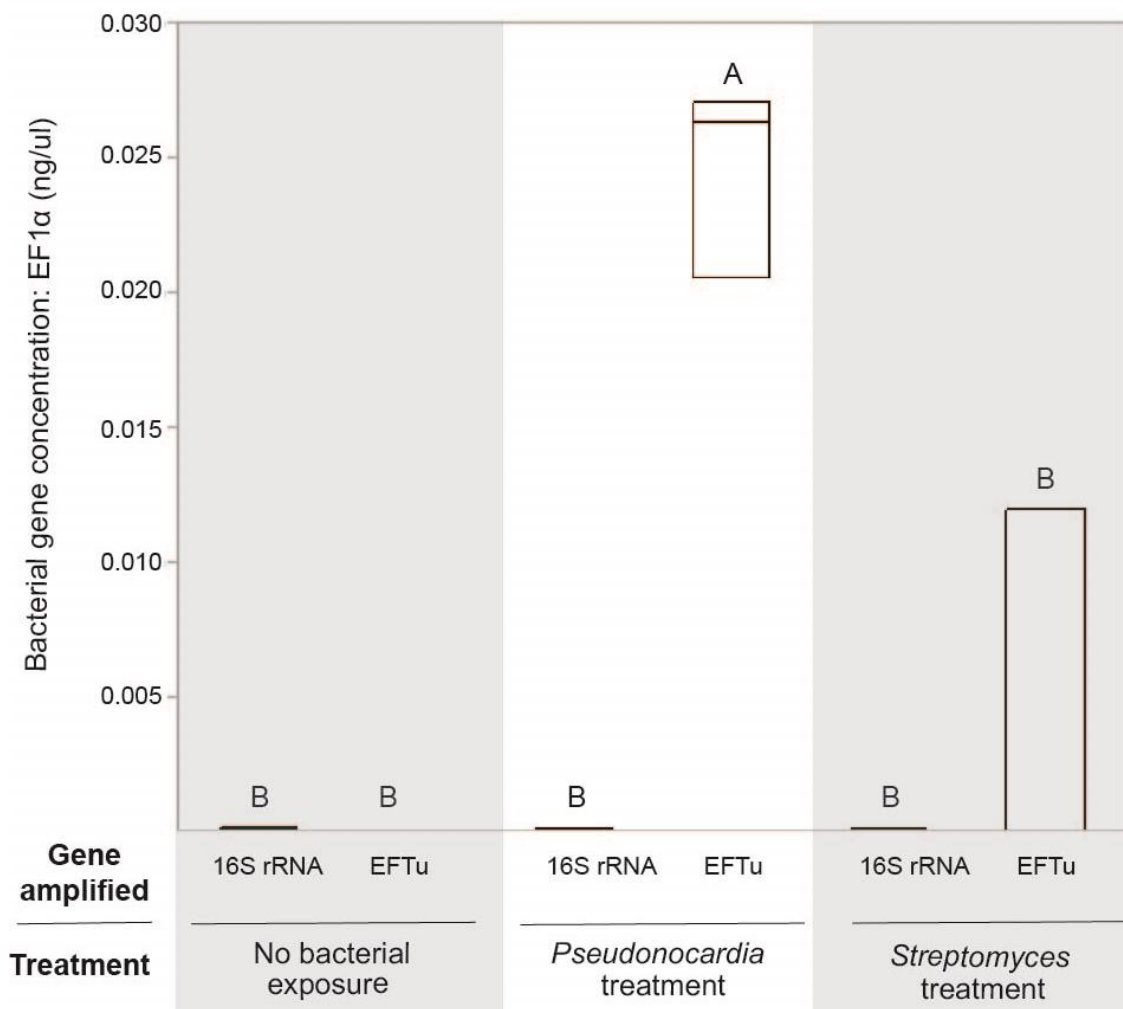


Figure 2.3 Box plot of the average concentration of *Pseudonocardia* (ng EFTu:ng EF1 α) or *Streptomyces coelicor* (ng 16S rRNA: ng EF1 α) for different *A. octospinosus* workers. Ants were exposed to different treatments—no bacterial exposure, *Pseudonocardia*, or *S. coelicor*—and qPCR was used to determine bacterial acquisition. Connecting letters denote treatments that not significantly different. N=3 for all treatments.

2.8 References

- Bentley, S. D., Chater, K. F., Cerdeño-Tárraga, A.-M., Challis, G. L., Thomson, N. R., James, K. D., ... Hopwood, D. A. (2002). Complete genome sequence of the model actinomycete *Streptomyces coelicolor* A3(2). *Nature*, *417*(6885), 141–7. <https://doi.org/10.1038/417141a>
- Camargo, R. S., Forti, L. C., Lopes, J. F. S., Andrade, A. P. P., & Ottati, A. L. T. (2007). Age polyethism in the leaf-cutting ant *Acromyrmex subterraneus brunneus* Forel, 1911 (Hym., Formicidae). *Journal of Applied Entomology*, *131*(2), 139–145. <https://doi.org/10.1111/j.1439-0418.2006.01129.x>
- Carr, G., Derbyshire, E. R., Caldera, E., Currie, C. R., & Clardy, J. (2012). Antibiotic and antimalarial quinones from fungus-growing ant-associated *Pseudonocardia* sp. *Journal of Natural Products*, *75*(10), 1806–9. <https://doi.org/10.1021/np300380t>
- Clay, K. (2014). Defensive symbiosis: a microbial perspective. *Functional Ecology*, *28*, 293–298. <https://doi.org/10.1111/1365-2435.12258>
- Currie, C. R., Bot, A. N. M., & Boomsma, J. J. (2003). Experimental evidence of a tripartite mutualism : bacteria protect ant fungus gardens from specialized parasites. *Oikos*, *1*(July 2002), 91–102.
- Currie, C. R., Poulsen, M., Mendenhall, J., Boomsma, J. J., & Billen, J. (2006). Coevolved crypts and exocrine glands support mutualistic bacteria in fungus-growing ants. *Science (New York, N.Y.)*, *311*(5757), 81–3. <https://doi.org/10.1126/science.1119744>
- Currie, C. R., & Scott, J. A. (1999). Fungus-growing ants use antibiotic-producing bacteria to control garden parasites, *398*(April), 701–705.
- Hölldobler, B., & Wilson, E. O. (1990). *The Ants*. Harvard University Press. Retrieved from <https://books.google.com/books?hl=en&lr=&id=R-7TaridBX0C&pgis=1>
- Kaltenpoth, M., & Engl, T. (2014). Defensive microbial symbionts in Hymenoptera. *Functional Ecology*, *28*(2), 315–327. <https://doi.org/10.1111/1365-2435.12089>
- Li, H., Sosa-Calvo, J., Horn, H. A., Pupo, M. T., Clardy, J., Rabeling, C., ... Currie, C. R. (2018). Convergent evolution of complex structures for ant–bacterial defensive symbiosis in fungus-farming ants. *Proceedings of the National Academy of Sciences*, 201809332. <https://doi.org/10.1073/pnas.1809332115>
- Marsh, S. E., Poulsen, M., Pinto-Tomás, A., & Currie, C. R. (2014). Interaction between workers during a short time window is required for bacterial symbiont transmission in *Acromyrmex* leaf-cutting ants. *PloS One*, *9*(7), e103269. <https://doi.org/10.1371/journal.pone.0103269>
- Moran, N. A. (2007). Symbiosis as an adaptive process and source of phenotypic complexity.

Proceedings of the National Academy of Sciences of the United States of America, 104 Suppl 1(suppl 1), 8627–33. <https://doi.org/10.1073/pnas.0611659104>

- Mueller, U. G. (2012). Symbiont recruitment versus ant-symbiont co-evolution in the attine ant-microbe symbiosis. *Current Opinion in Microbiology*, 15(3), 269–277. <https://doi.org/10.1016/J.MIB.2012.03.001>
- Oh, D.-C., Poulsen, M., Currie, C. R., & Clardy, J. (2009). Dentigerumycin: a bacterial mediator of an ant-fungus symbiosis. *Nature Chemical Biology*, 5(6), 391–3. <https://doi.org/10.1038/nchembio.159>
- Oliver, K. M., Russell, J. A., Moran, N. A., & Hunter, M. S. (2003). Facultative bacterial symbionts in aphids confer resistance to parasitic wasps. *Proceedings of the National Academy of Sciences of the United States of America*, 100(4), 1803–7. <https://doi.org/10.1073/pnas.0335320100>
- Poulsen, M., Bot, a. N. M., Currie, C. R., Nielsen, M. G., & Boomsma, J. J. (2003). Within-colony transmission and the cost of a mutualistic bacterium in the leaf-cutting ant *Acromyrmex octospinosus*. *Functional Ecology*, 17(2), 260–269. <https://doi.org/10.1046/j.1365-2435.2003.00726.x>
- Steffan, S. A., Chikaraishi, Y., Currie, C. R., Horn, H., Gaines-Day, H. R., Pauli, J. N., ... Ohkouchi, N. (2015). Microbes are trophic analogs of animals. *Proceedings of the National Academy of Sciences*, 112(49), 201508782. <https://doi.org/10.1073/pnas.1508782112>
- Van Arnam, E. B., Ruzzini, A. C., Sit, C. S., Horn, H., Pinto-Tomás, A. A., Currie, C. R., & Clardy, J. (2016). Selvamicin, an atypical antifungal polyene from two alternative genomic contexts. *Proceedings of the National Academy of Sciences of the United States of America*, 113(46), 12940–12945. <https://doi.org/10.1073/pnas.1613285113>
- Wilson, E. O. (1980). Caste and division of labor in leaf-cutter ants (Hymenoptera: Formicidae: Atta). *Behavioral Ecology and Sociobiology*, 7(2), 157–165. <https://doi.org/10.1007/BF00299521>

Chapter 3

Imaging with Mass Spectrometry of Bacteria on the Exoskeleton of Fungus-Growing Ants

Authors: Erin Gemperline,* Heidi A. Horn,* Kellen DeLaney, Cameron R. Currie, and Lingjun Li

Reprinted with permission from Gemperline, E., Horn, H. A., DeLaney, K., Currie, C. R., & Li, L. (2017). Imaging with Mass Spectrometry of Bacteria on the Exoskeleton of Fungus-Growing Ants. *ACS chemical biology*, 12(8), 1980-1985. Copyright 2017 American Chemical Society. <https://pubs.acs.org/doi/abs/10.1021/acscchembio.7b00038>

Author contributions: (*authors contributed equally) Conceived of project (HAH, EG, CRC), designed and carried out experiment (HAH), performed mass spectrometry (EG, KD), performed data analysis (HAH, EG), and wrote the manuscript (HAH, EG, KD, LL, CRC).

3.1 Abstract

Mass spectrometry imaging is a powerful analytical technique for detecting and determining spatial distributions of molecules within a sample. Typically, mass spectrometry imaging is limited to the analysis of thin tissue sections taken from the middle of a sample. In this work, we present a mass spectrometry imaging method for the detection of compounds produced by bacteria on the outside surface of ant exoskeletons in response to pathogen exposure. Fungus-growing ants have a specialized mutualism with *Pseudonocardia*, a bacterium that lives on the ants' exoskeletons and helps protect their fungal garden food source from harmful pathogens. The developed method allows for visualization of bacterial-derived compounds on the ant exoskeleton. This method demonstrates the capability to detect compounds that are specifically localized to the bacterial patch on ant exoskeletons, shows good reproducibility across individual ants, and achieves accurate mass measurements within 5 ppm error when using a high-resolution, accurate-mass mass spectrometer.

3.2 Introduction

Microbial organisms produce many secondary metabolite compounds that have been extensively studied as potential drug leads in natural product research. Much of this research examines the production of these small molecules when microbes are grown in isolation. These compounds may act in chemical communication between microbes (Davies, 2006; Romero, Traxler, López, & Kolter, 2011; Yim, Wang, & Davies, 2006); as such, recent work examined pairwise interactions between microbes and detected induction of differential compounds (Seyedsayamdost, 2014; Seyedsayamdost, Traxler, Clardy, & Kolter, 2012; Traxler, Seyedsayamdost, Clardy, & Kolter, 2012; Traxler, Watrous, Alexandrov, Dorrestein, & Kolter, 2013). While this is an effective tool, particularly for natural product discovery, it still overlooks the diversity and complexity of species interactions that occur within a microbial niche. Improved approaches to examine small molecules produced by microbes *in situ* will greatly benefit microbial ecology and have great implications for natural product research. Here, we developed a method using mass spectrometry imaging to examine *in situ* chemical interactions in the leaf-cutter ant symbiosis, an established, multipartite symbiosis.

Leaf-cutter ants participate in a multispecies symbiosis. These ants provide leaf substrate to a fungus that they cultivate as their sole food source (Chapela, Rehner, Schultz, & Mueller, 1994; Weber, 1966). This association is an obligate mutualism and the ants are under strong selective pressure to protect their food source. To do this, the ants maintain a mutualism with Actinobacteria in the genus *Pseudonocardia*. The *Pseudonocardia* symbionts live on the ants' propleural plates (the plate on the ventral side of the ant thorax directly posterior to the head, see photograph in **Figure 3.1**) and provide antimicrobial protection against pathogens, including the system-specific pathogen *Escovopsis* (C. R. Currie, Mueller, & Malloch, 1999; C R Currie,

Bot, & Boomsma, 2003; Cameron R Currie & Scott, 1999; Poulsen et al., 2010). The quadripartite symbiosis between the ant host, the fungal cultivar, antibiotic-producing *Pseudonocardia*, and garden pathogen *Escovopsis* is particularly well-suited for ecological studies as each player can be isolated from the system for individual study and the intact association can be manipulated *in vivo*. Developing an approach to study secondary metabolites *in vivo* could reveal functionally and ecologically relevant chemical interactions between microbial species as well as unlock a vast array of natural products.

In this study, matrix-assisted laser desorption/ionization (MALDI)-mass spectrometry imaging (MSI) was used to examine *in situ* species interactions between *Pseudonocardia* and *Escovopsis*. MSI has rapidly emerged as a powerful analytical technique for understanding the spatial distributions of molecules within a variety of biological samples (Baig et al., 2015; Bhandari et al., 2015; Caprioli, 2015; Dunham et al., 2016; Khalil, Römpf, Pretzel, Becker, & Spengler, 2015; Van de Plas, Yang, Spraggins, & Caprioli, 2015; Yang et al., 2012), and more recently, scientists have taken advantage of the capabilities of MSI and applied this technique toward the discovery of new natural products (Bouslimani, Sanchez, Garg, & Dorrestein, 2014; Lane et al., 2009; Nyadong et al., 2009). Although LAESI-MSI techniques have been used to characterize compounds on nonflat sample surfaces (Bartels et al., 2017), typically MALDI-MSI is limited to the analysis of thin tissue sections or bacterial colonies in culture. However, this study aimed to analyze metabolites produced by *Pseudonocardia* in its native ecological niche on the organism's outer surface. There have been few reports of studies using ultraviolet (UV)-LDI-MS and MALDI-MSI to analyze other insects, such as flies (Vrkoslav, Muck, Cvačka, & Svatoš, 2010; Yew et al., 2009). A previous study used MALDI-MSI to examine whole ants but did not analyze bacteria specifically localized to the ants' propleural plates (Schoenian et al.,

2011). Thus, a unique sample preparation method was developed to analyze chemical compounds produced by bacteria localized to the ant propleural plate in an accurate and reproducible manner *via* MALDI-MSI. The uniqueness in the sample preparation comes from using modified glass slides in which three-dimensional (3D) samples (ants) can be inlaid so that the outer surface of the organism can be analyzed, in comparison to traditional MALDI-MSI sample preparation in which thin sections are sliced from the middle of a 3D sample and the inside of the organism is analyzed. We take advantage of the high-resolution, accurate-mass capabilities of a MALDI-LTQ Orbitrap mass spectrometer which maintains <5 ppm mass accuracy even with slight differences in the sample height, unlike the more common MALDI-time-of-flight (TOF) systems. This approach will increase our understanding of this host/microbe symbiosis and has the capability to provide ecological insights into chemical interactions between microbial species in a unique biological system (Horn et al. in review).

3.3 Results

3.3.1 MSI Method

We developed a method for MSI of *Pseudonocardia* on the surface of the ants' propleural plates, as described in the Materials and Methods section and shown in **Figure 3.1**. A photograph of the ants and glass slides coated with DHB matrix is shown in **Figure A3.1**. As proof-of-principle, ants were raised without *Pseudonocardia* and ProteoMass MALDI-MS calibration mix (Sigma-Aldrich) was spiked onto ant propleural plates laid into the modified glass slide in different ways (see Supporting Information for more details) and directly onto the glass slide. Images were obtained for six calibration standards spiked onto ant propleural plates,

and the glass slide in the mass range of 300–1800 m/z and the mass spectra collected for each imaged area were averaged to report the average m/z value detected of each standard. **Table A3.1** details the calibrant m/z values measured and the calculated mass errors. The method displayed a Δ ppm mass error of 2.1 ± 0.1 ppm for the calibrants spiked onto the ants, which is comparable to the 1.9 Δ ppm mass error observed for the calibration mix that was measured directly from the glass slide. The absolute ppm error measurements varied but could be minimized with instrument calibration. These results suggest that any nonplanarity of the ant samples does not greatly affect the mass accuracy of the experiment, highlighting the unique advantage of using an Orbitrap-based mass analyzer compared to a time-of-flight mass analyzer, where even the difference of 100 μm in sample height can change the detected mass by up to 0.1 Da. We further examined the necessity of the groove in the glass slide by spiking a metabolite standard of ergothioneine (m/z 230.096) on ant propleural plates. The spiked propleural plates were then laid in the groove of the modified slides or laid onto standard glass slides and secured with double-sided tape. The ant thoraxes were either secured with a lateral tilt (tilted to the right or left), a longitudinal tilt (tilted up or down), or left planar. The results, shown in **Figure S3.2**, show that ergothioneine was not able to be detected on several of the ant thoraxes placed on the standard glass slides and tilted either laterally or longitudinally, likely due to being out of the plane of the MALDI laser. This issue was not observed when the ant thoraxes were placed in the groove of the slide. Placing the ant thoraxes in the groove of the glass slide minimized the impact of any tilt of the sample, or nonplanarity, when compared to ant thoraxes placed on standard glass slides. The mass accuracy was not affected by the tilt of the ants. Furthermore, laying the ants into the groove of the glass slide keeps the samples in a sturdy, fixed position for the entire

analysis time which ranged from 2 to 7 days depending on the number of ants being imaged and the spatial resolution selected.

Three ants from three different subcolonies (nine ants in total) were imaged over the course of several months and the representative images are displayed in **Figure 3.2**. The images show that many of the same m/z values could be detected on multiple biological replicates. Furthermore, multiple groups of ants were analyzed at different times, and still many of the same m/z values were detected across individual and groups of biological replicates, thus demonstrating overall strong reproducibility of the method. Some biological variation, mainly in the spatial distributions of the detected compounds, was expectedly observed as the localization of the bacteria varies slightly from ant to ant.

3.3.2 MSI of Ant/*Pseudonocardia*/*Escovopsis* Interactions

Representative MS images of compounds produced by *Pseudonocardia* on the ant propleural plate are displayed in **Figure 3.3**, showing that this method can clearly and confidently distinguish bacterial-derived compounds (localized to the propleural plate) from ant or environment derived compounds (no specific localizations). These data show that a lack of *Pseudonocardia* results in fewer detectable compounds on the ant propleural plate. Furthermore, many compounds were observed to be produced only in response to *Escovopsis* exposure (such as m/z 390.098, 490.084, 533.166, and 620.009 shown in **Figure 3.3**). The results showing that *Pseudonocardia* only synthesizes these compounds in response to pathogen exposure led to the hypothesis that these molecules could be natural products or drug leads with antimicrobial properties. Compound identifications were attempted by searching collected MS/MS data via several metabolomics and natural products databases. The preliminary database searches either resulted in tens of potential identifications or no search results for a given mass, which could

indicate the detection of unique compounds. Future work will focus on additional compound elucidation and identifications. The MSI data have been made publically available on METASPACE (<http://annotate.metaspaces2020.eu>) (Palmer et al., 2017).

Interestingly, the compound detected at m/z 230.096 (shown in **Figure 3.3**) is only observed when *Pseudonocardia* is present on the ant propleural plates. This compound was identified as ergothioneine. Ergothioneine is a unique compound that is only known to be specifically synthesized by certain species of Cyanobacteria, Mycobacteria, Actinobacteria, and certain fungi such as *Ascomycetes* and *Basidiomycetes* (Cheah & Halliwell, 2012; Genghof, 1970). Currently, the physiological role of ergothioneine is unknown; however, *in vitro* studies have shown antioxidant properties of this compound (Cheah & Halliwell, 2012). The ergothioneine identification was confirmed by comparing the sample to a purchased ergothioneine standard (Sigma-Aldrich). The retention time was identical to that of the ergothioneine standard, and the MS/MS spectra were also nearly identical. Differences in the MS/MS spectra are due to co-isolation of a similar-mass metabolite because of a wide isolation width (3 Da). A mirror plot of the MS/MS spectra for the experimental sample and the ergothioneine standard is shown in **Figure 3.4**. These results indicate that ergothioneine is indeed being produced by *Pseudonocardia* and not by the fungal pathogen, *Escovopsis*, because this compound is detected when *Pseudonocardia* is present (regardless of *Escovopsis* exposure) but is absent when the ants without *Pseudonocardia* were exposed to *Escovopsis*. A followup analysis of the *Pseudonocardia* genome showed that *Pseudonocardia* do indeed possess the genes required for ergothioneine synthesis.

From a technological standpoint, the work presented here demonstrates a method for MALDI-MSI of metabolites from a host/microbe system *in situ*. It was essential to use MSI for

this study in order to be truly confident that the detected compounds were indeed being produced by *Pseudonocardia* and not from the ants or the environment. This protocol can be used as a tool for chemical biologists and adapted in the future for MALDI-MS imaging of the surface of other organisms with three-dimensional shapes, rather than thin tissue sections, in order to tackle difficult biological questions. We demonstrated the usefulness of this protocol by studying the ant/*Pseudonocardia* symbiosis. The approach developed here can provide important insights into metabolites that mediate the microbial interactions within the fungus-growing ant symbiosis and provide insights into the expression of cryptic secondary metabolite clusters.

3.4 Methods

3.4.1 Sample Preparation for MALDI-MSI

Prior to sample preparation, grooves were cut into glass slides, and double-sided tape was applied to the back of the slide. The double-sided tape allows for a flexible backing in which ants of different sizes can still be positioned so that their propleural plate is parallel to the top of the slide.

Ants were randomly assigned to one of three treatments: *Pseudonocardia*/pathogen treatment, no-*Pseudonocardia*/pathogen treatment, or *Pseudonocardia*/control treatment (see Supporting Information for ant colony preparation and pathogen treatment details). The ants were dissected by removing the head, abdomen, and appendages from the thorax with a razor blade. The thorax was placed in the groove of the slide with additional tape over the bottom portion of the thorax (posterior to the *Pseudonocardia* patch on the propleural plate) to secure into place. Ant thoraxes were then inlaid into the groove of the slide with the propleural plate

facing outward and parallel with the top of the slide. Additional dissection methods were evaluated (see Supporting Information).

A matrix (40 mg mL⁻¹ DHB in 50:50 water/methanol) was applied to the ants using a TM-Sprayer (HTX Technologies, LLC). DHB was purchased from Sigma-Aldrich. The TM-Sprayer method for applying DHB to the ants was as follows: 80 °C, 0.2 mL/min flow rate, eight passes—rotate/offset, 3 mm spacing, 30 s dry time between passes, velocity of 950 mm/min.

3.4.2 MALDI-Orbitrap MSI

A MALDI- LTQ Orbitrap mass spec- trometer (Thermo Scientific) equipped with an N₂ laser (spot diameter of 75 µm) was used in positive ion mode for MSI. Multiple ants of each treatment type ($n = 3-4$) were imaged with a step size (pixel size) of 75 µm using a mass range of m/z 100–1700 and a mass resolution of 60 000. The region to be imaged and the raster step size were controlled using the LTQ software (Thermo Scientific) and the instrument methods were created using Xcalibur (Thermo Scientific). MALDI-MSI data were processed using MSiReader (Robichaud, Garrard, Barry, & Muddiman, 2013) (see Supporting Information for more information).

LC-ESI-MS and MS/MS. Metabolites were extracted from the propleural plates of ants that were and were not exposed to *Escovopsis* (see Supporting Information for additional extraction procedure details). MS and MS/MS data of the ant extracts were acquired on a quadrupole-orbital trapping instrument (Q-Exactive Orbitrap, Thermo Scientific) equipped with an ESI source operated in positive ion mode. The MS scan range was m/z 135–1300. The MS/MS scan range was adjusted depending on the parent mass and high-energy collisional dissociation (HCD) was used for fragmentation with collision energy of 35 eV and an isolation

width of 3 Da. See the Supporting Information for LC parameters and links to publically available LC-MS and LC-MS/MS data sets.

3.4.3 Metabolite Identifications

Online databases were used to search the accurate mass and MS/MS data for potential metabolite identifications. Ergothioneine was identified by searching the accurate mass and MS/MS data against reference MS/MS spectra in the METLIN database (Smith et al., 2005) and then comparing the LC retention time and MS/MS spectra to a purchased ergothioneine standard.

3.5 Acknowledgments

The authors would like to thank T. Drier in the UW-Madison Chemistry Glass Shop for creating the custom glass slides for the *in situ* MALDI-MSI experiments. Support for this research was provided in part by the University of Wisconsin Madison (UW-Madison), Office of the Vice Chancellor for Research and Graduate Education with funding from the Wisconsin Alumni Research Foundation (WARF), and National Institutes of Health R56MH110215 (to L.L.). L.L. acknowledges a Vilas Distinguished Achievement Professorship and a Janis Apinis Professorship with funding provided by the WARF and UW- Madison School of Pharmacy. C.C. acknowledges National Institutes of Health U19TW009872-01. E.G. acknowledges an NSF Graduate Research Fellowship (DGE-1256259). The MALDI-Orbitrap was purchased through a National Institutes of Health shared instrument grant (NCRR S10RR029531). TOC/abstract graphic: photo courtesy of Alex Wild.

3.6 Figures

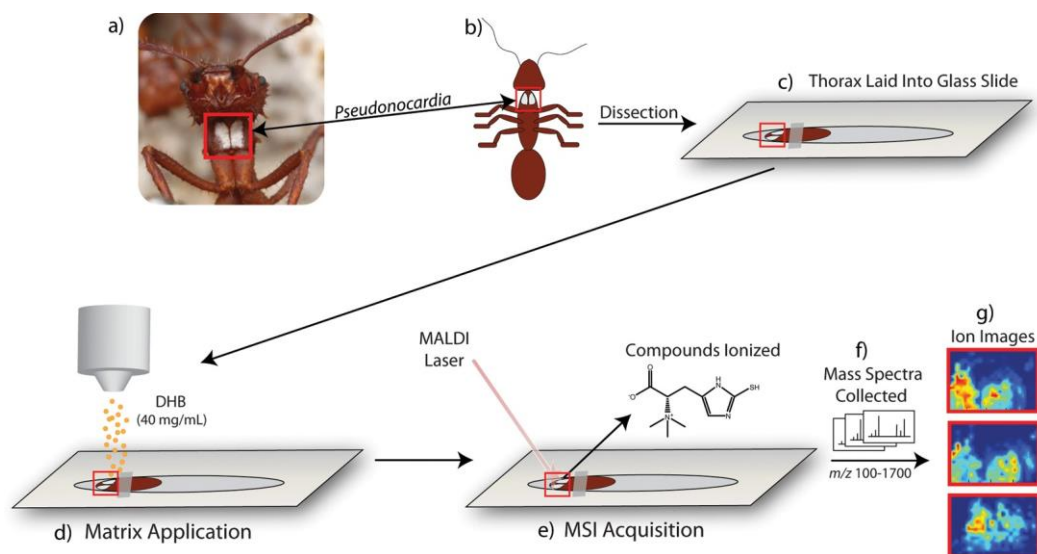


Figure 3.1 Workflow for MS imaging of *Pseudonocardia* on the ant propleural plate. a) Photograph and b) cartoon of *Pseudonocardia* on the ant exoskeleton. c) Grooves were cut into glass slides and double-sided tape was applied to the back of the slide. The ant thoraxes were removed and positioned into the groove of the slide with the propleural plate facing outward and even with the top of the slide. An additional thin strip of double-sided tape was applied below the propleural plate to stabilize and secure the thorax into place. d) Matrix was applied to the slide using an automatic sprayer. e) A laser was fired at the sample to ionize compounds of interest and introduce them into the mass spectrometer. f) An array of mass spectra was acquired using a MALDI-LTQ Orbitrap and g) compiled into MS images. Photo courtesy of Alex Wild.

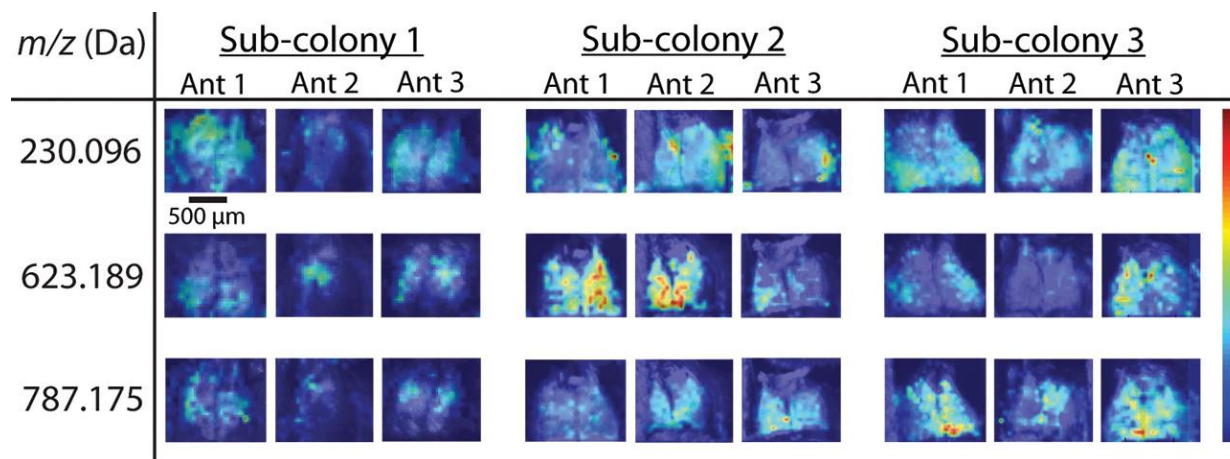


Figure 3.2 Representative MS images. The images demonstrate the reproducibility of the developed method by comparing ant propleural plates from nine technical replicates. The color scale represents low (blue) to high (red) relative intensity (0–100%). Scale bar = 500 μm . All images are the m/z value ± 5 ppm.

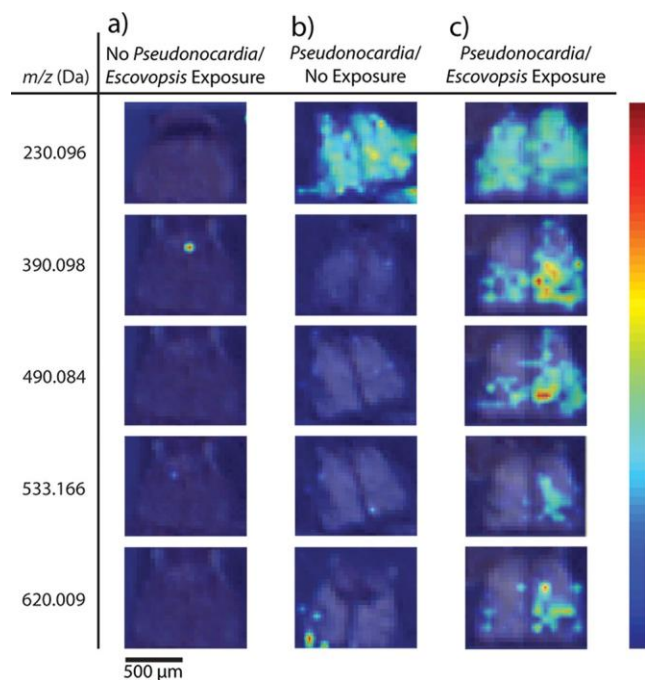


Figure 3.3 Representative MS images comparing ant propleural plates. (a) without the presence of their native *Pseudonocardia* and also exposed to the pathogen, (b) *Escovopsis*, with the presence of *Pseudonocardia*/ no pathogen exposure, and (c) with *Pseudonocardia* and exposed to *Escovopsis*. The color scale represents low (blue) to high (red) relative intensity (0–100%). Scale bar = 500 μm . All images are the m/z value ± 5 ppm.

Ergothioneine
m/z 230.09558

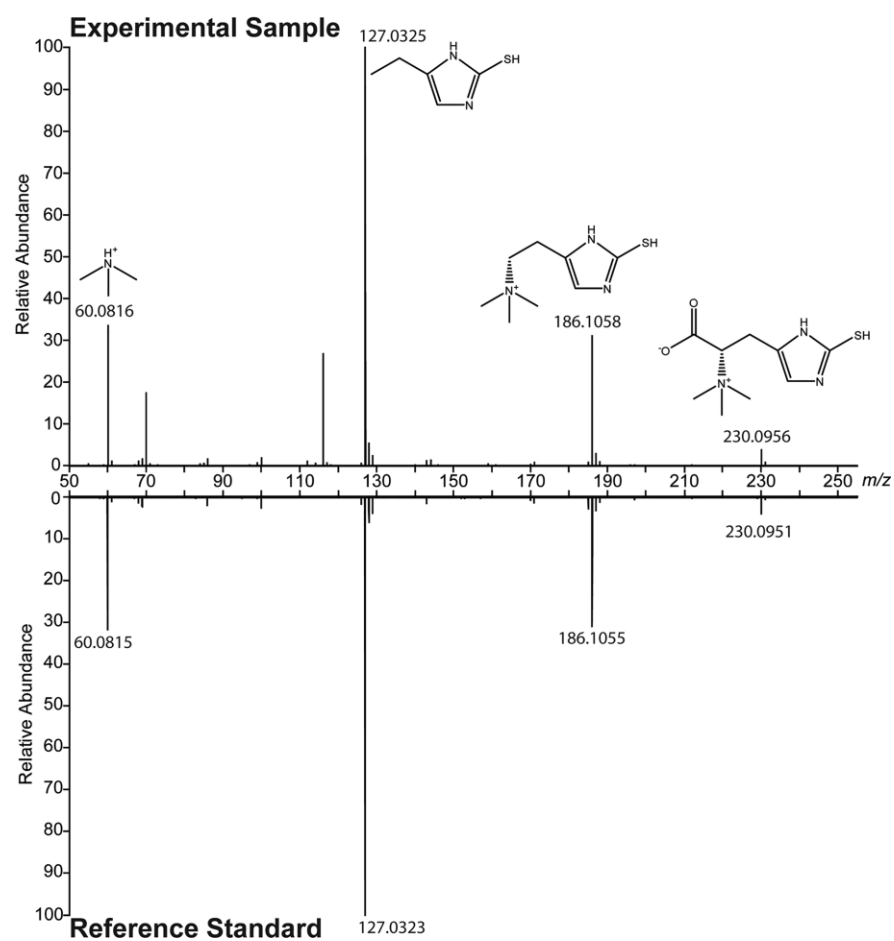


Figure 3.4 Mirror plot of the MS/MS spectrum of the identified metabolite, ergothioneine (*m/z* 230.09558), compared to the MS/MS spectrum of a purchased ergothioneine standard. Differences in the MS/MS spectra are due to coisolation of a similar-mass metabolite because of a wide isolation width (3 Da). The spectrum is annotated with structures corresponding to fragment ions that match fragments reported in the literature spectra in the MELTIN database.

3.7 References

- Davies, J. (2006) Are antibiotics naturally antibiotics? *J. Ind. Microbiol. Biotechnol.* *33*, 496–499.
- Yim, G., Huimi Wang, H., and Davies, J. (2006) The truth about antibiotics. *Int. J. Med. Microbiol.* *296*, 163–170.
- Romero, D., Traxler, M. F., Lopez, D., and Kolter, R. (2011) Antibiotics as signal molecules. *Chem. Rev.* *111*, 5492–5505.
- Seyedsayamdost, M. R., Traxler, M. F., Clardy, J., and Kolter, R. (2012) Old meets new: using interspecies interactions to detect secondary metabolite production in actinomycetes. *Methods Enzymol.* *517*, 89–109.
- Traxler, M. F., Seyedsayamdost, M. R., Clardy, J., and Kolter, R. (2012) Interspecies modulation of bacterial development through iron competition and siderophore piracy. *Mol. Microbiol.* *86*, 628–644.
- Traxler, M. F., Watrous, J. D., Alexandrov, T., Dorrestein, P. C., and Kolter, R. (2013) Interspecies interactions stimulate diversification of the *Streptomyces coelicolor* secreted metabolome. *mBio* *4*, e00459-13.
- Seyedsayamdost, M. R. (2014) High-throughput platform for the discovery of elicitors of silent bacterial gene clusters. *Proc. Natl. Acad. Sci. U. S. A.* *111*, 7266–7271.
- Weber, N. A. (1966) Fungus-growing ants. *Science* *153*, 587–604.
- Chapela, I. H., Rehner, S. A., Schultz, T. R., and Mueller, U. G. (1994) Evolutionary History of the Symbiosis between Fungus-Growing Ants and Their Fungi. *Science* *266*, 1691–1694.
- Currie, C. R., Scott, J. A., Summerbell, R. C., and Malloch, D. (1999) Fungus-growing ants use antibiotic-producing bacteria to control garden parasites. *Nature* *398*, 701–704.
- Currie, C. R., Mueller, U. G., and Malloch, D. (1999) The agricultural pathology of ant fungus gardens. *Proc. Natl. Acad. Sci. U. S. A.* *96*, 7998–8002.
- Currie, C. R., Bot, A. N. M., and Boomsma, J. J. (2003) Experimental evidence of a tripartite mutualism: bacteria protect ant fungus gardens from specialized parasites. *Oikos* *101*, 91–102.
- Poulsen, M., Cafaro, M. J., Erhardt, D. P., Little, A. E. F., Gerardo, N. M., Tebbets, B., Klein, B. S., and Currie, C. R. (2010) Variation in *Pseudonocardia* antibiotic defence helps govern parasite-induced morbidity in *Acromyrmex* leaf-cutting ants. *Environ. Microbiol. Rep.* *2*, 534–540.
- Yang, J. Y., Phelan, V. V., Simkovsky, R., Watrous, J. D., Trial, R. M., Fleming, T. C., Wenter, R., Moore, B. S., Golden, S. S., Pogliano, K., and Dorrestein, P. C. (2012) Primer on agar-based microbial imaging mass spectrometry. *J. Bacteriol.* *194*, 6023–6028.

- Baig, N. F., Dunham, S. J., Morales-Soto, N., ShROUT, J. D., Sweedler, J. V., and Bohn, P. W. (2015) Multimodal chemical imaging of molecular messengers in emerging *Pseudomonas aeruginosa* bacterial communities. *Analyst* 140, 6544–6552.
- Dunham, S. J., Comi, T. J., Ko, K., Li, B., Baig, N. F., Morales-Soto, N., ShROUT, J. D., Bohn, P. W., and Sweedler, J. V. (2016) Metal-assisted polyatomic SIMS and laser desorption/ionization for enhanced small molecule imaging of bacterial biofilms. *Biointerphases* 11, 02A325.
- Bhandari, D. R., Wang, Q., Friedt, W., Spengler, B., Gottwald, S., and Rompp, A. (2015) High resolution mass spectrometry imaging of plant tissues: towards a plant metabolite atlas. *Analyst* 140, 7696–7709.
- Khalil, S. M., Rompp, A., Pretzel, J., Becker, K., and Spengler, B. (2015) Phospholipid Topography of Whole-Body Sections of the *Anopheles stephensi* Mosquito, Characterized by High-Resolution Atmospheric-Pressure Scanning Microprobe Matrix-Assisted Laser Desorption/Ionization Mass Spectrometry Imaging. *Anal. Chem.* 87, 11309–11316.
- Caprioli, R. M. (2015) Imaging Mass Spectrometry: Enabling a New Age of Discovery in Biology and Medicine Through Molecular Microscopy. *J. Am. Soc. Mass Spectrom.* 26, 850–852.
- Van de Plas, R., Yang, J. H., Spraggins, J., and Caprioli, R. M. (2015) Image fusion of mass spectrometry and microscopy: a multimodality paradigm for molecular tissue mapping. *Nat. Methods* 12, 366–U138.
- Bouslimani, A., Sanchez, L. M., Garg, N., and Dorrestein, P. C. (2014) Mass spectrometry of natural products: current, emerging and future technologies. *Nat. Prod. Rep.* 31, 718–729.
- Lane, A. L., Nyadong, L., Galhena, A. S., Shearer, T. L., Stout, E. P., Parry, R. M., Kwasnik, M., Wang, M. D., Hay, M. E., Fernandez, F. M., and Kubanek, J. (2009) Desorption electrospray ionization mass spectrometry reveals surface-mediated antifungal chemical defense of a tropical seaweed. *Proc. Natl. Acad. Sci. U. S. A.* 106, 7314–7319.
- Nyadong, L., Hohenstein, E. G., Galhena, A., Lane, A. L., Kubanek, J., Sherrill, C. D., and Fernandez, F. M. (2009) Reactive desorption electrospray ionization mass spectrometry (DESI-MS) of natural products of a marine alga. *Anal. Bioanal. Chem.* 394, 245–254.
- Bartels, B., Kulkarni, P., Danz, N., Böcker, S., Saluz, H. P., and Svatos, A. (2017) Mapping metabolites from rough terrain: laser ablation electrospray ionization on non-flat samples. *RSC Adv.* 7, 9045–9050.
- Vrkoslav, V., Muck, A., Cvacka, J., and Svatos, A. (2010) MALDI imaging of neutral cuticular lipids in insects and plants. *J. Am. Soc. Mass Spectrom.* 21, 220–231.
- Yew, J. Y., Dreisewerd, K., Luftmann, H., Muthing, J., Pohlentz, G., and Kravitz, E. A. (2009) A new male sex pheromone and novel cuticular cues for chemical communication in *Drosophila*. *Curr. Biol.* 19, 1245–1254.

Schoenian, I., Spiteller, M., Ghaste, M., Wirth, R., Herz, H., and Spiteller, D. (2011) Chemical basis of the synergism and antagonism in microbial communities in the nests of leaf-cutting ants. *Proc. Natl. Acad. Sci. U. S. A.* 108, 1955–1960.

Horn, H., Gemperline, E., Chevrette, M., Mevers, E., Clardy, J., Li, L., and Currie, C. R. Specialized chemical responses to pathogens in the defensive symbionts of fungus-growing ants. In preparation.

Palmer, A., Phapale, P., Chernyavsky, I., Lavigne, R., Fay, D., Tarasov, A., Kovalev, V., Fuchser, J., Nikolenko, S., Pineau, C., Becker, M., and Alexandrov, T. (2016) FDR-controlled metabolite annotation for high-resolution imaging mass spectrometry. *Nat. Methods* 14, 57–60.

Genghof, D. S. (1970) Biosynthesis of ergothioneine and hercynine by fungi and Actinomycetales. *J. Bacteriol.* 103, 475–478.

Cheah, I. K., and Halliwell, B. (2012) Ergothioneine; antioxidant potential, physiological function and role in disease. *Biochim. Biophys. Acta, Mol. Basis Dis.* 1822, 784–793.

Robichaud, G., Garrard, K. P., Barry, J. A., and Muddiman, D. C. (2013) MSiReader: an open-source interface to view and analyze high resolving power MS imaging files on Matlab platform. *J. Am. Soc. Mass Spectrom.* 24, 718–721.

Smith, C. A., O'Maille, G., Want, E. J., Qin, C., Trauger, S. A., Brandon, T. R., Custodio, D. E., Abagyan, R., and Siuzdak, G. (2005) METLIN: a metabolite mass spectral database. *Ther. Drug Monit.* 27, 747–751.

Chapter 4

Specialized chemical responses to pathogens in the defensive symbionts of fungus-growing ants

This manuscript has been submitted to *Molecular Ecology* and is under review at the time of this thesis submission.

Authors: Heidi A. Horn*, Erin Gemperline*, Marc G. Chevrette, Bradon R. McDonald, Jennifer R. Bratburd, Lingjun Li, Cameron R. Currie

*These authors contributed equally

Author Contributions: Designed experiments (H.A.H., E.G., L.L., C.R.C.), performed experiments (H.A.H., E.G.), performed genome sequencing and analysis (M.G.C., B.R.M., J.R.B.), performed statistical analysis and data analysis (H.A.H., E.G.), wrote the manuscript (H.A.H., E.G., C.R.C., L.L.).

4.1 Abstract

Microbes interact largely through the production of small molecules. These natural products influence the evolutionary trajectories of populations and have been extensively investigated as potential drug leads. Nevertheless, our current understanding of the ecological and evolutionary dynamics of chemical signaling between microbes remains limited. Here we examine the chemical ecology of bacterially produced molecules within an ancient ant-microbe symbiosis. Fungus-growing ants engage in a multi-partite mutualism with a fungus they grow for food and an exosymbiotic *Pseudonocardia* bacterium that produces small molecules with antimicrobial properties to help protect the fungus garden from pathogens. Here, using a high-resolution, accurate-mass matrix-assisted laser desorption/ionization Orbitrap mass spectrometer, we examine changes in the small molecules produced by two *Pseudonocardia*

defensive symbionts associated with *Acromyrmex* leaf-cutter ants when exposed to three different fungal pathogens, in Petri plate assays (*in vitro*) and ant sub-colony infections (*in vivo*). *Pseudonocardia* from *in vitro* cocultures exhibit markedly different metabolic fingerprints compared to growth in isolation indicating that metabolites are induced by particular pathogen interactions. Under *in vivo* conditions, the overall chemical profiles of *Pseudonocardia* differ strikingly compared to the same conditions *in vitro* suggesting species interactions *in vivo* induce different small molecules than interactions in culture. Finally, we detected several molecules unique to each treatment condition, suggesting an apparent distinct and dynamic response in small molecules produced under different infection conditions. Taken together, these results suggest that the diversity of chemical communication in this ant-bacterial defensive symbiosis may be highly dynamic and involve greater chemical diversity than previously appreciated.

4.2 Introduction

The diversity of life is shaped by species interactions. In microbes, the interactions between and within species are largely mediated by small molecules. These metabolites have been extensively studied as potential drug leads, however the ecological role of most is largely unknown (Bérdy, 2005; Clardy, Fischbach, & Currie, 2009; Romero, Traxler, López, & Kolter, 2011). Nevertheless, it is viewed that they are important as microbial signaling and are implicated in associations ranging from competition and warfare to cooperation and

mutualism (Diggle, Gardner, West, & Griffin, 2007; Fajardo & Martínez, 2008; Kinkel, Schlatter, Xiao, & Baines, 2014; Linares, Gustafsson, Baquero, & Martinez, 2006; O'Brien & Wright, 2011; Seyedsayamdost, Traxler, Clardy, & Kolter, 2012; Traxler, Seyedsayamdost, Clardy, & Kolter, 2012; Traxler, Watrous, Alexandrov, Dorrestein, & Kolter, 2013; Yim, Wang, & Davies, 2007). Greater understanding of the diversity and ecological function of these compounds is crucial to elucidate the interactions and associations between microbes that affect evolutionary trajectories. Here we examine small molecule signals within a coevolved system that has defended against fungal pathogens for millions of years.

Fungus-growing ants (Tribe Attini) participate in an ancient, multi-partite symbiosis whose associations span from mutualistic to pathogenic. For ~55 million years attine ants have cultivated a basidiomycetous fungus that they consume as their sole food source (Nygaard et al., 2016; Weber, 1966). The fungal cultivar is grown in a monoculture within colonies (Mueller et al., 2010) and is highly susceptible to pathogens including the coevolved fungal pathogen *Escovopsis* (C. R. Currie, Mueller, & Malloch, 1999). The ants, under selective pressure to protect their food source, have evolved defense mechanisms to protect their fungal garden including an association with an Actinobacteria in the genus *Pseudocardia* (C R Currie, Bot, & Boomsma, 2003; Cameron R Currie & Scott, 1999; Poulsen et al., 2010). In this defensive mutualism the bacterium produces antimicrobial small molecules that inhibit pathogen growth; in return *Pseudocardia* resides in crypts and tubercles on the ant exoskeleton and is fed nutrients through specialized glands (Cameron R

Currie, Poulsen, Mendenhall, Boomsma, & Billen, 2006; Li et al., 2018; Steffan et al., 2015).

Although several small molecules produced by *Pseudonocardia* have been characterized *in vitro* (Carr, Derbyshire, Caldera, Currie, & Clardy, 2012; Oh, Poulsen, Currie, & Clardy, 2009; Van Arnam et al., 2016), few studies to date have examined these molecules *in vivo* (Gemperline, Horn, DeLaney, Currie, & Li, 2017; Schoenian et al., 2011). Moreover, the diversity of compounds produced by these ant-associated bacteria is relatively unexplored.

Here, we explore the ecological dynamics of small molecule production by two *Acromyrmex*-associated *Pseudonocardia*. Our overarching hypothesis is ant-*Pseudonocardia*-pathogen interactions impact the small molecules produced by symbiotic *Pseudonocardia*. We combine experimental microbial ecology with mass spectrometry imaging (MSI), to answer the following questions: (i) Does the interaction with a pathogen induce the production of different small molecules by *Pseudonocardia*? (ii) Are the small molecules produced by *Pseudonocardia* highly similar when present on the ant host (i.e., *in vivo*) versus growing in pure culture (i.e., *in vitro*)? (iii) Do different pathogens induce the production of different small molecules by *Pseudonocardia*?

To address these questions, we first sequenced the genomes of 16 strains of ant-associated *Pseudonocardia* and 1 free-living *Pseudonocardia* in order to examine their biosynthetic potential. We then focus on 2 strains of *Pseudonocardia* with highly similar genomes and near identical biosynthetic potential from *Acromyrmex* leaf-cutter ants to serve as biological replicates. Using these strains, we first conducted bioassay inhibition challenges

between *Pseudonocardia* and three fungal pathogens: 2 different strains of *Escovopsis*, a system-specific pathogen, and *Trichoderma viridae*, a general fungal pathogen. In addition, we performed these same inhibition challenges *in vivo* – when *Pseudonocardia* resides on the ant exoskeleton. To compare the diversity of small molecules produced in these interactions, we performed MSI using a high-resolution, accurate-mass matrix-assisted laser desorption/ionization (MALDI) Orbitrap mass spectrometer. Further, for *in vivo* MSI, we use a recently developed technique to detect and compare metabolic profiles produced by *Pseudonocardia* on the surface of the ant's propleural plate (Gemperline et al., 2017). We take an untargeted approach in order to observe molecules not detected under normal growth conditions. *Pseudonocardia* from *Acromyrmex* hosts have been extensively studied in *in vitro* conditions yet few compounds have been identified (unpublished data). This suggests that there are few compounds constitutively produced by these lineages and the context of the bacterium is likely an important factor in influencing small molecule production.

4.3 Methods

4.3.1 Ant colony collection and maintenance

Two colonies of *Acromyrmex* leaf-cutter ants were used: colony ST040116-01 *Acromyrmex octospinosus* and colony CC031209-02 *A. echinator*. These colonies were originally collected in the canal region of Panama and subsequently maintained in a temperature controlled room (27°C) at the University of Wisconsin-Madison prior to this

experiment. Colonies were fed *Quercus* and *Acer* leaves (fresh in summer and thawed from -20°C in winter) 3 days/week prior to and during the experiment.

4.3.2 In vitro bioassays

From each of the two ant colonies, *Pseudonocardia* symbionts were isolated from the propleural plates of young callow workers exhibiting visible growth of the bacteria (*Pseudonocardia* sp. AOST16-01 from colony ST040116-01 *A. octospinosus*; *Pseudonocardia* sp. AECC09-02 from colony CC031209-02 *A. echinator*). Growth inhibition bioassays were performed between *Pseudonocardia* and 3 fungal strains that are known to infect the fungus gardens of leaf-cutter ants: *Escovopsis* strain 1 isolated from *Atta sexdens* colony SES030113-01, *Escovopsis* strain 2 isolated from *Atta cephalotes* colony AL031210-29, and *Trichoderma viridae*. Each bioassay was performed in triplicate on YMEA media (4g yeast extract, 4 g dextrose, 10 g malt extract, 15g agar in 1 L distilled H₂O). *Pseudonocardia* was inoculated in the center of a 15 mm Petri plate and allowed to grow for 2 weeks. Fungal pathogens were then point inoculated on the edge of each Petri plate and grew for 1 week after which samples from the zone of inhibition were prepared for MSI.

4.3.3 Genome sequencing

Pseudonocardia were isolated following previous methods (Cafaro & Currie, 2005) from diverse ant hosts (*Acromyrmex* sp., *Trachymyrmex* sp., *Apterostigma* sp.) from Panama, Costa Rica, and Peru. Genomic DNA was extracted from isolates using standard phenol-chloroform extraction protocols for Actinomycetes. Paired-end Illumina libraries were generated and

loaded in 2x250 format on the Illumina MiSeq platform. Sequencing data was quality filtered and assembled using SPAdes v3.7.0 (Nurk et al., 2013). Open reading frames were called by Prodigal v2.60 (Hyatt et al., 2010) and functionally annotated by COG (Galperin, Makarova, Wolf, & Koonin, 2015). Secondary metabolic content was assessed by antiSMASH v4.0 (Blin et al., 2017) and PRISM (Skinnider et al., 2015). Biosynthetic gene clusters were compared at both amino acid and nucleotide levels by MAFFT v7.123b (Katoh & Standley, 2013) and nucmer v3.1 (Kurtz et al., 2004) respectively. Genomic assemblies for all strains were mapped by nucmer to the biosynthetic gene clusters identified in *Pseudonocardia* sp. AEC09-02.

All strains of *Pseudonocardia* used to infer the molecular phylogeny fall within clade VI of a previous multi-locus phylogenetic analysis of *Pseudonocardia* (Cafaro et al., 2011). In addition to genomes sequenced in this study, three previously sequenced genomes (*Pseudonocardia* sp. AEC25-04 (EC080625-04), *Pseudonocardia* sp. TCAL05-10 (AL041005-10), *Pseudonocardia* sp. AHH29-09 (HH130629-09))(Sit et al., 2015) were included in the analysis as well as one publically available free-living strain that was used as an outgroup (*Pseudonocardia spinosipora* DSM44797 (INSDC: [AUBB000000000.1](https://www.ncbi.nlm.nih.gov/nuccore/AUBB000000000.1))).

4.3.4 Subcolony preparation and pathogen treatment

For our *in vivo* infection experiment, subcolonies of ants and fungus garden were made from each colony and placed in a sterile 8 cm Petri plate. Approximately 1 g of fungus garden was placed in a plastic weigh boat with approximately 4-6 minor worker ants included and placed within the Petri plate. To each subcolony, one major worker was added from the main

fungus garden. Care was taken to ensure the approximate same age among all major workers, based on the degree of sclerotization of the exoskeleton (*e.g.*, callow works are lighter color) and degree of *Pseudonocardia* bloom; workers that are approximately 2-4 weeks old have a lighter color and *Pseudonocardia* bloom covering their whole exoskeleton (Poulsen et al. 2005). Subcolonies were randomly assigned to one of four treatments: water, *Escovopsis* strain 1, *Escovopsis* strain 2, or *T. viridae*. Each treatment was replicated in 3 subcolonies and at 3 separate time points (n=9 for each treatment). Cultures of *Escovopsis* strain 1 and *Escovopsis* strain 2 and *T. viridae* were grown one week on Potato Dextrose Medium (39 g Potato Dextrose Medium, 15 g agar in 1 L distilled H₂O) prior to infection. Infection of subcolonies occurred by applying mature fungal spores from a 6 mm² area of agar and inoculating directly to the fungus garden with a sterile inoculation loop. Control subcolonies were similarly disturbed with a sterile inoculation loop and filter sterilized water. Subcolonies were left for 20 hours after which focal ants were removed and frozen at -20°C for further processing.

4.3.5 Sample Preparation for MALDI

Bacterial colonies and their neighboring zone of inhibition were cut from the agar plate using a razor blade and transferred to a glass slide using a spatula. The colony and agar were dehydrated in a desiccator overnight. Samples for the *in vivo* ant imaging were prepared as previously described (Gemperline et al., 2017; Moree et al., 2012; Yang et al., 2012).

For both agar and ant MSI, matrix (40 mg/mL 2,5-dihydroxybenzoic acid (DHB) in 50:50 water:methanol) was applied to the dried agar or ants using a TM Sprayer (HTX Technologies, LLC, Carrboro, NC, USA). DHB was purchased from Sigma-Aldrich (St. Louis, MO, USA).

4.3.6 MALDI-Orbitrap MSI

A MALDI-Orbitrap LTQ mass spectrometer (Thermo Scientific, Waltham, MA, USA), equipped with a N₂ laser, was used in positive ion mode for MS imaging. Three bacterial colonies of each inhibition assay were imaged at a spatial resolution of 100 µm for the bioassays using a mass range of m/z 100-1700, a mass resolution of 60,000 and a mass error of ≤ 5 ppm. For *in vivo* MSI, three rounds of imaging were conducted over the course of several months in which three ants of each treatment type were imaged at a spatial resolution of 75 µm using the same instrumental settings listed above. MSiReader (Robichaud, Garrard, Barry, & Muddiman, 2013) was used to create a list of compounds of interest for each sample that were ultimately combined into one list. Ion images (normalized to the total ion current) were automatically generated from the combined mass lists using MSiReader.

4.3.7 MALDI-MSI Data Processing and Analysis

Raw data files acquired from MALDI-MSI were uploaded to MSiReader. MSiReader was used to create a list of compounds of interest by selecting the propleural plate as the “interrogated zone” and subtracting the matrix peaks chosen as the “reference zone”. A list of m/z values was generated in this way for 9 control ants and 9 ants for each treatment type and

the lists were combined into one list; duplicated masses (within 5 ppm mass error) and isotopic peaks were removed. Note that m/z values for ion adducts were not verified and removed from the mass list. This process was used for both ant species and three biological replicates of all co-culture controls and treatments. Ion images were automatically generated with MSiReader for every sample/ treatment using the combined mass lists. All images were normalized to the TIC. Mass lists were manually cross-checked between all treatment and sample types to determine if each compound was unique to a specific treatment or shared between treatments. Compounds were determined to be valid target compounds if they were present in at least 6 of the 9 biological replicates for the *in vivo* assays and at least two of the three biological replicates for the *in vitro* assays. Unique compounds (potential target compounds) were defined as compounds present in pathogen treated samples and not in the control samples.

4.3.8 Statistical Analysis

Mass intensity lists were compiled using ImageQuest software (Thermo Scientific) and then analyzed using MetaboAnalyst (J. Xia, Sinelnikov, Han, & Wishart, 2015; Jianguo Xia, Psychogios, Young, & Wishart, 2009). Masses under m/z 300.0000 were removed before analysis. Mass peak lists were analyzed with a mass tolerance of 0.003 m/z and retention time tolerance set to 1. Data were filtered using standard deviation to eliminate non-informative variables and then normalized by sum and auto-scaled. PLS-DA was performed on the normalized data.

4.4 Results

4.4.1 Genomics

Using PacBio SMRT sequencing technology (Eid et al., 2009), we sequenced four strains (*Pseudo* sp. AOST16-01, *Pseudo* sp. AECC09-02, *Pseudo* sp. AHUGM27-02, and *Pseudo* sp. TAL02-03) of ant-associated *Pseudonocardia*. These assemblies are either complete or have N50 values between 4.26 Mbp and 6.22 Mbp. Complete genome sizes range from 5.6 Mbp to 6.6 Mbp with approximately 73-74% global GC content (**Figure 4.1a**). An additional 13 strains of *Pseudonocardia* (twelve ant-associated strains and one free-living strain of *Pseudonocardia*) were sequenced with Illumina sequencing technology resulting in assemblies with N50 values ranging from 4.9 Kbp to 7.91 Kbp. A molecular phylogeny of these *Pseudonocardia*, inferred using 94 conserved genes, fits previously inferred patterns of host specificity and geographic distribution of ant-associated *Pseudonocardia* in which there appears to be some specificity between *Pseudonocardia* lineage and ant host although there is evidence of some host switching (Cafaro et al., 2011).

Examination of biosynthetic gene clusters (BGCs) across the seven complete genomes reveals substantial biosynthetic potential and diversity across ant-associated *Pseudonocardia* (**Figure A2.1**). Strains range from having between 10 and 16 BGCs on both their chromosome and putative plasmids, accounting for an average of 9.25% of the genome. Despite the genomic diversity present across the ant-associated strains examined in this study,

the BGCs of 2 strains, *Pseudonocardia* sp. AOST16-01 and *Pseudonocardia* sp. AECC09-02, are nearly identical. These two strains were isolated from two sympatric species of *Acromyrmex* ants (*A. octospinosus* and *A. echinator*, strains AOST16-01 and AECC09-02, respectively) from Panama, and show high sequence similarity and gene synteny at the whole genome scale (98.89% average mapped nucleotide identity). Further, *Pseudonocardia* sp. AOST16-01 contains 15 BGCs, 14 of which are homologous to those found in *Pseudonocardia* sp. AECC09-02 (**Figure 4.1b**). In contrast, the closely related symbiont strain *Pseudonocardia* sp. AHH29-09 (97.09% average mapped nucleotide identity with *Pseudonocardia* sp. AECC09-02), isolated from a colony of *Apterostigma* ants, has differential BGC potential when compared to *Pseudonocardia* sp. AOST16-01 and *Pseudonocardia* sp. AECC09-02. *Pseudonocardia* sp. AHH29-09 contains 14 BGCs, 9 of which are shared with *Pseudonocardia* sp. AOST16-01 and *Pseudonocardia* sp. AECC09-02 (**Figure 4.1b**).

4.4.2 In vitro *small molecule induction*

To address our first question, does the interaction with a pathogen induce the production of different small molecules, we conducted MSI on cultures of *Pseudonocardia* sp. AOST16-01 and *Pseudonocardia* sp. AECC09-02 in isolation and in inhibition bioassay pairings with pathogenic fungi, focusing on regions where zones of inhibition would form (*i.e.*, in the medium on the margins of the *Pseudonocardia* culture). An ion was considered present in a

given treatment if there was signal detected in at least 2 out of 3 petri plate replicates. Overall, we detected a diverse suite of ions, mass-to-charge ratios (m/z) between 300 to 1700 Da, with individual treatments producing between 186-337 distinct ions (**Figure A2.2**).

The majority of ions are detected in all or multiple treatments. An example is shown in m/z of 655.275 (**Figure 4.2a**). In contrast, a molecule with m/z 760.296 is produced by *Pseudonocardia* sp. AOST16-01 *in vitro* when challenged with *Escovopsis* sp. 1, but is largely missing from *Pseudonocardia* sp. AECC09-02 (except for some signal in the *T. viridae* challenge) (**Figure 4.2a**). Further, across the three *in vitro* replicates of each treatment, ion m/z 671.028 is detected in both bacterial strains and in both *Escovopsis* interactions, however this ion is not induced in interactions with *Trichoderma* (**Figure 4.2a**). These differential ion patterns suggest that particular molecules are produced by *Pseudonocardia* only under particular species interactions.

Total mass spectra were analyzed using a Partial Least Squares-Discriminant Analysis (PLS-DA), demonstrating a ‘metabolic fingerprint’ for each treatment with replicates of each treatment grouped together (**Figure 4.2b**). The control treatment of each *Pseudonocardia* strain produces a metabolic profile that separates from the opposite strain. Further, molecules group more similarly by producing strain (*Pseudonocardia* sp. AOST16-01 or *Pseudonocardia* sp. AECC09-02), regardless of the pathogen treatment, and each strain produces a distinct suite of molecules in response to each pathogen as seen by the separate metabolic fingerprints in the PLS-DA (**Figure 4.2b**).

For each *Pseudonocardia* sp. AOST16-01 and *Pseudonocardia* sp. AECC09-02, we detected 77 ions shared in at least two out of three replicates of each of the control and 3 pathogen treatments, suggesting these metabolites are constitutively produced and secreted (**Figure 4.2c**). Of these 77 ions detected in each strain, 38 are shared between the two strains (**Table A2.1**). We also detected ions that appear to be induced by particular pathogen interactions. For example, in interactions with both *Escovopsis* sp. 1 and *Escovopsis* sp. 2, 67 unique ions are induced in *Pseudonocardia* sp. AOST16-01 and 38 unique ions are induced in *Pseudonocardia* sp. AECC09-02. Of these ions, 17 are shared between the two bacterial strains, indicating molecules that are induced by the presence of *Escovopsis* (**Figure 4.2c; Table A2.1**). We also detected 3 ions in both strains of *Pseudonocardia* that are present in any interaction with a pathogen – *Escovopsis* sp. 1, *Escovopsis* sp. 2 or *T. viridae* — indicating molecules that appear to be induced by interactions with a range of fungi. *Pseudonocardia* sp. AOST16-01 produces 21 unique ions that are found in interactions with all pathogens and *Pseudonocardia* sp. AECC09-02 produces 37 unique ions under these conditions (**Figure 4.2c**). Additionally, there are ions found in various combinations of treatments and the control in both strains of *Pseudonocardia* and are found in **Table A2.1**.

4.4.3 In vitro-in vivo comparison

To compare the small molecules produced by *Pseudonocardia* when present on the ant host (i.e., *in vivo*) with those produced when growing in culture (i.e., *in vitro*), we use a newly

developed method for MALDI-MSI of *Pseudonocardia* directly on the exoskeleton of fungus-growing ants (Gemperline et al., 2017). We focus on ant workers, associated with *Pseudonocardia* sp. AOST16-01 and *Pseudonocardia* sp. AECC09-02, maintained in sub-colonies with fungus garden and experimentally treated with and without the same pathogen strains employed in our *in vitro* work. Comparison between the *in vitro* and *in vivo* metabolomic fingerprints for *Pseudonocardia* sp. AOST16-01 and *Pseudonocardia* sp. AECC09-02 reveals global differences in ions detected between the 2 conditions. PLS-DA of mass spectra comparing the *in vitro* and *in vivo* conditions for *Pseudonocardia* sp. AOST16-01 (**Figure 4.3a**) and *Pseudonocardia* sp. AECC09-02 (**Figure 4.3b**) yields assay-specific metabolic fingerprints; all *in vitro* pairings are more similar to one another, distinct from the *in vivo* treatments. Overall, metabolic fingerprints for each *in vivo* treatment (*i.e.*, different pathogen interactions) show less variation from one another than *in vitro* treatments; greater differential response is seen among treatments *in vitro* as seen by separation of metabolic fingerprints of each treatment group (**Figure 4.3**).

Total ions detected in the *in vivo* treatments range from 54-139 ions (**Figure A2.3**).

Although fewer total ions were detected *in vivo* compared to *in vitro* (this is likely due to the larger number of ant replicates compared to Petri plate replicates), a large percentage (55%-86%) of these ions are only detected in *Pseudonocardia in vivo* (**Table 4.1**). *Pseudonocardia* sp. AOST16-01 produced 64 ions in control conditions on its ant host and 85.94% of these are not detected when this strain is grown in control conditions *in vitro*. Our experimental

pathogen infections of sub-colonies reveal similar results. For example, in *in vivo* interactions with *Escovopsis* sp. 1 we detect 90 ions from *Pseudonocardia* sp. AOST16-01, 65.56% of which were not found *in vitro*, and 60 ions were detected in *in vivo* interactions with *Escovopsis* sp. 2, 68.33% of which are not found *in vitro* (**Table 4.1**). Likewise, similar incongruence between the ions detected under *in vitro* and *in vivo* conditions is seen in *Pseudonocardia* sp. AECC09-02. For example, 113 ions are detected in the control, 86.73% of which are not found *in vitro* and for *in vivo* interactions with *Escovopsis* sp. 1 105 ions were detected, 78.10% of which are not present *in vitro*. Interactions with *Escovopsis* sp. 2 induce 139 ions *in vivo* and 74.82% are not present *in vitro* (**Table 4.1**). For our *T. viridae* infection treatments, 54 and 115 ions were detected for *Pseudonocardia* sp. AOST16-01 and *Pseudonocardia* sp. AECC09-02, respectively. 55.56% of these ions are unique to *Pseudonocardia* sp. AOST16-01 in *in vivo* conditions and 74.78% are unique *Pseudonocardia* sp. AECC09-02 *in vivo* conditions (**Table 4.1**). In all treatments, a greater number of ions are shared between the two strains *in vivo* than both strains and their *in vitro* equivalent (**Table 4.1**).

4.4.4 Specificity of pathogen interaction

To determine if *Pseudonocardia* responds to different pathogens by producing different small molecules, we compared the ion profiles among pathogen treatments. In our *in vitro* assays we detect a number of ions that appear to be induced in response to interactions with a

specific pathogen – each treatment produced unique ions only found in that particular interaction. We detected, in at least 2 or 3 replicates, 6 unique ions from *Pseudonocardia* sp. AOST16-01 in *in vitro* interactions with *Escovopsis* sp. 1; 7 unique ions when interacting with *Escovopsis* sp. 2; and 77 unique ions in interactions with *T. viridae*. We also detected unique ions produced by *Pseudonocardia* sp. AECC09-02 in specific pathogen interactions: 5 unique ions were detected in interactions with *Escovopsis* sp. 1; 45 unique ions in interactions with *Escovopsis* sp. 2; 115 unique ions in interactions with *T. viridae* (**Figure A2.2; Table A2.2**). A search for these condition specific metabolites in MetaboSearch (Zhou et al., 2012) and Antibase (Laatsch, 2014) (searched [M+H], [M+Na], [M+K], and [M+NH₄] adducts) reveals that some of these ions correspond to no known references, suggesting they may be uncharacterized compounds or ion adducts. For example, 6 unique ions were detected in *Pseudonocardia* sp. AOST16-01 in bioassays with *Escovopsis* sp. 1, of which 1 has no known reference. Similarly, 45 unique ions were detected in *Pseudonocardia* sp. AECC09-02 when interacting with *Escovopsis* sp. 2, and 5 of these ions have no known reference.

Similarly to the *in vitro* comparison of ions detected in response to different treatments, we compared metabolic profiles of *Pseudonocardia* on the ant host to determine if ions specific to particular pathogen infections are also observed *in vivo*. As in the *in vitro* challenges, ions specific to individual conditions were detected for all treatments (presence in a treatment indicated by an ion present in at least 6 out of 9 ant replicates). *Pseudonocardia* sp. AOST16-01 produced 12 ions specific to the control treatment, 15 ions were unique in

challenges with *Escovopsis* sp. 1, 4 ions in the *Escovopsis* sp. 2 treatment, and 1 unique ion is detected in challenges with *T. viridae* (**Figure 4.4a; Table A2.3; Figure A2.3**).

Pseudonocardia sp. AECC09-02 produced 1 ion specific to the control treatment, 5 ions were unique in challenges with *Escovopsis* sp. 1, 14 unique in the *Escovopsis* sp. 2 treatment, and 9 ions were unique to the challenges with *T. viridae* (**Figure 4.4a; Table A2.3; Figure A2.3**).

Searches for these unique ions in MetaboSearch (Zhou et al., 2012) and Antibase (Laatsch, 2014) revealed no known hits for the 3 and 4 unique ions detected in *Pseudonocardia* sp.

AOST16-01 and *Pseudonocardia* sp. AECC09-02, respectively (**Table A2.3**). In addition to pathogen-specific ions, both strains produce ions that are present only when the fungus garden is infected with specific combinations of pathogens. Under infection with both strains of *Escovopsis*, *Pseudonocardia* sp. AOST16-01 repeatedly produces 2 unique ions and 5 ions are detected in *Pseudonocardia* sp. AECC09-02 (**Figure 4.4a; Table A2.4**). In global analyses, the *in vivo* mass spectra reveal a colony specific response as seen in a PLS-DA of these data (**Figure 4.4b**); metabolic fingerprints for each ant-*Pseudonocardia* pairing appear more similar to the host ant colony regardless of pathogen present.

4.5 Discussion

Here we outline an ecological and mass spectrometry approach for examining the small molecule dynamics in a defensive symbiosis. Traditional approaches to understand bacterial-derived small molecules have primarily been performed in *in vitro* cultures, typically with the

microbe growing in pure culture. While this approach is informative, it has the potential to miss many important molecules that are induced by the ecological conditions associated with the dynamics present *in vivo*. The reason for this is that production of antimicrobial small molecules is energetically costly, and thus constitutive production is unlikely. A genomics approach has more recently been employed and confirmed the presence of BGCs associated with small molecules not observed in culture (Abdelmohsen et al., 2015). To explore the role of ecological interactions on the production of small molecules, we take an untargeted MSI approach allowing us to examine metabolites that vary under different experimental conditions in *Pseudonocardia* associated with *Acromyrmex* ant hosts. Previous *in vitro* chemical characterization of *Pseudonocardia* isolated from *Acromyrmex* ant hosts has not successfully isolated compounds when grown in culture (unpublished data). These same strains exhibit variation in their ability to inhibit *Escovopsis* when grown in coculture suggesting they produced diverse small molecules, consistent with the hypothesized arms race dynamics between the organisms. This evidence suggests that there are complicated dynamics that influence the production of small molecules in this ancient symbiosis.

We first examined ion profiles of *Pseudonocardia* in *in vitro* pairings with 3 different pathogens to examine the induction of products by *Pseudonocardia* from pathogen interactions. We hypothesize that *Pseudonocardia* induces production of antimicrobial molecules in pathogen interactions because it is costly for an organism to produce secondary metabolites (Stubbenieck, Vargas-Bautista, & Straight, 2016) and constitutive production is predicted to

increase the selection for resistance in the associated pathogen. Indeed, our results suggest that *in vitro* interactions with pathogens do induce small molecule production in *Pseudonocardia* compared to growth in isolation. While many ions were detected in all conditions and are constitutively produced, we detect ions specific to particular pathogen interactions in both strains. Both *Pseudonocardia* strains appear to have a suite of ions that are only induced when *Escovopsis* is present, suggesting there is an *Escovopsis*-specific small molecule response. In addition, there are ions detected when any pathogen is present, *Escovopsis* or *Trichoderma*, which may indicate a general response to interactions with a fungal pathogen. These results corroborate other *in vitro* studies examining the induction of microbial small molecules (Bertrand et al., 2013, 2014; Traxler & Kolter, 2015; Traxler et al., 2013). Co-culture of 2 organisms is a technique to induce the production of so-called cryptic gene clusters and is increasingly used in drug discovery efforts (Adnani et al., 2017; Bertrand et al., 2013, 2014; Traxler & Kolter, 2015). Here, we use ecologically relevant species pairings to understand the conditions influencing microbial produced small molecules rather than attempting to induce cryptic biosynthetic gene clusters. While we were unable to elucidate these compounds using MALDI-MS/MS or LC-MS/MS, it is critical to develop methods that are better able to detect these exclusive ions as they appear to be important in the ecological response to fungal pathogens. Although we were unable to identify specific molecules, we focused on ions that were present across replicates of a given treatment. The reproducibility of these ions gives confidence that they are indeed induced in a particular treatment. Examination of shifts in these

small molecule profiles provides insight into the ecological contexts that influence the diversity of bacterial derived metabolites.

To address our second question, we explored the metabolic profile of these interactions within their coevolved system and examined the small molecule response to pathogen presence at the ant-*Pseudonocardia* interface. Comparisons of metabolites produced under *in vitro* and *in vivo* conditions reveal a large number of differences between the 2 conditions, including a high percentage of ions only detected *in vivo*. This finding emphasizes the complexity of multi-species interactions and suggests the ant host plays an important role, in conjunction with *Pseudonocardia*, in mediating the chemistry involved in colony protection. The largest separation of metabolic fingerprints of compounds produced by *Pseudonocardia in vivo* occurred between the 2 colonies examined rather than in response to different pathogens. This may be a result of colony-specific responses to pathogen infection as well as an interplay between the ant host and bacterial mutualist. Morphological adaptations on the ant host and congruent molecular phylogenies of *Pseudonocardia* and the ant host are highly suggestive of coevolutionary dynamics between the two organisms (Cafaro et al. 2011; Cafaro and Currie 2005; Cameron R Currie et al. 2006, Li et al. 2018). Recent work demonstrated that *Pseudonocardia* derives its nutrition from the ant, suggesting a strong metabolic connection between the two organisms (Steffan et al., 2015). These specific associations between the ant and bacterium may be influencing the production of small molecules. Interactions between domains is not an uncommon occurrence, and these interactions often have profound ecological

consequences (Moree et al., 2012; Nihorimbere et al., 2012; Song et al., 2015). Overall these findings emphasize a dynamic association between *Pseudonocardia* and the ant host that may influence the production of small molecules that affect the ecology of this symbiotic system.

We also examine the hypothesis that different pathogens induce specific small molecule responses by *Pseudonocardia*. Indeed, we did observe unique ions in each strain of *Pseudonocardia* during different pathogen interactions, and unique ions are detected in every fungal pathogen treatment, both *in vivo* and *in vitro*. These results suggest that there may be system-specific (*Escovopsis*) small molecule induction by *Pseudonocardia* as well as general (*Escovopsis* and *Trichoderma*) fungal pathogen induction of small molecules. These pathogen-specific small molecules may be important in describing the variation of bacterial inhibition of fungal pathogens and other species interactions (Cafaro et al. 2011; Poulsen et al. 2010; Vetsigian, Jajoo, and Kishony 2011) and suggest that there is either variation in each strain's ability to recognize and/or respond to pathogen infections. It is possible that this variation within species interactions is due to gene regulation or post-translational modification changes between bacterial strains which could be explored in future studies (Goh et al., 2002; Tsui et al., 2004). These findings indicate the potential for seemingly identical strains of bacteria with different ecologies (i.e. different host associations) to produce diverse chemical compounds. The ecological approach outlined here may be a promising strategy to discover novel anti-fungal compounds.

Although the bacterial symbionts examined in this study have high genomic similarity, the metabolic profiles of each strain was surprisingly different, including in pure culture as well as in pair-wise pathogen interactions. *Pseudonocardia* sp. AOST16-01 and *Pseudonocardia* sp. AECC09-02 were respectively isolated from *A. octospinosus* and *A. echinator*, sympatric species of ants found in the Canal Zone of Panama. These ant species appear to host one of two *Pseudonocardia* phylotypes (Andersen et al. 2013; Holmes et al. 2016; Poulsen et al. 2005), and the 2 strains of *Pseudonocardia* used in this experiment identify as the same phylotype. Interestingly, MSI reveals shifted metabolic profiles between *Pseudonocardia* strains, indicating that the small molecule potential within a single phylotype may be more diverse than previously expected. This variation in metabolic response may have important implications on the nature of the attine ant-*Pseudonocardia* symbiosis.

It has long been recognized that species interactions help generate biological diversity. In microbes, species interactions are likewise important, but contemporary research has been largely limited to *in situ* natural history (*i.e.*, describing ‘who’ is there) or *in vitro* interactions (*i.e.*, examining interactions in culture conditions). Recent efforts to better understand microbial interactions have included experimental construction of microbial communities (Evans et al., 2017; Lewin et al., 2016; Lindemann et al., 2016; Tiunov & Scheu, 2005), mathematical modeling (Vetsigian et al., 2011; Zomorodi & Segrè, 2016), and *in vivo* manipulation experiments (Kastman et al., 2016; Khadempour et al., 2016; Martiny et al., 2017; Parker, Hrček, McLean, & Godfray, 2017; Turnbaugh et al., 2009; Wolfe, Button, Santarelli, & Dutton, 2014).

Here we examine chemical ecology of microbial interactions by combining *in vitro* and *in vivo* experimental manipulations and mass spectrometry imaging in the well-characterized fungus-growing ant symbiosis. Through this approach we show a surprisingly dynamic and diverse response in the microbial-derived small molecules associated with changes in a multi-species interaction network, including differential small molecule production between two exceedingly similar bacterial strains (*i.e.*, two strains sharing 99.98% sequence identity). The variation in microbial-produced small molecules seen here in two closely-related strains of *Pseudonocardia* suggests that the diversity of chemical communication may be vastly greater than expected (or predicated). This chemical variation may play a significant role in the evolution and maintenance of the symbiosis as there is the opportunity for selection to act on this variation. Through the utilization of ecological interactions, we see a diverse bacterial reaction to pathogenic fungi both *in vitro* and *in vivo*.

4.6 Acknowledgements

Support for this research was provided by the University of Wisconsin–Madison (UW-Madison), Office of the Vice Chancellor for Research and Graduate Education with funding from the Wisconsin Alumni Research Foundation (WARF). M.G.C. is supported by NIH National Research Service Award T32 GM008505. L.L. acknowledges an H. I. Romnes Faculty Research Fellowship and a Vilas Distinguished Achievement Professorship with funding provided by the WARF and UW-Madison School of Pharmacy. C.C. acknowledges NIH U19TW009872-01. E.G. acknowledges an NSF Graduate Research Fellowship (DGE-1256259). The MALDI-Orbitrap was purchased through an NIH shared instrument grant (NCRR S10RR029531).

4.7 Tables and figures

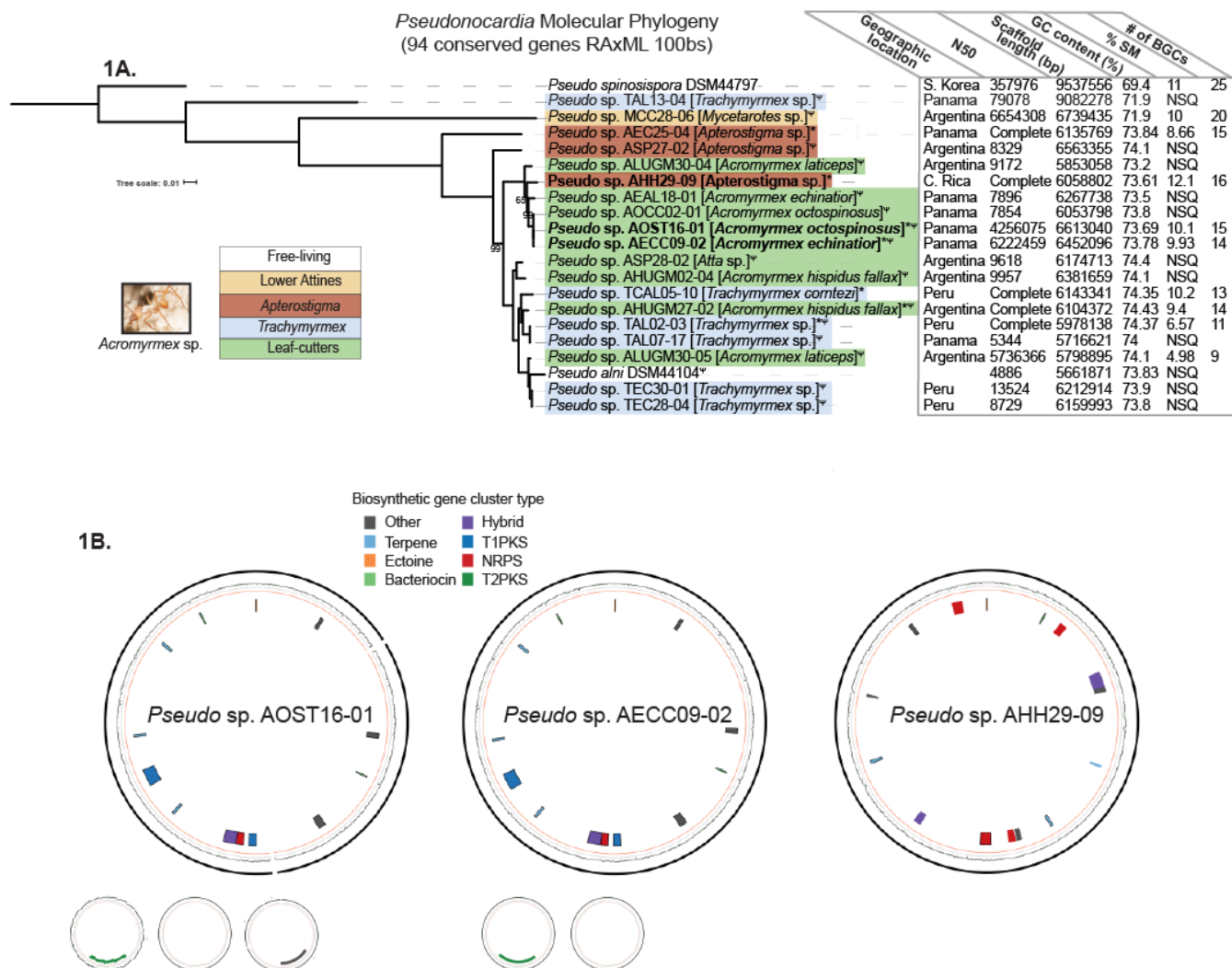


Figure 4.1 A) Molecular phylogeny of ant-associated *Pseudonocardia* using maximum likelihood methods on 94 conserved genes with 100 bootstraps (bootstrap values above 99 not shown). Color corresponds to ant host lineage (all *Acromyrmex* ants denoted by *A. species name*) and geographic location of ant host and genomic metadata are represented in table. Asterisks denote strains that were sequenced using PacBio sequencing technology; all other strains were Illumina sequenced. Ψ indicates strains sequenced in this study; *Pseudonocardia spinospora* DSM44797 (INSDC: [AUBB000000001](https://www.ncbi.nlm.nih.gov/nuccore/AUBB000000001)); all others were sequenced by Sit et al. 2015. SM (secondary metabolism); NSQ (not of sufficient quality). Photograph of *Acromyrmex* worker courtesy of Don Parsons bugpix@charter.net. B) Genome maps (chromosome and plasmids) of bolded strains from Figure 4a. Colored boxes indicate biosynthetic gene cluster type (type I polyketide synthase (T1PKS); type II polyketide synthase (T2PKS); hybrid= multiple cluster types) and relative location in the genome. Black, outer ring corresponds to each contig; inner black ring represents GC content (orange line=25% GC, gray=50% GC, green=75% GC).

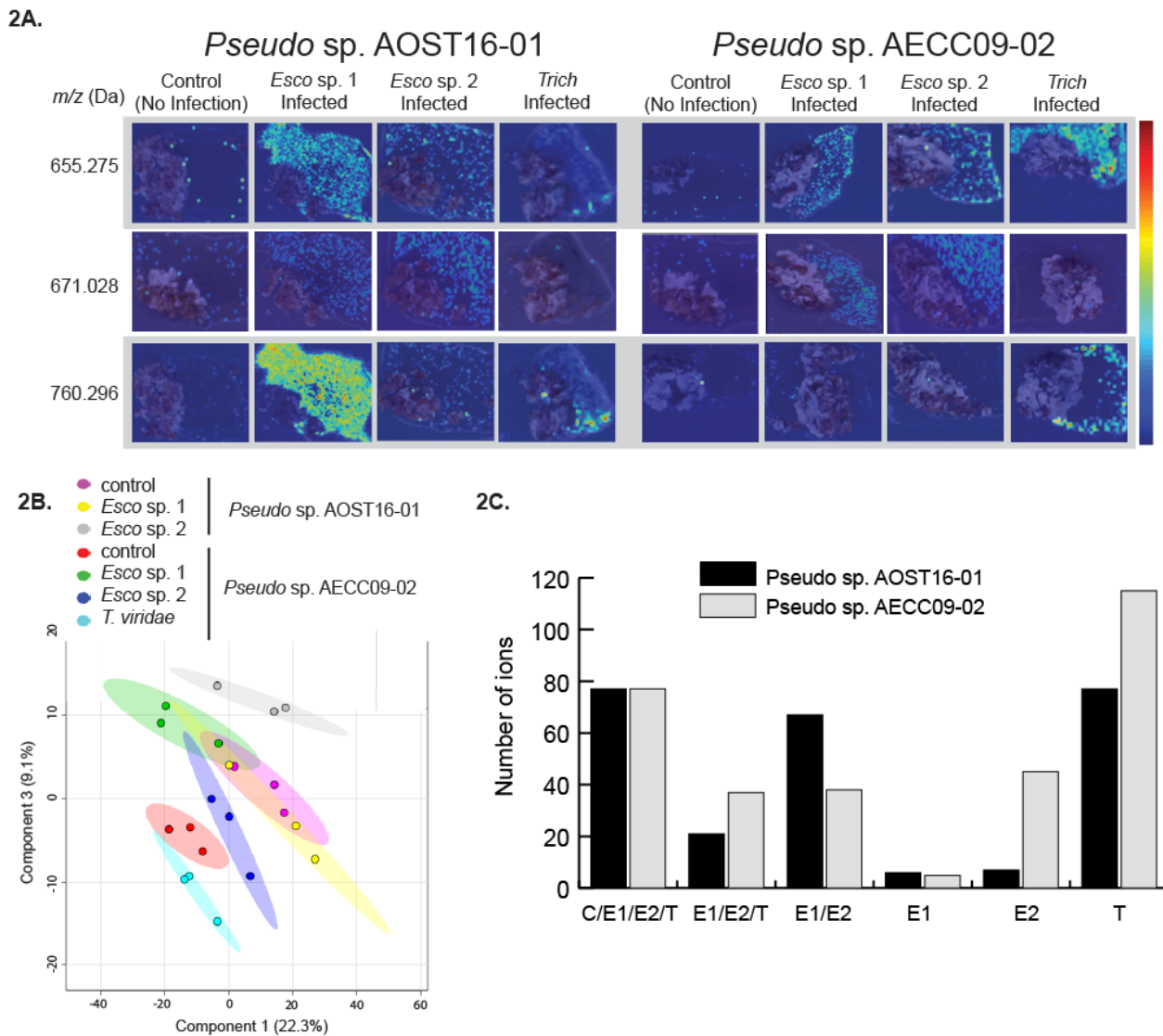


Figure 2.2 A) Representative MS images of *Pseudonocardia* co-cultures. Ion images are overlaid with optical images of each sample. Bacterial colonies are the lighter, textured areas and the surrounding agar is the smooth, dark blue background. Agar sections were excised next to the bacterial colony and fungal pathogens are not pictured. Control treatments represent *Pseudonocardia* grown in culture with no pathogen exposure. B) Partial Least Squares-Discriminant analysis (PLS-DA) of mass intensity spectra for each treatment group *in vitro* ($\geq m/z$ 300). Individual points represent one replicate. Shaded areas represent the 95% confidence area for each treatment ($R^2=0.96751$; $Q^2=0.726$). *Pseudonocardia* sp. AOST16-01 and the *T. viridae* treatment has been removed due to issues in MALDI acquisition. C) Number of unique ions specific to each combination of treatments in each strain of *Pseudonocardia* under *in vitro* conditions. C (control); E1 (*Escovopsis* sp. 1); E2 (*Escovopsis* sp. 2); T (*T. viridae*).

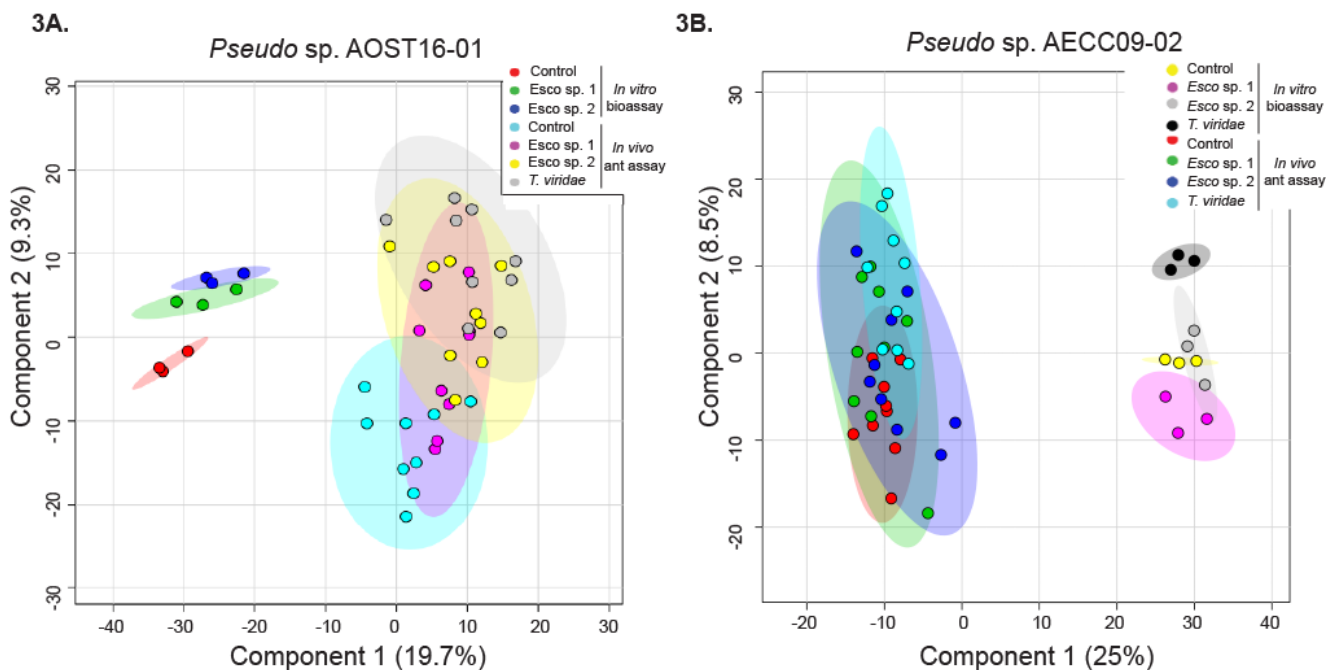


Figure 4.3 PLS-DA of mass intensity spectra for each treatment group *in vitro* and *in vivo* ($\geq m/z$ 300) for A) *Pseudonocardia* sp. AOST16-01 ($R^2=0.87044$; $Q^2=0.74962$) and B) *Pseudonocardia* sp. AECC09-02 ($R^2=0.85647$; $Q^2=0.744$). Control treatments represent *Pseudonocardia* with no pathogen exposure. Individual points represent one replicate, and shaded areas represent the 95% confidence area for each treatment. *Pseudonocardia* sp. AOST16-01 and the *T. viridae* *in vitro* treatment has been removed due to issues in MALDI acquisition.

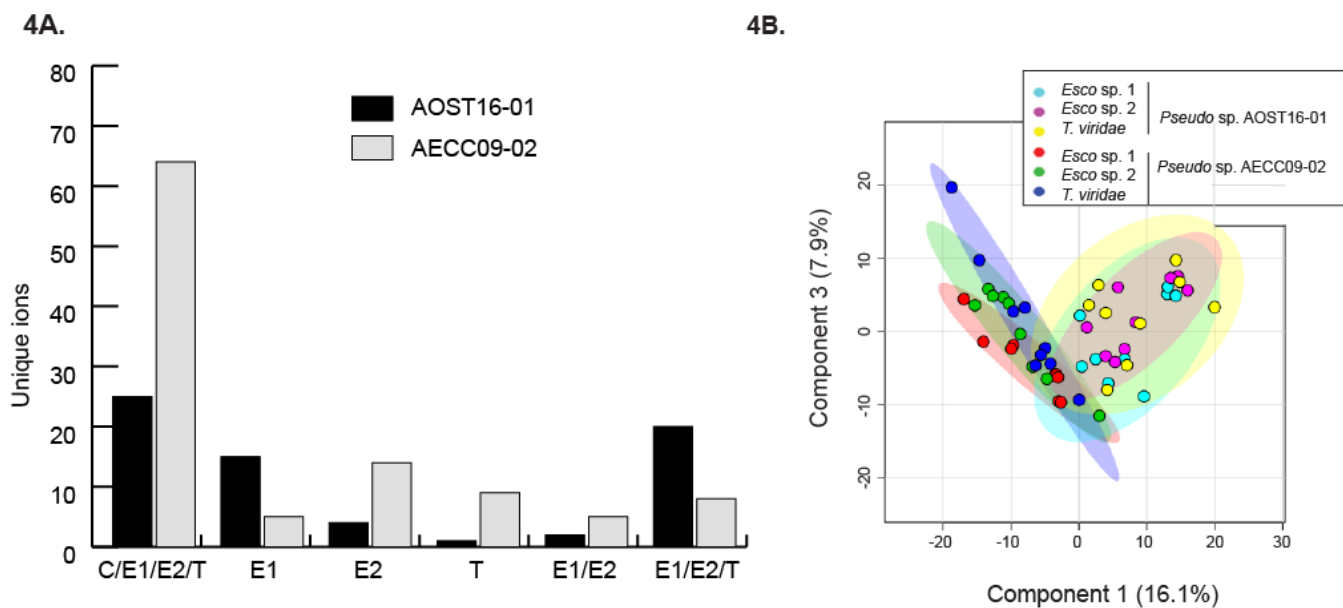


Figure 4.4 A) Number of unique ions in each combination of treatments in each strain of *Pseudonocardia* under *in vivo* conditions. C (control); E1 (*Escovopsis* sp. 1); E2 (*Escovopsis* sp. 2); T (*T. viridae*). B) PLS-DA of mass intensity spectra for each treatment group *in vivo* ($\geq m/z$ 300). Individual points represent one replicate. Shaded areas represent the 95% confidence area for each treatment ($R^2=0.9172$; $Q^2=0.66287$)

Table 4.1 Total number of m/z detected in each *Pseudonocardia* strain in *in vitro* and *in vivo* conditions. Ions detected *in vitro* are detected in 2 out of 3 replicates; ions detected *in vivo* are found in 6 out of 9 replicates.

	<i>Pseudonocardia</i> sp. AOST16-01				<i>Pseudonocardia</i> sp. AECC09-02				shared between strains <i>in situ</i>
	<i>in vitro</i>	<i>in vivo</i>	shared	% unique to <i>in vivo</i>	<i>in vitro</i>	<i>in vivo</i>	shared	% unique to <i>in vivo</i>	
Control	253	55	9	85.94%	158	98	15	86.73%	40
<i>Esco</i> sp. 1	306	59	31	65.56%	216	82	23	78.10%	54
<i>Esco</i> sp. 2	304	41	19	68.33%	263	104	35	74.82%	48
<i>T. viridae</i>	162	30	24	55.56%	229	86	29	74.78%	42

4.8 References

- Abdelmohsen, U. R., Grkovic, T., Balasubramanian, S., Kamel, M. S., Quinn, R. J., & Hentschel, U. (2015). Elicitation of secondary metabolism in actinomycetes. *Biotechnology Advances*, 33(6), 798–811. <http://doi.org/10.1016/J.BIOTECHADV.2015.06.003>
- Adnani, N., Chevrette, M. G., Adibhatla, S. N., Zhang, F., Yu, Q., Braun, D. R., ... Bugni, T. S. (2017). Coculture of Marine Invertebrate-Associated Bacteria and Interdisciplinary Technologies Enable Biosynthesis and Discovery of a New Antibiotic, Keyicin. *ACS Chemical Biology*, 12(12), 3093–3102. <http://doi.org/10.1021/acschembio.7b00688>
- Andersen, S. B., Hansen, L. H., Sapountzis, P., Sørensen, S. J., & Boomsma, J. J. (2013). Specificity and stability of the Acromyrmex-Pseudonocardia symbiosis. *Molecular Ecology*, 22(16), 4307–21. <http://doi.org/10.1111/mec.12380>
- Bérdy, J. (2005). Bioactive microbial metabolites. *The Journal of Antibiotics*, 58(1), 1–26. <http://doi.org/10.1038/ja.2005.1>
- Bertrand, S., Bohni, N., Schnee, S., Schumpp, O., Gindro, K., & Wolfender, J.-L. (2014). Metabolite induction via microorganism co-culture: A potential way to enhance chemical diversity for drug discovery. *Biotechnology Advances*, 32(6), 1180–1204. <http://doi.org/10.1016/J.BIOTECHADV.2014.03.001>
- Bertrand, S., Schumpp, O., Bohni, N., Monod, M., Gindro, K., & Wolfender, J.-L. (2013). De novo production of metabolites by fungal co-culture of *Trichophyton rubrum* and *Bionectria ochroleuca*. *Journal of Natural Products*, 76(6), 1157–65. <http://doi.org/10.1021/np400258f>
- Blin, K., Wolf, T., Chevrette, M. G., Lu, X., Schwalen, C. J., Kautsar, S. A., ... Medema, M. H. (2017). antiSMASH 4.0—improvements in chemistry prediction and gene cluster boundary identification. *Nucleic Acids Research*, 45(18), 1019–1037. <http://doi.org/10.1093/nar/gkx319>
- Cafaro, M. J., & Currie, C. R. (2005). Phylogenetic analysis of mutualistic filamentous bacteria associated with fungus-growing ants. *Canadian Journal of Microbiology*, 51(6), 441–6. <http://doi.org/10.1139/w05-023>
- Cafaro, M. J., Poulsen, M., Little, A. E. F., Price, S. L., Gerardo, N. M., Wong, B., ... Currie, C. R. (2011). Specificity in the symbiotic association between fungus-growing ants and protective *Pseudonocardia* bacteria. *Proceedings. Biological Sciences / The Royal Society*,

278(1713), 1814–22. <http://doi.org/10.1098/rspb.2010.2118>

- Carr, G., Derbyshire, E. R., Caldera, E., Currie, C. R., & Clardy, J. (2012). Antibiotic and antimalarial quinones from fungus-growing ant-associated *Pseudonocardia* sp. *Journal of Natural Products*, 75(10), 1806–9. <http://doi.org/10.1021/np300380t>
- Clardy, J., Fischbach, M. A., & Currie, C. R. (2009). The natural history of antibiotics. *Current Biology : CB*, 19(11), R437-41. <http://doi.org/10.1016/j.cub.2009.04.001>
- Currie, C. R., Bot, A. N. M., & Boomsma, J. J. (2003). Experimental evidence of a tripartite mutualism : bacteria protect ant fungus gardens from specialized parasites. *Oikos*, 1(July 2002), 91–102.
- Currie, C. R., Mueller, U. G., & Malloch, D. (1999). The agricultural pathology of ant fungus gardens. *Proceedings of the National Academy of Sciences*, 96(14), 7998–8002. <http://doi.org/10.1073/pnas.96.14.7998>
- Currie, C. R., Poulsen, M., Mendenhall, J., Boomsma, J. J., & Billen, J. (2006). Coevolved crypts and exocrine glands support mutualistic bacteria in fungus-growing ants. *Science (New York, N.Y.)*, 311(5757), 81–3. <http://doi.org/10.1126/science.1119744>
- Currie, C. R., & Scott, J. A. (1999). Fungus-growing ants use antibiotic-producing bacteria to control garden parasites, 398(April), 701–705.
- Diggie, S. P., Gardner, A., West, S. A., & Griffin, A. S. (2007). Evolutionary theory of bacterial quorum sensing: when is a signal not a signal? *Philosophical Transactions of the Royal Society of London. Series B, Biological Sciences*, 362(1483), 1241–9. <http://doi.org/10.1098/rstb.2007.2049>
- Eid, J., Fehr, A., Gray, J., Luong, K., Lyle, J., Otto, G., ... Turner, S. (2009). Real-Time DNA Sequencing from Single Polymerase Molecules. *Science*, 323(5910).
- Evans, R., Alessi, A. M., Bird, S., McQueen-Mason, S. J., Bruce, N. C., & Brockhurst, M. A. (2017). Defining the functional traits that drive bacterial decomposer community productivity. *The ISME Journal*. <http://doi.org/10.1038/ismej.2017.22>
- Fajardo, A., & Martínez, J. L. (2008). Antibiotics as signals that trigger specific bacterial responses. *Current Opinion in Microbiology*, 11(2), 161–7. <http://doi.org/10.1016/j.mib.2008.02.006>
- Galperin, M. Y., Makarova, K. S., Wolf, Y. I., & Koonin, E. V. (2015). Expanded microbial

- genome coverage and improved protein family annotation in the COG database. *Nucleic Acids Research*, 43(Database issue), D261-9. <http://doi.org/10.1093/nar/gku1223>
- Gemperline, E., Horn, H. A., DeLaney, K., Currie, C. R., & Li, L. (2017). Imaging with Mass Spectrometry of Bacteria on the Exoskeleton of Fungus-Growing Ants. *ACS Chemical Biology*, 12(8), 1980–1985. <http://doi.org/10.1021/acscchembio.7b00038>
- Goh, E.-B., Yim, G., Tsui, W., McClure, J., Surette, M. G., & Davies, J. (2002). Transcriptional modulation of bacterial gene expression by subinhibitory concentrations of antibiotics. *Proceedings of the National Academy of Sciences of the United States of America*, 99(26), 17025–30. <http://doi.org/10.1073/pnas.252607699>
- Holmes, N. A., Innocent, T. M., Heine, D., Bassam, M. Al, Worsley, S. F., Trottmann, F., ... Hutchings, M. I. (2016). Genome Analysis of Two Pseudonocardia Phylotypes Associated with Acromyrmex Leafcutter Ants Reveals Their Biosynthetic Potential. *Frontiers in Microbiology*, 7, 2073. <http://doi.org/10.3389/fmicb.2016.02073>
- Hyatt, D., Chen, G.-L., Locascio, P. F., Land, M. L., Larimer, F. W., & Hauser, L. J. (2010). Prodigal: prokaryotic gene recognition and translation initiation site identification. *BMC Bioinformatics*, 11, 119. <http://doi.org/10.1186/1471-2105-11-119>
- Kastman, E. K., Kamelamela, N., Norville, J. W., Cosetta, C. M., Dutton, R. J., & Wolfe, B. E. (2016). Biotic Interactions Shape the Ecological Distributions of Staphylococcus Species. *MBio*, 7(5), e01157-16. <http://doi.org/10.1128/mBio.01157-16>
- Katoh, K., & Standley, D. M. (2013). MAFFT multiple sequence alignment software version 7: improvements in performance and usability. *Molecular Biology and Evolution*, 30(4), 772–80. <http://doi.org/10.1093/molbev/mst010>
- Khadempour, L., Burnum-Johnson, K. E., Baker, E. S., Nicora, C. D., Webb-Robertson, B.-J. M., White, R. A., ... Currie, C. R. (2016). The fungal cultivar of leaf-cutter ants produces specific enzymes in response to different plant substrates. *Molecular Ecology*, 25(22), 5795–5805. <http://doi.org/10.1111/mec.13872>
- Kinkel, L. L., Schlatter, D. C., Xiao, K., & Baines, A. D. (2014). Sympatric inhibition and niche differentiation suggest alternative coevolutionary trajectories among Streptomyces. *The ISME Journal*, 8(2), 249–56. <http://doi.org/10.1038/ismej.2013.175>
- Kurtz, S., Phillippy, A., Delcher, A. L., Smoot, M., Shumway, M., Antonescu, C., & Salzberg, S. L. (2004). Versatile and open software for comparing large genomes. *Genome Biology*, 5(2), R12. <http://doi.org/10.1186/gb-2004-5-2-r12>

- Laatsch, H. (2014). AntiBase 2014: The Natural Compound Identifier.
- Lewin, G. R., Johnson, A. L., Soto, R. D. M., Perry, K., Book, A. J., Horn, H. A., ... Currie, C. R. (2016). Cellulose-Enriched Microbial Communities from Leaf-Cutter Ant (*Atta colombica*) Refuse Dumps Vary in Taxonomic Composition and Degradation Ability. *PLOS ONE*, *11*(3), e0151840. <http://doi.org/10.1371/journal.pone.0151840>
- Li, H., Sosa-Calvo, J., Horn, H. A., Pupo, M. T., Clardy, J., Rabeling, C., ... Currie, C. R. (2018). Convergent evolution of complex structures for ant-bacterial defensive symbiosis in fungus-farming ants. *Proceedings of the National Academy of Sciences of the United States of America*, 201809332. <http://doi.org/10.1073/pnas.1809332115>
- Linares, J. F., Gustafsson, I., Baquero, F., & Martinez, J. L. (2006). Antibiotics as intermicrobial signaling agents instead of weapons. *Proceedings of the National Academy of Sciences of the United States of America*, *103*(51), 19484–9. <http://doi.org/10.1073/pnas.0608949103>
- Lindemann, S. R., Bernstein, H. C., Song, H.-S., Fredrickson, J. K., Fields, M. W., Shou, W., ... Beliaev, A. S. (2016). Engineering microbial consortia for controllable outputs. *The ISME Journal*, *10*(9), 2077–2084. <http://doi.org/10.1038/ismej.2016.26>
- Martiny, J. B., Martiny, A. C., Weihe, C., Lu, Y., Berlemont, R., Brodie, E. L., ... Allison, S. D. (2017). Microbial legacies alter decomposition in response to simulated global change. *The ISME Journal*, *11*(2), 490–499. <http://doi.org/10.1038/ismej.2016.122>
- Moree, W. J., Phelan, V. V, Wu, C.-H., Bandeira, N., Cornett, D. S., Duggan, B. M., & Dorrestein, P. C. (2012). Interkingdom metabolic transformations captured by microbial imaging mass spectrometry. Moree, W. J., Phelan, V. V, Wu, C.-H., Bandeira, N., Cornett, D. S., Duggan, B. M., & Dorrestein, P. C. (2012). Interkingdom metabolic transformations captured by micro. *Proceedings of the National Academy of Sciences of the United States of America*, *109*(34), 13811–6. <http://doi.org/10.1073/pnas.1206855109>
- Mueller, U. G., Scott, J. J., Ishak, H. D., Cooper, M., Rodrigues, A., Mueller, U., ... Hartl, D. (2010). Monoculture of Leafcutter Ant Gardens. *PLoS ONE*, *5*(9), e12668. <http://doi.org/10.1371/journal.pone.0012668>
- Nihorimbere, V., Cawoy, H., Seyer, A., Brunelle, A., Thonart, P., & Ongena, M. (2012). Impact of rhizosphere factors on cyclic lipopeptide signature from the plant beneficial strain *Bacillus amyloliquefaciens* S499. *FEMS Microbiology Ecology*, *79*(1), 176–91. <http://doi.org/10.1111/j.1574-6941.2011.01208.x>
- Nurk, S., Bankevich, A., Antipov, D., Gurevich, A. A., Korobeynikov, A., Lapidus, A., ...

- Pevzner, P. A. (2013). Assembling single-cell genomes and mini-metagenomes from chimeric MDA products. *Journal of Computational Biology : A Journal of Computational Molecular Cell Biology*, 20(10), 714–37. <http://doi.org/10.1089/cmb.2013.0084>
- Nygaard, S., Hu, H., Li, C., Schiøtt, M., Chen, Z., Yang, Z., ... Tunlid, A. (2016). Reciprocal genomic evolution in the ant–fungus agricultural symbiosis. *Nature Communications*, 7, 12233. <http://doi.org/10.1038/ncomms12233>
- O’Brien, J., & Wright, G. D. (2011). An ecological perspective of microbial secondary metabolism. *Current Opinion in Biotechnology*, 22(4), 552–8. <http://doi.org/10.1016/j.copbio.2011.03.010>
- Oh, D.-C., Poulsen, M., Currie, C. R., & Clardy, J. (2009). Dentigerumycin: a bacterial mediator of an ant–fungus symbiosis. *Nature Chemical Biology*, 5(6), 391–3. <http://doi.org/10.1038/nchembio.159>
- Palmer, A., Phapale, P., Chernyavsky, I., Lavigne, R., Fay, D., Tarasov, A., ... Alexandrov, T. (2017). FDR-controlled metabolite annotation for high-resolution imaging mass spectrometry. *Nature Methods*, 14(1), 57–60. <http://doi.org/10.1038/nmeth.4072>
- Parker, B. J., Hrčák, J., McLean, A. H. C., & Godfray, H. C. J. (2017). Genotype specificity among hosts, pathogens, and beneficial microbes influences the strength of symbiont-mediated protection. *Evolution*, 71(5), 1222–1231. <http://doi.org/10.1111/evo.13216>
- POULSEN, M., CAFARO, M., BOOMSMA, J. J., & CURRIE, C. R. (2005). Specificity of the mutualistic association between actinomycete bacteria and two sympatric species of *Acromyrmex* leaf-cutting ants. *Molecular Ecology*, 14(11), 3597–3604. <http://doi.org/10.1111/j.1365-294X.2005.02695.x>
- Poulsen, M., Cafaro, M. J., Erhardt, D. P., Little, A. E. F., Gerardo, N. M., Tebbets, B., ... Currie, C. R. (2010). Variation in *Pseudonocardia* antibiotic defence helps govern parasite-induced morbidity in *Acromyrmex* leaf-cutting ants. *Environmental Microbiology Reports*, 2(4), 534–540. <http://doi.org/10.1111/j.1758-2229.2009.00098.x>
- Robichaud, G., Garrard, K. P., Barry, J. A., & Muddiman, D. C. (2013). MSiReader: an open-source interface to view and analyze high resolving power MS imaging files on Matlab platform. *Journal of the American Society for Mass Spectrometry*, 24(5), 718–21. <http://doi.org/10.1007/s13361-013-0607-z>
- Romero, D., Traxler, M. F., López, D., & Kolter, R. (2011). Antibiotics as signal molecules. *Chemical Reviews*, 111(9), 5492–505. <http://doi.org/10.1021/cr2000509>

- Schoenian, I., Spitteller, M., Ghaste, M., Wirth, R., Herz, H., & Spitteller, D. (2011). Chemical basis of the synergism and antagonism in microbial communities in the nests of leaf-cutting ants. *Proceedings of the National Academy of Sciences of the United States of America*, *108*(5), 1955–60. <http://doi.org/10.1073/pnas.1008441108>
- Seyedsayamdost, M. R., Traxler, M. F., Clardy, J., & Kolter, R. (2012). *Natural Product Biosynthesis by Microorganisms and Plants, Part C. Methods in enzymology* (Vol. 517). Elsevier. <http://doi.org/10.1016/B978-0-12-404634-4.00005-X>
- Sit, C. S., Ruzzini, A. C., Van Arnem, E. B., Ramadhar, T. R., Currie, C. R., & Clardy, J. (2015). Variable genetic architectures produce virtually identical molecules in bacterial symbionts of fungus-growing ants. *Proceedings of the National Academy of Sciences*, *112*(43), 13150–13154. <http://doi.org/10.1073/pnas.1515348112>
- Skinnider, M. A., Dejong, C. A., Rees, P. N., Johnston, C. W., Li, H., Webster, A. L. H., ... Magarvey, N. A. (2015). Genomes to natural products PRediction Informatics for Secondary Metabolomes (PRISM). *Nucleic Acids Research*, *43*(20), 9645–62. <http://doi.org/10.1093/nar/gkv1012>
- Song, C., Mazzola, M., Cheng, X., Oetjen, J., Alexandrov, T., Dorrestein, P., ... Trede, D. (2015). Molecular and chemical dialogues in bacteria-protozoa interactions. *Scientific Reports*, *5*, 12837. <http://doi.org/10.1038/srep12837>
- Steffan, S. A., Chikaraishi, Y., Currie, C. R., Horn, H., Gaines-Day, H. R., Pauli, J. N., ... Ohkouchi, N. (2015). Microbes are trophic analogs of animals. *Proceedings of the National Academy of Sciences*, *112*(49), 201508782. <http://doi.org/10.1073/pnas.1508782112>
- Stubbendieck, R. M., Vargas-Bautista, C., & Straight, P. D. (2016). Bacterial Communities: Interactions to Scale. *Frontiers in Microbiology*, *7*, 1234. <http://doi.org/10.3389/fmicb.2016.01234>
- Tiunov, A. V., & Scheu, S. (2005). Facilitative interactions rather than resource partitioning drive diversity-functioning relationships in laboratory fungal communities. *Ecology Letters*, *8*(6), 618–625. <http://doi.org/10.1111/j.1461-0248.2005.00757.x>
- Traxler, M. F., & Kolter, R. (2015). Natural products in soil microbe interactions and evolution. *Natural Product Reports*, *32*(7), 956–970. <http://doi.org/10.1039/C5NP00013K>
- Traxler, M. F., Seyedsayamdost, M. R., Clardy, J., & Kolter, R. (2012). Interspecies modulation

- of bacterial development through iron competition and siderophore piracy. *Molecular Microbiology*, *86*(3), 628–44. <http://doi.org/10.1111/mmi.12008>
- Traxler, M. F., Watrous, J. D., Alexandrov, T., Dorrestein, P. C., & Kolter, R. (2013). Interspecies interactions stimulate diversification of the *Streptomyces coelicolor* secreted metabolome. *MBio*, *4*(4), e00459-13-. <http://doi.org/10.1128/mBio.00459-13>
- Tsui, W. H. W., Yim, G., Wang, H. H., McClure, J. E., Surette, M. G., & Davies, J. (2004). Dual effects of MLS antibiotics: transcriptional modulation and interactions on the ribosome. *Chemistry & Biology*, *11*(9), 1307–16. <http://doi.org/10.1016/j.chembiol.2004.07.010>
- Turnbaugh, P. J., Ridaura, V. K., Faith, J. J., Rey, F. E., Knight, R., & Gordon, J. I. (2009). The Effect of Diet on the Human Gut Microbiome: A Metagenomic Analysis in Humanized Gnotobiotic Mice. *Science Translational Medicine*, *1*(6). Retrieved from <http://stm.sciencemag.org/content/1/6/6ra14.short>
- Van Arnam, E. B., Ruzzini, A. C., Sit, C. S., Horn, H., Pinto-Tomás, A. A., Currie, C. R., & Clardy, J. (2016). Selvamycin, an atypical antifungal polyene from two alternative genomic contexts. *Proceedings of the National Academy of Sciences of the United States of America*, *113*(46), 12940–12945. <http://doi.org/10.1073/pnas.1613285113>
- Vetsigian, K., Jajoo, R., & Kishony, R. (2011). Structure and evolution of *Streptomyces* interaction networks in soil and in silico. *PLoS Biology*, *9*(10), e1001184. <http://doi.org/10.1371/journal.pbio.1001184>
- Weber, N. A. (1966). Fungus-growing ants. *Science (New York, N.Y.)*, *153*(3736), 587–604. <http://doi.org/10.1126/science.153.3736.587>
- Wolfe, B. E., Button, J. E., Santarelli, M., & Dutton, R. J. (2014). Cheese Rind Communities Provide Tractable Systems for In Situ and In Vitro Studies of Microbial Diversity. *Cell*, *158*(2), 422–433. <http://doi.org/10.1016/j.cell.2014.05.041>
- Xia, J., Psychogios, N., Young, N., & Wishart, D. S. (2009). MetaboAnalyst: a web server for metabolomic data analysis and interpretation. *Nucleic Acids Research*, *37*(Web Server issue), W652-60. <http://doi.org/10.1093/nar/gkp356>
- Xia, J., Sinelnikov, I. V., Han, B., & Wishart, D. S. (2015). MetaboAnalyst 3.0--making metabolomics more meaningful. *Nucleic Acids Research*, gkv380-. <http://doi.org/10.1093/nar/gkv380>

- Yang, J. Y., Phelan, V. V., Simkovsky, R., Watrous, J. D., Trial, R. M., Fleming, T. C., ... Dorrestein, P. C. (2012). Primer on agar-based microbial imaging mass spectrometry. *Journal of Bacteriology*, *194*(22), 6023–8. <http://doi.org/10.1128/JB.00823-12>
- Yim, G., Wang, H. H., & Davies, J. (2007). Antibiotics as signalling molecules. *Philosophical Transactions of the Royal Society of London. Series B, Biological Sciences*, *362*(1483), 1195–200. <http://doi.org/10.1098/rstb.2007.2044>
- Zhou, B., Wang, J., Ransom, H. W., Cui, Q., Lewis, I., Hegeman, A., ... Beger, R. (2012). MetaboSearch: Tool for Mass-Based Metabolite Identification Using Multiple Databases. *PLoS ONE*, *7*(6), e40096. <http://doi.org/10.1371/journal.pone.0040096>
- Zomorodi, A. R., & Segrè, D. (2016). Synthetic Ecology of Microbes: Mathematical Models and Applications. *Journal of Molecular Biology*, *428*(5), 837–861. <http://doi.org/10.1016/j.jmb.2015.10.019>

Chapter 5

Partner fidelity of host-microbe symbiosis influences small molecule production *in vivo* in the leaf-cutter ant symbiosis

Authors: Heidi A. Horn, Kellen Delaney, Erin Gemperline, Linjun Li, and Cameron R. Currie

Author contributions: conceptualized experiment (HAH, CRC), designed experiment (HAH) performed field work and experimental manipulations (HAH), performed mass spectrometry (KD, EG), analyzed data (HAH, KD), performed statistical analysis (HAH), wrote manuscript (HAH, KD, LL, CRC).

*This chapter is in preparation for submission

5.1 Abstract

Host-microbe symbioses are ubiquitous and greatly influence the evolution of eukaryotes. The dynamics of a host-microbe association are important to establish as microbial strain diversity and specificity can influence the ecology of the host. Here, we use the well-characterized leaf-cutter ant symbiosis, to ask questions regarding how host-microbe partner fidelity influences the ecology of the system. Leaf-cutter ants maintain a fungus that they cultivate as their main food source. To help defend their fungal cultivar from pathogens, these ants maintain an antibiotic-producing bacterium, *Pseudonocardia*, on their exoskeleton. Little is known about how the association is maintained or how the interaction between the two organisms influences antibiotic production by *Pseudonocardia*. Here we ask how manipulations of the host-symbiont association in *Acromyrmex* leaf-cutter ants influence *Pseudonocardia*-produced small molecules. We perform imaging mass spectrometry to identify the small molecule profiles in conspecific ant-bacterial switches, between colonies of *Acromyrmex echinator*, and allospecific switches,

between *A. echinator* and *A. octospinosus* colonies. We find no consistent difference in the small molecule profiles in conspecific switches, suggesting there is no significant influence of host-microbe association on conspecific pairings. In contrast, comparisons of small molecule profiles in allospecific switches produce variable results. There is some separation of metabolic fingerprints in one switch but not in the remaining allospecific switches. These results indicate a complex relationship between ant host species and *Pseudonocardia* strain may be influencing small molecule production in the leaf-cutter ant system.

5.2 Introduction

Microbes greatly influence the ecological functions of their hosts. Crucial to understanding how host-microbe interactions evolve and are maintained is characterizing the influence of microbial strain diversity on the ecological outcomes of their host. A holobiont theory has emerged that posits that a host and its associated microbial community are a unit upon which selection may act. This idea has garnered controversy as the theory disregards the effect microbial strain variation has on host ecology (Doolittle & Booth, 2017; Douglas & Werren, 2016; Rosenberg & Zilber-Rosenberg, 2018; Theis et al., 2016; Zilber-Rosenberg & Rosenberg, 2008). Characterization of how microbial strain diversity and specificity influences the ecological function of a host is needed to evaluate these assumptions. While exploration of the effects of diverse microbial symbiotic communities, such as in the gastrointestinal tract of animals, on host ecology is challenging, studies focusing on comparatively simpler associations, such as pairwise host-microbe interactions, can inform how microbial strain diversity influences hosts. Here, we examine how the interaction between a leaf-cutter ant and its bacterial mutualist influences small molecule production.

Fungus-growing ants are well-known for maintaining several microbial partners. These Neotropical ants grow and cultivate a basidiomycetous fungus as their sole food source (Hölldobler & Wilson, 1990; Weber, 1966). To defend their fungal cultivar from disease, the ants have evolved defense mechanisms to protect it, including a mutualistic association with a bacterium, *Pseudonocardia*. *Pseudonocardia* is an exosymbiont and resides on the ant exoskeleton. The ant provides nutrients to the bacterium (Steffan et al., 2015), which in exchange produces antibiotic molecules to protect the colony from infection (Cameron R Currie & Scott, 1999). Removal of *Pseudonocardia* from the ant results in greater pathogen overgrowth in the colony (C R Currie, Bot, & Boomsma, 2003). Some of the antimicrobial molecules produced by *Pseudonocardia* have been characterized (Carr, Derbyshire, Caldera, Currie, & Clardy, 2012; Oh, Poulsen, Currie, & Clardy, 2009; Van Arnam et al., 2016) although the variation and full diversity of compounds is unknown. Genomic analysis, phylogenetics, and inhibition bioassays indicate that *Pseudonocardia* produces variable antibiotic small molecules (Cafaro et al., 2011; Cafaro & Currie, 2005; Holmes et al., 2016; Sit et al., 2015; McDonald et al., in prep). While there is great diversity in the biosynthetic gene potential in ant-associated *Pseudonocardia*, the influence of the interaction between ant host and *Pseudonocardia*, which is likely influencing small molecule production, is largely unknown.

Pseudonocardia is transmitted from worker to worker, and for successful acquisition callow workers must be exposed to the symbiont within a 1-2 hour window following eclosion (Marsh, Poulsen, Pinto-Tomás, & Currie, 2014). Symbiont acquisition can be altered using a cross-fostering approach during this window and is a powerful experimental tool. Cross-fostering experiments between two ant hosts, where workers from one colony raise a pupa from an allospecific colony (Armitage, Broch, Marín, Nash, & Boomsma, 2011), reveals differences in

the colonizing ability of different strains of *Pseudonocardia* (Sandra B Andersen, Yek, Nash, & Boomsma, 2015). *Acromyrmex echinator* and *A. octospinosus* in Panama appear to maintain one of two genomically similar phylotypes of *Pseudonocardia*, PS1 and PS2 (Holmes et al., 2016), however PS2 is a better colonizer and grows to greater abundance on the ant host in cross-fostering experiments (Sandra B Andersen et al., 2015). Other species of *Acromyrmex* ants, that maintain more diverse lineages of *Pseudonocardia*, are also able to acquire non-native *Pseudonocardia* in cross-fostering experiments yet at a lower abundance compared to their native association (Bruner, unpublished). These results suggest that interaction between ant host and *Pseudonocardia* can influence the abundance of the symbiont and perhaps influencing the ecology of the system. It is unknown if the interaction between the two is also influencing the small molecules *Pseudonocardia* produces to protect the system from disease. Here we use a newly developed imaging mass spectrometry technique (Gemperline, Horn, DeLaney, Currie, & Li, 2017) to assess small molecule profiles produced by *Pseudonocardia* on the ant host during native and non-native host-symbiont pairings.

To determine if host-symbiont interactions influence antimicrobial production, we ask if the interactions between ant and *Pseudonocardia* at two different ant host levels influence the small molecules that *Pseudonocardia* produces. We perform ant-bacterial switches in which ants maintain bacteria from another host colony and then compared small molecule profiles of the resulting switched host-symbiont pairs under disease conditions. We first ask if ants of the same species (*Acromyrmex echinator*) but different colonies (conspecific switches) produce different small molecules when the same strain of bacterium is maintained. Secondly, we perform symbiont switches between two ant species (*Acromyrmex echinator* and *Acromyrmex*

octospinosus) to determine if the small molecule response to pathogen infection is maintained when ant host species (allospecific switches) are switched.

5.3 Methods

5.3.1 Colony collection and maintenance

Colonies of *Acromyrmex echinator* and *A. octospinosus* were collected in Gamboa, Panama in October 2015 (**Figure 5.1**). They were housed in laboratory conditions (approximately 27°C) for the duration of the experiment and fed hibiscus leaves and flower petals, polenta, and oats *ad libitum*. Ant-symbiont switches occurred at two ant host levels: switches between ant colonies of the same species, *A. echinator* (conspecific switches) (**Figure 5.2**) and switches between ant colonies of different species, *A. echinator* and *A. octospinosus* (allospecific switches) (**Figure 5.3**).

5.3.2 Conspecific switches

Five colonies of *A. echinator* were chosen for the conspecific switches: A.e col1, A.e col2, A.e col3, A.e col4, A.e col5 (**Table 5.1**). Colonies were chosen based on the size and health of the colony—only large colonies, which contained a large amount of brood, that were incorporating leaf-material were used. Host-symbiont switches occurred by creating subcolonies to cross-foster pupae (Armitage et al., 2011). A subcolony consisted of a Petri plate containing a plastic weigh boat filled with 1-5 g of fungus garden. Fungus garden was the same for all subcolonies and came from one host colony: an *Acromyrmex echinator* colony with colony code GB102315-02. A pupa of one colony (from either A.e col1, A.e col2, or A.e col3) was placed inside the fungus garden and workers, 6 minors and 2 majors, from a confocal colony were added to the subcolony. A positive control included a pupa and workers from the same colony; a

negative control included a focal pupa raised by *Atta colombica* workers (colony code Atta col7), another genus of leaf-cutter ant. *Atta* do not possess the external symbiont therefore there is no *Pseudonocardia* transmission. Subcolonies were monitored until the pupa reached eclosion and then the developing ant was moved to its own subcolony in isolation. The focal ant remained in the subcolony until there was a full bloom of *Pseudonocardia* on the exoskeleton (a 12 on the scale according to Poulsen et al. 2003). Focal ants that were part of the negative control treatment (acquired no bacterial symbiont) developed for 2 weeks when bloom is typically at its peak. This protocol was performed on ants from each of 3 colonies (A.e col1, A.e. col2, A.e col3) such that ants from one colony maintained *Pseudonocardia* from each of 4 other colonies (**Figure 5.2**). Eight pupae and subcolonies were prepared for each treatment (combination of ant-*Pseudonocardia* pairing), although not all 8 pupae survived to maturity. An individual colony (A.e col1, A.e col2, or A.e col3) is considered one replicate.

Once the focal ant developed full bacterial bloom, the subcolony was infected with the pathogen, *Escovopsis*. All subcolonies were infected with the same strain of *Escovopsis* which was isolated from a colony A.e col1 following the protocol of Currie et al 1999a. Once isolated, *Escovopsis* was grown on potato dextrose agar (Potato Dextrose Medium (39 g Potato Dextrose Medium, 15 g agar in 1 L distilled H₂O) for one week prior to infection. Infection occurred by taking dry spores from a 6 mm² area with an inoculation loop and rubbing the dry spores of the fungus garden of the subcolony. Infection occurred for 20 hours after which the focal ant was removed and preserved at -80°C until further processing.

5.3.3 *Allopecific switches*

The above cross-fostering protocol was also followed for colonies of two different ant host species. Colonies of *A. echinator* and *A. octospinosus* were chosen for these host-symbiont

switches (**Table 5.1; Figure 5.3**). Reciprocal switches were performed on colonies A.e. col1 and A.o col1 and are considered replicate 1 (**Figure 5.3**). A second replicate was performed with reciprocal switches in A.e col2 and A.o col2; a third replicate was performed with colonies A.e col6 and A.o col3 (**Figure 5.3**). *Escovopsis* infection occurred as described above and ants were removed and stored at -80°C until further processing. Samples were shipped from the Smithsonian Tropical Research Institute in Gamboa, Panama to the University of Wisconsin-Madison on dry ice.

5.3.4 MALDI mass spectrometry imaging

Ants that were removed from their colony were frozen at -80°C and prepared for MALDI-MSI as described elsewhere (Gemperline et al., 2017). Briefly, ants were dissected by removing the thorax from the rest of the body with a razor blade. The ants were placed on plain glass microscope slides that had a grooved surface cut into them. The ants were secured to the slides with double-sided tape placed on the back of the slide, with the propleural plate facing upward. To prevent the ants' position from shifting during imaging acquisition, a piece of tape was also placed on the thorax below the propleural plate. 2,5-dihydroxybenzoic acid (DHB, Acros Organics, Morris, New Jersey) matrix (40 mg/mL dissolved in 50:50 methanol water) was applied using a TM sprayer (HTX Technologies, LLC, Carraboro, NC) using 8 passes at 80 °C and 0.2 mL/min flow rate, with a spray velocity of 950 mm/min and 30 s dry time between passes.

Ant samples were run on a MALDI-LTQ-Orbitrap XL mass spectrometer (Thermo Scientific, Bremen, Germany) in positive-ion mode with a mass-to-charge ratio (m/z) range of 300 to 1700 and 25 kJ laser energy. The instrument was equipped with a 337.1 nm, 60 Hz nitrogen laser. Optical images were obtained by an HP scanner and imported into the LTQ tune

page. A raster plate motion was used with a step size of 75 μm to acquire MS images of the ant propleural plates.

5.3.5 Data analysis

Resulting raw MS data was loaded into Thermo ImageQuest (Thermo Scientific, Bremen, Germany) and exported as imzml files using profile mode. The files were then loaded into MSiReader (Robichaud, Garrard, Barry, & Muddiman, 2013), normalized to the total ion current (TIC), and smoothed with 5th order linear smoothing. The scanned optical image was then overlaid on the MS image. The software's peak-finder tool was used to generate a list of m/z values of peaks present in more than 10% of the propleural plate and less than 1% of the background or with an average intensity ratio greater than 1000. Images were generated for each m/z value. The images were then manually inspected to ensure that each was due to signal from the propleural plate and not matrix or background interference or the exoskeleton of the ant.

Statistical analyses were performed using Metaboanalyst (J. Xia, Sinelnikov, Han, & Wishart, 2015; Jianguo Xia, Psychogios, Young, & Wishart, 2009). Principal component analysis (PCA) was performed with the following parameters: mass peak lists were analyzed with a mass tolerance of 0.003 m/z and retention time tolerance set to 1. Data were filtered using standard deviation to eliminate non-informative variables and then normalized by sum and auto-scaled. Principal component analysis and partial least squares discriminant analysis (PLS-DA) were performed on the normalized data. Two-way permutational analysis of variance (PERMANOVA) was performed on data with mass intensities removed using PAST (Hammer, Ryan, Hammer, & Harper, 2001). Groups were designated either as ant host colony or *Pseudonocardia* strain.

5.4 Results

5.4.1 Conspecific switches

Small molecule profiles were compared across *A. echinator* colonies with each ant-*Pseudonocardia* pairing. Principal component analysis was performed for each colony replicate, n=3 (**Figure 5.4 a**). The PCA for colony 1 shows no separation of profiles when *Pseudonocardia* from non-native colonies resides on ants from colony 1 (**Figure 5.4 a**). Similarly, colonies 2 and 3 also show no separation of profiles in a PCA – there is no distinct fingerprint for any ant-*Pseudonocardia* pairing (**Figure 5.4 b,a**). Furthermore, within treatment variation is approximately equal to between treatment variation for each replicate. Partial least squares discriminant analysis was performed on the same groupings and separation of small molecule fingerprints is observed (**Figure 5.5**). However these models are overfit as observed by large Q^2 values (A.e col1: $R^2=0.99481$, $Q^2=0.21285$; A.e. col2: $R^2=0.99405$, $Q^2=0.64133$; A.e col3: $R^2=0.87224$, $Q^2=0.075956$) and the observed separation is an artifact of overfitting.

Small molecule fingerprints were also compared using *Pseudonocardia* strain as the group assignment rather than ant host. Again, there is no observed separation of profiles across all three replicates (**Figure 5.4 b**). Variation within replicates is again approximately equal to variation between treatments (**Figure 5.4 b**).

5.4.2 Allospecific switches

Similarly, small molecule fingerprints were compared for two allospecific switches (**Figure 5.6 a,b**). A PCA of replicate one shows separation of small molecule fingerprints of all treatments: the *A. echinator* native pairing, *A. echinator* allospecific switch, *A. octospinosus* native pairing, and the *A. octospinosus* allospecific switch all have distinct profiles (**Figure 5.6**

a). A two-way PERMANOVA of these groups reveals a significant colony effect ($F=1.0708$; $p=0.0056$) and *Pseudonocardia* effect ($F=1.1292$; $p=0.0016$) (**Figure 5.6 a**). An interaction between the two components is also observed ($p=0.0405$).

Interestingly, a second replicate (an allospecific switch with two different colonies of *A. echinator* and *A. octospinosus*) reveals a different pattern. Small molecule fingerprints show no separation when compared in a PCA. Further, there is no significant colony or *Pseudonocardia* effect in a two-way PERMANOVA ($F=1.001$, $p=0.226$ and $F=0.93642$, $p=0.5072$ respectively). There is also no interaction between colony and *Pseudonocardia* ($p=0.7886$) (**Figure 5.6 b**).

A third replicate of allospecific switches was performed, although PCA could not be performed because one treatment group had too few ant pseudo-replicates. However, a two-way PERMANOVA indicates there is a significant *Pseudonocardia* effect in this replicate ($F=1.111$, $p=0.0099$) but no ant host colony effect ($F=0.81953$, $p=0.8287$). There is also no interaction effect between ant colony and *Pseudonocardia* in this replicate ($p=0.5668$).

5.5 Discussion

Here we performed host-symbiont switches in the leaf-cutter ants *A. echinator* and *A. octospinosus* to determine the effect of the interaction between host ant genotype and microbial strain on bacterial small molecule production. *Pseudonocardia* displays variation in its inhibition of pathogens in culture although little is known about this diversity *in vivo* or how strain specificity and ant host influences this antimicrobial protection. We find that conspecific switches do not alter the small molecule profiles of the *A. echinator* colonies tested. Further, the results of allospecific switches are not consistent between replicates. One replicate displayed a separation of small molecule fingerprints suggesting that *Pseudonocardia* produces different

small molecules when on an ant host of a different species. However, the other two allospecific switch replicates do not demonstrate the same separation of profiles. These discordant results suggest that some combination of symbiont strain and ant host species is necessary to maintain a native small molecule response to pathogen infection.

As expected, conspecific switches in *A. echinator* did not result in significantly different small molecule profiles. Within treatment variation is similar to between treatment variation. This is expected as a large number of changes in small molecule profiles at this local population would be unlikely as there has been little evolutionary time for divergence to generate global changes. It is possible that there is variation in several specific small molecules produced, yet this would not be seen in global comparisons of small molecule fingerprints.

Comparison of small molecule profiles between allospecific switches varies more than the conspecific switches, although this is largely dependent on the replicate pair. One replicate, a switch between one colony of *A. echinator* and one colony of *A. octospinosus*, did show significant separation of metabolite profiles of the different ant-*Pseudonocardia* pairings. This was supported by a two-way PERMANOVA which indicated a significant colony and *Pseudonocardia* affect. However, the other two replicates, sets of different *A. echinator* and *A. octospinosus* colonies, did not show any separation of profiles between treatments. Increased replication to include more colonies of each species or perform reciprocal switches between all colonies is necessary to further assess the variation at this level of host-symbiont association. Unfortunately, it was not possible to perform all pairwise switches (i.e. all *A. echinator* colonies switched reciprocally with all *A. octospinosus* colonies) due to the small size of the *A. octospinosus* colonies and a limited number of pupae. It is possible that this variation is due to the combination of *Pseudonocardia* phylotype and ant host. *Acromyrmex echinator* and *A.*

octospinosus in Panama both maintain one of two phylotypes of *Pseudonocardia*, PS1 and PS2 (S B Andersen, Hansen, Sapountzis, Sørensen, & Boomsma, 2013; Holmes et al., 2016).

Genome sequencing of these two strains revealed that they have differing biosynthetic gene clusters from one another and are capable of producing different compounds (Holmes et al., 2016). While this may explain differences in small molecule profiles between phylotypes on their host ant, it does not explain why a phylotype would produce a different profile when it resides on a different host species (as in replicate one of the allospecific switches). This suggests that there is an ant host effect influencing the production of small molecules.

Understanding how strain level difference influence host ecology is important and may have implications on bacterial species concept. Currently, microbial ecology is strongly based on genomic analysis and nucleic acid similarity as a primary means to determine ecological function. Sequencing of microbial communities associated with hosts has, in part, led to the adoption of the holobiont theory. Sequencing may be informative but it does not allow inference of microbial function for a given host. Critics of the theory call for more research investigating the ecological interactions and outcomes of microbe-host associations (Douglas & Werren, 2016). The results in this study suggest that genome comparison alone is insufficient to determine ecological consequence of microbial strain specificity on microbial interactions.

5.6 Acknowledgments

We thank Gaspar Bruner Montero and the Smithsonian Tropical Research Institute for assistance in obtaining field collection permits and export permits. We also thank C. Francoeur and J. Bratburd for comments and suggestions on the manuscript.

5.7 Figures and tables

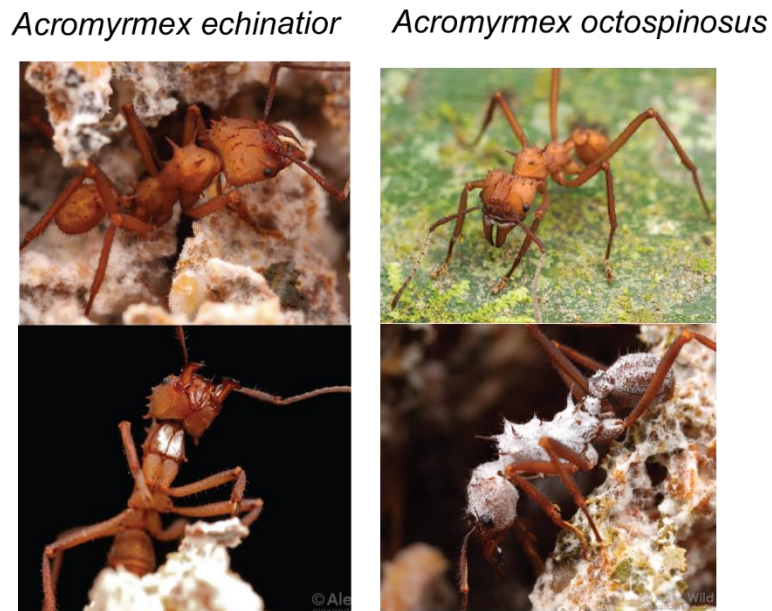


Figure 5.1 Worker ants of *Acromyrmex echinator* and *A. octospinosus*, sympatric species of leaf-cutter ant found in Panama. White film on workers in the symbiont, *Pseudonocardia*. Photos courtesy of Don Parsons.

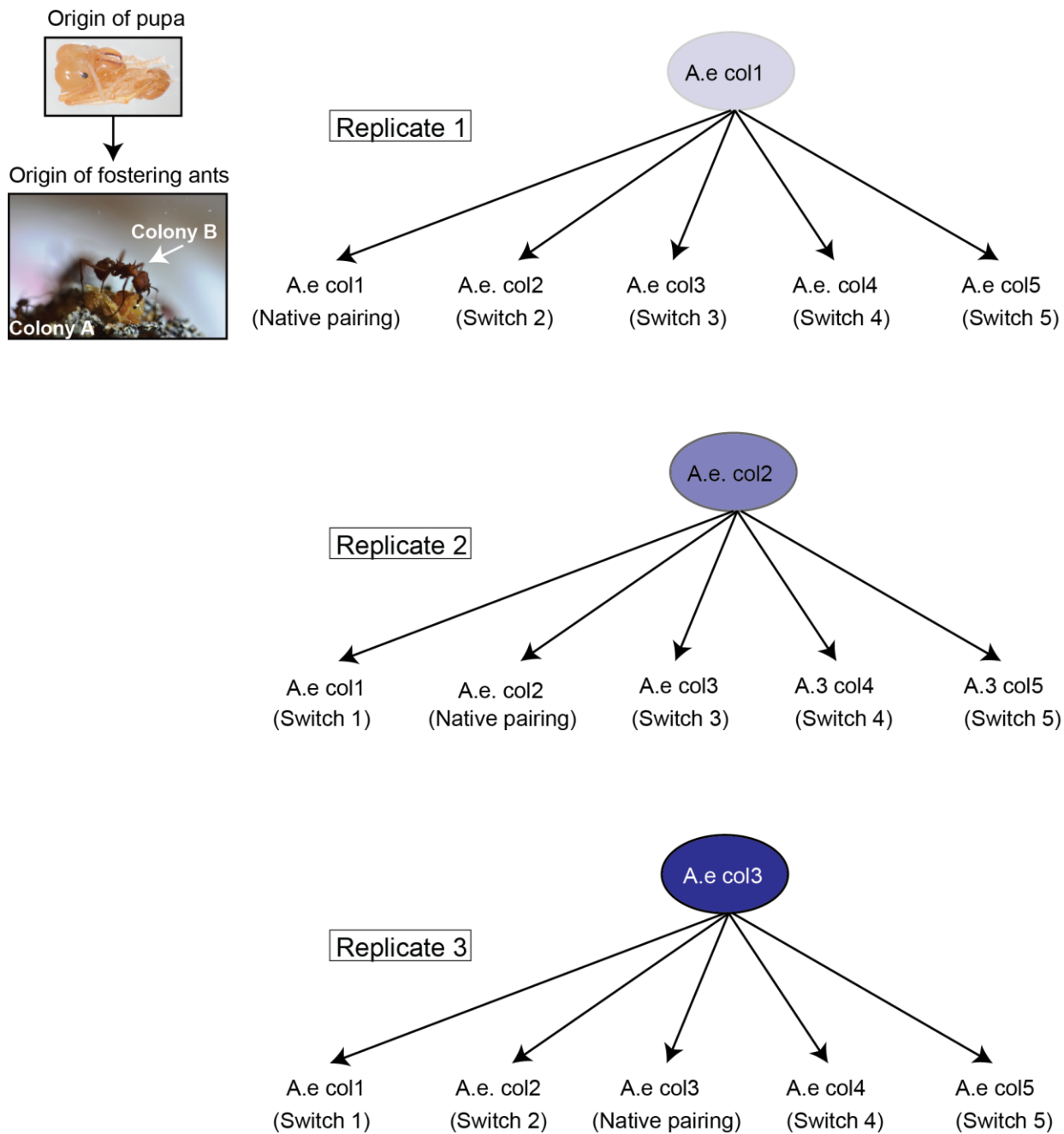


Figure 5.2 Conspecific experimental design. Pupae from one colony are raised by workers of a foster colony. Colonies of *A. echinator* were cross-fostered with colonies of *A. echinator*; each pairing represents one replicate switch. N=number of individual ants that survived and were preserved for imaging mass spectrometry. Photos courtesy of Don Parsons and Gaspar Bruner Montero.

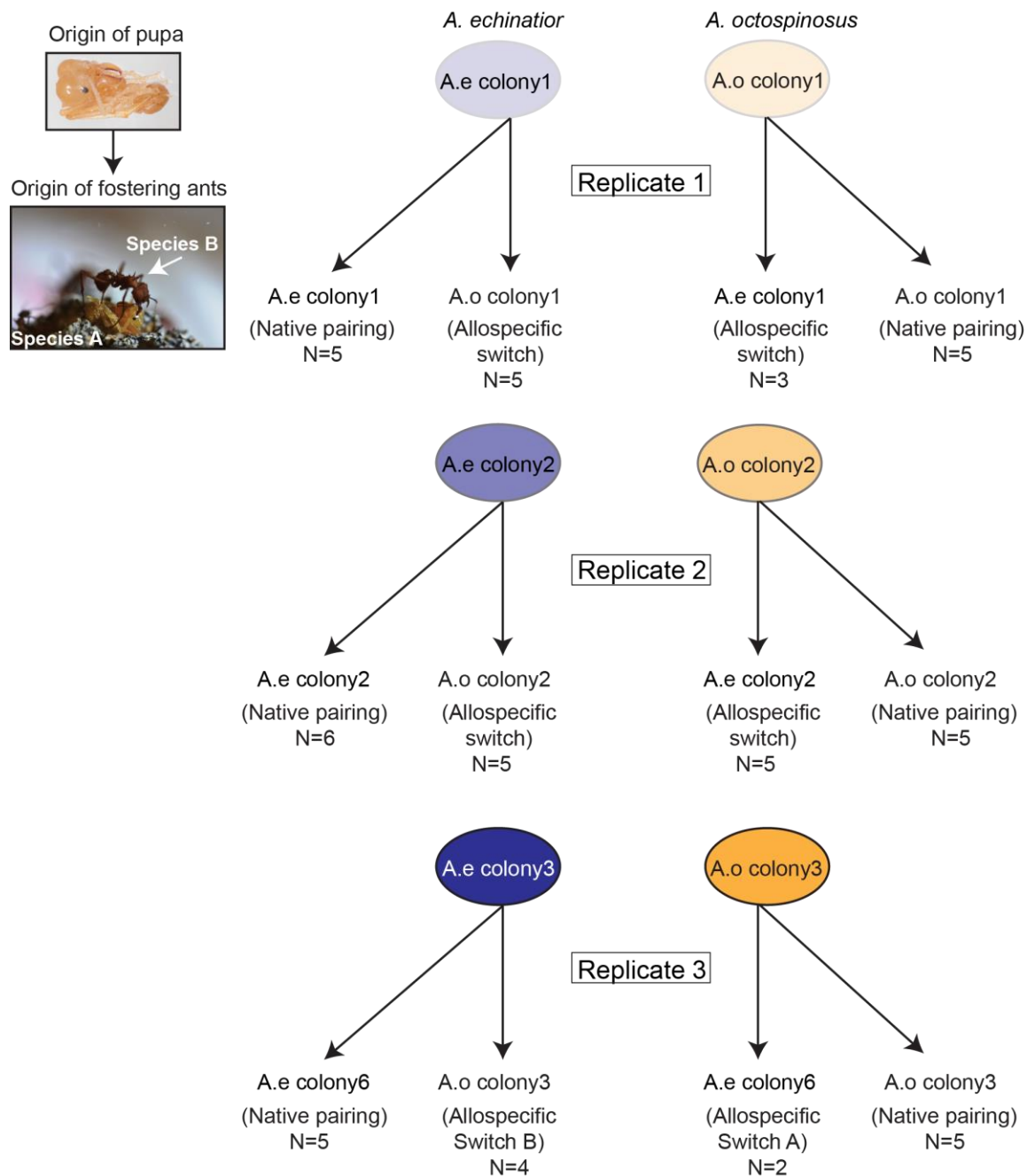


Figure 5.3 Allospecific experimental design. Pupae from one ant host species are raised by workers of a foster colony. Colonies of *A. echinator* were cross-fostered with colonies of *A. octospinosus*; each pairing represents one replicate switch. N=number of individual ants that survived and were preserved for imaging mass spectrometry. Photos courtesy of Done Parsons and Gaspar Bruner Montero.

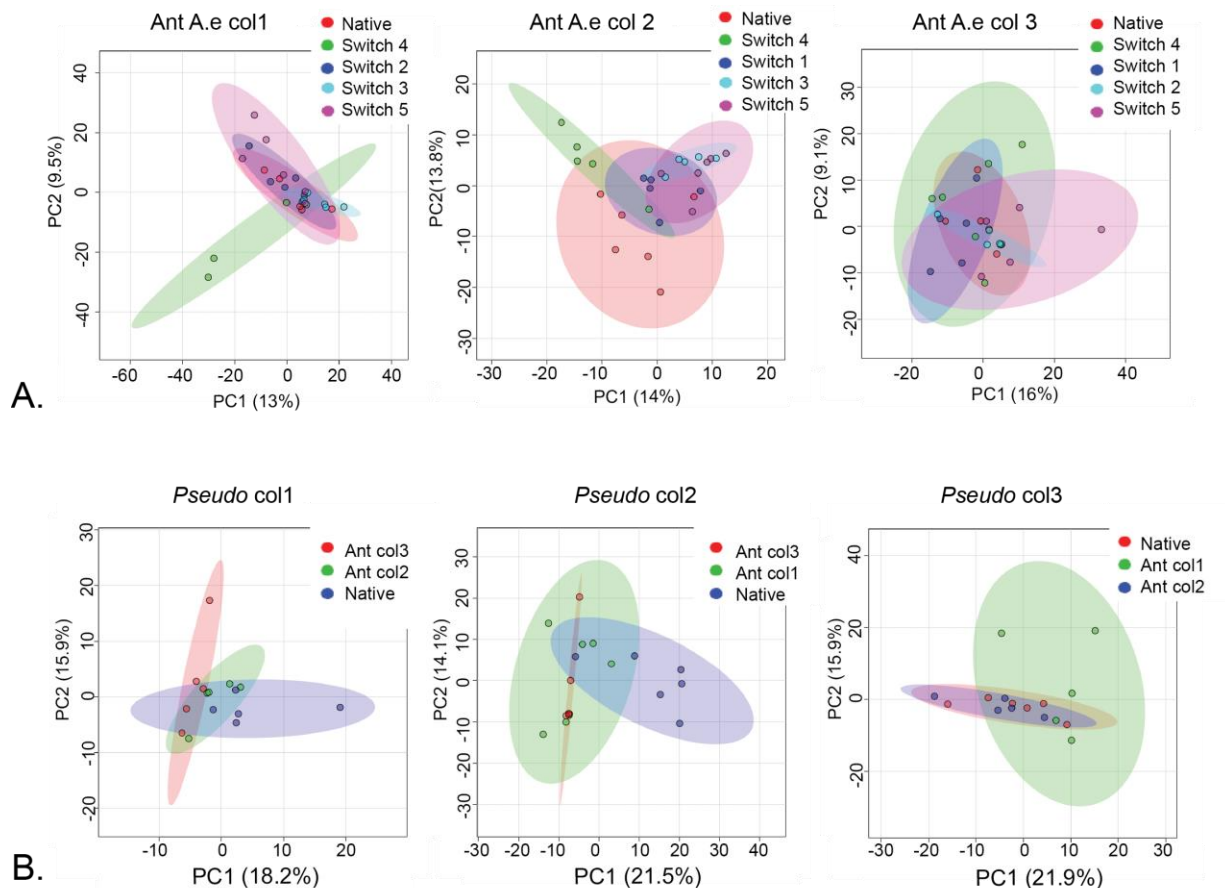


Figure 5.4 A) Principle component analysis of all masses and intensities for each of three conspecific switch replicates: A.e col1, A.e col2, A.e col3. Colored dots represent one ant replicate of each given conspecific switch. Area represents 95% confidence area for each metabolic fingerprint. B) Principle component analysis for each *Pseudoncoardia* strain on 3 different conspecific ant hosts. Colored dots represent one ant replicate of each given conspecific switch. Area represents 95% confidence area for each metabolic fingerprint.

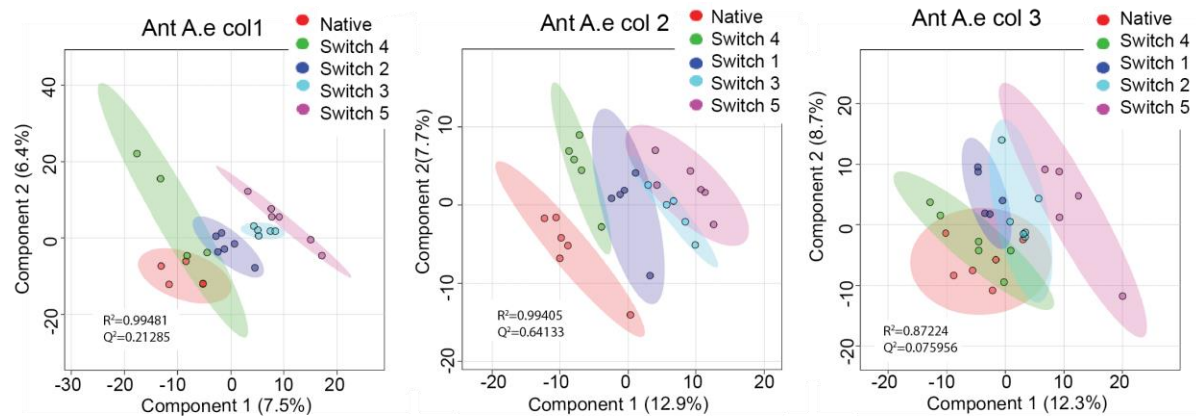


Figure 5.5 Partial least squares discriminant analysis of 3 replicates of conspecific switches. Colored dots represent one ant replicate of each given conspecific switch. Area represents 95% confidence area for each metabolic fingerprint. R^2 and Q^2 values are given in the plot.

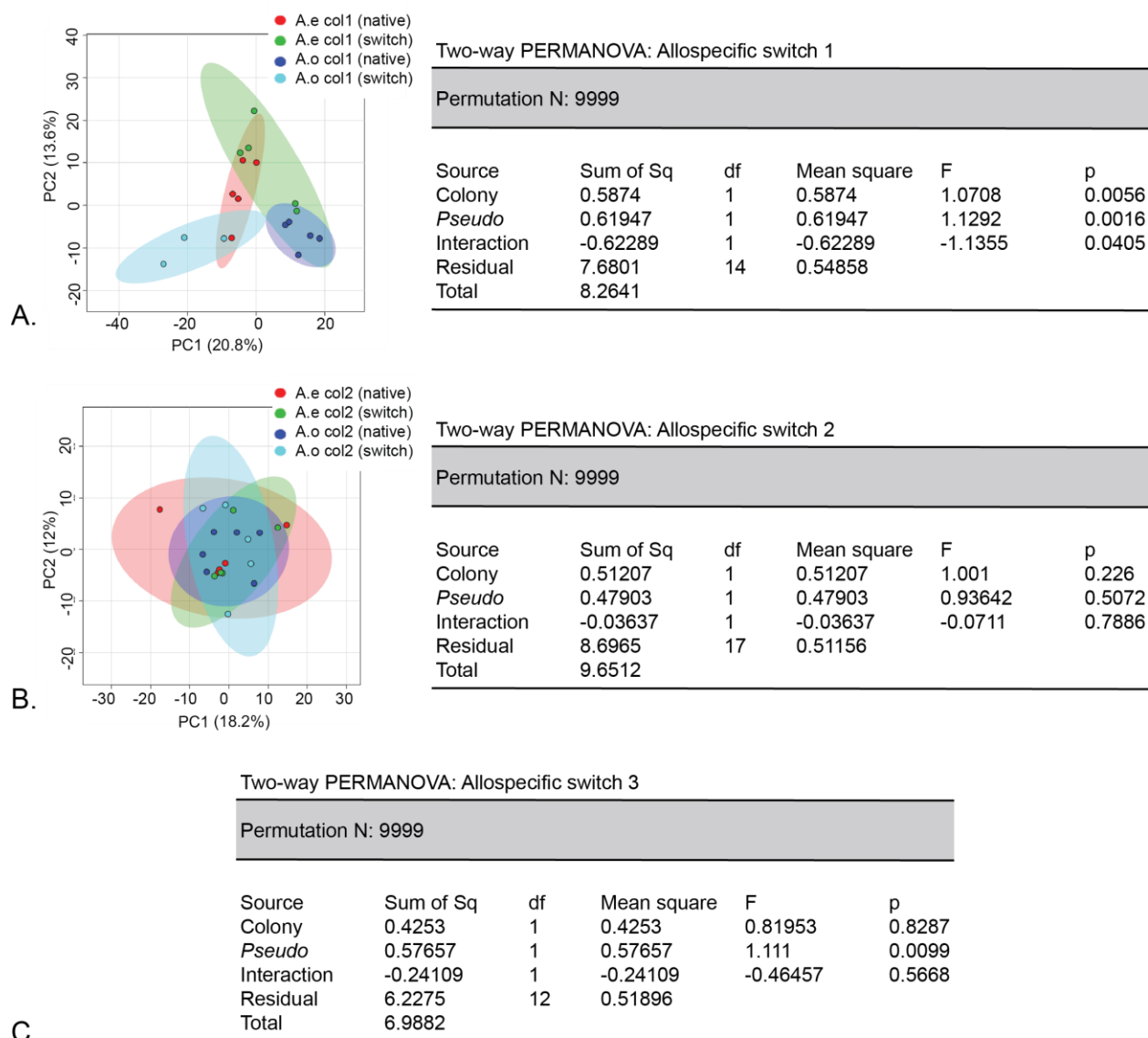


Figure 5.6 Principle component analyses and two-was PERMANOVA for allospecific switch replicates: A) allospecific switch 1; B) allospecific switch 2; C) allospecific switch 3. PCAs include all masses and intensities and colored dots represent one ant replicate of each given allospecific switch. Area represents 95 confidence area for each metabolic fingerprint. There is no PCA for part C due to low ant replicates in one treatment. Two-way PERMANOVA are performed on mass presence-absence and intensity data is not included.

Table 5.1 Ant colony information for colonies used in this experiment. Abbreviations as used in this manuscript are included along with collection information. All colonies were collected in Gamboa, Panama.

Name in manuscript	Colony number	Collection code	Ant host species
A.e col1	colony7	GB093001-01	<i>Acromyrmex echinator</i>
A.e col2	colony9	GB100502-02	<i>Acromyrmex echinator</i>
A.e col3	colony10	GB0927-01	<i>Acromyrmex echinator</i>
A.e col4	colony2	GB092601-01	<i>Acromyrmex echinator</i>
A.e col5	colony11	GB100501-01	<i>Acromyrmex echinator</i>
A.e col6	colony5	Ae5	<i>Acromyrmex echinator</i>
A.o col1	colony8	Ao8	<i>Acromyrmex octospinosus</i>
A.o col2	colony3	Ao3	<i>Acromyrmex octospinosus</i>
A.o col3	colony12	Ao12	<i>Acromyrmex octospinosus</i>

5.8 References

- Andersen, S. B., Hansen, L. H., Sapountzis, P., Sørensen, S. J., & Boomsma, J. J. (2013). Specificity and stability of the *Acromyrmex*-*Pseudonocardia* symbiosis. *Molecular Ecology*, 22(16), 4307–21. <https://doi.org/10.1111/mec.12380>
- Andersen, S. B., Yek, S., Nash, D. R., & Boomsma, J. J. (2015). Interaction specificity between leaf-cutting ants and vertically transmitted *Pseudonocardia* bacteria. *BMC Evolutionary Biology*, 15(1), 27. <https://doi.org/10.1186/s12862-015-0308-2>
- Armitage, S. A. O., Broch, J. F., Marín, H. F., Nash, D. R., & Boomsma, J. J. (2011). IMMUNE DEFENSE IN LEAF-CUTTING ANTS: A CROSS-FOSTERING APPROACH. *Evolution*, 65(6), 1791–1799. <https://doi.org/10.1111/j.1558-5646.2011.01241.x>
- Cafaro, M. J., & Currie, C. R. (2005). Phylogenetic analysis of mutualistic filamentous bacteria associated with fungus-growing ants. *Canadian Journal of Microbiology*, 51(6), 441–6. <https://doi.org/10.1139/w05-023>
- Cafaro, M. J., Poulsen, M., Little, A. E. F., Price, S. L., Gerardo, N. M., Wong, B., ... Currie, C. R. (2011). Specificity in the symbiotic association between fungus-growing ants and protective *Pseudonocardia* bacteria. *Proceedings. Biological Sciences / The Royal Society*, 278(1713), 1814–22. <https://doi.org/10.1098/rspb.2010.2118>
- Carr, G., Derbyshire, E. R., Caldera, E., Currie, C. R., & Clardy, J. (2012). Antibiotic and antimalarial quinones from fungus-growing ant-associated *Pseudonocardia* sp. *Journal of Natural Products*, 75(10), 1806–9. <https://doi.org/10.1021/np300380t>
- Currie, C. R., Bot, A. N. M., & Boomsma, J. J. (2003). Experimental evidence of a tripartite mutualism : bacteria protect ant fungus gardens from specialized parasites. *Oikos*, 1(July 2002), 91–102.
- Currie, C. R., & Scott, J. A. (1999). Fungus-growing ants use antibiotic-producing bacteria to control garden parasites, 398(April), 701–705.
- Doolittle, W. F., & Booth, A. (2017). It's the song, not the singer: an exploration of holobiosis and evolutionary theory. *Biology & Philosophy*, 32(1), 5–24. <https://doi.org/10.1007/s10539-016-9542-2>
- Douglas, A. E., & Werren, J. H. (2016). Holes in the Hologenome: Why Host-Microbe Symbioses Are Not Holobionts. *MBio*, 7(2), e02099. <https://doi.org/10.1128/mBio.02099-15>
- Gemperline, E., Horn, H. A., DeLaney, K., Currie, C. R., & Li, L. (2017). Imaging with Mass Spectrometry of Bacteria on the Exoskeleton of Fungus-Growing Ants. *ACS Chemical Biology*, 12(8), 1980–1985. <https://doi.org/10.1021/acscchembio.7b00038>
- Hammer, D. A. T., Ryan, P. D., Hammer, Ø., & Harper, D. A. T. (2001). *Past: Paleontological Statistics Software Package for Education and Data Analysis*. *Palaeontologia Electronica* (Vol. 4). Retrieved from http://palaeo-electronica.orghttp://palaeo-electronica.org/2001_1/past/issue1_01.htm.

- Hölldobler, B., & Wilson, E. O. (1990). *The Ants*. Harvard University Press. Retrieved from <https://books.google.com/books?hl=en&lr=&id=R-7TaridBX0C&pgis=1>
- Holmes, N. A., Innocent, T. M., Heine, D., Bassam, M. Al, Worsley, S. F., Trottmann, F., ... Hutchings, M. I. (2016). Genome Analysis of Two *Pseudonocardia* Phylotypes Associated with *Acromyrmex* Leafcutter Ants Reveals Their Biosynthetic Potential. *Frontiers in Microbiology*, 7, 2073. <https://doi.org/10.3389/fmicb.2016.02073>
- Marsh, S. E., Poulsen, M., Pinto-Tomás, A., & Currie, C. R. (2014). Interaction between workers during a short time window is required for bacterial symbiont transmission in *Acromyrmex* leaf-cutting ants. *PLoS One*, 9(7), e103269. <https://doi.org/10.1371/journal.pone.0103269>
- Oh, D.-C., Poulsen, M., Currie, C. R., & Clardy, J. (2009). Dentigerumycin: a bacterial mediator of an ant-fungus symbiosis. *Nature Chemical Biology*, 5(6), 391–3. <https://doi.org/10.1038/nchembio.159>
- Robichaud, G., Garrard, K. P., Barry, J. A., & Muddiman, D. C. (2013). MSiReader: an open-source interface to view and analyze high resolving power MS imaging files on Matlab platform. *Journal of the American Society for Mass Spectrometry*, 24(5), 718–21. <https://doi.org/10.1007/s13361-013-0607-z>
- Rosenberg, E., & Zilber-Rosenberg, I. (2018). The hologenome concept of evolution after 10 years. *Microbiome*, 6(1), 78. <https://doi.org/10.1186/s40168-018-0457-9>
- Sit, C. S., Ruzzini, A. C., Van Arnem, E. B., Ramadhar, T. R., Currie, C. R., & Clardy, J. (2015). Variable genetic architectures produce virtually identical molecules in bacterial symbionts of fungus-growing ants. *Proceedings of the National Academy of Sciences*, 112(43), 13150–13154. <https://doi.org/10.1073/pnas.1515348112>
- Steffan, S. A., Chikaraishi, Y., Currie, C. R., Horn, H., Gaines-Day, H. R., Pauli, J. N., ... Ohkouchi, N. (2015). Microbes are trophic analogs of animals. *Proceedings of the National Academy of Sciences*, 112(49), 201508782. <https://doi.org/10.1073/pnas.1508782112>
- Theis, K. R., Dheilly, N. M., Klassen, J. L., Brucker, R. M., Baines, J. F., Bosch, T. C. G., ... Bordenstein, S. R. (2016). Getting the Hologenome Concept Right: an Eco-Evolutionary Framework for Hosts and Their Microbiomes. *MSystems*, 1(2), e00028-16. <https://doi.org/10.1128/mSystems.00028-16>
- Van Arnem, E. B., Ruzzini, A. C., Sit, C. S., Horn, H., Pinto-Tomás, A. A., Currie, C. R., & Clardy, J. (2016). Selvamycin, an atypical antifungal polyene from two alternative genomic contexts. *Proceedings of the National Academy of Sciences of the United States of America*, 113(46), 12940–12945. <https://doi.org/10.1073/pnas.1613285113>
- Weber, N. A. (1966). Fungus-growing ants. *Science (New York, N.Y.)*, 153(3736), 587–604. <https://doi.org/10.1126/science.153.3736.587>
- Xia, J., Psychogios, N., Young, N., & Wishart, D. S. (2009). MetaboAnalyst: a web server for metabolomic data analysis and interpretation. *Nucleic Acids Research*, 37(Web Server issue), W652-60. <https://doi.org/10.1093/nar/gkp356>
- Xia, J., Sinelnikov, I. V., Han, B., & Wishart, D. S. (2015). MetaboAnalyst 3.0--making metabolomics more meaningful. *Nucleic Acids Research*, gkv380-.

<https://doi.org/10.1093/nar/gkv380>

Zilber-Rosenberg, I., & Rosenberg, E. (2008). Role of microorganisms in the evolution of animals and plants: the hologenome theory of evolution. *FEMS Microbiology Reviews*, 32(5), 723–735. <https://doi.org/10.1111/j.1574-6976.2008.00123.x>

Chapter 6

Conclusions and Future Directions

Microbes are ubiquitous and form symbioses with all organisms. Increased sequencing technology has allowed a greater description of microbial diversity in host associations although the characterization of microbial influence on host ecology is often limited. Characterization of small molecule dynamics, the mediators of microbial interactions, is particularly limited. Once the ecological characterization of a symbiosis is described (i.e. defining the dominant players, the nature of the interactions, and the diversity or specificity of associations), what topics should be explored next? Evolutionarily-minded inquiry about small molecule diversity and dynamics can more easily be addressed once the basic ecology is established. Specifically, the following questions remain unresolved and should be addressed: i) When, why, and how are small molecules produced *in vivo*? ii) Is there variation in the small molecules produced or are small molecules conserved throughout interactions? iii) What evolutionary processes generate any observed diversity in small molecule profiles? These questions are difficult to answer but developing models along with interdisciplinary approaches including population and community ecology, phylogenetics, and mass spectrometry can help address these problems in microbial ecology. Investigating these questions will not only shed light on microbial communication *in vivo* but also the evolutionary processes generating this diversity. The work in this thesis represents an attempt to characterize microbial interactions within the fungus-growing ant symbiosis and the influence of these interactions on small molecule dynamics.

In chapter 2 of this thesis, I outline a quantitative polymerase chain reaction (qPCR) method to detect the abundance of *Pseudonocardia* on its ant host. I then use the approach to examine differences in symbiont abundance on different ant worker castes and find evidence that

the bacterial symbiont is linked to the social structure of the ant colony. I find that garden workers of *Acromyrmex echinator* and *A. octospinosus* maintain higher abundance of *Pseudocardia* compared to foragers. This corresponds to a shift in age of ant worker suggesting that symbiont abundance may be tied to the colony caste-based social structure. I also find that *Acromyrmex* gynes had detectable *Pseudocardia* supporting that symbiont transmission occurs vertically from gyne to founding colony. Lastly, I show that developing worker ants exposed to a non-native symbiont, *Streptomyces*, do not acquire detectable amounts via qPCR. This qPCR technique can be used to further characterize ant-*Pseudocardia* switches and address questions regarding partner fidelity or specificity. Indeed, the method was applied in Li et al. 2018 and is included in Appendix 1 of this thesis.

Chapter 3 combines experimental approaches with mass spectrometry imaging (MSI) and develops improved methods to assess small molecule production by *Pseudocardia* on the ant exoskeleton. Matrix-assisted laser desorption ionization (MALDI) MSI was used on ants with and without *Pseudocardia* to detect and visualize small molecules produced by the bacterium under pathogen infection *in situ*. This method used MSI to localize small molecule detection specifically where *Pseudocardia* grows on the ant exoskeleton and replication of ants indicates core small molecule profiles that are reproducible. This technique is used in chapters 4 and 5 to address ecological questions regarding small molecule production and dynamics in the fungus-growing ant system.

Chapter 4 of this dissertation uses MSI to address questions regarding the influence of species interactions on small molecule production in ant-associated *Pseudocardia*. We first ask if interactions with pathogens induces chemistry in *Pseudocardia*. Indeed, in *in vitro* interactions, *Pseudocardia* produces small molecules during pathogen interactions not

observed in control treatments. Furthermore, we observe shifts in the small molecules profiles of *Pseudonocardia* when it resides on its ant host compared to when it is isolated in culture. This indicates a complex relationship between the ant host and the bacterium that may be influencing small molecule production. Lastly, we observe particular molecules induced only under particular treatments which supports a specialized chemical response to pathogen interactions. Future work elucidating the chemical structures of molecules that are important in particular species interactions would inform on the chemical ecology of this system.

The last chapter in this dissertation again use a MSI approach to characterize the influence of the ant-*Pseudonocardia* interaction on small molecule production. A set of host-symbiont switches are performed between conspecific and allospecific colonies of *Acromyrmex* leaf-cutter ants. Preliminary results suggest that there is some variation in small molecule profiles in some, but not all, conspecific switches. The shift in profile signifies there may be an incongruence between ant and *Pseudonocardia* that prevents small molecule production. This may be a result of interactions between particular phylotypes of *Pseudonocardia* and ant hosts. Future experiments that account for *Pseudonocardia* phylotype or more distant lineages of *Pseudonocardia* would address questions about partner fidelity and its influence on chemical diversity. Further, assessment of the ecological consequences of this observed small molecule variation may allow for better characterization of the implications partner fidelity in this system and its impact.

The work in this dissertation is the first attempt to characterize ant-microbe interactions and their effect on small molecule production in leaf-cutter ants. *In vivo* small molecule dynamics and diversity in *Pseudonocardia* has never been characterized, and this work is the first step to understand the complex chemically-mediated interactions of this well-described

symbiosis. We observed interactions between *Pseudonocardia* and its ant host as well as interactions with pathogens are influencing the small molecules produced in the system. Future work exploring antibiotic production in this system must account for the complexity of these associations that are influencing small molecule dynamics.

Appendix 1

Supplementary material for Chapter 3

Imaging with Mass Spectrometry of Bacteria on the Exoskeleton of Fungus-Growing Ants

Authors: Erin Gemperline*, Heidi A. Horn*, Kellen DeLaney, Cameron R. Currie, Lingjun Li

Author contributions: Author contributions are the same as Chapter 3 of this thesis.

A1.1 Supplementary materials and methods

A1.1.1 Ant Dissection Evaluation

Three methods of dissecting the ants and placing them on the slide were evaluated: 1- (propleural plate) The propleural plate was removed from the ant with a tweezer by pulling the prothoracic legs attached to the propleural plate until it was released from the thorax and placed into the groove of the slide; 2- (partial thorax) the anterior portion of the thorax, which contains the propleural plate, was removed from the ant with a razor blade by first removing the head and legs and then cutting through the thorax directly posterior to the *Pseudonocardia* patch on the propleural plate and the partial thorax was placed in the groove of the slide; and 3- (whole thorax) the entire thorax was removed with a razor blade after the head, abdomen, and legs were removed and the thorax was placed in the groove of the slide with additional tape over the bottom portion of the thorax (posterior to the *Pseudonocardia* patch on the propleural plate) to secure into place. Ant thoraxes were then inlaid into the groove of the slide with the propleural plate facing outward and parallel with the top of the slide. As proof-of-principle and to determine the best method of placing the ants on the slide, ants were raised without *Pseudonocardia* and ProteoMass MALDI-MS calibration mix (Sigma-Aldrich) was spiked onto the propleural plate. Mass accuracy and

overall ease of sample preparation were evaluated. Method 3 (whole thorax) was determined to provide the most accurate results and was used for the remainder of the study.

A1.1.2 Ant Colony Preparation and Pathogen Treatment

Acromyrmex octospinosus leaf-cutter ants were collected in the Canal Zone in Panama (colony ST040116-01). Subcolonies of ants were made by placing approximately 1 g of fungus garden in a Petri plate followed by four major workers from the main fungus garden. Additional subcolonies were made to raise workers that were symbiont (*Pseudonocardia*)-free. The subcolonies and ants were randomly assigned to one of three treatments: *Pseudonocardia*/pathogen treatment, no-*Pseudonocardia*/pathogen treatment, or a *Pseudonocardia*/control treatment. Pathogen-treated subcolonies were inoculated with the fungus *Escovopsis*. Control subcolonies were similarly inoculated with a sterile inoculation loop. Subcolonies were left for 20 hours after which focal ants were removed and frozen at 20°C for further processing.

A1.1.3 MALDI-MSI Data Processing and Analysis

Raw data files acquired from MALDI-MSI were uploaded to MSiReader (Robichaud, Garrard, Barry, & Muddiman, 2013).⁴ MSiReader was used to create a list of compounds of interest by selecting the propleural plate as the “interrogated zone” and subtracting the matrix peaks chosen as the “reference zone”. A list of m/z values was generated in this way for all ants and the lists were combined into one list; duplicated masses (within 5 ppm mass error) and isotopic peaks were removed. Note that m/z values for ion adducts were not verified and

removed from the mass list. Ion images were automatically generated with MSiReader for every sample/ treatment using the combined mass lists. All images were normalized to the total ion current (TIC). Mass lists were manually cross-checked between control and treated ants to determine if each detected compound was explicitly expressed only in response to *Escovopsis* exposure.

A1.1.4 Ant Propleural Plate Extractions

Seven ants with *Pseudonocardia* without garden infection (un-exposed) and seven ants with *Pseudonocardia* exposed to the pathogen *Escovopsis* were used for metabolite extractions. The seven propleural plates were detached from the ants, placed into a prechilled mortar, flash-frozen with liquid nitrogen and ground to powder. The powder was transferred to a pre-chilled 1.5-mL Eppendorf tube. The metabolites were extracted with 3:1:4 methanol:chloroform:water (v/v/v), briefly vortexed, and centrifuged for 10 min at 5000 xg. The resulting aqueous supernatant was removed and collected in new tubes. An additional 4 parts methanol was added to the tubes with the remaining organic and protein layers. The tubes were vortexed and centrifuged for 5 min at 1500 xg to pellet the protein layer. The organic layer was removed and collected in new tubes. Both the aqueous and organic fractions were dried and concentrated via SpeedVac and stored at -80 °C until analysis.

A1.1.5 Q-Exactive Orbitrap for LC-ESI-MS and LC-ESI-MS/MS

To acquire LC-ESI-MS and MS/MS data, propleural plate extracts were resuspended in 40 μ L of either water + 0.1% formic acid (FA) (aqueous fractions) or acetonitrile (AcN) + 0.1% FA (organic fractions). Samples were separated on a Kinetix C18 column (2.1 \times 150 mm, 1.7- μ m particle size; Phenomenex), equipped with a corresponding guard column, and heated to 35 $^{\circ}$ C. Mobile phases were (A) water with 0.1% FA and (B) AcN with 0.1% FA. Aqueous fractions were separated within 35 min under the following conditions: 0-5 min, 1% B; 5-10 min, 1-3% B; 10-18 min, 3-40% B; 18-22 min, 40-80% B; column cleaning at 95% B for 5 min and system re-equilibration at 1% B for 8 min. Organic fractions were separated within 35 min under the following conditions: 0-22 min, 1-95 % B; column cleaning at 95% B for 5 min and re-equilibration at 1% B for 8 min. The flow rate was 0.3 mL/min and the injection volume was 5 μ L. The samples were kept at 10 $^{\circ}$ C during the analysis.

A1.1.6 Publically Available Data

The MSI data have been made publically available on METASPACE (<http://annotate.metaspaces2020.eu>) (Palmer et al., 2017). The LC-MS and LC-MS/MS metabolomics data have been deposited to the EMBL-EBI MetaboLights database (Haug et al., 2013) with the identifier MTBLS471. The complete dataset can be accessed here: <http://www.ebi.ac.uk/metabolights/MTBLS471>. The metabolomics data have also been deposited to GNPS (Global Natural Products Social Molecular Networking) (Wang et al., 2016) through the MassIVE database with the identifier MSV000081131. The complete dataset can be accessed here:

<http://massive.ucsd.edu/ProteoSAFe/dataset.jsp?task=45496a5995e04c83b7a5b0935288c42>

f.

A1.2 Supplemental Tables and Figures

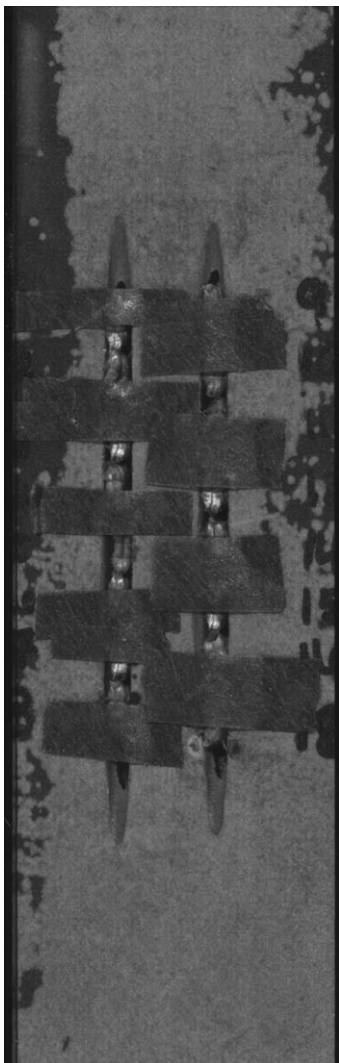


Figure A1.1 Photograph of ants and glass slides coated with DHB matrix.

Table A1.1. Proof-of-principle comparison of calibrants spiked onto ant propleural plates

Calibration Standards on Glass Slide					
Calibrant	Expected m/z	Detected m/z	ppm error	Δppm	Avg. Absolute Error (ppm)
MRFA	524.2650	524.2662	2.34		2.6
Bradykinin 1-7	757.3992	757.4003	1.56	1.9	
Bradykinin	1060.569	1060.572	2.97		
Angiotensin I	1296.685	1296.689	3.46		
Neurotensin	1672.917	1672.922	3.24		
Renin Substrate	1758.933	1758.937	2.34		
Entire Thorax					
Calibrant	Expected m/z	Detected m/z	ppm error	Δppm	Avg. Absolute Error (ppm)
MRFA	524.2650	524.2653	0.58		1.5
Bradykinin 1-7	757.3992	757.3998	0.86	2.1	
Bradykinin	1060.569	1060.571	1.72		
Angiotensin I	1296.685	1296.687	2.08		
Neurotensin	1672.917	1672.921	2.68		
Renin Substrate	1758.933	1758.935	1.29		
Upper Thorax					
Calibrant	Expected m/z	Detected m/z	ppm error	Δppm	Avg. Absolute Error (ppm)
MRFA	524.2650	524.2671	4.15		5.3
Bradykinin 1-7	757.3992	757.4027	4.69	2.3	
Bradykinin	1060.569	1060.5741	5.13		
Angiotensin I	1296.685	1296.692	5.75		
Neurotensin	1672.917	1672.928	6.44		
Renin Substrate	1758.933	1758.943	5.91		
Removed Propleural Plate					
Calibrant	Expected m/z	Detected m/z	ppm error	Δppm	Avg. Absolute Error (ppm)

MRFA	524.2650	524.2666	3.10		
Bradykinin 1-7	757.3992	757.4019	3.62		
Bradykinin	1060.569	1060.574	5.00	2.3	4.3
Angiotensin I	1296.685	1296.692	5.39		
Neurotensin	1672.917	1672.926	5.26		
Renin Substrate	1758.933	1758.939	3.48		

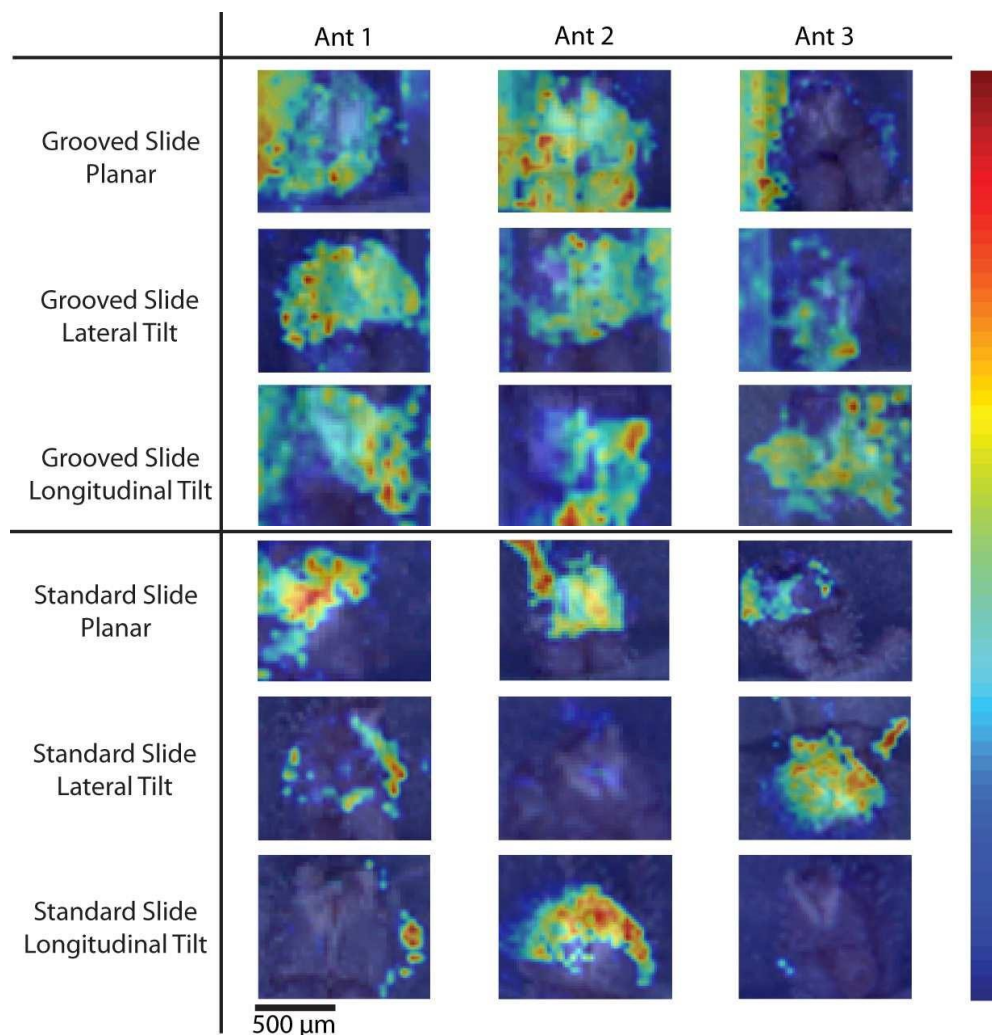


Figure A1.2 Representative MS images of ergothioneine standard spiked onto ant propleural plates that were either not tilted, tilted laterally (right or left), or tilted longitudinally (up or down). Note that the spiked ergothioneine standard sometimes dripped off of the ant thorax due to the hydrophobicity of the ant exoskeleton. Placing the ant thoraxes in the groove of the glass slide minimized the impact of any tilt of the sample, or non-planarity, when compared to ant thoraxes placed on standard glass slides. Ergothioneine was not able to be detected on several of the ant thoraxes placed on the standard glass slides and tilted either laterally or longitudinally (Standard Slide, Lateral Tilt- Ant 2; Standard Slide, Longitudinal Tilt- Ant 1 & Ant 3), likely due to being out of the plane of the MALDI laser. This issue was not observed when the ant thoraxes were placed in the groove of the slide.

A1.3 References

- Haug, K., Salek, R. M., Conesa, P., Hastings, J., de Matos, P., Rijnbeek, M., ... Steinbeck, C. (2013). MetaboLights—an open-access general-purpose repository for metabolomics studies and associated meta-data. *Nucleic Acids Research*, *41*(D1), D781–D786. <http://doi.org/10.1093/nar/gks1004>
- Palmer, A., Phapale, P., Chernyavsky, I., Lavigne, R., Fay, D., Tarasov, A., ... Alexandrov, T. (2017). FDR-controlled metabolite annotation for high-resolution imaging mass spectrometry. *Nature Methods*, *14*(1), 57–60. <http://doi.org/10.1038/nmeth.4072>
- Robichaud, G., Garrard, K. P., Barry, J. A., & Muddiman, D. C. (2013). MSiReader: an open-source interface to view and analyze high resolving power MS imaging files on Matlab platform. *Journal of the American Society for Mass Spectrometry*, *24*(5), 718–21. <http://doi.org/10.1007/s13361-013-0607-z>
- Wang, M., Carver, J. J., Phelan, V. V., Sanchez, L. M., Garg, N., Peng, Y., ... Bandeira, N. (2016). Sharing and community curation of mass spectrometry data with Global Natural Products Social Molecular Networking. *Nature Biotechnology*, *34*(8), 828–837. <http://doi.org/10.1038/nbt.3597>

Appendix 2

Supplementary material for Chapter 4

Specialized chemical responses to pathogens in the defensive symbionts of fungus-growing ants

Authors: Heidi A. Horn*, Erin Gemperline*, Marc G. Chevrette, Bradon R. McDonald, Jennifer R. Bratburd, Lingjun Li, Cameron R. Currie

Author contributions: Author contributions are the same as Chapter 4 of this thesis.

A2.1 Data Accessibility

MSI data is publically available on METASPACE (<http://annotate.metaspaces2020.eu>) (Palmer et al., 2017). Genomes will be deposited to NCBI and are available to reviewers upon request. There are no restrictions on data availability.

A2.2 Figures and Tables

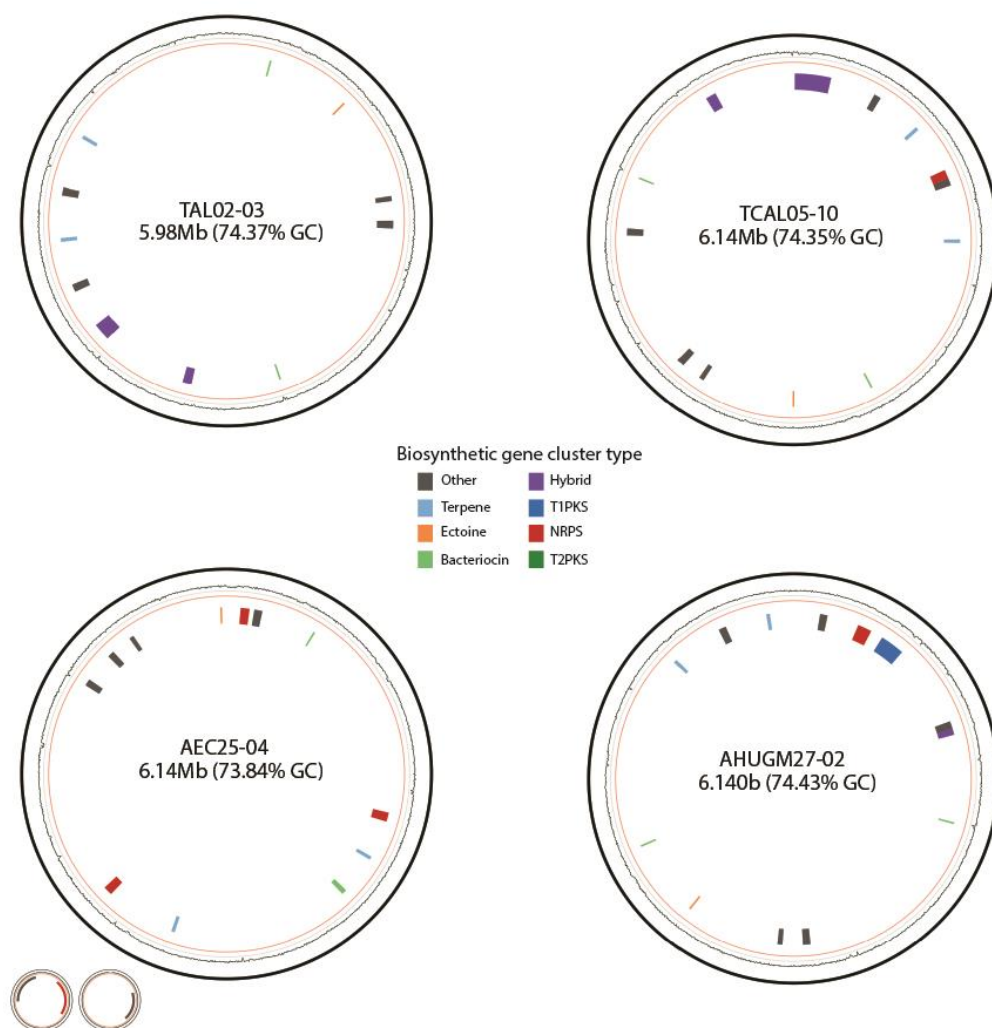


Figure A2.1 Genome maps (chromosome and plasmids) of *Pseudonocardia* strains TAL02-03 (*Trachymyrmex* ant host), TCAL05-10 (*Trachymyrmex corntezi* ant host), AEC25-04 (*Apterostigma* ant host), AHUGM27-02 (*Acromyrmex hispidus fallax* ant host) included in Figure 1a. Colored boxes indicate biosynthetic gene cluster type (type I polyketide synthase (T1PKS); type II polyketide synthase (T2PKS); hybrid=multiple cluster types) and relative location in the genome. Black, outer ring corresponds to each contig; inner black ring represents GC content (orange line=25% GC, gray= 50% GC, green=75% GC).

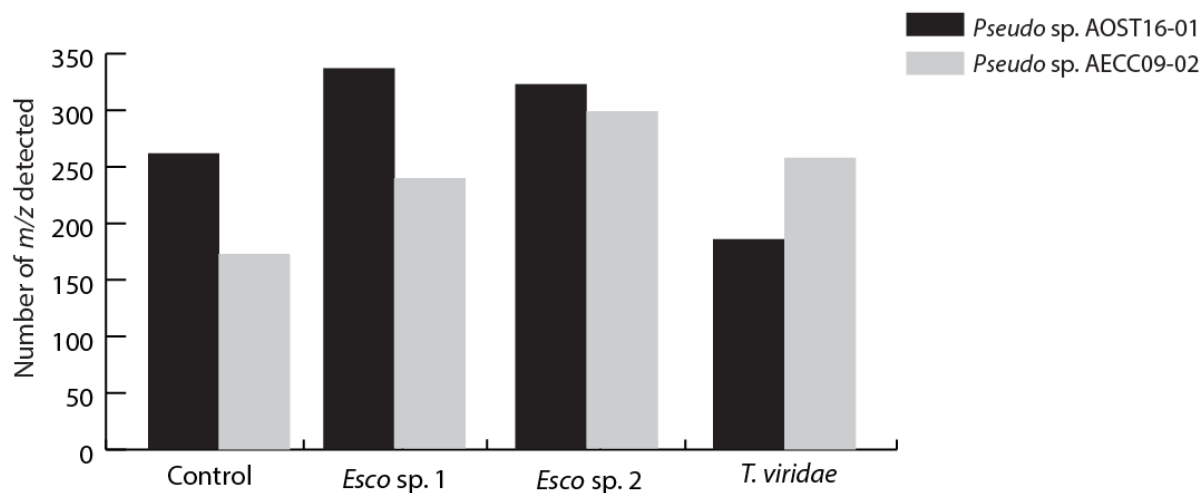


Figure A2.2 Total numbers of m/z detected ($\geq m/z$ 300) in at least 2 out of 3 replicates through MSI for each strain of *Pseudonocardia in vitro* under control treatment (no pathogen exposure) as well as 3 pathogen treatments.

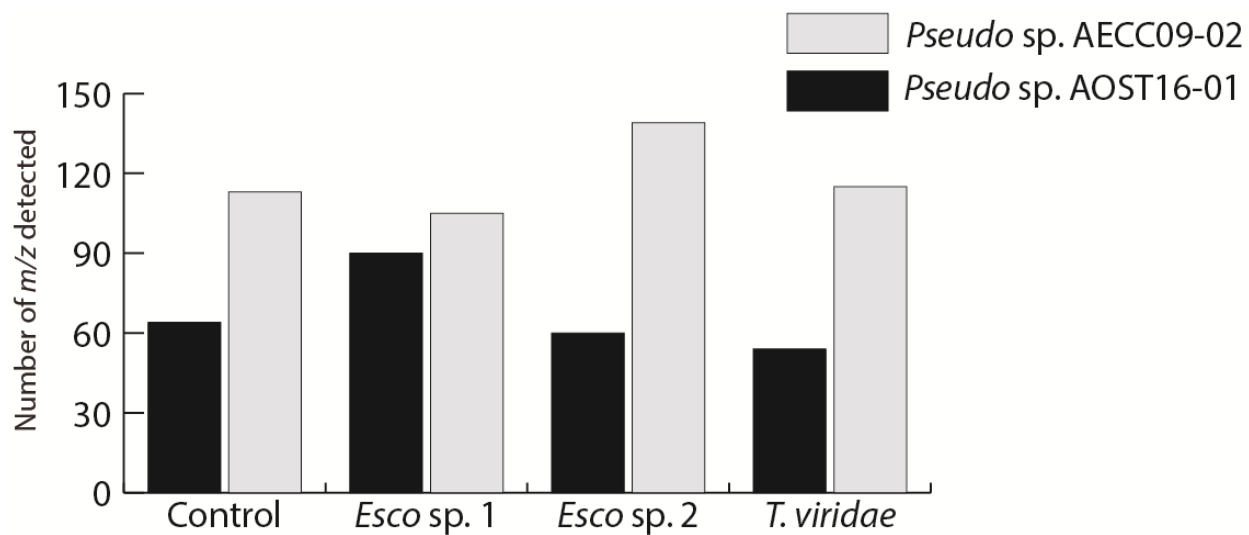


Figure A2.3 Total numbers of m/z detected ($\geq m/z$ 300) through MSI for each strain of *Pseudonocardia in situ* under no exposure control treatment as well as pathogen treatments. Each m/z was detected in 6 out of 9 ant replicates.

Table A2.1 Ions (m/z), over 300 Da, detected in each strain of *Pseudonocardia* shared between treatments under *in vitro* conditions. Each ion was detected in 2 out of 3 Petri plate replicates. Bold m/z are found in the same treatment of the opposite strain of *Pseudonocardia*.

<i>Pseudonocardia</i> sp. AOST16-01	
<i>Esco</i> sp. 1/ <i>Esco</i> sp. 2 [67]:	304.176 , 305.304, 306.080, 310.912, 314.182, 320.974, 322.054, 326.378, 329.015, 333.334, 334.930, 343.187, 350.904, 356.903, 360.151, 360.361, 366.112, 368.001, 372.876, 378.141 , 403.024 , 411.160, 425.980, 439.390, 471.211, 500.046, 510.939, 522.030 , 526.912, 527.177, 538.002, 542.970, 546.061 , 548.885, 551.309, 555.134 , 559.368, 568.041 , 570.144, 580.949, 581.319, 597.928, 599.940, 611.099, 635.111, 641.342, 649.047 , 650.032 , 657.084 , 658.066, 671.028 , 673.056 , 675.092 , 679.065, 687.176, 691.068, 693.010, 695.460, 696.022 , 703.191, 708.982 , 714.033, 725.451 , 744.283 , 744.302, 757.961, 950.951
<i>Esco</i> sp. 1/ <i>T. viridae</i> [5]:	362.134, 376.183, 399.145, 619.121, 737.345
<i>Esco</i> sp. 2/ <i>T. viridae</i> [6]:	310.902, 440.109, 472.000, 574.129, 693.334, 723.345
<i>Esco</i> sp. 1/ <i>Esco</i> sp. 2/ <i>T. viridae</i> [21]:	329.187, 331.128, 337.171, 341.193, 361.159, 365.105, 379.150, 408.952 , 428.036 , 450.018, 462.102, 526.173, 640.334, 646.475, 649.106, 655.275 , 705.321, 721.316, 727.301, 743.276, 760.296
Control/ <i>Esco</i> sp. 1/ <i>Esco</i> sp. 2/ <i>T. viridae</i> [77]:	306.201, 314.964, 315.202 , 328.184 , 330.060, 337.162 , 337.184 , 344.157 , 348.071, 353.158 , 353.164, 359.143 , 366.962, 369.155, 375.119 , 377.134 , 386.027 , 405.946 , 406.953, 408.008 , 422.928 , 427.139, 465.993 , 487.974 , 503.948, 524.058, 527.159, 542.069, 542.148, 543.132 , 544.456 , 558.365, 558.375 , 562.012 , 566.438 , 569.453 , 574.349 , 580.025 , 581.955, 582.412 , 582.961, 583.965, 583.996 , 584.410 , 586.032, 587.314, 591.434, 598.936 , 602.006 , 617.981 , 623.988 , 639.961, 656.308 , 657.316 , 662.450 , 664.117, 666.130, 689.211, 702.073, 704.089, 705.185, 743.297 , 758.972, 759.272 , 759.292, 772.525, 774.945 , 775.267, 777.281, 777.302, 851.262, 867.238, 934.982 , 1013.320, 1029.292 , 1175.366, 1191.344
Control/ <i>Esco</i> sp. 1 [18]:	558.063, 622.035 , 635.180, 669.105, 672.419, 745.019 , 751.027, 759.065, 767.00, 767.984, 828.303, 848.094, 891.704, 905.054, 913.090 , 941.274, 1015.377, 1035.509
Control/ <i>Esco</i> sp. 2 [2]:	481.094, 1339.431
Control/ <i>Esco</i> sp. 1/ <i>Esco</i> sp. 2 [143]:	303.166 , 306.048, 312.049 , 320.171, 328.030 , 346.041, 347.094, 347.175, 350.006 , 350.012 , 350.086, 350.996 , 352.042 , 352.920 , 365.986 , 366.970 , 368.016 , 368.022 , 370.052, 374.024, 381.078, 381.960 , 382.083 , 382.107, 383.997, 385.130 , 386.048, 389.997 , 392.034, 399.970 , 402.021, 405.970 , 420.061, 420.080 , 423.983, 424.003 , 424.926, 428.995 , 439.976 , 442.132, 443.045, 444.091 , 444.969 , 445.239, 449.129, 466.951, 483.195, 509.146, 540.040, 541.023 , 554.169, 556.998, 559.983 , 561.391, 562.054 , 574.430, 578.030 , 578.978 , 580.045 , 584.016, 594.003 , 596.020, 599.990, 600.011 , 603.144, 607.409, 609.072, 610.443, 615.985 , 625.268, 633.075, 633.081, 634.057, 635.102, 636.083, 654.095, 670.090, 671.199, 672.011, 672.204, 675.105, 688.394, 691.088, 691.216, 692.073, 693.117, 695.038, 697.088 , 707.062, 707.181 , 708.047, 711.434, 713.050 , 713.449, 715.100 , 718.003, 727.467 , 729.044, 729.387, 730.028, 731.074 , 735.037 , 737.082 , 741.483 , 745.314, 752.011, 753.055 , 756.493, 758.509, 759.975, 761.286, 761.309, 767.342, 769.030 , 770.509 , 775.037 , 778.278, 784.526 , 786.542, 791.013 , 793.276, 798.539 , 799.222, 800.557, 805.299 , 814.572, 833.255, 871.460, 884.486 , 909.416, 929.066 , 995.308, 1012.333, 1013.534, 1051.490, 1058.097 , 1155.608, 1157.360, 1177.376, 1193.567, 1337.418, 1353.399, 1499.474
Control/ <i>T. viridae</i> [0]:	
Control/ <i>Esco</i> sp. 1/ <i>T. viridae</i> [0]:	
Control/ <i>Esco</i> sp. 2/ <i>T. viridae</i> [0]:	
<i>Pseudonocardia</i> sp. AECC09-02	
<i>Esco</i> sp. 1/ <i>Esco</i> sp. 2 [38]:	304.176 , 306.201, 340.185, 346.041, 378.141 , 402.021, 402.196, 403.024 , 445.239, 522.030 , 546.061 , 555.134 , 556.998, 568.041 , 587.314, 610.443, 649.047 , 649.106, 650.032 , 657.084 , 671.028 , 672.011, 673.056 , 675.092 , 675.105, 695.038, 696.022 , 708.982 , 721.316, 725.451 , 744.283 , 745.314, 756.493, 758.509, 772.525, 786.542, 800.557, 814.572
<i>Esco</i> sp. 1/ <i>T. viridae</i> [3]:	367.027, 411.160, 702.072
<i>Esco</i> sp. 2/ <i>T. viridae</i> [23]:	337.171, 366.962, 370.052, 407.957, 462.102, 465.121, 509.146, 524.058, 526.173, 527.159, 542.069, 542.970, 543.152, 581.319, 591.434, 634.057, 639.961, 659.200, 666.130, 690.214, 704.089, 723.345 , 833.255
<i>Esco</i> sp. 1/ <i>Esco</i> sp. 2/ <i>T. viridae</i> [37]:	354.161, 392.034, 406.953, 408.952 , 427.139, 428.036 , 467.168, 542.148, 558.365, 581.955, 582.961, 583.965, 586.032, 633.075, 655.275 , 664.117, 671.199, 689.211, 691.216, 705.185, 706.189, 758.972, 775.267, 799.222, 846.316, 847.322, 851.262, 867.238, 995.308, 1012.333, 1013.32, 1155.608, 1175.366, 1177.376, 1191.344, 1337.418, 1353.399
Control/ <i>Esco</i> sp. 1/ <i>Esco</i> sp. 2/ <i>T. viridae</i> [77]:	315.202 , 328.184 , 331.128, 334.930, 337.162 , 337.184 , 339.177, 341.193, 344.157 , 350.904, 353.158 , 359.143 , 360.151, 375.119 , 377.134 , 379.150, 381.078, 383.997, 386.027 , 399.145, 405.946 , 408.008 , 422.928 , 423.983, 424.926, 465.993 , 483.195, 487.974 , 510.939, 526.912, 543.132 , 544.135, 544.456 , 558.375 , 562.012 , 566.438 , 569.453 , 574.349 , 580.025 , 582.412 , 583.996 , 584.016, 584.410 , 597.928, 598.936 , 599.990, 602.006 , 603.144, 607.409, 617.981 , 623.988 , 625.268, 633.081, 635.102, 640.334, 641.342, 656.308 , 657.316 , 662.450 , 727.301, 729.387, 743.276, 743.297 , 757.961, 759.272 , 759.975, 767.342, 774.945 , 871.460, 885.278, 909.416, 934.982 , 950.951, 1013.534, 1029.292 , 1051.49, 1193.567
Control/ <i>Esco</i> sp. 1 [8]:	355.155, 596.020, 622.035 , 707.062, 729.044, 730.044, 745.019 , 913.090
Control/ <i>Esco</i> sp. 2 [5]:	306.048, 314.182, 374.024, 636.083, 953.531
Control/ <i>Esco</i> sp. 1/ <i>Esco</i> sp. 2 [71]:	303.166 , 310.912, 312.049 , 314.964, 320.974, 326.378, 328.030 , 330.060, 333.334, 343.187, 350.006 , 350.012 , 350.996 , 352.042 , 352.920 , 356.903, 360.188, 360.361, 361.159, 365.986 , 366.970 , 368.016 , 368.022 , 372.876, 381.960 , 382.083 , 385.130 , 389.997 , 399.970 , 405.970 , 420.080 , 424.003 , 428.995 , 439.976 , 444.091 , 444.969 , 500.046, 541.023 , 548.885, 559.368, 559.983 , 562.054 , 578.030 , 578.978 , 580.045 , 594.003 , 600.011 , 615.985 , 637.476, 697.088 , 707.181 , 713.050 , 715.100 , 727.467 , 731.074 , 735.037 , 737.082 , 741.483 , 744.302, 753.055 , 769.030 , 770.509 , 775.037 , 784.526 , 791.013 , 798.539 , 805.299 , 828.303, 884.486 , 929.066 , 1058.097
Control/ <i>T. viridae</i> [1]:	561.391
Control/ <i>Esco</i> sp. 1/ <i>T. viridae</i> [0]:	
Control/ <i>Esco</i> sp. 2/ <i>T. viridae</i> [0]:	
Control/ <i>Esco</i> sp. 1/ <i>Esco</i> sp. 2/ <i>T. viridae</i> [2]:	450.018, 503.948

[] denotes total number of unique ions in each particular treatment

Table A4.2 Unique ions (m/z), over 300 Da, detected in each strain of *Pseudonocardia* in each treatment under *in vitro* conditions. Each ion was detected in 2 out of 3 Petri plate replicates.

<i>Pseudonocardia</i> sp. AOST16-01	
Control [22]	321.219, 329.084, 356.200, 364.096*, 376.124, 402.051, 408.019, 429.240, 438.145, 450.976, 535.298, 548.310, 563.005*, 565.290, 614.910*, 666.434, 704.389, 768.122, 1247.372*, 1500.481, 1515.449, 1516.452
<i>Escovopsis</i> sp. 1 [6]	360.361, 599.094, 761.267, 790.919, 1018.400*, 1019.408
<i>Escovopsis</i> sp. 2 [7]	465.121, 525.121, 637.476*, 680.532, 697.477, 699.105, 953.531
<i>T. viridae</i> [77]	303.134, 306.121, 313.058, 314.084, 314.091, 318.129, 319.069, 324.214, 325.199, 326.123, 329.167, 330.938, 332.075, 334.140, 344.134, 356.167, 357.152, 363.147, 368.203, 369.189, 378.152, 396.338, 406.159, 407.145, 417.221, 433.155, 530.344, 556.099, 557.108, 559.378, 565.053, 575.502, 586.406, 596.095, 598.109, 598.297, 599.119, 599.968*, 600.120, 601.135, 601.489, 604.024*, 614.272, 615.297, 621.101, 630.265, 636.273, 637.075, 652.247, 654.268, 657.283, 657.291, 658.296, 664.377, 666.637, 671.271, 687.264, 688.112, 693.231, 696.096, 699.265, 706.630, 718.336, 719.083, 726.068*, 740.317, 756.293, 764.275, 804.552, 892.127*, 972.393, 973.567, 977.590, 988.366, 989.541, 991.560, 1130.592
<i>Pseudonocardia</i> sp. AECC09-02	
Control [9]	329.084, 420.061, 466.951, 635.180, 688.394, 708.047*, 768.122, 876.731*, 941.274
<i>Escovopsis</i> sp. 1 [5]	303.185, 330.938, 369.155, 596.095, 905.054*
<i>Escovopsis</i> sp. 2 [45]	305.304, 306.080, 314.091, 320.171, 322.054, 329.015, 336.074, 347.094, 348.071, 350.086, 365.105, 386.048, 404.171, 440.109, 443.045, 481.094, 538.002, 540.040, 551.309, 554.169, 570.144, 574.129, 574.430, 609.072, 611.099, 654.095, 658.066*, 679.065, 680.532, 687.176, 691.068*, 693.010*, 693.117, 693.334, 703.191, 705.321, 711.434, 713.449, 714.033*, 718.003*, 761.286, 761.309, 777.281, 1157.360, 1499.474
<i>T. viridae</i> [115]	306.121, 312.035, 324.214, 328.008, 328.115, 329.167, 330.046, 345.045, 345.142, 346.019, 347.175, 352.027, 353.164, 354.057, 365.164, 366.112, 368.001*, 368.203, 369.189, 370.031, 376.039, 378.994, 381.158, 383.002, 383.975, 398.975*, 406.159, 407.986, 412.100, 419.135, 425.012, 425.148*, 425.980, 435.108, 442.132, 445.093, 447.110, 447.130, 448.027, 449.129, 463.104, 472.000*, 490.038, 492.067, 505.037, 506.011*, 508.049, 510.078, 514.078, 521.011, 527.020, 530.045*, 530.344, 542.994*, 546.018, 549.975*, 558.295, 558.968*, 564.030*, 565.950, 576.248, 579.131, 580.949*, 583.254, 595.104, 599.940*, 619.092, 634.091*, 635.066*, 635.111, 643.109, 646.475, 650.066, 654.268, 656.075*, 657.047*, 657.283, 659.075*, 659.097, 669.256, 669.292, 670.263, 670.294, 671.271, 672.047*, 672.275, 674.096, 681.058*, 681.079*, 683.108, 687.264, 688.021*, 688.269, 690.070*, 693.231, 694.026*, 694.236, 697.053, 699.081*, 699.105, 703.039*, 712.054*, 719.021*, 719.036*, 719.083, 740.317, 759.292*, 761.267, 764.275, 780.250, 790.919*, 804.552, 809.302, 843.292, 1035.509

[] denotes total number of unique ions in each particular treatment

* denotes ions with no known reference when searched in MetaboSearch28 and Antibase29 (searched [M+H], [M+Na], [M+K], and [M+NH₄] adducts).

Table A2.3 Ions (m/z), over 300 Da, detected in each strain of *Pseudonocardia* shared between treatments under *in vivo* conditions. Each ion was detected in 6 out of 9 ant replicates.

<i>Pseudonocardia</i> sp. AOST16-01	
<i>Esco</i> sp. 1/ <i>Esco</i> sp. 2 [2]:	350.086, 622.035
<i>Esco</i> sp. 1/ <i>T. viridae</i> [4]:	378.141, 381.148, 464.086, 637.142
<i>Esco</i> sp. 2/ <i>T. viridae</i> [0]:	
<i>Esco</i> sp. 1/ <i>Esco</i> sp. 2/ <i>T. viridae</i> : [20]	319.069, 330.938, 348.071, 399.145, 428.036, 440.109, 465.993, 524.058, 533.166, 541.121, 542.069, 545.959, 562.012, 574.094, 580.025, 617.981, 704.089, 768.122, 786.166, 824.122
Control/ <i>Esco</i> sp. 1/ <i>Esco</i> sp. 2/ <i>T. viridae</i> [25]:	320.076, 324.167, 325.199, 337.162, 341.193, 353.192, 355.208, 364.114, 366.129, 369.189, 379.15, 383.204, 402.196, 407.145, 446.185, 649.106, 664.117, 666.130, 696.096, 702.073, 729.072, 787.175, 825.130, 1015.377, 1018.4
Control/ <i>Esco</i> sp. 1 [15]:	334.14, 448.14, 452.134, 484.141, 504.209, 591.167, 595.233, 618.113, 640.122, 644.118, 646.207, 655.275, 705.321, 721.316, 737.311
Control/ <i>Esco</i> sp. 2 [1]:	307.186
Control/ <i>Esco</i> sp. 1/ <i>Esco</i> sp. 2 [6]:	339.213, 402.070, 458.120, 522.218, 560.174, 1019.408
Control/ <i>T. viridae</i> [0]:	
Control/ <i>Esco</i> sp. 1/ <i>T. viridae</i> [2]:	452.206, 527.039
Control/ <i>Esco</i> sp. 2/ <i>T. viridae</i> [2]:	340.185, 421.160
<i>Pseudonocardia</i> sp. AECC09-02	
<i>Esco</i> sp. 1/ <i>Esco</i> sp. 2 [5]:	307.095, 376.183, 410.250, 545.959, 555.117
<i>Esco</i> sp. 1/ <i>T. viridae</i> [2]:	375.100, 576.900
<i>Esco</i> sp. 2/ <i>T. viridae</i> [10]:	303.185, 377.134, 382.107, 503.948, 504.209, 511.059, 562.012, 721.316, 768.122, 868.138
<i>Esco</i> sp. 1/ <i>Esco</i> sp. 2/ <i>T. viridae</i> [8]:	313.140, 331.151, 380.145, 436.156, 441.155, 669.112, 729.072, 828.303
Control/ <i>Esco</i> sp. 1/ <i>Esco</i> sp. 2/ <i>T. viridae</i> [64]:	303.137, 319.069, 320.076, 324.167, 325.199, 335.055, 337.162, 340.185, 341.193, 346.103, 353.192, 355.155, 355.208, 364.114, 369.189, 378.141, 379.150, 380.151, 383.204, 385.130, 399.145, 402.196, 407.145, 421.160, 427.139, 428.036, 440.109, 446.185, 448.140, 452.134, 456.201, 458.120, 464.086, 467.168, 477.130, 490.084, 508.003, 524.058, 526.029, 527.039, 531.151, 533.166, 542.069, 580.025, 591.167, 622.035, 640.122, 643.109, 644.118, 649.106, 664.117, 666.130, 694.026, 702.073, 704.089, 708.245, 719.021, 783.147, 787.175, 811.105, 843.292, 846.316, 847.322, 885.278
Control/ <i>Esco</i> sp. 1 [3]:	339.213, 507.176, 541.121
Control/ <i>Esco</i> sp. 2 [9]:	322.122, 330.938, 361.143, 431.207, 448.165, 522.218, 637.142, 743.276, 748.587
Control/ <i>Esco</i> sp. 1/ <i>Esco</i> sp. 2 [14]:	310.122, 311.125, 366.129, 399.192, 402.070, 439.101, 525.115, 531.105, 561.391, 565.519, 604.024, 619.121, 744.082, 775.267
Control/ <i>T. viridae</i> [3]:	430.052, 473.103, 768.931
Control/ <i>Esco</i> sp. 1/ <i>T. viridae</i> [4]:	415.110, 566.170, 620.010, 732.560
Control/ <i>Esco</i> sp. 2/ <i>T. viridae</i> [15]:	310.06, 330.060, 334.140, 360.188, 404.171, 465.993, 484.141, 529.135, 696.096, 705.321, 734.570, 759.272, 762.603, 786.166, 825.130

[] denotes total number of unique ions in each particular treatment

Table A2.4 Unique ions (m/z), over 300 Da, detected in each strain of *Pseudonocardia* in each treatment under *in vivo* conditions. Each ion was detected in 6 out of 9 ant replicates.

<i>Pseudonocardia</i> sp. AOST16-01	
Control [12]:	315.202, 331.151, 338.145, 376.183, 498.176, 561.391, 565.290, 623.189, 719.299, 775.267, 783.147, 848.041
<i>Escovopsis</i> sp. 1:	360.188, 382.107, 399.192, 439.101, 456.201, 478.064, 490.084, 503.948, 507.176, 561.222, 619.121, 620.009*, 643.109, 655.152, 755.367
[15]	
<i>Escovopsis</i> sp. 2:	361.143, 444.091*, 604.024*, 744.082
[4]	
<i>T. viridae</i> [1]:	331.168
<i>Pseudonocardia</i> sp. AECC09-02	
Control [1]:	471.234
<i>Escovopsis</i> sp. 1:	409.246, 569.453, 618.113*, 704.250, 737.311
[5]	
<i>Escovopsis</i> sp. 2:	311.182, 331.168, 347.175, 355.171, 366.112, 383.110, 385.120, 399.199, 412.100, 414.097, 453.245, 494.224, 623.189, 824.122*
[14]	
<i>T. viridae</i> [9]:	348.071, 350.086, 478.064, 496.339, 607.409, 617.981*, 772.525, 773.139*, 786.542

[] denotes total number of unique ions in each particular treatment

* denotes ions with no known reference when searched in MetaboSearch28 and Antibase29 (searched [M+H], [M+Na], [M+K], and [M+NH₄] adducts).

Appendix 3

Convergent evolution of complex structures for ant-bacterial defensive symbiosis in fungus-farming ants

Authors: Hongjie Li, Jeffrey Sosa-Calvo, Heidi A. Horn, Mônica T. Pupo, Jon Clardy, Christian Rabeling, Ted R. Schultz, Cameron R. Currie

Reprinted with permission from Li, Hongjie, Jeffrey Sosa-Calvo, Heidi A. Horn, Mônica T. Pupo, Jon Clardy, Christian Rabeling, Ted R. Schultz, and Cameron R. Currie. "Convergent evolution of complex structures for ant–bacterial defensive symbiosis in fungus-farming ants." *Proceedings of the National Academy of Sciences* 115, no. 42 (2018): 10720-10725.

*This work is included in this dissertation as it is an application of the technique developed in Chapter 2 of this thesis. HAH performed all quantitative polymerase chain reaction experiments and generated data for Figure A3.3, Table A3.9.1, and Figure A3.9.1.

A3.1 Abstract

Evolutionary adaptations for maintaining beneficial microbes are hallmarks of mutualistic evolution. Fungus-farming “attine” ant species have complex cuticular modifications and specialized glands that house and nourish antibiotic-producing Actinobacteria symbionts, which in turn protect their hosts' fungus gardens from pathogens. Here we reconstruct ant-Actinobacteria evolutionary history across the full range of variation within subtribe Attina by combining dated phylogenomic and ultra-morphological analyses. Ancestral-state analyses indicate the ant-Actinobacteria symbiosis arose early in attine-ant evolution, a conclusion consistent with direct observations of Actinobacteria on fossil ants in Oligo-Miocene amber. qPCR indicates that the dominant ant-associated Actinobacteria belong to the genus *Pseudonocardia*. Tracing the evolutionary trajectories of *Pseudonocardia*-maintaining mechanisms across attine ants reveals a continuum of adaptations. In *Myrmicocrypta* species, which retain many ancestral morphological and behavioral traits, *Pseudonocardia* occur in

specific locations on the legs and antennae, unassociated with any specialized structures. In contrast, specialized cuticular structures, including crypts and tubercles, evolved at least three times in derived attine-ant lineages. Conspicuous caste differences in *Pseudonocardia*-maintaining structures, in which specialized structures are present in worker ants and queens but are reduced or lost in males, are consistent with vertical *Pseudonocardia* transmission. Although the majority of attine ants are associated with *Pseudonocardia*, there have been multiple losses of bacterial symbionts and of bacteria-maintaining structures in different lineages over evolutionary time. The early origin of the ant-*Pseudonocardia* mutualism and the multiple evolutionary convergences on strikingly similar anatomical adaptations for maintaining bacterial symbionts indicate that *Pseudonocardia* have played a critical role in the evolution of ant fungiculture.

A3.2 Introduction

Evolutionary adaptations associated with mutualistic associations are ubiquitous in nature and mutualistic evolution is an important driver of phenotypic complexity (1–4). In animals, internal specialized cells, tissues, and/or organs often evolve in host organisms to accommodate and maintain mutualists, such as bacteriocytes in the aphid-*Buchnera* symbiosis (5, 6) and light organs in the squid-*Vibrio* symbiosis (7). Likewise, in many insect groups, external cuticular modifications have arisen frequently to house microbial symbionts, such as antennal gland reservoirs in the beewolf wasp-*Streptomyces* symbiosis (8) and mycangia in beetle-fungus symbioses (9). Such symbiont-associated traits are often regarded as inherently contingent evolutionary outcomes, the results of complex sequences of unique historical events (10).

Attine ants (subfamily Myrmicinae, tribe Attini, subtribe Attina), an exclusively New World monophyletic group of 17 genera that comprise approximately 250 described species, have cultivated fungi for some 55-65 My (11-13). Primitively, attine ants forage on insect frass,

seeds, flower parts, and other organic detritus as substrates for their fungus gardens, but higher-attine leaf-cutting ants cut fresh vegetation, making them dominant herbivores in Neotropical ecosystems. As part of the fungus-farming life history, attine ants participate in elaborate symbiotic associations with multiple microbial lineages, spanning fungi and bacteria (14-17). Species in the genus *Escovopsis* (Ascomycota, Hypocreales), specialized parasitic fungi that are only known to occur in attine fungus gardens, constitute a "crop disease" of attine agriculture, competing with the ants to use their fungal cultivars for food. As a defense against *Escovopsis*, attine ants participate in mutualistic associations with Actinobacteria that produce antibiotics with potent antagonistic properties against *Escovopsis* parasites (16, 18, 19). The attine ant-cultivar-parasite-bacterium association is therefore, minimally, a quadripartite symbiosis and so far one of the most complex symbiotic interactions discovered in nature (20).

The exoskeletons of numerous attine-ant species are anatomically modified in order to house Actinobacteria symbionts and nourish them with glandular secretions through pores lining the specialized cuticle (21), as indicated by the trophic position of the symbionts one level higher than the trophic position of the ants (22). This key evolutionary innovation likely favors the resident Actinobacteria, thereby stabilizing the attine ant-Actinobacteria mutualistic association. An earlier survey of specialized structures that maintain Actinobacteria in attine ants revealed high diversity (21). In the early-diverging paleoattine genus *Apterostigma*, filamentous Actinobacteria occur on the propleura (in between the forelegs) and the mesopleura (between the forelegs and middle legs), where they grow directly on the ventral surface of the cuticle, which is lined with gland-cell-associated pores. In the "higher" attine-ant genus *Trachymyrmex*, the Actinobacteria symbiont occurs on the propleura (in between the forelegs), where they grow on tubercles within crypts, in which each tubercle is connected to an internal glandular cell. In the

leaf-cutting genus *Acromyrmex* (Fig. A3.1A), the bacteria grow on tubercles directly on the exoskeleton rather than in crypts (Fig. A3.1B and C). When interpreted with reference to the ant phylogeny, this diversity in cuticular structures conforms to broad evolutionary patterns, with important implications for understanding evolutionary adaptations associated with ant-bacteria mutualism.

Despite the apparent advantages of mutualism with Actinobacteria, some extant higher-attine ants have nearly or completely lost the cuticular structures associated with the maintenance of bacterial symbionts (e.g., *Atta* spp.) (21, 23). Such secondary losses of complex structural traits and, presumably, of the symbiosis with Actinobacteria implies alternative evolutionary interpretations, including (i) a single principal origin followed by multiple losses, (ii) multiple independent origins and no losses, or (iii) some combination of multiple origins and losses. Each scenario, in turn, has implications for the evolution of the ant-bacteria symbiosis. To date, these scenarios have not been tested phylogenetically due both to the lack of ultra-morphological studies of ants sampled from all major attine-ant clades and the lack of a well-supported phylogeny for those sampled ants. To address these issues, we perform a phylogenomic analysis that includes 69 taxa, covering 15 of the 17 fungus-farming attine-ant genera as well as closely related, non-fungus-growing ants. Only two monotypic genera *Paramyctophylax* and *Pseudoatta* were excluded. In addition, we conduct scanning electron microscopy (SEM), quantitative polymerase chain reaction (qPCR), divergence dating, and ancestral-state character reconstruction analyses in order to reconstruct the origin and subsequent evolution of specialized cuticular structures for maintaining and nourishing bacteria in fungus-farming ants.

A3.3 Results and Discussion

A3.3.1 Ancient Ant-Pseudonocardia Symbiosis.

To reconstruct the phylogenetic relationships of attine fungus-farming ants, we obtained phylogenomic data for 69 taxa (five outgroup and 64 ingroup taxa) consisting of 672 ultraconserved-element (UCE) loci, resulting in a concatenated alignment containing 416,786 bp with 13% missing data and 131,357 parsimony-informative sites (PIS). Maximum-likelihood analyses resulted in a resolved phylogeny of the fungus-farming ants in which nearly all nodes are maximally well supported (Fig. A3.2, details provided in the *SI Appendix*, Fig. S1 and Table S1). The recovered phylogenetic relationships are fully congruent with those proposed in a recent study with more outgroup taxa by Branstetter et al. (2017) (11).

To gauge the timescale over which the ant-Actinobacteria symbiosis emerged and diversified, we conducted divergence-dating analysis in which four nodes were calibrated using information from four Dominican amber fossils. The posterior dates of three of our four fossil-calibrated nodes (N1, N3, and N4; Fig. S2) are significantly older (59 Ma, 27 Ma, and 22 Ma, respectively) than our prior dates based on the minimum age of Dominican amber (15 Ma), indicating that the UCE data are highly decisive. Our results indicate that fungus-farming ants arose at the end of the Paleocene around 57 Ma (95% HPD interval: 48-66 Ma) (details provided in the *SI Appendix*, Fig. S2). The crown clades of the ‘Paleoattina’ and ‘Neoattina’, the two major sister clades within fungus-farming ants, originated 49 (41-58) Ma and 48 (40-57) Ma, respectively. Although our inferred dates are largely congruent with those of other molecular studies, they imply a slightly younger date for the origin of fungus-farming ants (11, 12), possibly due to our sparser taxon sampling.

Our electron microscopy survey established the presence/absence of filamentous bacterial symbionts across a broad, representative sample of fungus-farming ants (Fig. A3.2, details provided in *SI Appendix*, Fig. S3). Combined evidence from maximum-likelihood ancestral-state

reconstruction, divergence-dated phylogenetic analysis, and electron-microscopic ultra-morphological study indicates that the ant-Actinobacteria association originated coincident with or shortly after the origin of fungus-farming ants, no later than 49 Ma (Fig. A3.2).

Ants embedded in amber (i.e., fossilized tree resin) are often extremely well preserved, providing the opportunity to study microscopic morphological structures. We examined two attine-ant fossils in Oligo-Miocene amber from the Dominican Republic, which has been dated variously at 15-20 million years old (24, 25), *Trachymyrmex primaevus* and *Apterostigma eowilsoni* (26, 27). We found crypts housing filamentous bacteria in a modern *Trachymyrmex* species (Fig. A3.1D, E and F) and we likewise observed crypts in the fossil *T. primaevus* (Fig. A3.1G) in the same locations on the head (Fig. A3.1H) and propleural plates (Fig. A3.1I and J). For extant *Apterostigma* species, dense filamentous Actinobacteria are found in the area of the mesopleura under the forelegs (Fig. A3.1K), corresponding to the location on *A. eowilsoni* where we found conspicuous bubbles that are likely due to bacterial respiration (Fig. A3. 1L). The presence of Actinobacteria on ants fossilized in 17-20 million-year-old amber is consistent with an early origin of the ant-Actinobacteria symbiosis.

To reconstruct the evolution of specialized cuticular structures for maintaining Actinobacteria, we conducted micromorphological examinations of 69 ant species, sampled from across the full range of the tribe Attina, with electron microscopy (Fig. A3.2, details provided in *SI Appendix*, Fig. S4 and S5). This led to the unexpected discovery of numerous conspicuous crypts distributed across large parts of the integuments of *Myrmicocrypta tuberculata* and *Apterostigma ierense* and of diverse specialized structures in other *Apterostigma* species. The presence of such structures in both the Paleoattina and the Neoattina, sister clades resulting from

the basal-most split in the attine ant phylogeny, adds further support to an early origin of the ant-Actinobacteria mutualism.

To assess the presence and relative abundance of filamentous bacterial symbionts across attine ants, we screened 25 species representing all attine-ant genera for the abundance of *Pseudonocardia* with a combination of qPCR and electron microscopy (Fig. A3.3, *SI Appendix*, Table A3.1). Ant genera closely related to attine ants, including *Blepharidatta conops*, *Wasmannia auropunctata*, *Tranopelta subterranea*, *Acanthognathus ocellatus*, and *Daceton armigerum*, the latter two in the subtribe Dacetina, the sister group of the Attina, do not have *Pseudonocardia* bacteria nor any filamentous bacteria on their integuments. *Pseudonocardia* bacteria were found to be present in the paleoattine genera *Mycocepurus*, *Myrmicocrypta*, and *Apterostigma* by both qPCR and eSEM. In most species of early-diverging Neoattina, qPCR found relatively low abundances of *Pseudonocardia* (e.g., in *Cyphomyrmex costatus*, *C. longiscapus*, *C. muelleri*, *Mycetarotes parallelus*, *Mycetosoritis hartmanni*, and *Mycetophylax asper*), which is in agreement with our microscopic observations of lower densities on workers. Relatively lower abundances in these groups are likely due to the substantially smaller bodies of these workers (28). Both qPCR and microscopy found relatively high concentrations of *Pseudonocardia* in *Mycetophylax morschi*. Similarly, qPCR detected high concentrations of *Pseudonocardia* in most ‘higher’ attine ants such as *Trachymyrmex* cf. *bugnioni* and *T. septentrionalis* but not in *Sericomyrmex mayri* and *Xerolitor explicatus* (microscopic study found visible filamentous bacteria absent in *Sericomyrmex* and present in low density in *X. explicatus*). Also, no *Pseudonocardia* is detectable in the fungus gardens of *S. mayri* (*SI Appendix*, Fig. A3.9.1). In the leaf-cutting genus *Atta*, *Pseudonocardia* is completely undetectable via qPCR, consistent with microscopic observations. In leaf-cutting *Acromyrmex* species, the highest

concentration of *Pseudonocardia* was found in *Ac. echinator* and *Ac. laticeps*, but *Pseudonocardia* was absent in *Ac. versicolor*. Our direct qPCR evidence, considered together with past long-term isolation experiments (29) as well as culture-independent studies by us and others (30, 31), indicate that the genus *Pseudonocardia* is the dominant filamentous Actinobacteria symbiont found on attine ant exoskeletons.

A3.3.2 Evolutionary Trajectory of Pseudonocardia Maintenance in Fungus-Farming Ants.

To reconstruct the evolutionary history of the ant-*Pseudonocardia* symbiosis, we examined the locations of bacteria on the ant cuticle and the specialized cuticular structures for maintaining bacteria across the phylogeny of attine ants (Fig. A3.2, details provided in *SI Appendix*, Fig. S3). Species in the genera closely related to attine ants, *Tranopelta*, *Wasmannia*, *Blepharidatta*, *Acanthognathus*, and *Daceton* (the latter two representing the Dacetina, the sister group of the fungus-farming ants) do not have any specialized structures for maintaining *Pseudonocardia* bacteria. Similarly, species in the paleoattine genera *Mycocepurus* and *Myrmicocrypta* have no *Pseudonocardia*-associated morphological structures present on the external exoskeleton. The only exception is the species *Myrmicocrypta tuberculata*, which has been recovered as the sister group of all other *Myrmicocrypta* species and has obvious crypts both on the propleural plate and distributed over the rest of the exoskeleton (Fig. A3.2) (32). Despite the absence of specialized structures in other *Myrmicocrypta* species, in 24 out of 26 species examined, dense concentrations of filamentous *Pseudonocardia* occur on the antennae and legs, specifically on the antennal scape and on the femora and tibiae (*SI Appendix*, Table S3 and Figure S7). In the paleoattine genus *Apterostigma*, diverse specialized cuticular structures were found on both the propleural and mesopleural plates, including, on the former, crypts and tubercles. In species with tubercles only (e.g., *A. megacephala* and *A. jubatum*, Fig. A3.2), the

tubercles have pores in the locations where the filamentous *Pseudonocardia* are cultured. In species in which crypts are present (e.g., *A. ierense*, Fig. 2), each crypt contains dense concentrations of filamentous *Pseudonocardia*. In the neoattine species, tubercles are absent in *Kalathomyrmex emeryi* and *Cyatta abscondita*, but present in the clade containing *Mycetosoritis hartmanni* and *Mycetarotes parallelus*. Crypts are also present in *Cyphomyrmex* and *Mycetophylax* species. In these species, each crypt contains a tubercle with a duct connected to a glandular cell in the ant body (in Fig. A3.2) (21). In the paraphyletic higher-attine genus *Trachymyrmex*, tubercles were found in the clade that is the sister group of *Sericomyrmex*. Tubercles are also present in *Sericomyrmex* species and *Xerolitor explicatus* but were highly reduced in terms of size and abundance. In the clade containing *T. cornetzi*, *T. bugnioni*, and *T. diversus*, crypts are present, with the exception of *T. intermedius*, in which tubercles are present. Significantly, *T. intermedius* is the sister to all other species in that clade. Interestingly, tubercles are present in the clade containing *T. septentrionalis* and *T. arizonensis*, which is the sister clade to the leaf-cutter ants. Similarly, tubercles are present in the leaf-cutting species *Acromyrmex echinator*, *Ac. octospinosus*, and *Ac. rugosus*, whereas specialized cuticular structures are absent in the leaf-cutter species *Ac. striatus*, *Ac. versicolor*, *Ac. heyeri*, *Ac. lundii*, and *Atta* spp. Interestingly, the inquiline social parasite *Acromyrmex charruanus*, which is considered a close relative of its host *Ac. heyeri* (33), is also lacking specialized cuticular modifications to house *Pseudonocardia* symbionts. The specialized cuticular modifications for maintaining *Pseudonocardia* symbionts across the attine ants represent an apparent continuum of adaptive traits, from antennal gland reservoirs to gland-associated crypts and tubercles. Maximum-likelihood ancestral-state reconstruction indicates that specialized cuticular structures for maintaining *Pseudonocardia* originated separately three times (Fig. A3.2). Repeated anatomical

convergent evolution is consistent with the defensive role of *Pseudonocardia* against the garden pathogen *Escovopsis*, an ubiquitous and ancient "crop disease" of fungus-farming ant agriculture (14, 16).

A3.3.3 Caste Differences in Maintenance of Pseudonocardia Symbionts.

Comparisons of the worker castes (minor and major workers) in *Acromyrmex echinator* revealed significant differences in the structure and height of tubercles (*SI Appendix*, Fig. S8). These differences are correlated with the abundance of visible filamentous *Pseudonocardia*, which achieve their highest densities in major workers, the caste most likely to apply *Pseudonocardia*-produced antibiotics. We further compared workers, males, and alate queens of five attine-ant species, *Acromyrmex echinator*, *Mycetophylax faunulus*, *Mycetophylax asper*, *Mycetosoritis hartmanni*, and *Trachymyrmex septentrionalis*. Specialized *Pseudonocardia*-associated cuticular structures, including crypts and tubercles, were consistently present in workers and queens, but absent or highly reduced in males (*SI Appendix*, Fig. S9). These differences across castes in the presence/absence of cuticular structures, together with observed differences in the abundance of bacterial symbionts, indicate that *Pseudonocardia* symbionts are transferred from worker to worker within colonies (34) and vertically by daughter queens when they found new colonies. In contrast to some marine and terrestrial symbioses with consistent horizontal acquisition, the vertical transmission of bacterial symbionts from mother to daughter colonies in fungus-farming ants, while not precluding occasional horizontal transmission, can be expected to reinforce the stability of particular pairs of mutualistic partners.

A3.3.4 Repeated Loss of Symbiosis.

Despite the apparent benefits of ant-*Pseudonocardia* symbiosis in attine ants, our results indicate the occurrence of multiple losses of ant-*Pseudonocardia* associations and of

Pseudonocardia-maintaining structures during the course of attine ant evolution. Specialized cuticular structures are absent in *Mycetophylax conformis*, *Mycetagroicus inflatus*, *Acromyrmex striatus*, *Ac. versicolor*, *Ac. heyeri*, *Ac. lundii*, and the genus *Atta*. Reduced tubercles are present in *Sericomyrmex*, even though *Pseudonocardia* are absent. Our maximum-likelihood ancestral-state reconstruction indicates that *Pseudonocardia* symbionts have been lost at least six times and that specialized *Pseudonocardia*-maintaining cuticular structures have been lost at least seven times. Thus, ant-*Pseudonocardia* mutualistic associations have been lost repeatedly, possibly due to environmental factors such as migration into dry or colder environments where parasite pressure might be reduced or where the growth of the exosymbionts may not be possible. Given the high metabolic cost associated with maintaining the *Pseudonocardia* (35), the repeated loss of *Pseudonocardia* symbionts when pressure is removed is perhaps not surprising.

A3.4 Conclusion

Many animals and plants have important morphological, physiological, and behavioral traits that help establish and maintain beneficial microbes (3, 36). In this study, we demonstrate the convergent origin of elaborate cuticular structures for maintaining *Pseudonocardia* in multiple fungus-farming ant lineages. These multiple convergences, each producing strikingly similar yet complex morphological structures, indicate the presence of strong selection pressures for maintaining *Pseudonocardia* to help control the ancient garden parasite *Escovopsis*. The vertical transmission of *Pseudonocardia* across ant colony generations, coupled with the provision by the ants of glandular nutrients to the bacteria, is expected to reinforce the stability of partner associations with *Pseudonocardia*. Considered together, these results indicate that the

mutualism between fungus-farming ants and antibiotic-producing *Pseudonocardia* is an ancient defensive symbiosis.

The medicinal use of antibiotics by humans dates only from 1945, yet the rapid evolution of antibiotic resistance in human pathogens has rendered the original antibiotics largely ineffective. In contrast, our results indicate that fungus-farming ants have effectively used antibiotics for millions of years. Understanding the mechanisms associated with the long-term use of antibiotics in this ancient symbiosis has the potential to inform our own attempts to counter antibiotic resistance in human pathogens. Likewise, the small molecules produced by ant-associated *Pseudonocardia* for controlling the *Escovopsis* crop disease represent a promising resource for novel antibiotic drug discovery (18, 37, 38).

A3.5 Experimental Procedures

A3.5.1 Taxon sampling and UCE data preparation.

We sampled a total of 69 ant species for phylogenetic analysis, representing the phylogenetic diversity of the tribe Attini for both fungus-farming and non-fungus-farming ant species (*SI Appendix*, Table S1). Within the fungus-farming ants (subtribe Attina), we included 64 species representing ~26% of the 245 currently known species and covering 15 of the 17 currently recognized genera. We did not have material for the genera *Paramyctophylax* and *Pseudoatta*, each of which contains a single species, and the latter of which is a derived social parasite of *Acromyrmex* known to be nested within that genus. The monophyly/non-monophyly of the included genera has been previously tested in multiple studies (*SI Appendix*, Table S4). Five outgroup taxa were included, two from the sister group Dacetina and three from other distantly related clades in the tribe Attini. Our analyses are based on a modified version of the alignment used in Branstetter et al. (2017) (11), into which we incorporated new sequences for

seven species belonging to the fungus-farming ants (ingroup). The output from the demultiplexed FASTQ data was trimmed for adapter contamination and low-quality bases using Illumiprocessor (39), which contains the package Trimmomatic (40, 41). Further data processing followed a series of scripts available in the Phyluce package v1.5 (42) to process the reads and extract targeted UCE loci, and is similar to that employed in Branstetter et al. (2017) (11) and Ješovnik et al. (2017) (43) (*SI Appendix*, Table S5 and S6).

Alignment of each UCE locus was performed using MAFFT v7.310 (44) and the resulting alignments were trimmed with GBLOCKS v0.91b (45) using relaxed settings (-b1=0.5 -b2=0.5 -b3=12 -b4=7).

A3.5.2 Phylogenetic inference.

After removing loci with poor taxon representation and gap-rich regions, our data consisted of 672 UCE loci, which were on average 620 bp long. We employed IQ-TREE (46) to infer the best substitution model under the AICc criterion for each UCE locus, performed 2000 ultrafast bootstrap approximations (47), and increased the number of unsuccessful attempted iterations to 200 (from the default 100) using the command (*iqtree-omp -s \$f -nt 2 -bb 2000 -merit AICc -wbt -nstop 200*).

We then constructed a 70% complete (data from ≥ 48 of the 69 taxa for each locus) concatenated alignment (416,786 bp long, including 13.1% of missing data and gaps) using the program AMAS (48) and created a by-locus partition file with the appropriate model selected for each UCE locus based on the IQ-TREE analysis described above. We used this concatenated alignment to infer a maximum likelihood tree using IQ-TREE. Node support was obtained by performing 2000 ultrafast bootstrap approximations (47).

A3.5.3 Divergence-dating analyses.

Estimation of species divergence times was conducted using the approximate likelihood approach implemented in the program MCMCTREE as part of the PAML package (49). To calibrate the analysis, information from four Dominican amber fossils (*Acanthognathus poinari*, *Apterostigma electropilosum*, *Cyphomyrmex* spp., and *Trachymyrmex primaevus*) were employed as independent constraints to calibrate our analysis (*SI Appendix*, Table S7, S8 and Fig. S2, black box symbols indicate constraints, N1-N4). We employed lower bounds (minimum-age bounds) for all four calibrations following Branstetter et al. (2017) (11). Except for the root age, all four fossil calibration points were specified as a truncated Cauchy distribution indicated by $L(tL, p, c)$, where tL = minimum-age bound (set as 15 Ma), p = offset value (default value of 0.1), and c = scale parameter value (default value of 1) representing a heavy-tailed density (50). The minimum (lower) bounds here specified represent 'soft' bounds, allowing molecular data to correct for conflicting fossil information (51), with a 2.5% probability that the bounds may be violated. The 97.5% upper limit of the probability distribution is at 366 Ma, there is no mean and variance is infinite (49). Since the dating of Dominican amber is ambiguous, ranging from 15 to 20 Ma (24, 25), we chose a conservative minimum age of 15 Ma and employed relatively flat priors to accommodate a wide range of posterior dates. Because of the lack of a fossil for directly calibrating the root node, we employed an admittedly more problematic secondary calibration based on the inferred age of the corresponding internal node of the phylogeny of Branstetter et al. 2017. For the root of the tree we employed soft minimum and maximum bounds (as B (0.56, 0.76), representing the secondary calibration range of 56–76 Ma), in order to incorporate the 95% HPD value range estimated by Branstetter et al. (2017) for the node corresponding to our root, with lower (pL) and upper (pU) tail probabilities set at $pL=pU= 0.025$ (default values). In

this case the prior density distribution is a flat uniform density between 56 and 76 Ma with 2.5% of density mass lying outside this range (52). To decrease computation time, we performed the analyses using an unpartitioned dataset (*n*_{data}= 1) using the HKY+G4 substitution model (*model*= 4 and *alpha*= 0.5). We conducted two independent MCMCTREE runs using the following settings: *sampfreq*= 5000, *nsample*= 10000, and *burnin*= 5000000. We assessed run convergence and performance by examining *mcmc.txt* files in Tracer v1.6 (53) and convergence plots in either Excel or R v.3.4.3 (R Development Core Team, 2014).

A3.5.4 Fossil ants.

Two amber fossils were available for morphological study: 1) *Apterostigma eowilsoni* (Holotype); worker caste; Oligo-Miocene; Dominican Republic. 2) *Trachymyrmex primaevus*; worker caste; Oligo-Miocene; Dominican Republic (details provided in *SI Appendix, SI Materials and Methods*).

A3.5.5 Electron microscopy.

Besides the 69 taxa in the phylogeny, 21 additional taxa were chosen for electron microscopic study, 17 species of the genus *Myrmicocrypta* (*SI Appendix, Table S3*), *Mycocephurus obsoletus*, and *Acromyrmex silvestrii*. In addition, we included the two inquiline social parasites *Mycocephurus castrator* and *Acromyrmex charruanus*, which exploit colonies of *M. goeldii* and *Ac. heyeri*, respectively (33) (*SI Appendix, Table S9*). See details in *SI Appendix, SI Materials and Methods*.

A3.5.6 qPCR.

A total of 25 species were screened for the abundance of *Pseudonocardia* using qPCR, representing all major taxa in the phylogeny (*SI Appendix, Table A3.9.1*). Material from four

fungus gardens was also included. See *SI Appendix, SI Materials and Methods* for details of DNA extraction, primer sets, and gene amplification.

A3.5.7 Ancestral-State Reconstruction.

We carried out maximum-likelihood-based ancestral-state reconstruction analyses in the software program Mesquite (54) (details provided in *SI Appendix, SI Materials and Methods*).

A3.6 Acknowledgements

We are grateful to R. Noll, S. Swanson, and J.G. Pennington for expert help conducting SEM work. We thank D. Grimaldi (American Museum of Natural History) for the loan of amber fossil specimens. We thank E. Okonski for fossil amber ant imaging and laboratory assistance. We thank M. Borowiec and M. Lloyd for assistance with UCE statistics. This study was funded by the National Institutes of Health (NIH) grant U19 TW009872-05 (to C.R.C., M.T.P., and J.C.), NIH grant U19 AI109673 (to C.R.C.), National Science Foundation grants DEB 1456964 and 1654829 (to C.R. and T.R.S.), São Paulo Research Foundation-FAPESP #2013/50954-0 (to M.T.P.), and partially supported by the University of Wisconsin-Madison College of Engineering Shared Research Facilities and the NSF through the Materials Science Research and Engineering Center (DMR-1720415) using instrumentation provided at the UW-Madison Materials Science Center. Collections of Brazilian samples are approved according to SISBIO #46555-5 and CNPq #010936/2014-9 authorizations.

A3.7 Figures

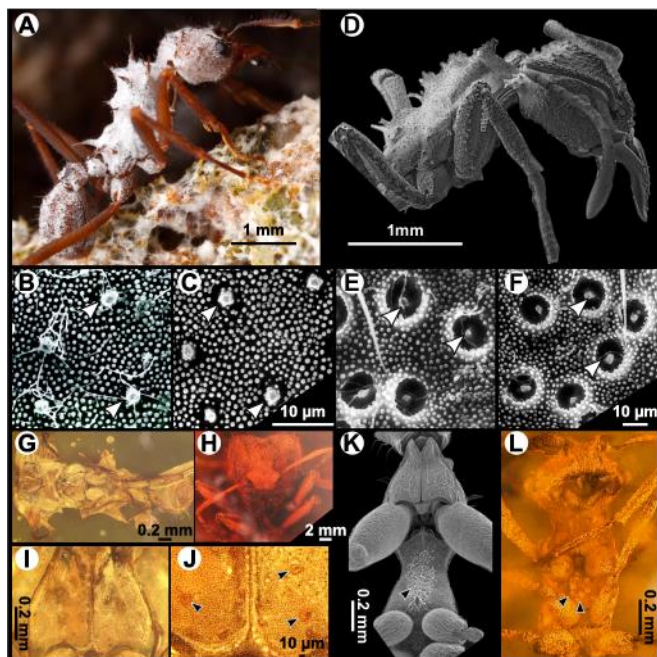


Figure A3.1 Cuticular structures associated with bacterial symbionts of extant and extinct attine ants. (A) Extant *Acromyrmex octospinosus* garden-tending ant with Actinobacteria (white) covering the entire body. Photo by Alex Wild, used by permission. (B) Actinobacteria growing directly on tubercles (arrows) on the propleural plate of *Ac. octospinosus* and (C) *Ac. octospinosus* tubercles from which Actinobacteria have been removed, revealing details. (D) Extant *Trachymyrmex bugnioni* ant with crypts over the entire body. (E) Actinobacteria growing directly on tubercles within crypts (arrows) on the propleural plate of *T. bugnioni*, and (F) *T. bugnioni* crypts from which Actinobacteria have been removed, revealing details in which each crypt contains a tubercle. (G) *Trachymyrmex primaevus* ant fossil embedded in Oligo-Miocene amber from the Dominican Republic, ventral view. (H) Detail of *T. primaevus* head showing foveae (i.e., pits or crypts). (I) Detail of *T. primaevus* propleural plate and (J) enlargement, showing dense foveae (arrows indicate pits or crypts). (K) Extant *Apterostigma dentigerum*, ventral view. Arrows indicate Actinobacteria on mesopleura. (L) *Apterostigma eowilsoni* ant fossil embedded in Oligo-Miocene amber from the Dominican Republic, ventral view. Arrows indicate plumes of bubbles on the mesopleura.

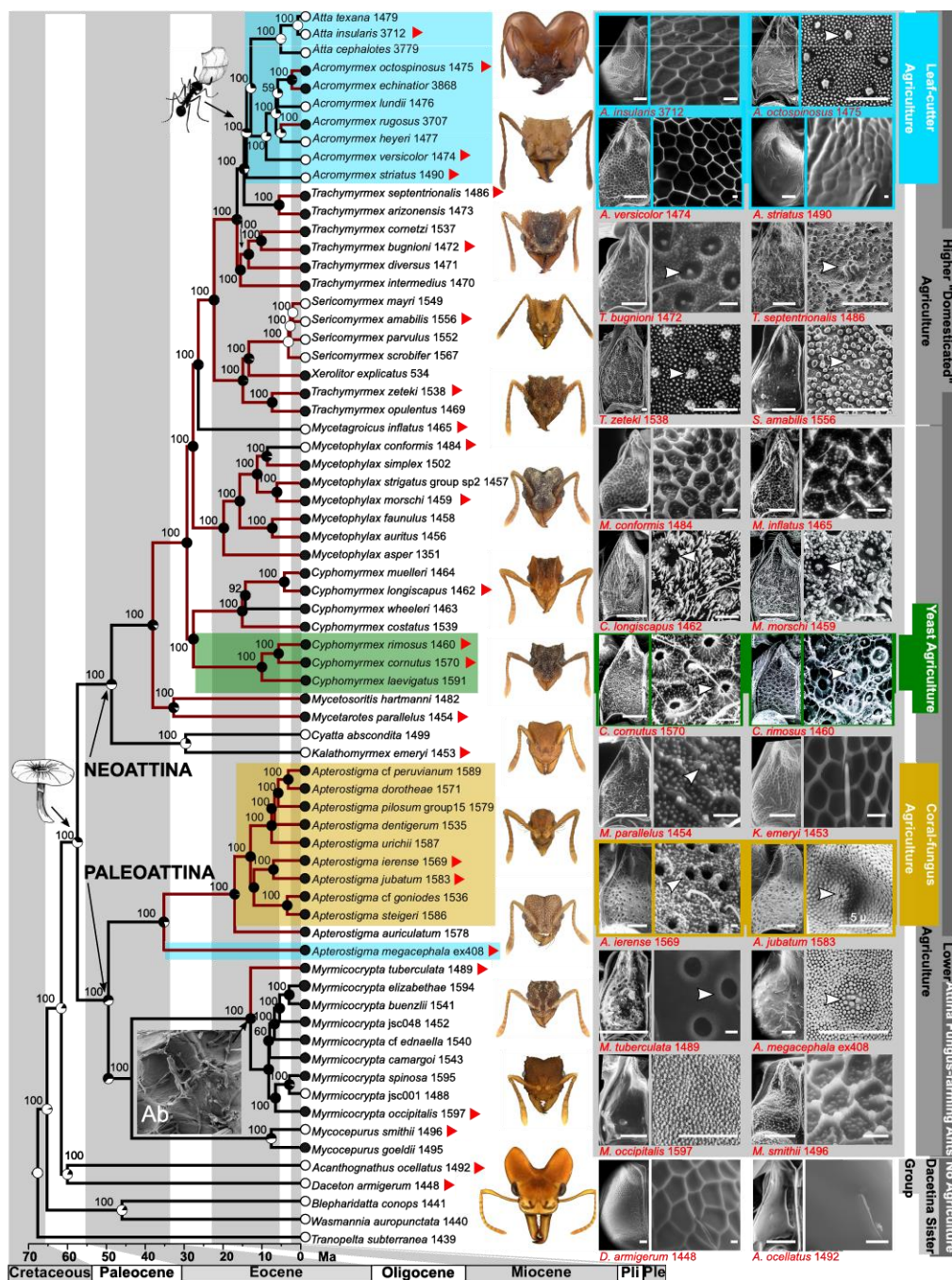


Figure A3.2 A time-calibrated phylogeny of the fungus-farming 'attine' ants, indicating the ancestral-state reconstruction probabilities (circles at nodes and tips) for the presence (black) or absence (white) of associated Actinobacteria. Branch colors indicate the status of specialized structures for housing and maintaining mutualistic Actinobacteria: brown branches indicate the presence of cuticular structures on the propleural plate and black branches indicate the absence of such structures. Red arrows adjacent to taxon names refer to the images on the right (additional images are in the *SI Appendix* Fig. S5). Numbers above branches are maximum-likelihood bootstrap proportions. Scale bar: 100 μm for propleural plate; 10 μm for other images (except *A. jubatum*, for which scale bar is 5 μm). Ab: antennal Actinobacteria (*Myrmicocrypta* spp.).

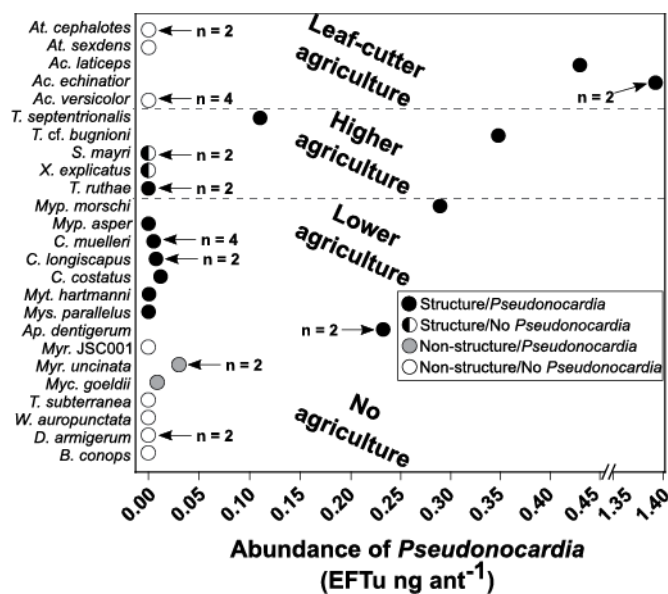


Figure A3.3 qPCR for measurement of abundance of *Pseudonocardia*. Sample sizes (maximum number of biological replicates) are provided next to their respective data points.

A3.8 Reference

- Joy JB (2013) Symbiosis catalyses niche expansion and diversification. *Proc R Soc B* 280:2012–2820.
- Moran NA (2007) Symbiosis as an adaptive process and source of phenotypic complexity. *Proc Natl Acad Sci USA* 104:8627–8633.
- McFall-Ngai M, et al. (2013) Animals in a bacterial world, a new imperative for the life sciences. *Proc Natl Acad Sci USA* 110:3229–3236.
- Douglas AE (1994) Symbiotic interactions. (Oxford University Press, Oxford).
- Baumann P, Moran NA and Baumann LC (2013) Bacteriocyte-associated endosymbionts of insects. *The Prokaryotes*, eds Rosenberg E, DeLong EF, Lory S, Stackebrandt E, Thompson F (Springer, Berlin, Heidelberg), pp 465–496.
- Braendle C, et al. (2003) Developmental origin and evolution of bacteriocytes in the aphid-*Buchnera* symbiosis. *PLoS Biol* 1:070–076.
- Nyholm SV, McFall-Ngai MJ (2004) The winnowing: Establishing the squid-*Vibrios* symbiosis. *Nat Rev Microbiol* 2:632–642.
- Kaltenpoth M, et al. (2014) Partner choice and fidelity stabilize coevolution in a Cretaceous-age defensive symbiosis. *Proc Natl Acad Sci USA* 111:6359–6364.

9. Hulcr J, Stelinski LL (2017) The Ambrosia symbiosis: From evolutionary ecology to practical management. *Annu Rev Entomol* 62:285–303.
10. Gerardo NM (2015) Harnessing evolution to elucidate the consequences of symbiosis. *PLoS Biol* 13:1–6.
11. Branstetter MG, et al. (2017) Dry habitats were crucibles of domestication in the evolution of agriculture in ants. *Proc R Soc B* 284:20170095.
12. Schultz TR, Brady SG (2008) Major evolutionary transitions in ant agriculture. *Proc Natl Acad Sci USA* 105:5435–5440.
13. Sosa-Calvo J, Schultz TR, Ješovnik A, Dahan RA, Rabeling C (2018) Evolution, systematics, and natural history of a new genus of cryptobiotic fungus-growing ants. *Syst Entomol* 43:549–567.
14. Currie CR, et al. (2003) Ancient tripartite coevolution in the Attine ant-microbe symbiosis. *Science* 299:386–388.
15. Pinto-Tomás AA, et al. (2009) Symbiotic nitrogen fixation in the fungus gardens of leaf-cutter ants. *Science* 326:1120–1123.
16. Currie CR, Scott JA, Summerbell RC, Malloch D (1999) Fungus-growing ants use antibiotic-producing bacteria to control garden parasites. *Nature* 398:701–704.
17. Currie CR, Mueller UG, Malloch D (1999) The agricultural pathology of ant fungus gardens. *Proc Natl Acad Sci USA* 96:7998–8002.
18. Van Arnam EB, et al. (2016) Selvamycin, an atypical antifungal polyene from two alternative genomic contexts. *Proc Natl Acad Sci USA* 113:12940–12945.
19. Van Arnam EB, Currie CR, Clardy J (2017) Defense contracts: molecular protection in insect-microbe symbioses. *Chem Soc Rev* 47:1638–1651.
20. Focus N (2008) All that makes fungus gardens grow. *Science* 320:1006–1008.
21. Currie CR, Poulsen M, Mendenhall J, Boomsma JJ, Billen J (2006) Coevolved crypts and exocrine glands support mutualistic bacteria in fungus-growing ants. *Science* 311:81–83.
22. Steffan SA, et al. (2015) Microbes are trophic analogs of animals. *Proc Natl Acad Sci USA* 112:15119–15124.
23. Boomsma JJ, Aanen DK (2009) Rethinking crop-disease management in fungus-growing ants. *Proc Natl Acad Sci USA* 106:17611–17612.
24. Iturralde-Vinent MA, MacPhee DE (1996) Age and paleogeographical origin of Dominican amber. *Science* 273:1850–1852.
25. Grimaldi DA, Agosti D (2000) A formicine in New Jersey Cretaceous amber and early evolution of ants. *Proc Natl Acad Sci USA* 97:13678–83.
26. Grimaldi D, Engel MS (2005) *Evolution of Insects* (Cambridge University Press, Cambridge, UK).
27. Schultz T (2007) The fungus-growing ant genus *Apterostigma* in Dominican amber. *Mem Am Entomol Inst* 80:425–436.
28. Andersen SB, Hansen LH, Sapountzis P, Sørensen SJ, Boomsma JJ (2013) Specificity and stability of the *Acromyrmex-Pseudonocardia* symbiosis. *Mol Ecol* 22:4307–4321.
29. Cafaro MJ, et al. (2011) Specificity in the symbiotic association between fungus-growing ants and protective *Pseudonocardia* bacteria. *Proc R Soc B* 278:1814–22.

30. Andersen SB, Yek SH, Nash DR, Boomsma JJ (2015) Interaction specificity between leaf-cutting ants and vertically transmitted *Pseudonocardia* bacteria. *BMC Evol Biol* 15:1–13.
31. Poulsen M, Cafaro M, Boomsma JJ, Currie CR (2005) Specificity of the mutualistic association between actinomycete bacteria and two sympatric species of *Acromyrmex* leaf-cutting ants. *Mol Ecol* 14:3597–3604.
32. Sosa-Calvo J, Fernando Fernández, Schultz TR (2018) Phylogeny and evolution of the cryptic fungus-farming ant genus *Myrmicocrypta* F. Smith (Hymenoptera: Formicidae) inferred from multilocus data. *Syst Entomol* DOI: 10.1111/syen.12313.
33. Rabeling C, Schultz TR, Bacci M, Bollazzi M (2015) *Acromyrmex charruanus*: a new inquiline social parasite species of leaf-cutting ants. *Insectes Soc* 62(3):335–349.
34. Marsh SE, Poulsen M, Pinto-Tomás A, Currie CR (2014) Interaction between workers during a short time window is required for bacterial symbiont transmission in acromyrmex leaf-cutting ants. *PLoS One* 9:e103269.
35. Poulsen M, Bot ANM, Currie CR, Nielsent MG (2003) Within-colony transmission and the cost of transmission in the leaf-cutting bacterium a mutualistic ant *Acromyrmex octospinosus*. *Funct Ecol* 17:260–269.
36. Parniske M (2008) Arbuscular mycorrhiza: The mother of plant root endosymbioses. *Nat Rev Microbiol* 6:763–775.
37. Sit CS, et al. (2015) Variable genetic architectures produce virtually identical molecules in bacterial symbionts of fungus-growing ants. *Proc Natl Acad Sci USA* 112:13150–13154.
38. Oh DC, Poulsen M, Currie CR, Clardy J (2009) Dentigerumycin: A bacterial mediator of an ant-fungus symbiosis. *Nat Chem Biol* 5:391–393.
39. Faircloth BC, Sorenson L, Santini F, Alfaro ME (2013) A Phylogenomic Perspective on the Radiation of Ray-Finned Fishes Based upon Targeted Sequencing of Ultraconserved Elements (UCEs). *PLoS One* 8:e65923.
40. Bolger AM, Lohse M, Usadel B (2014) Trimmomatic: A flexible trimmer for Illumina sequence data. *Bioinformatics* 30:2114–2120.
41. Del Fabbro C, Scalabrin S, Morgante M, Giorgi FM (2013) An extensive evaluation of read trimming effects on illumina NGS data analysis. *PLoS One* 8:e85024.
42. Faircloth BC (2016) PHYLUCE is a software package for the analysis of conserved genomic loci. *Bioinformatics* 32:786–788.
43. Ješovnik A, et al. (2017) Phylogenomic species delimitation and host-symbiont coevolution in the fungus-farming ant genus *Sericomyrmex* Mayr (Hymenoptera: Formicidae): ultraconserved elements (UCEs) resolve a recent radiation. *Syst Entomol* 42:523–542.
44. Katoh K, Standley DM (2013) MAFFT multiple sequence alignment software version 7: Improvements in performance and usability. *Mol Biol Evol* 30:772–780.
45. Castresana J (2000) Selection of conserved blocks from multiple alignments for their use in phylogenetic analysis. *Mol Biol Evol* 17:540–552.
46. Nguyen LT, Schmidt HA, Von Haeseler A, Minh BQ (2015) IQ-TREE: A fast and effective stochastic algorithm for estimating maximum-likelihood phylogenies. *Mol Biol Evol* 32:268–274.
47. Minh BQ, Nguyen MAT, Von Haeseler A (2013) Ultrafast approximation for phylogenetic

- bootstrap. *Mol Biol Evol* 30:1188–1195.
48. Borowiec ML (2016) AMAS: a fast tool for alignment manipulation and computing of summary statistics. *PeerJ* 4:e1660.
 49. Yang Z (2007) PAML 4: Phylogenetic analysis by maximum likelihood. *Mol Biol Evol* 24:1586–1591.
 50. Inoue J, Donoghue PCJ, Yang Z (2010) The impact of the representation of fossil calibrations on Bayesian estimation of species divergence times. *Syst Biol* 59:74–89.
 51. Barba-Montoya J, dos Reis M, Yang Z (2017) Comparison of different strategies for using fossil calibrations to generate the time prior in Bayesian molecular clock dating. *Mol Phylogenetics Evol* 114:386–400.
 52. Yang Z, Rannala B (2006) Bayesian estimation of species divergence times under a molecular clock using multiple fossil calibrations with soft bounds. *Mol Biol Evol* 23:212–226.
 53. Rambaut A, Suchard M, Xie W, Drummond AJ (2014) Tracer 1.6.0. *University of Edinburgh, Edinburgh, UK*.
 54. Maddison WP, Maddison DR (2017) Mesquite: A modular system for evolutionary analysis. Version 3.2. Available at mesquiteproject.org.

A3.9 Supplementary material

All supplementary material for this manuscript is found online at:

<http://www.pnas.org/content/pnas/suppl/2018/10/02/1809332115.DCSupplemental/pnas.1809332115.sapp.pdf>

Only figures and data generated by HAH are included here.

Table A3.9.1. Quantitive PCR (qPCR) of fungus-farming ant species.

Species	Collection Code	Collection Country	No. of Workers*
<i>Acromyrmex</i>			
<i>Acromyrmex_echinator</i>	AL050505-11	Panama	1, 1
<i>Acromyrmex_versicolor</i>	CR080724-01	USA	1, 1, 1, 1
<i>Acromyrmex_laticeps</i>	UGM030330-05	Panama	1
<i>Apterostigma</i>			
<i>Apterostigma_dentigerum</i>	AL050512-17	Panama	4,4
<i>Atta</i>			
<i>Atta_sexdens</i>	CC030329-01	USA	1
<i>Atta_cephalotes</i>	HH120223-02	Panama	1,1
<i>Cyphomyrmex</i>			
<i>Cyphomyrmex_costatus</i>	20140902-38 HFM	Panama	10
<i>Cyphomyrmex_longiscapus</i>	20150812-165 MV/PG	Panama	5, 6
<i>Cyphomyrmex_muelleri</i>	20150807-16MV/PG	Panama	6, 6, 6
<i>Mycetarotes</i>			

<i>Mycetarotes_parallelus</i>	JSC111027-01	Brazil	6
Mycetophylax			
<i>Mycetophylax_asper</i>	AJ141020-02	Brazil	5
<i>Mycetophylax_morschi</i>	TRS141026-03	Brazil	8
Mycetosoritis			
<i>Mycetosoritis_hartmanni</i>	CR107042702	USA	5
Mycocephurus			
<i>Mycocephurus_goeldii</i>	CR151006-02	Brazil	4
Myrmicocrypta			
<i>Myrmicocrypta_uncinata</i>	TRS111024-01	Brazil	6, 7
<i>Myrmicocrypta_JSC001</i>	JSC051102-14	Guyana	6
Sericomyrme			
<i>Sericomyrmex_mayri</i>	JSC111122-13	Brazil	5, 4
Trachymyrmex			
<i>Trachymyrmex_bugnioni</i>	TRS141003-04	Brazil	6
<i>Trachymyrmex_ruthae</i>	TRS910324-02	Brazil	4, 3
<i>Trachymyrmex_septentrionalis_1486</i>	TRS170427-01	USA	5
Xerolitor			
<i>Xerolitor_explicatus</i>	CR151031-07	Paraguay	5
Outgroups			
<i>Tranopelta_subterranea</i>	JSC120726-03	Peru	5
<i>Wasmannia_auropunctata</i>	CR111122-48	Cuba	6
<i>Blepharidatta_conops</i>	CR080724-01	Brazil	5
<i>Daceton_armigerum</i>	CR151006-02	Guyana	1, 1
Fungal Garden			
<i>Sericomyrmex_mayri</i>	AJ141004-01	Brazil	
<i>Myrmicocrypta_uncinata</i>	JSC151103-07	Brazil	
<i>Myrmicocrypta_uncinata</i>	TRS111024-01	Brazil	
<i>Myrmicocrypta_uncinata</i>	JSC051102-14	Brazil	

* Separated number indicate numbers of pooled ant individuals in each qPCR run.

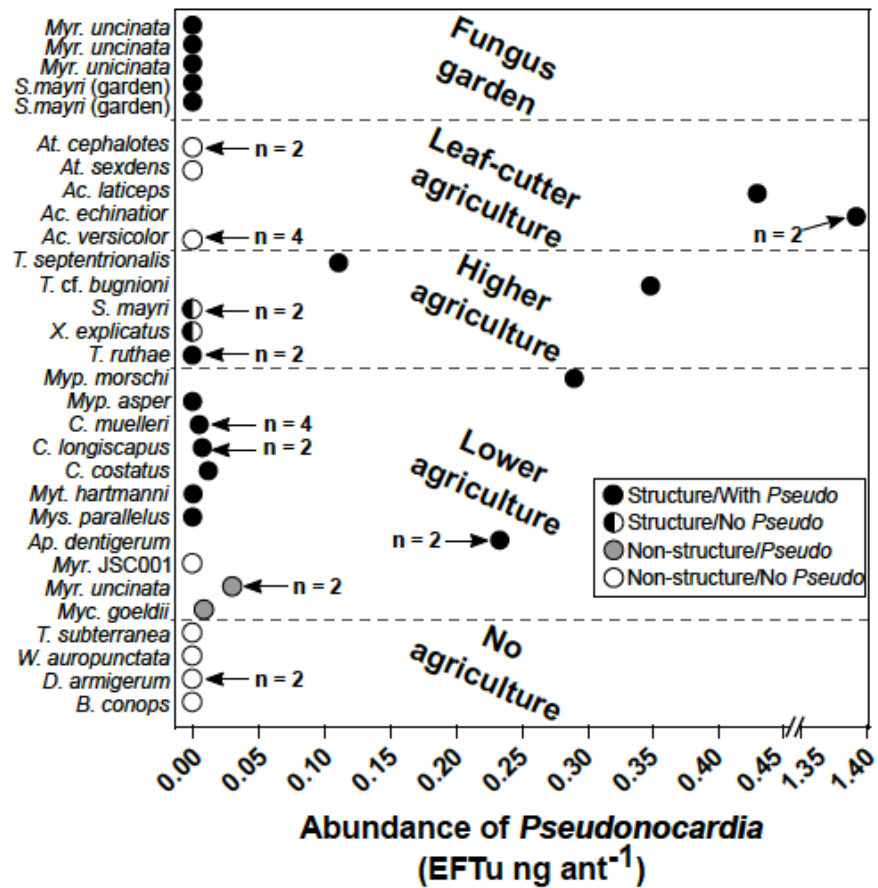


Figure A.3.9.1 qPCR for measurement of abundance of *Pseudonocardia* including fungus garden samples.

Appendix 4

Microbes are trophic analogs of animals

Authors: Shawn A. Steffana, Yoshito Chikaraishi, Cameron R. Currie, Heidi Horn, Hannah R. Gaines-Day, Jonathan N. Pauli, Juan E. Zalapa, and Naohiko Ohkouchi

Reprinted with permission from Steffan, Shawn A., Yoshito Chikaraishi, Cameron R. Currie, Heidi Horn, Hannah R. Gaines-Day, Jonathan N. Pauli, Juan E. Zalapa, and Naohiko Ohkouchi. "Microbes are trophic analogs of animals." *Proceedings of the National Academy of Sciences* 112, no. 49 (2015): 15119-15124.

*This work is included in this dissertation because HH contributed to the conceptualization, design, and execution of the assessment of trophic positions in the leaf-cutter ant system. It was decided to include this work in the broader context of this manuscript rather than publish independently. HH collected data or contributed to Figure A4.1, Figure A4.4, and Table A4.1.

A4.1 Abstract

In most ecosystems, microbes are the dominant consumers, commandeering much of the heterotrophic biomass circulating through food webs. Characterizing functional diversity within the microbiome, therefore, is critical to understanding ecosystem functioning, particularly in an era of global biodiversity loss. Using isotopic fingerprinting, we investigated the trophic positions of a broad diversity of heterotrophic organisms. Specifically, we examined the naturally occurring stable isotopes of nitrogen ($^{15}\text{N}:\text{}^{14}\text{N}$) within amino acids extracted from proteobacteria, actinomycetes, ascomycetes, and basidiomycetes, as well as from vertebrate and invertebrate macrofauna (crustaceans, fish, insects, and mammals). Here, we report that patterns of intertrophic ^{15}N -discrimination were remarkably similar among bacteria, fungi, and animals, which permitted unambiguous measurement of consumer trophic position, independent of phylogeny or ecosystem type. The observed similarities among bacterial, fungal, and animal consumers suggest that within a trophic hierarchy, microbiota are equivalent to, and can be interdigitated with, macrobiota. To further test the universality of this finding, we examined

Neotropical fungus gardens, communities in which bacteria, fungi, and animals are entwined in an ancient, quadripartite symbiosis. We reveal that this symbiosis is a discrete fourlevel food chain, wherein bacteria function as the apex carnivores, animals and fungi are meso-consumers, and the sole herbivores are fungi. Together, our findings demonstrate that bacteria, fungi, and animals can be integrated within a food chain, effectively uniting the macro- and microbiome in food web ecology and facilitating greater inclusion of the microbiome in studies of functional diversity.

A4.2 Introduction

The trophic functions of species sculpt the unique characteristics of the communities in which they are embedded (1, 2). It is not surprising, then, that sustained biodiversity losses (3, 4) are fueling the “trophic downgrading” of Earth (5) and altering the functioning of all major ecosystem types (6). The most abundant, ubiquitous organisms in most ecosystems—the microbiota—are also likely being impacted, and these organisms are often the least understood, particularly in terms of functional diversity (7, 8). If we are to better understand the impacts of biodiversity loss on ecosystem functioning, we will need to have a means to more comprehensively measure the trophic niches of both the macro- and microbiome. Further, such organisms must be examined while integrated within their respective communities (1). Assessing the trophic niches of microbial and animal species has too often been a theoretical endeavor (9), with macrofauna generally associated with plant-based food webs (“green food webs”) and the microfauna relegated to the sphere of decomposition (“brown food webs”) (9–11). It has proven difficult to merge these two spheres using a shared trophic metric, not only because of the difficulties in identifying microbial diversity (8), but also because of methodological obstacles in

measuring the trophic position of a microbe. Consequently, trophic ecology has tended to focus on green food webs, often leaving the trophic hierarchies of brown webs less resolved.

Uniting green and brown food webs is critically important to studies of biodiversity and ecosystem functioning because in most ecosystems, microbes are the dominant heterotrophs (3, 7, 12).

These organisms commandeer most of the heterotrophic biomass circulating through the food web (13). Indeed, in terrestrial systems, the vast majority of primary production is not captured by herbivores; rather, it falls to the ground and is consumed by microbes and small invertebrate detritivores (7, 12, 14). Higher-order carnivores consume the detritivores, conjoining the upward flow of detritivore and herbivore biomass (9, 11, 15, 16), but if the trophic positions in the basal layers of the food web cannot be accurately measured, the entire food web rests on a poorly known, tenuous platform (9).

Here, we investigate whether the trophic positions of microorganisms can be measured empirically, testing whether microbes are trophically equivalent to the macrobiotic consumers in a food-chain. Using amino acid stable isotope fingerprinting (17–20), we measure with high accuracy the trophic positions (TPs) of cultured and free-roaming organisms. In past work, this method has produced accurate TP estimates of zooplankton (18, 21), fish (17), gastropods (17), amphibians (22), and insects (19, 20), ranging from simple herbivores to higher-order carnivores. Although the utility of isotopic fingerprinting has been demonstrated in both aquatic (17, 21, 23, 24) and terrestrial ecosystems (19, 20), there remains an unbridged knowledge gap between the macro- and microbiome.

Recent studies have documented evidence of feeding guilds among the animals of brown food webs (11, 15, 25), and this finding sets up questions as to the trophic positions of the resident microbiota. For example, when microbes feed on a resource, do they register trophically just as animals do? More specifically, what is the trophic position of a fungus consuming a leaf, or an arthropod consuming that fungus? We address these questions, testing the hypothesis that fungi and bacteria are trophically equivalent to animals. We do so by measuring the degree of intertrophic ^{15}N -discrimination within amino acids extracted from consumer taxa, focusing on two key compounds: glutamic acid and phenylalanine (17, 19, 20, 26). For microbial organisms to be trophically equivalent to animals, their respective patterns of intertrophic ^{15}N -discrimination in glutamic acid and phenylalanine must mirror those of animals. In multiple controlled feeding studies involving a diversity of vertebrate and invertebrate consumers, net ^{15}N -discrimination between glutamic acid (glu) and phenylalanine (phe), commonly referred to as the trophic discrimination factor ($\text{TDF}_{\text{glu-phe}}$) (27), has tended to be centered near $+7.64 \pm 0.60\text{‰}$ (17, 20, 21). Although centered at 7.64, variability in the $\text{TDF}_{\text{glu-phe}}$ can generate “noise” around the trophic position ($\text{TP}_{\text{glu-phe}}$) estimate for any given consumer (Eq. 1). Variability in the $\text{TDF}_{\text{glu-phe}}$ among consumer groups, therefore, must be assessed using known, homogeneous diets. Ultimately, the degree to which the $\text{TDF}_{\text{glu-phe}}$ is consistent among microbial and animal consumers will dictate whether macro- and microbiota can be considered trophically equivalent.

To assess the universality of our approach, we examine the trophic identities of the organisms in leaf-cutter ant fungus gardens. Fungus gardens represent discrete community modules in which animals (ants), fungi, and bacteria have coevolved within an ancient symbiosis (28, 29) (Fig. 1). Leaf-cutter ants (*Acromyrmex* or *Atta*) are prodigious harvesters of leaf

material and have been referred to as the dominant herbivores of the Neotropics (30). The success of leaf-cutter ants derives largely from their mutualism with the fungus, *Leucoagaricus gongylophorus*, which is cultivated within the fungus gardens as the ants' sole food source (31). This mutualism is frequently parasitized, however, by another fungus (*Escovopsis*) that can invade and overwhelm the colony (28). Leafcutter ants (specifically, *Acromyrmex*) have evolved a defense against *Escovopsis* via a second mutualism with a bacterium (*Pseudonocardia*) that selectively suppresses the growth of the invading fungus (28, 29). The fungus garden, therefore, represents a complex, quadripartite symbiosis (ant-fungus-fungus-bacterium), with major impacts on tropical food web ecology (29, 30). Our findings uncover distinct trophic identities within this community, reframing how microbes may be viewed within a food web, and demonstrating the ecological portability of our approach.

A4.3 Results

A4.3.1 Controlled-Feeding Studies (TDF_{glu-phe} and TP_{glu-phe} Estimates)

Trophic discrimination factors (¹⁵N-discrimination between a consumer and its diet) were measured for specific amino acids extracted from fungal, bacterial, and animal consumers. The degree of ¹⁵N-discrimination in glutamic acid (glu) was consistently high among all consumers ($7.06 \pm 1.64\text{‰}$), whereas that of phenylalanine (phe) ($-0.16 \pm 1.55\text{‰}$) was trivial. This pattern stood in stark contrast to the more variable patterns observed in other amino acids (Table S1), whether feeding on a plant-derived (Fig. 2A) or animal-derived diet (Fig. 2B). Here, the “glu-phe elbow” highlights the value of glu and phe as trophic and source amino acids, respectively. Trophic amino acids (TrAA) enrich significantly between trophic levels, whereas source amino acids (SrcAAs) tend to be insensitive to intertrophic enrichment (17, 21). As such, these two classes of amino acids have served to indicate the TPs of animal taxa (17, 20, 23, 32).

We were able to consistently measure the $\delta^{15}\text{N}$ of the following TrAAs: alanine, glutamic acid, leucine, valine, and isoleucine. Among the SrcAAs, we were able to consistently measure glycine, and phenylalanine (Table S1). Across the three biological kingdoms examined in our study, glu and phe produced the most consistent, least variable TDF value, the parameter critical for accurate trophic position estimation.

Among the plant-feeding fungi in our controlled-feeding trials, these consumers produced a TDF_{glu-phe} (mean $\pm 1\sigma$) of $7.26 \pm 1.22\text{‰}$ (Table 1). This value was not significantly different ($t_{30} = 1.01$, $P = 0.320$) from that of our plant-feeding animals ($6.79 \pm 0.76\text{‰}$), nor was it significantly dissimilar from the standard TDF_{glu-phe}, $+7.64\text{‰}$ ($t_{23} = -1.38$, $P = 0.181$). Carnivorous fungi produced a mean TDF_{glu-phe} of $7.21 \pm 1.29\text{‰}$, which was not significantly different ($t_8 = -0.305$, $P = 0.768$) from that of animals fed the same diet ($7.43 \pm 0.92\text{‰}$), nor from the standard TDF_{glu-phe} ($t_2 = -0.575$, $P = 0.624$). Similarly, the bacteria cultured on yeast-extract media produced a mean TDF_{glu-phe} value of $6.65 \pm 0.33\text{‰}$. This degree of enrichment was not significantly different from those of either fungi or animals ($F_{2,45} = 0.803$, $P = 0.454$). Pooling together the bacterial and fungal consumers into a single microbial group, the microbial TDF_{glu-phe} was not dissimilar from that of the animals in our study ($t_{46} = 0.251$, $P = 0.803$).

Because our fungal, bacterial, and animal species were kept in pure culture and fed an isotopically characterized, homogeneous diet, their trophic positions were known. We were thus able to compare the known TP of a consumer with its empirically measured TP_{glu-phe} (Table 1). The mean TP_{glu-phe} values of plantfeeding fungi (1.96 ± 0.153) and animals (1.90 ± 0.093) were not different from each other ($t_{31} = 0.97$, $P = 0.338$; Fig. 3A). Similarly, the mean TP_{glu-phe} of fungi (3.01 ± 0.170) and animals (3.04 ± 0.113) feeding exclusively on the animal-based diet were not different from each other ($t_8 = -0.39$, $P = 0.710$; Fig. 3B). Bacterial trophic

positions were examined using diets more suited to bacterial culture (yeast-based growth media). *Streptomyces* and *Escherichia coli* were cultured on broths in which yeast extracts (fungus-derived amino acids) comprised the primary protein sources. The yeasts used in these diets (*Saccharomyces* spp., typically *S. cerevisiae*) are cultured on plant biomass, thus the yeasts are herbivorous organisms and registered as such: the TP_{glu-phe} of the yeast-based diet registered 2.00 ± 0.075 . *Streptomyces*, the bacterium consuming this diet, registered at 2.91 ± 0.039 , which was one trophic level higher and distinctly carnivorous (Table 1). The *E. coli* diet was a different broth blend consisting of both yeast extract and tryptone (amino acids of unknown origin), and this diet registered a mean TP_{glu-phe} of 2.54 ± 0.025 . The TP of *E. coli* cultured on this diet was 3.40 ± 0.043 . Again, the bacterium registered one trophic level higher than its diet.

To further test the hypothesis that microbes are trophically equivalent to animals, homogenized diets of fungus-derived proteins were fed to animal and bacterial species. Dried shiitake mushrooms, *Lentinula edodes*, were fed to the larvae of a moth, *Plodia interpunctella*. Shiitake mushrooms are wood-eating fungi and registered as herbivores (TP_{glu-phe} = 1.98 ± 0.120). The *Plodia* larvae feeding on the mushrooms registered as carnivores, with a mean TP_{glu-phe} of 3.04 ± 0.073 (Table 1). As mentioned previously, the bacterium, *Streptomyces*, was grown on media containing extracts from herbivorous yeast cultures. *Streptomyces* registered as a carnivore, with a TP_{glu-phe} of 2.91 ± 0.039 , approximately one trophic level higher than its yeast-based diet.

The plant-based diets in our study represented TP = 1 and were measured as such (Fig. 3A). When these measurements were arrayed within a $\delta^{15}\text{N}$ biplot, they closely aligned with the trophic isocline corresponding to primary producers. Trophic isoclines (trophoclines) are pairings of $\delta^{15}\text{N}_{\text{glu}}$ and $\delta^{15}\text{N}_{\text{phe}}$ values that, when plotted across a wide gradient of $\delta^{15}\text{N}$

signatures, represent the integer TPs within a food chain (e.g., TP = 1, 2, or 3). The herbivores in our controlled-feeding trials (known TP = 2) were closely aligned with trophocline 2 (Fig. 3A), and the carnivores (known TP = 3) were all clustered along trophocline 3 (Fig. 3B). Among all fungal, bacterial, and animal taxa, the observed TP_{glu-phe} values were not significantly different from their respective, known TPs (n = 17, paired Wilcoxon signed rank test: $W = -31.00$, $P = 0.074$).

A4.3.2 Fungus-Garden Study

An examination of leaf-cutter ant fungus gardens (Fig. 1) revealed that the ant-cultivated fungus, *Leucoagaricus*, was an herbivorous organism (TP_{glu-phe} = 1.9 ± 0.12), whereas the ants, long known to be fungivorous (28), registered at a distinctly carnivorous TP: 2.9 ± 0.17 (Fig. 4). The invading fungus, *Escovopsis*, also registered at a carnivorous TP, 3.0 ± 0.15 , and the bacterium deployed by the ants to defend the fungus garden registered a TP of 4.0 ± 0.17 . Arrayed across trophoclines, the bacterial, fungal, and animal consumer groups within the fungus garden registered as four discrete trophic groups (Fig. 4).

A4.4 Discussion

Viewed under the lens of amino acid isotopic analysis, the bacteria, fungi, and animals in our study exhibited strikingly similar patterns of intertrophic ¹⁵N-discrimination. Specifically, the consistent TDF_{glu-phe} among all consumers reflected predictable patterns of ¹⁵N-discrimination in glutamic acid and phenylalanine, the two amino acids previously shown to be critically important to accurate TP estimation among animals (17, 20, 26, 33). The degree of intertrophic ¹⁵N-discrimination in glu was relatively high, whereas that of phe was characteristically low, which contrasted with the more variable patterns observed in the

remaining aminoacids. This glu-phe ^{15}N -discrimination pattern held true across not only a broad phylogenetic spectrum (three biological kingdoms), but also a diversity of ecosystem types (terrestrial vs. aquatic) and trophic groups (plant- vs. animal-based diets). Trophically, therefore, the macro- and microfauna in our study were equivalent. Such constancy in the TDFglu-phe facilitates accurate, predictable trophic position estimation within the broader empire of heterotrophy.

The degree to which microbial and animal species can be integrated within a food web is particularly apparent when $\delta^{15}\text{N}_{\text{glu}}$ and $\delta^{15}\text{N}_{\text{phe}}$ values are arrayed across trophoclines. Trophoclines effectively couple $\delta^{15}\text{N}_{\text{glu}}$ and $\delta^{15}\text{N}_{\text{phe}}$ measurements within a 2D isotopic space and thereby provide a framework in which to view consumer trophic position. Within this framework, our microbial taxa registered as strict carnivores (trophic position 3) when feeding on herbivores, as did our animal taxa. Importantly, the animal taxa feeding on the same or analogous resources were trophically indistinguishable from the microbes, permitting the interdigitation of macro- and microfauna along each trophocline. Here, it is apparent that the consumers in our study registered one trophic level higher than their respective diets, regardless of consumer identity. Thus, whether it was crustaceans, fungi, insects, or mammals feeding on plant-based diets, the consumers registered as herbivores. Likewise, whether we measured moths eating fungi, fish eating homogenized insect powder, bacteria consuming yeast extracts, or fungi eating caterpillars, the consumer taxa registered as strict carnivores within the trophic hierarchy.

These findings suggest that when organisms feed on microbes, the consumers' trophic positions elevate predictably, regardless of whether the consumer is an animal or microbe. Trophically, therefore, a heterotrophic microbe represents "meat" in a food web. In light of the predominance of microbial detritivores within brown food webs (7, 12, 13), microbial biomass

may be a profoundly important source of protein flowing up through food chains. Indeed, as food chains shorten with the trophic downgrading of ecosystems (5), higher-order microbial carnivores may provide an important stabilizing buffer against the asymmetries caused by the loss of other trophic groups. Future work in this vein might investigate whether microbes and animals commonly swap trophic roles when the other is lost.

Within leaf-cutter ant fungus gardens, we examined the trophic roles of each symbiont in the community. Using amino acid stable isotope fingerprinting, we show that the cultivated fungus, *Leucoagaricus*, fed as an herbivore ($TP_{\text{glu-phe}} = 1.9 \pm 0.12$) and was the sole consumer of plant material in the fungus gardens. That a fungus was the sole herbivore within the fungus-garden community suggests that fungi, not ants, are the dominant herbivores of the Neotropics. The ants, long known to be fungivorous (28), registered at a distinctly carnivorous $TP_{\text{glu-phe}}: 2.9 \pm 0.17$. Importantly, the $TP_{\text{glu-phe}}$ of the ants was exactly one trophic level above their diet, and as strict consumers of herbivores, the ants were functional carnivores. In the trophic hierarchy of a fungus garden, the ants hold an intermediate position (trophic level 3) and thus are more analogous to “ranchers” than “gardeners.” The invading fungus, *Escovopsis*, also registered at a carnivorous $TP_{\text{glu-phe}}, 3.0 \pm 0.15$, indicating that it, too, fed on the herbivores of the community. At this $TP_{\text{glu-phe}}$, *Escovopsis* appears to be a direct competitor of the ants and not a consumer of the ants. To better compete with *Escovopsis*, the ants deploy their bacterial symbiont, *Pseudonocardia*, and interestingly, this bacterium registered a $TP_{\text{glu-phe}}$ of 4.0 ± 0.17 , one trophic level above the ants. Given that the bacterium grows on the ant exoskeleton (Fig. 1D) and is closely associated with specialized glands within cuticular crypts (29), the observed trophic position of *Pseudonocardia* strongly suggests it feeds exclusively on the ants. The tradeoff underlying the antibacterial mutualism, therefore, can be characterized as food for

protection, wherein the ants use their own tissues to culture a carnivorous bacterium, and in exchange, the bacterium protects the fungus garden from invaders. Collectively, these findings reveal the presence of four discrete trophic levels within the fungus garden community. Here, the bacterium is the trophic equivalent of an apex carnivore, whereas the ant colony and its fungal competitor feed as meso-carnivores, and all are supported by the foundational herbivore of the community, another fungus. By coupling isotopic fingerprinting with natural history information, we are able to better illuminate the trophic identities of fungal, bacterial, and animal consumers in an ancient, quadripartite symbiosis.

Our overarching goal in this work is to provide a basis to accurately interpret the trophic positions of free-roaming heterotrophic organisms, regardless of their phylogenetic origin or ecosystem type. We provide empirical evidence that isotopically derived trophic metrics are equally applicable to animal and microbial consumer groups. Whether feeding on plant- or animal-based biomass, fungi and bacteria are trophic analogs of animals. Although it is possible that the 15 taxa cultured in our controlled-feeding studies were not broadly representative of heterotrophic bacteria, fungi, and animals, the likelihood that we inadvertently selected the 15 anomalous species is quite small given the exceedingly high global diversity of heterotrophic fauna (3, 4, 7, 8). It is more parsimonious to conclude that the organisms in our study reflect real patterns within the broader heterotrophic empire and that microbes can be considered the trophic equivalents of animals within a food chain. For food web ecology, this reframes how the microbiome can be viewed and resolves long-standing questions as to where microbes fit within the food chain. Fungal, bacterial, and animal species can be integrated within a single trophic hierarchy, thereby uniting the macro- and microbiome and facilitating more comprehensive assessments of functional diversity within ecosystems.

A4.5 Materials and Methods

A.4.5.1 Culturing of Consumer Species

Fifteen heterotrophic species, spanning six phyla (Proteobacteria, Actinobacteria, Ascomycota, Basidiomycota, Arthropoda, and Chordata) and three kingdoms (Fungi, Bacteria, and Animalia), were kept in pure culture on homogeneous, isotopically characterized diets (SI Materials and Methods). Among the animal taxa cultured were crustaceans, fish, insects, and mammals. Among the microbiota, we cultured ascomycete and basidiomycete fungi, as well as proteobacteria and filamentous bacteria (actinomycetes). When a consumer had developed to maturity on a given diet, the entire organism was homogenized and the $\delta^{15}\text{N}$ values of amino acids within its tissues were measured using established analytical protocols (17, 26, 34). Cultures of fungus gardens were maintained within a controlled-environment laboratory setting (24–26 °C, 16:8 photoperiod). Leaf-cutter ant (*Acromyrmex echinatior*) colonies were provisioned with leaves harvested from oak trees (*Quercus macrocarpa*). Colonies were confined to clear plastic mesocosms and maintained according to established rearing protocols (29).

4.5.2 Compound-Specific Isotope Analysis

Each specimen was collected, euthanized, and desiccated in a drying oven for 7–14 d and then homogenized before drawing aliquots for stable nitrogen isotope analysis of amino acids. Compound-specific isotope analysis of N was conducted via protocols (17, 34) developed and refined at the Department of Biogeochemistry, Japan Agency of Marine-Earth Science and Technology (JAMSTEC), Yokosuka, Japan. In brief, specimens were hydrolyzed and derivatized, allowing for the extraction of amino acids. The identities of the amino acids were verified via gas chromatography (GC) and then combusted (C) within a furnace interfaced with

an isotopic ratio MS (IRMS). Using an integrated GC-C-IRMS system, each target amino acid had its isotope ratio quantified independently. The $\delta^{15}\text{N}$ values were determined for a suite of amino acids, generally including alanine, glutamic acid, leucine, valine, isoleucine, glycine, and phenylalanine (Datasets S1–S30).

A4.5.3 Trophic Computations and Statistics

Trophic position (TP_{glu-phe}) estimates were generated using the following equation (17):

$$\text{TP} = \delta^{15}\text{N}_{\text{glu}} - \delta^{15}\text{N}_{\text{phe}} + |\beta| |\Delta\text{glu-phe}| + \lambda, \text{TP} = \delta^{15}\text{N}_{\text{glu}} - \delta^{15}\text{N}_{\text{phe}} + |\beta| |\Delta\text{glu-phe}| + \lambda \quad [1],$$

where $\delta^{15}\text{N}_{\text{glu}}$ represents the nitrogen isotopic ratio of glutamic acid, $\delta^{15}\text{N}_{\text{phe}}$ represents the nitrogen isotopic ratio of phenylalanine, β corrects for the difference in ^{15}N values between glutamic acid and phenylalanine within the primary producers of the food web (e.g., $\beta \sim 8.4\%$ for C_3 plants), $\Delta\text{glu-phe}$ represents the net trophic discrimination between glutamic acid and phenylalanine, and λ represents the basal trophic level ($=1$) of the food web. The trophic discrimination factor, $\Delta\text{glu-phe}$ (also referred to as the TDF), represents the net intertrophic ^{15}N -discrimination between glutamic acid and phenylalanine (SI Materials and Methods). Discernment of significant differences between known and observed TP values was examined using univariate ANOVA and nonparametric tests (paired Wilcoxon signed rank tests where data were heteroscedastic). Distinguishing among TDF values was accomplished using paired t tests.

A4.6 Acknowledgments

We thank Janet van Zoeren, Rachel Arango, Sacha Horn, Lindsay Wells, Brian Hudelson, Christopher Watson, Merritt Singleton, and Drs. Patricia McManus, Bhadriraju Subramanyam, Tess Killpack, and Bill Karasov for assistance with animal and microbial cultures. Leaf-cutter ant photos appear courtesy of Don Parsons. Drs. Prarthana Dharampal, Peggy Ostrom, Stephen Carpenter, and Elissa Chasen provided helpful suggestions on earlier manuscript drafts. This work was supported by the University of Wisconsin Vilas Lifecycle Professorship (awarded to

S.A.S.), the US Department of Agriculture–Agricultural Research Service (Current Research Information System 3655-21220-001, awarded to S.A.S. and J.E.Z.), and the Japan Agency for Marine–Earth Science and Technology.

A4.7 Figures

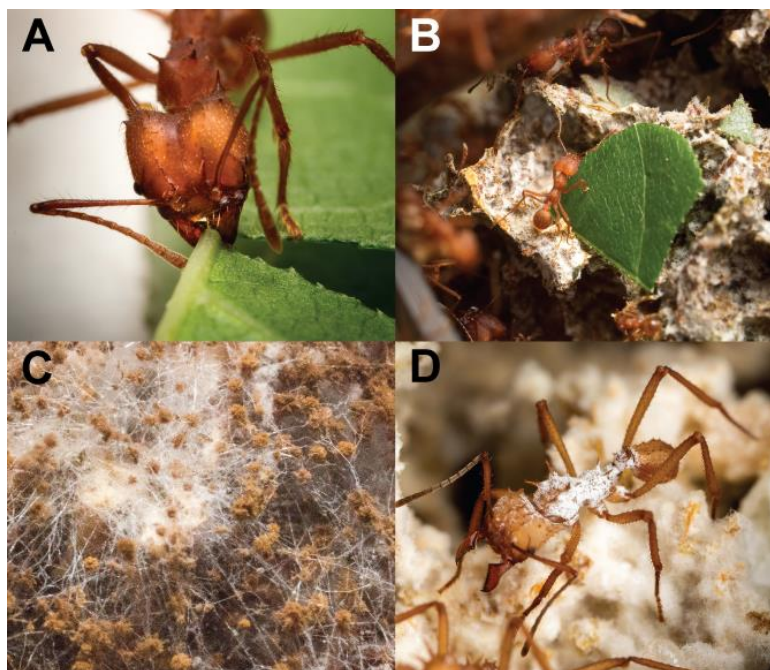
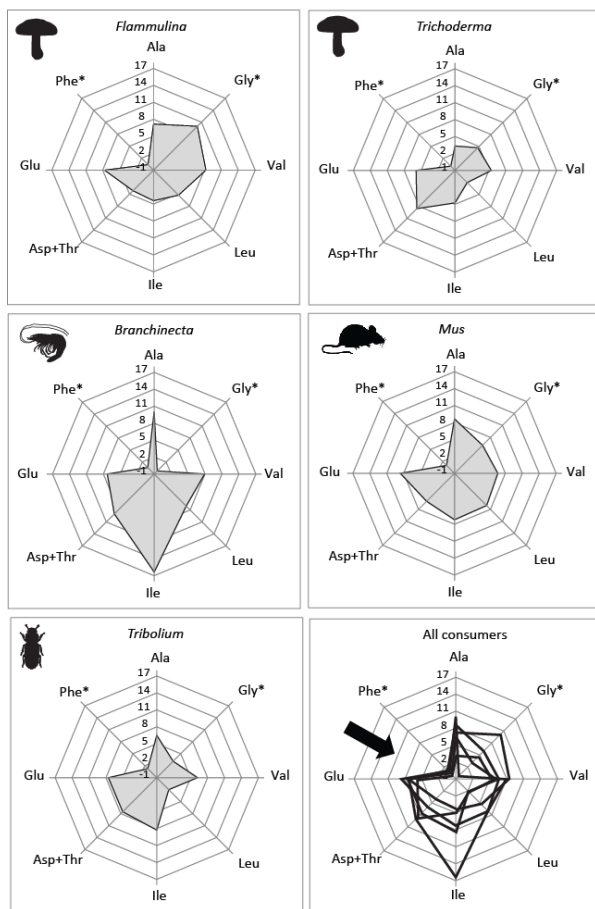


Figure A4.1 Denizens of a leaf-cutter ant fungus garden. (A) Forager ant cutting out a leaf fragment. (B) Incorporation of leaf material into the fungus garden. (C) Mycelia and fruiting bodies of *Leucoagaricus*, the fungus cultivated by the ants. (D) The bacterium, *Pseudonocardia* (white, powder-like substance on the ant dorsum), growing within specialized structures on the ant cuticle. The five taxa in our fungus gardens: oak (*Quercus macrocarpa*), cultivated fungi (Basidiomycota: *Leucoagaricus gongylophorus*), parasitic fungi (Ascomycota: *Escovopsis*), leaf-cutter ants (*Acromyrmex echinator*), and the filamentous bacterium (Actinobacteria: *Pseudonocardia*) grown by the ants to suppress the invading fungus, *Escovopsis* (29).

A. Herbivorous organisms



B. Carnivorous organisms

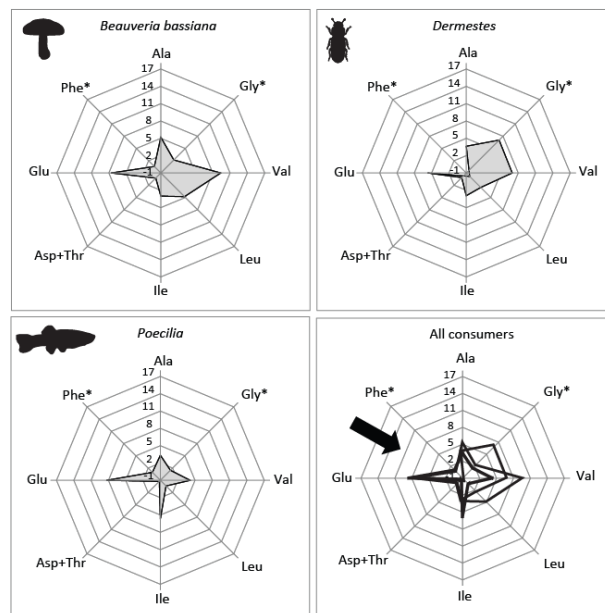


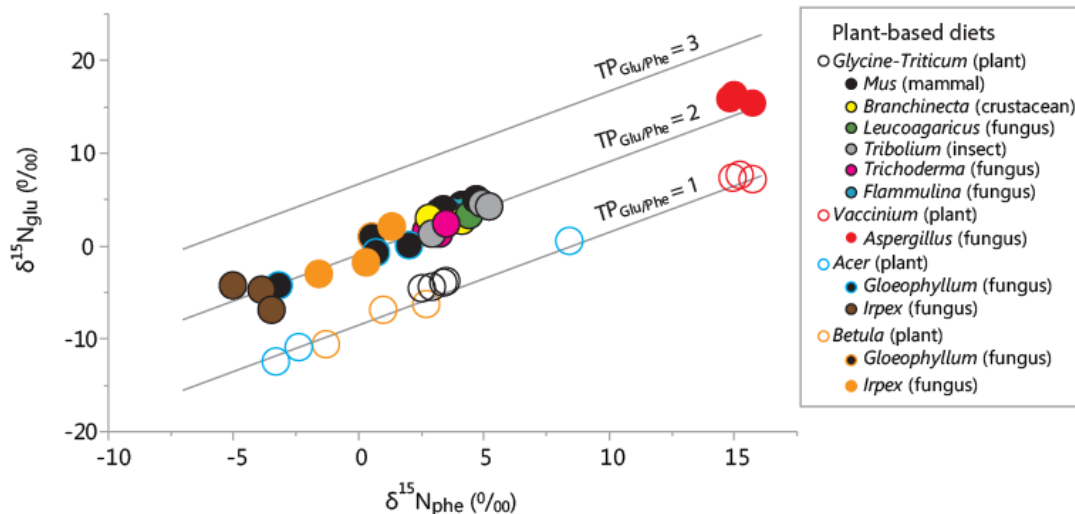
Figure A4.2. Patterns of intertrophic ^{15}N -discrimination within specific amino acids, across a broad diversity of heterotrophic organisms. For each amino acid (AA) extracted from a given consumer, the net change in $\delta^{15}\text{N}_{\text{AA}}$ between the consumer and its diet has been arrayed within a radar plot. This net change is also commonly referred to as the TDF, an important parameter in trophic position estimation. All consumers were fed exclusively on either (A) a plant-based diet (soy and wheat flour) or (B) an animal-based diet. The consistently high degree of ^{15}N -discrimination in glutamic acid (glu) stands in stark contrast to the consistently low discrimination in phenylalanine (phe). When these intertrophic discrimination patterns are superimposed over one another, a distinct “elbow” is formed by the high glu, low phe pattern (creating the “glu-phe elbow,” indicated by bold arrows). This phenomenon is typical of isotopic fractionation in animal tissues (17, 20, 21, 23) and underscores the finding that $\delta^{15}\text{N}_{\text{glu}}$ and $\delta^{15}\text{N}_{\text{phe}}$ discrimination patterns in fungi and bacteria mirror those of animals. *Source AAs.

Table 4.1 Comparison of the TDFs and TPs of fungal, bacterial, and animal taxa

Consumer		Dietary protein type	Trophic discrimination factor (TDF)		Trophic position (TP)	
			TDF _{glu-phe}	TDF _{TrAA-SrcAA}	TP _{expected}	TP _{glu-phe}
Fungi	<i>Aspergillus</i>	Plant	8.59	0.95	2	2.1
	<i>Beauveria</i>	Animal (herbivore)	7.02	3.20	3	3.0
	<i>Flammulina</i>	Plant	7.32	0.88	2	2.0
	<i>Gloeophyllum</i> (on birch)	Plant	7.99	10.77	2	2.0
	<i>Gloeophyllum</i> (on maple)	Plant	7.10	5.18	2	1.9
	<i>Irpex</i> (on birch)	Plant	7.74	3.65	2	2.0
	<i>Irpex</i> (on maple)	Plant	7.36	1.37	2	2.0
	<i>Leucoagaricus</i>	Plant	6.35	7.12	2	1.8
	<i>Trichoderma</i>	Plant	5.83	1.92	2	1.8
Bacteria	<i>Escherichia</i>	Yeast-extract, tryptone	6.48	3.62	3.5	3.4
	<i>Streptomyces</i>	Yeast extract, tryptic soy	6.82	3.72	3.0	2.9
Insects	<i>Dermestes</i>	Animal (herbivore)	7.50	0.89	3	3.1
	<i>Plodia</i>	Fungus (herbivore)	8.05	4.62	3	3.0
	<i>Tribolium</i>	Plant	6.31	3.93	2	1.8
Crustaceans	<i>Branchinecta</i>	Plant	6.70	9.55	2	1.9
Fish	<i>Poecilia</i>	Animal (herbivore)	7.37	1.51	3	3.0
Mammals	<i>Mus</i>	Plant	7.59	4.12	2	2.0
Mean:			7.20	3.94		
Standard deviation:			0.72	2.91		
% RSD:			10.0%	73.8%		

Values calculated using glutamic acid and phenylalanine, as well as multicomponent groupings of TrAA and SrcAA. TP_{expected} indicates the expected trophic position of a consumer, given the known trophic position of its diet. TP_{glu-phe} indicates the observed trophic position of each consumer, based on its 15N_{glu} and 15N_{phe} values. TrAA = alanine, valine, leucine, isoleucine, glutamic acid. SrcAA = glycine, phenylalanine. The % relative SD (% RSD) quantifies the ratio of the SD to its corresponding mean ($\times 100$) and conveys the degree of variability as a proportion of the mean. Among the 17 consumer-diet combinations examined in this study, the TDF_{TrAA-SrcAA} was much more variable than the TDF_{glu-phe} (equal variance test, $P < 0.01$).

A. Plant-based diet



B. "Meat"-based diet

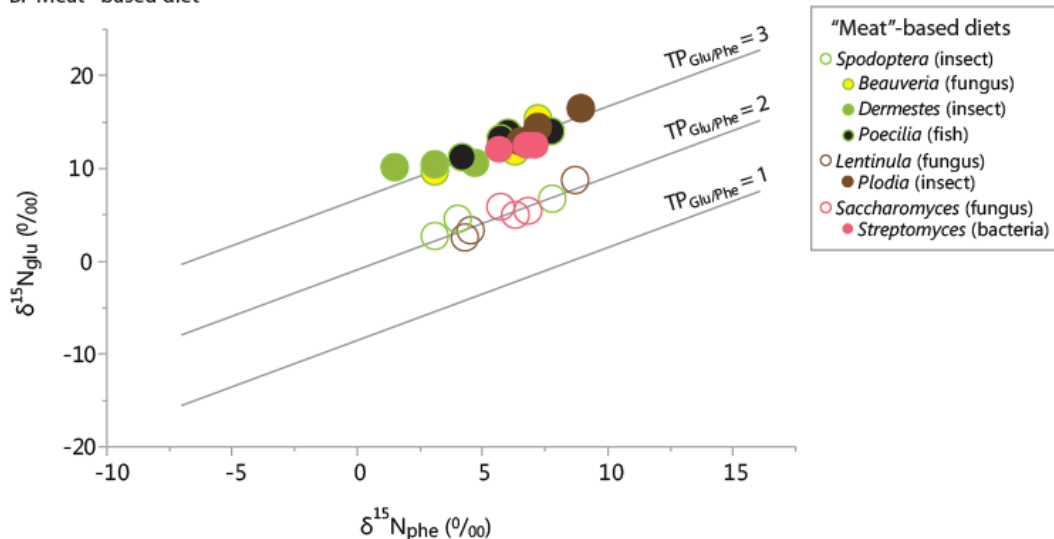


Figure A4.3 Amino acid isotope compositions ($\delta^{15}\text{N}_{\text{glu}}$ and $\delta^{15}\text{N}_{\text{phe}}$) of fungal and animal species, arrayed across trophic isoclines. (A) Organisms cultured on a plant-based diet. (B) Organisms cultured on an animal-based diet. For each organism, the glutamic acid $\delta^{15}\text{N}$ value ($\delta^{15}\text{N}_{\text{glu}}$) is plotted against its corresponding phenylalanine $\delta^{15}\text{N}$ value ($\delta^{15}\text{N}_{\text{phe}}$). ○, samples of a given diet; ●, consumers. Trophic isoclines (plotted as solid lines) represent pairings of $\delta^{15}\text{N}_{\text{glu}}$ and $\delta^{15}\text{N}_{\text{phe}}$ values over a wide gradient, with each line corresponding to an integer trophic position (TP = 1, 2, and 3).

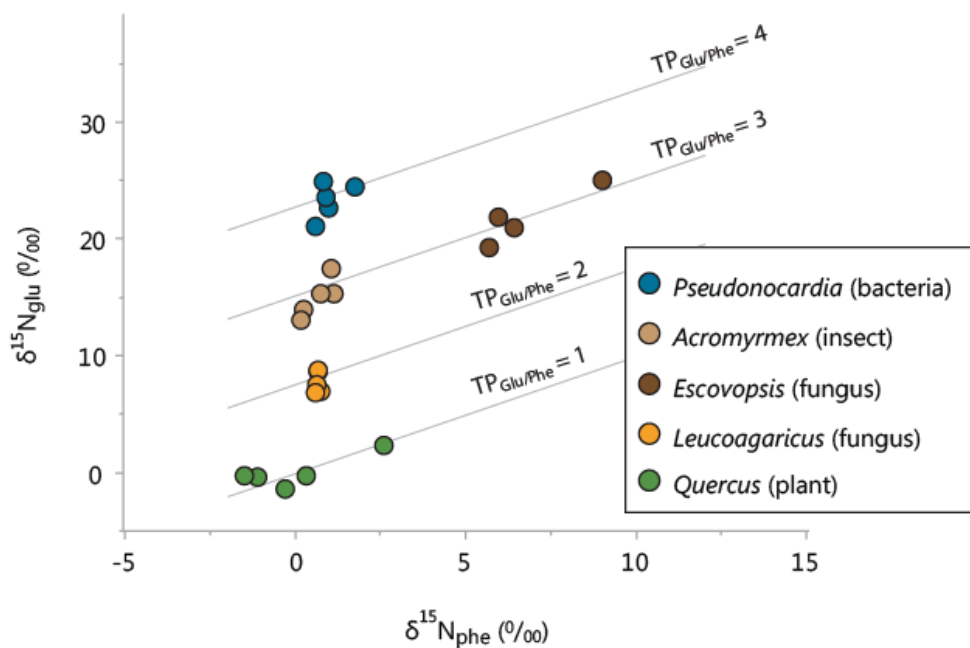


Figure A4.4 Amino acid isotope compositions ($\delta^{15}\text{N}_{\text{glu}}$ and $\delta^{15}\text{N}_{\text{phe}}$) of each trophic group within ant fungus gardens. For each organism, the glutamic acid $\delta^{15}\text{N}$ value ($\delta^{15}\text{N}_{\text{glu}}$) is plotted against its corresponding phenylalanine $\delta^{15}\text{N}$ value ($\delta^{15}\text{N}_{\text{phe}}$). All isotopic values ($\delta^{15}\text{N}$) are arrayed across trophic isoclines. Trophic isoclines (plotted as solid lines) represent pairings of $\delta^{15}\text{N}_{\text{glu}}$ and $\delta^{15}\text{N}_{\text{phe}}$ values over a wide gradient, with each line corresponding to an integer trophic level ($\text{TP}_{\text{glu/phe}} = 1\text{--}4$).

A4.8 References

1. Chase J, Leibold M (2003) *Ecological Niches: Linking Classical and Contemporary Approaches* (Univ of Chicago Press, Chicago).
2. Cohen J, et al. (1993) Improving food webs. *Ecology* 74(1):252–258.
3. May RM (1988) How many species are there on Earth? *Science* 241(4872):1441–1449.
4. Pimm SL, et al. (2014) The biodiversity of species and their rates of extinction, distribution, and protection. *Science* 344(6187):1246752.
5. Estes JA, et al. (2011) Trophic downgrading of planet Earth. *Science* 333(6040):301–306.
6. Hooper D, et al. (2005) Effects of biodiversity on ecosystem functioning: A consensus of current knowledge. *Ecol Monogr* 75(1):3–35.
7. Beattie A, Ehrlich P (2010) The missing link in biodiversity conservation. *Science* 328(5976):307–308.
8. Hughes JB, Hellmann JJ, Ricketts TH, Bohannan BJ (2001) Counting the uncountable: Statistical approaches to estimating microbial diversity. *Appl Environ Microbiol* 67(10):4399–4406.
9. Polis G, Strong D (1996) Food web complexity and community dynamics. *Am Nat* 147(5):813–846.
10. Lindeman R (1942) The trophic-dynamic aspect of ecology. *Ecology* 23(4):399–417.
11. Kaspari M, Yanoviak SP (2009) Biogeochemistry and the structure of tropical brownfood webs. *Ecology* 90(12):3342–3351.
12. Coleman DC (1996) Energetics of detritivory and microbivory in soil in theory and practice. *Food Webs: Integration of Patterns and Dynamics*, eds Polis GA, Winemiller KO (Chapman & Hall, New York), pp 39–50.
13. Moore JC, de Ruiter PC (2012) *Energetic Food Webs* (Oxford Univ Press, Oxford, UK).
14. Colinvaux P (1978) *Why Big Fierce Animals Are Rare: An Ecologist's Perspective* (Princeton Univ Press, Princeton).
15. Haraguchi TF, Uchida M, Shibata Y, Tayasu I (2013) Contributions of detrital subsidies to aboveground spiders during secondary succession, revealed by radiocarbon and stable isotope signatures. *Oecologia* 171(4):935–944.

16. Tayasu I, Hyodo F (2010) Use of carbon—14 natural abundances in soil ecology: Implications for food web research. *Earth, Life, and Isotopes*, eds Ohkouchi N, Tayasu I, Koba K (Kyoto Univ Press, Kyoto), pp 3–16.
17. Chikaraishi Y, et al. (2009) Determination of aquatic food-web structure based on compound-specific nitrogen isotopic composition of amino acids. *Limnol Oceanogr* 7 (2003):740–750.
18. Hannides C, Popp B, Landry M, Graham B (2009) Quantification of zooplankton trophic position in the North Pacific Subtropical Gyre using stable nitrogen isotopes. *Limnol Oceanogr* 54(1):50–61.
19. Chikaraishi Y, Ogawa NO, Doi H, Ohkouchi N (2011) $^{15}\text{N}/^{14}\text{N}$ ratios of amino acids as a tool for studying terrestrial food webs: A case study of terrestrial insects (bees, wasps, and hornets). *Ecol Res* 26(4):835–844.
20. Steffan SA, et al. (2013) Trophic hierarchies illuminated via amino acid isotopic analysis. *PLoS One* 8(9):e76152.
21. McClelland J, Montoya J (2002) Trophic relationships and the nitrogen isotopic composition of amino acids in plankton. *Ecology* 83(8):2173–2180.
22. Chikaraishi Y, Steffan SA, Takano Y, Ohkouchi N (2015) Diet quality influences isotopic discrimination among amino acids in an aquatic vertebrate. *Ecol Evol* 5(10):2048–2059.
23. Popp B, et al. (2007) Insight into the trophic ecology of yellowfin tuna, *Thunnus albacares*, from compound-specific nitrogen isotope analysis of proteinaceous amino acids. *Stable Isotopes as Indicators of Ecological Change*, eds Dawson T, Siewolf R (Academic, London), pp 173–190.
24. Newsome SD, Fogel ML, Kelly L, Martínez del Río C (2011) Contributions of direct incorporation from diet and microbial amino acids to protein synthesis in Nile tilapia. *Funct Ecol* 25(5):1051–1062.
25. Maraun M, et al. (2011) Stable isotopes revisited: Their use and limits for oribatid mite trophic ecology. *Soil Biol Biochem* 43(5):877–882.
26. Chikaraishi Y, et al. (2014) High-resolution food webs based on nitrogen isotopic composition of amino acids. *Ecol Evol* 4(12):2423–2449.
27. Cerling T, Harris J (1999) Carbon isotope fractionation between diet and bioapatite in ungulate mammals and implications for ecological and paleoecological studies. *Oecologia* 120(3):347–363.
28. Currie C, Scott J, Summerbell R, Malloch D (1999) Fungus-growing ants use antibiotic-producing bacteria to control garden parasites. *Nature* 398:701–705.
29. Currie CR, Poulsen M, Mendenhall J, Boomsma JJ, Billen J (2006) Coevolved crypts and exocrine glands support mutualistic bacteria in fungus-growing ants. *Science* 311(5757):

81–83.

30. Hölldobler B, Wilson EO (1990) *The Ants* (Belknap Publishing, Cambridge, MA).
31. Currie CR, et al. (2003) Ancient tripartite coevolution in the attine ant-microbe symbiosis. *Science* 299(5605):386–388.
32. Décima M, Landry MR, Popp BN (2013) Environmental perturbation effects on baseline $\delta^{15}\text{N}$ values and zooplankton trophic flexibility in the southern California Current Ecosystem. *Limnol Oceanogr* 58(2):624–634.
33. Chikaraishi Y, Kashiyama Y, Ogawa NO, Kitazato H, Ohkouchi N (2007) Metabolic control of nitrogen isotope composition of amino acids in macroalgae and gastropods: Implications for aquatic food web studies. *Mar Ecol Prog Ser* 342(2003):85–90.
34. Chikaraishi Y, Takano Y, Ogawa NO, Ohkouchi N (2010) Instrumental optimization for compound-specific nitrogen isotope analysis of amino acids by gas chromatography/combustion/isotope ratio mass spectrometry. *Earth, Life, and Isotopes*, eds Ohkouchi N, Tayasu I, Koba K (Kyoto Univ Press, Kyoto), pp 367–386.

A4. 9 Supplementary material

All supplementary material for this manuscript is found online at:

<http://www.pnas.org/content/pnas/suppl/2015/11/19/1508782112.DCSupplemental/pnas.201508782SI.pdf>
<http://www.pnas.org/content/pnas/suppl/2015/11/19/1508782112.DCSupplemental/pnas.1508782112.sd01.pdf>